UNIVERSITÀ DI PARMA

UNIVERSITÀ DEGLI STUDI DI PARMA

DOTTORATO DI RICERCA IN "FISICA"

CICLO XXXVIII

Solving $\mathcal{N} = 2$ gauge theories through matrix models on the sphere

Coordinatore:

Chiar.ma Prof. Raffaella Burioni

Tutore:

Chiar.mo Prof. Luca Griguolo

Dottorando
Alessandro Testa

Anni Accademici 2022/2023 – 2024/2025

Abstract

In this thesis, we study different classes of four-dimensional $\mathcal{N} = 2$ super-Yang–Mills (SYM) theories, including both conformal and non-conformal setups. The extended but non-maximal supersymmetry of these models enables the development of non-perturbative approaches, such as integrability, gauge-gravity dualities, and localization techniques, while retaining a non-trivial low-energy dynamics. As a result, $\mathcal{N} = 2$ SYM theories provide an interpolating framework between maximally supersymmetric $\mathcal{N} = 4$ configurations and more realistic scenarios where we can improve our understanding of quantum field theory beyond usual perturbative regimes.

In the first part of this work, we study special $\mathcal{N} = 2$ superconformal models known as quiver theories. These setups offer a controlled playground for investigating several non-perturbative aspects of quantum field theory and are expected to exhibit higher-dimensional dynamics in certain regions of their parameter space. This phenomenon, known as deconstruction, was originally studied in ordinary (quiver-like) Yang–Mills theories where, however, the higher-dimensional dynamics appears in the low-energy regimes, thereby preventing explicit computations. In contrast, the $\mathcal{N} = 2$ quiver theories combine supersymmetry and conformal invariance, allowing us to explore their quantum dynamics through powerful non-perturbative tools, such as supersymmetric localization. More specifically, we study protected correlation functions which, in the 't Hooft limit, are mapped by localization to special Fredholm determinants of Bessel operators. These determinants are closely related to the celebrated Tracy–Widom distributions of random matrix theory and provide a representation of the observables valid for arbitrary parameter values. By exploiting the determinant formalism, we systematically explore the dynamics of quiver theories and obtain closed-form results at strong coupling. In particular, we show that in the deconstruction limit these models display effective five-dimensional dynamics with massive excitations propagating along an emergent dimension. The corresponding mass spectrum is described analytically by the zeros of Bessel functions and can be interpreted within an effective one-dimensional field theory.

The remarkable effectiveness of the matrix model description in conformal scenarios naturally raises the question of whether it can be extended to non-conformal theories in flat space. To address this problem, we consider $\mathcal{N} = 2$ models with massless matter and non-vanishing β-function, where conformal symmetry is dynamically broken at the quantum level. We study two classes of localizable observables: the expectation value of supersymmetric (half-BPS) Wilson loops and the correlation functions of chiral operators. In flat space, these quantities are computed through standard Feynman diagram techniques and renormalization procedures. Despite the breaking of conformal invariance, we demonstrate that supersymmetric localization on S^4 reproduces the corresponding perturbative results in flat space within a specific regime of validity. This agreement extends the applicability of matrix-model methods beyond conformal settings and opens new directions for exploring the strong-coupling regimes of $\mathcal{N} = 2$ theories with non-vanishing β-function and their possible holographic duals.

Acknowledgements

I am deeply grateful to my supervisor, Luca Griguolo, and Gregory Korchemsky for their constant support throughout my Ph.D. and for introducing me to their unique and inspiring approach to scientific research. Their guidance has been invaluable in shaping my understanding of physics and in cultivating my curiosity and independence.

My sincere thanks also go to my collaborators Marco Billo', Luigi Guerrini, and Alberto Lerda for the fruitful collaborations, stimulating discussions, and precious advice for the future. I am equally grateful to my friend and more recent collaborator Bercel Boldis for his genuine friendship and for the endless brainstorming sessions we shared over the past year.

Although they were not direct collaborators, I owe special thanks to Alessio Miscioscia and Federico Ambrosino for the inspiring scientific conversations we had over the years and for the many memorable moments spent together.

I am also very grateful to Congkao Wen and Konstantin Zarembo for kindly reading this thesis.

I wish to thank my office colleagues, Leonardo Bossi, Giacomo Sansone, Dennis Linde, and Sophie Mueller for the many laughs, the support, and the intense working hours we shared. I am also thankful to the University of Parma for creating such a vibrant research environment, and to all the Ph.D. students I have met throughout these years.

I would like to express my deep gratitude to the Institut de Physique Théorique and to its members for their kind hospitality during my visits.

My deepest gratitude goes to my wife, my cycling, hiking, and life partner for her unwavering support, patience, and love throughout these years. Without her encouragement, I would never have had the strength and serenity to pursue what I love and to reach this final goal.

I am profoundly grateful to my family for their constant love and support. I especially thank my parents, my aunt, and my grandmothers for their encouragement and motivation, particularly during difficult moments. You have raised me with dedication, and I hope to make you proud with this achievement.

Special thanks go to Luigi, who has been an incredible source of advice and affection since my childhood, and to his children, Mario, Lilliana, and Ludovica, who I consider more than a second family and with whom I share a deep emotional bond.

Finally, I wish to express my heartfelt gratitude to all my closest friends, Edoardo, Paolo B., Paolo C., Davide G., Davide A., Marta, Chiara, Valeria, Carlo, Massimiliano, and Nicolò, for always being so close to me during these years. I am immensely proud and grateful to have all of you by my side at the end of this remarkable academic journey.

Dedicated to all my family

Contents

Chapter I

Preliminaries

Introduction

Quantum field theory (QFT) represents the fundamental language in which modern theoretical physics is formulated. Historically, it emerged from the attempt to reconcile the principles of quantum mechanics with those of special relativity within the study of elementary particle physics. While traditional quantum mechanics provides remarkable predictions for the dynamics of atomic and molecular systems, it fails to describe relativistic phenomena. Quantum field theory resolves this limitation by promoting particles to excitations of spacetime fields, thereby offering a unified framework for describing interactions and revealing that the true fundamental building blocks of nature are, in fact, the fields themselves rather than particles.

Within this framework, a fundamental class of models is represented by *gauge theories*, where interactions are determined by local symmetries. The Standard Model of particle physics, our best description of the electromagnetic, weak, and strong forces to date, is formulated entirely using this language. Among its components, Quantum Chromodynamics (QCD), the non-Abelian gauge theory of strong interactions, provides a striking example of the complexity of such models. At high energies, interactions are weak and can be consistently treated by perturbation theory, allowing precise predictions for particle processes. At low energies, however, the theory becomes strongly coupled and involves non-perturbative phenomena, such as confinement.

The theoretical understanding of the low-energy dynamics of non-Abelian gauge theories remains one of the most intricate open problems in modern physics, reflecting the structural richness and complexity of quantum field theory. Except for free models and a few integrable cases, solving a quantum field theory exactly is notoriously difficult. Nevertheless, several powerful methods have been developed to improve our understanding of this formalism.

Among these, symmetries play a central role: they restrict the possible form of interactions, give rise to conservation laws and selection rules, and, in the case of spontaneous symmetry breaking, predict the appearance of Goldstone modes. Closely related to symmetries are anomalies, which in the modern formulation are understood as obstructions to gauging a global symmetry [1, 2]. They provide deep insights into the internal consistency and global structure of a theory, especially along its renormalization group flow [3].

Other remarkable and powerful tools are provided by dualities and enhanced spacetime symmetries. More specifically, dualities allow us to reformulate strongly coupled theories in terms of weakly coupled ones, which can then be treated with standard perturbative techniques. Concrete realizations of this principle range from the Kramers–Wannier duality in statistical systems [4] to the celebrated AdS/CFT correspondence [5–8]. Conversely, enhanced spacetime symmetries allow us to gain insights into the quantum dynamics of fields by introducing additional constraints in the theory. An explicit realization of this method is provided by supersymmetry and conformal symmetry, which lie at the heart of this thesis.

Supersymmetry is an enhanced spacetime symmetry that establishes a connection between bosons and fermions, making their dynamics more constrained than in standard gauge theories. In certain cases, the rigid constraints imposed by supersymmetry lead to remarkable cancella-

tions of quantum corrections, stabilizing the calculation of specific observables and allowing them to be exactly computed in regimes that would otherwise be intractable in ordinary models. These features make supersymmetric setups an ideal playground for exploring strong-coupling dynamics and developing non-perturbative techniques, including supersymmetric localization [9, 10] and integrability [11].

Conversely, conformal symmetry extends spacetime invariance by including scale and special conformal transformations. It emerges in various areas of theoretical physics, from the description of critical phenomena in statistical systems to two-dimensional models, where the conformal algebra becomes infinite-dimensional [12]. In higher dimensions, the conformal group is finite but still imposes strong constraints that can be exploited to develop powerful non-perturbative techniques, such as the conformal bootstrap.

When conformal symmetry is combined with supersymmetry, the resulting theories exhibit superconformal invariance. The natural framework where such models arise is string theory, which provides an exceptionally powerful theoretical laboratory where the interactions of the Standard Model can be reconciled with gravity at the quantum level. In this context, one of the most remarkable and successful dualities in theoretical physics was discovered: the AdS/CFT correspondence. In its canonical formulation, it relates a four-dimensional superconformal gauge theory with maximal supersymmetry, namely $\mathcal{N} = 4$ super-Yang–Mills, to a Type IIB string propagating on $\mathrm{AdS}_5 \times S^5$, providing a concrete realization of the long-sought connection between gauge and gravitational dynamics.

Although supersymmetry does not appear to be realized in nature at experimentally accessible scales, four-dimensional supersymmetric gauge theories, especially $\mathcal{N} = 2$ and $\mathcal{N} = 4$ super-Yang–Mills, provide an effective framework to explore non-perturbative dynamics at the quantum level. Moreover, these idealized models can also shed light on more realistic scenarios, such as QCD. A notable example is the *empirical principle of maximal transcendentality* [13], which relates the term of highest transcendental weight for several perturbative quantities computed in $\mathcal{N} = 4$ SYM, such as the cusp and twist-two anomalous dimensions [13–18], to the corresponding counterparts in QCD.

While this principle is not universal, it highlights the effectiveness of supersymmetric gauge theories as theoretical laboratories to improve our understanding of quantum field theory. These considerations naturally motivate the study of models with a lower degree of supersymmetry, *i.e.* $\mathcal{N} = 2$ super-Yang–Mills theories. With their extended, yet not maximal, supersymmetry these models provide an interpolating framework between maximally supersymmetric $\mathcal{N} = 4$ theories and more physical scenarios, allowing the development of non-perturbative methods and exhibiting rich low-energy dynamics, such as confinement [19] and the Seiberg electric-magnetic dualities [20–22].

A remarkable feature of $\mathcal{N} = 2$ supersymmetric gauge theories is that they exhibit a rich and elegant mathematical structure, connected with different areas of research, including geometry, topology, and the study of random matrices. We will discuss explicit examples of such correspondences throughout this thesis, whose primary goal is to study the dynamics of various $\mathcal{N} = 2$ models, including conformal and non-conformal setups. More specifically, we focus on special classes of $\mathcal{N} = 2$ superconformal theories, known as quiver models, which arise from orbifold projections of the maximally supersymmetric $\mathcal{N} = 4$ configuration, and on $\mathcal{N} = 2$ theories with massless matter and non-vanishing β-function, where conformal symmetry is dynamically broken at the quantum level.

Outline

The content of this thesis builds upon the original analyses developed in the following works [23–28]:

- M. Billo', L. Griguolo, A. Lerda, and A. Testa, "*Correlators in non-conformal $\mathcal{N} = 2$ gauge theories from localization*", JHEP 08 (2025) 282, arXiv: 2505.03940.
- G. P. Korchemsky and A. Testa, *"Correlation functions in four-dimensional superconformal long circular quivers"*, JHEP 07 (2025) 223, arXiv: 2501.17223.
- L. Griguolo, L. Guerrini, and A. Testa, *"Into the wedge of $\mathcal{N} = 2$ superconformal gauge theories"*, JHEP 07 (2025) 125, arXiv: 2411.04043.
- M. Billo', L. Griguolo, and A. Testa, "*1/2 BPS Wilson loops in non-conformal $\mathcal{N} = 2$ gauge theories and localization: a three-loop analysis*", JHEP 02 (2025) 076, arXiv: 2410.14847.
- M. Billo', L. Griguolo, and A. Testa. "*Supersymmetric Localization and Nonconformal $\mathcal{N}$=2 Supersymmetric Yang-Mills Theories in the Perturbative Regime*", Phys. Rev. Lett. 134 (2024), arXiv: 2407.11222.
- M. Billo', L. Griguolo, and A. Testa. "*Remarks on BPS Wilson loops in non-conformal $\mathcal{N} = 2$ gauge theories and localization*", JHEP 01 (2024) 160, arXiv: 2311.17692.

This thesis is organised as follows. We begin in Chapter 1 by reviewing the essential features of supersymmetry and conformal symmetry in four dimensions. After recalling the structure of the supersymmetry algebra, we introduce $\mathcal{N} = 2$ and $\mathcal{N} = 4$ super-Yang–Mills theories and the corresponding irreducible representations of the supersymmetry algebras. We emphasise the role of supersymmetry in constraining these models by providing a general overview of their properties at the quantum level.

Chapter 2 is devoted to the technique of supersymmetric localization on the four-sphere S^4. We first review the general principles underlying localization and describe how path integrals in $\mathcal{N} = 2$ gauge theories reduce to finite-dimensional matrix models. We then discuss the specific form of these matrix models, highlighting both the similarities and key differences between conformal and asymptotically free setups, where the β-function is non-vanishing. This framework provides the starting point for the analyses presented in the following chapters.

In Chapter 3, we turn our attention to a class of $\mathcal{N} = 2$ superconformal gauge theories known as quiver models. After introducing their structure and main features, we focus on special correlation functions of chiral operators, which serve as powerful probes for the underlying dynamics. We show how these quantities can be computed via localization and how, in the planar limit, their matrix-model representation can be reformulated in terms of special Fredholm determinants, also known in this context as generalisedd Tracy–Widom distributions. These tools allow us to probe interesting phenomena and limits, such as deconstruction mechanisms at strong coupling, where quiver theories are expected to exhibit higher-dimensional dynamics.

Chapter 4 develops this analysis further by employing the determinant formalism to explicitly compute the correlation functions introduced in the previous chapter across the parameter space

of the theory. We present explicit results at both weak and strong coupling, discussing the emergence of an extra dimension and interpreting the resulting massive excitations within an effective field theory. In particular, we provide an analytic expression of the corresponding mass spectrum, thereby giving a concrete realization of the deconstruction mechanism in this class of models.

In Chapters 5 and 6, we move beyond conformal setups and investigate $\mathcal{N} = 2$ super-Yang–Mills theories with massless hypermultiplets and non-vanishing β-function. Within the matrix-model description, we analyse two classes of localizable observables, namely chiral correlators and half-BPS Wilson loops, with the aim of understanding whether, and under which conditions, the results obtained on the four-sphere can still be related to their flat-space counterparts despite the quantum breaking of conformal symmetry. We show that, within well-defined perturbative regimes, this correspondence persists, thus extending the range of applicability of localization techniques beyond the conventional conformal domain.

Finally, in Chapter 7, we summarise the main results of this work and outline several possible directions for future research. A number of technical details are collected in the appendices, where we summarise the conventions used throughout the thesis and present perturbative calculations.

Chapter 1

Supersymmetric gauge theories in four dimensions

In this chapter, we present a self-contained overview of four-dimensional super-Yang–Mills theories with extended supersymmetry algebras. The aim of the following sections is to outline the fundamental features of these models, which form the main building blocks of the analysis developed throughout this thesis. Specifically, Section 1.1 discusses the general structure of supersymmetry in four dimensions, briefly describing its algebraic structure and some foundational concepts that play a central role in this work. Section 1.2 reviews conformal symmetry and outlines the peculiar features of conformal field theories in four dimensions, while Section 1.3 introduces supersymmetric gauge theories, describing the irreducible representations of the corresponding supersymmetry algebras and the distinctive aspects of these models.

1.1 Supersymmetry in four dimensions

Supersymmetry is a novel spacetime symmetry that extends the conventional framework of quantum field theory by unifying bosons and fermions within a common algebraic structure [1]. It was originally introduced to evade the constraints of the Coleman-Mandula no-go theorem [32], which states that under certain assumptions, such as analyticity of the S-matrix, locality, and the presence of non-trivial scattering processes, the symmetry group of an interacting quantum field theory in any spacetime dimension greater than $d = 1 + 1$ necessarily factorizes as

$$\text{Poincaré} \times \text{Internal Symmetries} . \tag{1.1}$$

In four-dimensional Minkowski spacetime with metric $\eta_{\mu\nu}$[2], the Poincaré group encodes translations and Lorentz transformations. These are generated, respectively, by the four-momentum operator P_μ and by the antisymmetric tensor $M_{\mu\nu}$. Conversely, the internal symmetries are generated by a set of conserved charges, such as the isospin or baryon number, which are Lorentz scalars and collectively denoted by T. The complete symmetry algebra is then spanned by the

[1] For a detailed review, we refer the reader to [29–31].

[2] In this section we follow the notations and conventions of [33].

generators $P_\mu, M_{\mu\nu}, T$, which satisfy the following commutation relations

$$[P_\mu, P_\nu] = 0 \ , \tag{1.2a}$$
$$[M_{\mu\nu}, M_{\rho\sigma}] = i(\eta_{\mu\sigma} M_{\nu\rho} + \eta_{\nu\rho} M_{\mu\sigma} - \eta_{\mu\rho} M_{\nu\sigma} - \eta_{\nu\sigma} M_{\mu\rho}) \ , \tag{1.2b}$$
$$[M_{\mu\nu}, P_\rho] = i(\eta_{\rho\nu} P_\mu - \eta_{\rho\mu} P_\nu) \ . \tag{1.2c}$$
$$[T, P_\mu] = [T, M_{\mu\nu}] = 0 \ . \tag{1.2d}$$

As already anticipated, the factorized structure imposed by the Coleman-Mandula theorem (1.1) relies on several key assumptions. Some of these are deeply physical, such as locality and causality, while others can be relaxed, leading to interesting loopholes. Historically, two of these loopholes have proven particularly relevant.

The first concerns the existence of a mass gap. Since the theorem is formulated in terms of the S-matrix, it presupposes the presence of asymptotic states, which are well-defined only in massive theories. However, many important models in modern theoretical physics, including those describing critical phenomena in statistical systems, are massless. Such theories frequently exhibit *conformal invariance*, which extends the usual spacetime symmetries of the Poincaré group (1.2) in a non-trivial way.

The second loophole is supersymmetry, which bypasses the Coleman-Mandula theorem by introducing a fundamentally different type of spacetime symmetry. Algebraically, its underlying structure is not a standard Lie algebra, as in the Poincaré case (1.2), but a $\mathbb{Z}_2$-graded Lie algebra, in which the generators obey both commutation and anticommutation relations.

More concretely, in a four-dimensional Minkowski spacetime the supersymmetry algebra is generated by the Poincaré charges (1.2) together with a set of left- and right-handed Weyl spinors $\left(Q^I_\alpha, \bar{Q}^I_{\dot\alpha}\right)$, where $I = 1, \ldots, \mathcal{N}$ labels the number of independent supersymmetries (or supercharges), while $\alpha, \dot\alpha = 1, 2$ are spinor indices associated with the fundamental and complex-conjugate representation of the double covering group $SL(2, \mathbb{C})$ [3]. Explicitly, we have

$$\left[P_\mu, Q^I_\alpha\right] = 0 \ , \tag{1.3a}$$
$$\left[M_{\mu\nu}, Q^I_\alpha\right] = i\,(\sigma_{\mu\nu})_\alpha{}^\beta\, Q^I_\beta \ , \tag{1.3b}$$
$$\left[M_{\mu\nu}, \bar{Q}^{I,\dot\alpha}\right] = i\,(\bar\sigma_{\mu\nu})^{\dot\alpha}{}_{\dot\beta}\, \bar{Q}^{I,\dot\beta} \ , \tag{1.3c}$$
$$\left\{Q^I_\alpha, \bar{Q}^J_{\dot\alpha}\right\} = 2\sigma^\mu_{\alpha\dot\alpha} P_\mu \delta^{IJ} \ , \tag{1.3d}$$
$$\left\{Q^I_\alpha, Q^J_\beta\right\} = \epsilon_{\alpha\beta} Z^{IJ} \ , \quad Z^{IJ} = -Z^{JI} \ , \tag{1.3e}$$
$$\left[Q^I_\alpha, T_a\right] = (B_a)^I{}_J\, Q^J_\alpha \ . \tag{1.3f}$$

Quantum field theories equipped with supersymmetry display novel structural properties. Some of them can be inferred directly from the algebra (1.3).

First, equation (1.3a) guarantees that $P^2 = P_\mu P^\mu$ is a Casimir operator. As a result, irreducible representations of the supersymmetry algebra, also known in this context as supermultiplets, retain the standard particle-state interpretation of Poincaré representations. However, unlike ordinary multiplets, supermultiplets necessarily contain both bosons and fermions. This follows from the relations (1.3b) and (1.3c), which show that the supercharges have spin $\frac{1}{2}$. As a result, acting with them on a bosonic state yields a fermion, and vice versa. Moreover, all states within a given supermultiplet satisfy the identity

$$n_f = n_b \ , \tag{1.4}$$

[3] The spinor conventions of this section follow those presented in the second chapter of [33].

where n_f and n_b denote the number of fermionic and bosonic states, respectively. This equality is a direct consequence of the anticommutation relation (1.3d), which captures the fundamental idea that supercharges act as "square roots" of translations. At the level of quantum field theory, the balance (1.4) manifests itself through remarkable cancellations of divergences, making supersymmetric models considerably more tractable.

Furthermore, in theories with extended supersymmetry ($\mathcal{N} > 1$), the algebra may include additional antisymmetric central charges Z^{IJ} (1.3e), which are Lorentz scalars that commute with all other generators. Their precise form and physical interpretation are model-dependent.

Finally, relation (1.3f) clarifies the interplay between supersymmetry and internal symmetries. Unlike the ordinary Poincaré charges, which commute with the internal symmetries (1.2d), supercharges may carry a representation of the internal symmetry group, known in this context as the *R-symmetry* group. In four dimensions, the maximal R-symmetry group consistent with the spinor structure is $U(\mathcal{N})_R$

1.2 Conformal symmetry and correlation functions in CFTs

In the previous section, we introduced supersymmetry as a way to evade the constraints of the Coleman-Mandula theorem (1.1). Another possibility to extend the Poincaré group arises from including spacetime symmetries that preserve angles but not necessarily distances. These transformations appear naturally in massless theories and, together with translations, rotations, and boosts, form the conformal group.

The goal of this section is to introduce conformal symmetry in flat spacetime, focusing on the relevant aspects for the remainder of this work. For a more detailed review, we refer to [34–36].

For concreteness, we consider a d-dimensional Minkowski spacetime with metric $\eta_{\mu\nu} = \mathrm{diag}(-1, 1, \ldots, 1)$. A coordinate transformation $x^\mu \mapsto x'^\mu$ is conformal if its Jacobian satisfies [4]

$$\frac{\partial x^\alpha}{\partial x'^\mu} = \Omega(x)\Lambda^\alpha{}_\mu(x) \ , \quad \text{where} \quad \Lambda \in O(1, d-1) \ . \tag{1.5}$$

This condition ensures that the metric transforms by a local rescaling, *i.e.* $\eta'_{\mu\nu} = \Omega^2(x)\eta_{\mu\nu}$. Moreover, it is straightforward to observe that both Poincaré transformations and dilatations satisfy (1.5) with $\Omega(x) = 1$ and $\Omega(x) = \text{const}$, respectively.

To study the conformal algebra, we consider infinitesimal transformations

$$x^\mu = x'^\mu + \delta^\mu(x) + \mathcal{O}(\delta^2) \ . \tag{1.6}$$

By imposing (1.5), it is straightforward to derive the following conformal Killing equation

$$\partial_\mu \delta_\nu + \partial_\nu \delta_\mu = \frac{2}{d}(\partial_\alpha \delta^\alpha)\eta_{\mu\nu} \ . \tag{1.7}$$

In two dimensions, (1.7) admits infinitely many solutions [37], while for $d > 2$, we find that

$$\delta^\mu(x) = a^\mu + \omega^{\mu\nu}x_\nu + \alpha\eta^{\mu\nu}x_\nu + b^\mu x^2 - 2x^\mu(b \cdot x) \ . \tag{1.8}$$

In the previous expression, a^μ generate translations, $\omega^{\mu\nu}$ Lorentz transformations, α dilatations, and b^μ special conformal transformations. Denoting the generators of special conformal

[4] In Euclidean space, the conformal group is defined by the condition (1.5) with $\Lambda \in O(d)$.

transformations and dilatations by K^μ and D, respectively, we find that they satisfy [5]

$$\begin{aligned}
[K_\mu, P_\nu] &= 2i(\eta_{\mu\nu} D - M_{\mu\nu}) \ , \\
[K_\rho, M_{\mu\nu}] &= i(\eta_{\rho\mu} K_\nu - \eta_{\rho\nu} K_\mu) \ , \\
[D, P_\mu] &= i P_\mu \ , \\
[D, K_\mu] &= -i K_\mu \ , \\
[K_\mu, K_\nu] &= [D, M_{\mu\nu}] = [P_\mu, P_\nu] = 0 \ .
\end{aligned} \tag{1.10}$$

Combined with the Poincaré algebra (1.2), the commutation relations (1.10) generate the full conformal algebra in d dimensions, which possesses $(d+2)(d+1)/2$ generators and is locally isomorphic to the Lie algebra $so(1, d+1)$. The structure of (1.10) allows us to deduce some interesting features of conformal field theories (CFTs).

First, unlike ordinary quantum field theories, CFTs do not admit the usual interpretation in terms of particle states. This follows from the fact that P^2 is not an invariant Casimir of the conformal algebra, meaning that asymptotic states and an S-matrix description are no longer meaningful. Instead, all physical information is encoded in local correlation functions.

Moreover, the algebra (1.10) reveals that scale invariance, generated by the dilatation operator D, does not automatically imply conformal invariance. Indeed, the generators $M_{\mu\nu}, P_\mu, D$ form a closed subalgebra, and the full conformal group arises only if the theory satisfies additional consistency conditions [38, 39].

Finally, it is important to emphasise that classical conformal symmetry does not necessarily survive quantization. The prototypical example is provided by pure Yang–Mills theories. Classically, these models exhibit conformal invariance, while at the quantum level this symmetry is broken as a mass scale is generated. In general, a quantum field theory preserves conformal symmetry only if it lies at a renormalization-group fixed point, where both the β-function and the trace of the stress-energy tensor vanish [40, 41].

Correlation functions

We previously mentioned that in conformal field theories, physical observables are encoded in correlation functions. However, only correlators of *primary operators* are fundamental quantities. To clarify this aspect, we have to discuss the irreducible representations of the conformal algebra (1.10). These are completely specified by the representations of the subalgebra $\{K_\mu, M_{\mu\nu}, D\}$ which, when exponentiated, leaves the origin invariant.

To study the representations of such a subalgebra, we consider a generic local operator $\phi(x)$ inserted at the origin. Under Lorentz transformations and dilatations, we have

$$M_{\mu\nu}\phi(0) = S_{\mu\nu}\phi(0) \ , \tag{1.11a}$$

$$D\phi(0) = -i\Delta\phi(0) \ , \tag{1.11b}$$

[5] We obtained the conformal algebra (1.10) by representing the generators as differential operators acting on functions of spacetime

$$\begin{aligned}
P_\mu &= -i\partial_\mu \ , \\
M_{\mu\nu} &= i(x_\mu \partial_\nu - x_\nu \partial_\mu) \ , \\
D &= -i x^\mu \partial_\mu \ , \\
K_\mu &= -i(2x_\mu x^\nu \partial_\nu - x^2 \partial_\mu) \ .
\end{aligned} \tag{1.9}$$

where $S_{\mu\nu}$ is the spin matrix, describing the irreducible representation of the Lorentz group carried by ϕ, while Δ defines the *conformal dimension* of the operator, which controls its behaviour under dilatations $x \to \lambda x$, *i.e.*

$$\phi(x) \to \lambda^{-\Delta}\phi(\lambda x) \ .$$

It remains to specify the action of K^μ. According to (1.5), K^μ lowers the scaling dimension of a local operator. However, in unitary conformal field theories, the spectrum of scaling dimensions is bounded from below. This means that any (unitary) irreducible representation of the conformal algebra must contain a *lowest-weight* operator $\Phi(x)$ such that

$$K_\mu \Phi(0) = 0 \ . \tag{1.12}$$

Local fields satisfying this condition are called *primary operators* which, together with their quantum numbers $\{S_{\mu\nu}, \Delta\}$, entirely determine the unitary representations of the conformal algebra (1.10). The remaining elements of the representations are obtained by repeatedly acting on the primary with the momentum generator P_μ. This action generates an infinite tower of local fields with increasing scaling dimension known as *descendants*.

This construction clarifies why the only fundamental correlations in CFTs are those involving primary operators. Therefore, our final goal is to show how we can constrain the structure of these correlation functions by imposing conformal invariance. To begin with, we consider the one-point function of a primary operator $\Phi(x)$ with scaling dimension Δ. By requiring invariance under the Poincaré group and dilatations, it is straightforward to show that

$$\langle \Phi_\Delta(x) \rangle = 0 \ . \tag{1.13}$$

The first non-vanishing correlator of primary operators is the two-point function. This is constrained by translational and Lorentz invariance to depend on

$$x_{12} \equiv |x_1 - x_2| \ , \tag{1.14}$$

while dilatations and special conformal transformations impose the conservation of the scaling dimension. As a result, the two-point function of primary operators takes the following form

$$\langle \Phi_{\Delta_1}(x_1)\Phi_{\Delta_2}(x_2) \rangle = \frac{G^{(2)}_{\Delta_1}\delta_{\Delta_1,\Delta_2}}{x_{12}^{\Delta_1+\Delta_2}} \ , \tag{1.15}$$

where $G^{(2)}_{\Delta_1}$ is usually a function of the theory parameters, which can always be reabsorbed into a redefinition of the fields Φ but is not fixed by symmetry arguments.

Finally, we consider the three-point functions. Their kinematic structure is still fixed by conformal symmetry which leads to the following expression

$$\langle \Phi_1(x_1)\Phi_2(x_2)\Phi_3(x_3) \rangle = \frac{G^{(3)}_{\Delta_1,\Delta_2,\Delta_3}}{x_{12}^{\Delta_1+\Delta_2-\Delta_3} x_{23}^{\Delta_2+\Delta_3-\Delta_1} x_{13}^{\Delta_1+\Delta_3-\Delta_2}} \ , \tag{1.16}$$

where $G^{(3)}_{\Delta_1,\Delta_2,\Delta_3}$ is a theory-dependent factor which, in contrast to the two-point functions, cannot be eliminated by a field redefinition.

Nevertheless, we can remove the operator-normalization dependence of two- and three-point functions by considering the ratio

$$C_{\Delta_1,\Delta_2,\Delta_3} = \frac{G^{(3)}_{\Delta 1,\Delta_2,\Delta_3}}{\sqrt{\prod_{i=1}^3 G^{(2)}\Delta_i}} \ , \tag{1.17}$$

which defines the structure constants of the theory. These play a fundamental role in conformal field theories as they enter the Operator Product Expansion (OPE). This is a powerful method to constrain higher-point functions [42], which relies on the idea that the product of two operators inserted at nearby points can be expressed as a sum of local fields at a single point. Schematically, if we denote by $\Phi_{\Delta_1}(x)$ and $\Phi_{\Delta_2}(0)$ two scalar primaries, then their OPE is

$$\Phi_{\Delta_1}(x)\Phi_{\Delta_2}(0) = \sum_{\text{primaries } \Phi} C_{\Delta_1,\Delta_2,\Delta_\Phi}\, \mathcal{C}_\Phi(y,\partial_y),\Phi(y)\Big|_{y=0} \,. \tag{1.18}$$

In generic quantum field theories, the OPE usually leads to an asymptotic series, whereas in conformal field theories the expansion (1.18) is convergent and provides the starting point for powerful non-perturbative techniques, such as conformal bootstrap.

1.3 Super-Yang–Mills theories with extended supersymmetry

The supersymmetry algebra (1.3) is characterized by a certain number $\mathcal{N}$ of supercharges, which defines the degree of supersymmetry. In four dimensions, the minimal supersymmetric models are based on the $\mathcal{N} = 1$ super-Poincaré algebra. This can feature a $U(1)_R$ R-symmetry and its irreducible representations include the $\mathcal{N} = 1$ vector, chiral, and supergravity multiplet. The latter corresponds to *locally* supersymmetric theories, which involve dynamical gravity with particles of spin higher than one. In this thesis, however, we are interested in *globally* supersymmetric gauge models, which are commonly denoted as *super-Yang–Mills* (SYM) theories and do not comprise dynamical gravity.

The fundamental building blocks of $\mathcal{N} = 1$ super-Yang–Mills theories are the vector and chiral multiplets, whose (on-shell) field contents are

$$\mathcal{N} = 1 \text{ vector-multiplet} = (A_\mu, \lambda_\alpha) \,, \tag{1.19a}$$

$$\mathcal{N} = 1 \text{ chiral multiplet} = (\phi, \psi_\alpha) \,. \tag{1.19b}$$

In (1.19a), A_μ is the usual Yang–Mills field, while λ_α is a two-component Weyl fermion, also known as the *gaugino* in this context. Both fields transform in the adjoint representation of the gauge group and are necessarily massless. Conversely, the components of the chiral multiplet (1.19b) may acquire a mass and transform in some representation of the gauge group. In general, the $\mathcal{N} = 1$ supersymmetry and the associated $U(1)_R$ R-symmetry allow us to specify the gauge group, (properly complexified) couplings and mass terms, as well as superpotential interactions. As a consequence, it is possible to construct *chiral* $\mathcal{N} = 1$ gauge theories, where left- and right-handed components experience different forces in analogy to the Standard Model.

Increasing the number of supercharges, we obtain more constrained theories. In four dimensions, the only models with global extended supersymmetry are those with $\mathcal{N} = 2$ and $\mathcal{N} = 4$ algebra. Both play a central role in this thesis, and in the rest of this section we will discuss their underlying structure and properties.

$\mathcal{N} = 2$ super-Yang–Mills theories

$\mathcal{N} = 2$ super-Yang–Mills theories are built from two types of irreducible representations: the vector multiplet, which encodes radiation, and the hypermultiplets, which describe the matter sector. More specifically, the (on-shell) field content of an $\mathcal{N} = 2$ vector multiplet can be obtained by combining one $\mathcal{N} = 1$ vector multiplet with one *adjoint* $\mathcal{N} = 1$ chiral multiplet, *i.e.*

$$\mathcal{N} = 2 \text{ vector multiplet} = (A_\mu, \lambda_\alpha) \oplus (\phi, \psi_\alpha) \,. \tag{1.20}$$

All fields in (1.20) are massless and transform in the adjoint representation of the gauge group. Similarly, the (on-shell) spectrum of an $\mathcal{N}=2$ hypermultiplet in a representation $\mathcal{R}$ of the gauge group is described by two independent $\mathcal{N}=1$ chiral multiplets

$$\mathcal{N}=2 \text{ hypermultiplet } = (q,\eta_\alpha)\oplus(\tilde{q},\tilde{\eta}_\alpha)\ , \tag{1.21}$$

where q and $\tilde{q}$ are complex scalars, while η_α and $\tilde{\eta}_\alpha$ are their fermionic partners.

In $\mathcal{N}=2$ field theories, the R-symmetry group is realized as follows

$$U(2)_R \simeq SU(2)_R \times U(1)_R\ . \tag{1.22}$$

In particular, the two gauginos of the vector multiplet (1.20) and the two matter scalars $q,\tilde{q}$ form doublets of the non-Abelian factor $SU(2)_R$, while the remaining fields are singlets but can carry a $U(1)_R$ charge. Importantly, this R-symmetry forbids self-interactions among hypermultiplets, meaning that $\mathcal{N}=2$ theories admit only gauge–matter interactions. More generally, an $\mathcal{N}=2$ theory is completely specified by the gauge group and the representation $\mathcal{R}$ in which matter transforms. As a result, it is not possible to construct $\mathcal{N}=2$ chiral models.

The extended supersymmetry of $\mathcal{N}=2$ theories makes them powerful laboratories for controlling the dynamics of fields at the quantum level, while still permitting rich low-energy physics. In particular, the non-Abelian R-symmetry and non-renormalization theorems ensure that $\mathcal{N}=2$ theories are *one-loop exact* [43–48]. Perturbatively, this means the β-function takes this form

$$\beta(g_*)=\mu\frac{\mathrm{d}g_*}{\mathrm{d}\mu}=-\frac{\beta_0}{16\pi^2}g_*^3\ , \tag{1.23}$$

where g_* denotes the renormalized coupling evaluated at the *renormalization scale* μ, while β_0 is a group-theoretic coefficient depending on the gauge group and the matter representation. For a general Yang–Mills theory with simple gauge group G, real scalars and Weyl fermions, the general form of β_0 is given by [49]

$$\beta_0=\frac{11}{3}C_2(G)-\sum_{\text{scalars}}\frac{1}{6}i_{\mathcal{R}_s}-\sum_{\text{fermions}}\frac{2}{3}i_{\mathcal{R}_f}\ , \tag{1.24}$$

where $C_2(G)$ is the quadratic Casimir (B.2b) of the adjoint representation, while $i_{\mathcal{R}_s}$ and $i_{\mathcal{R}_f}$ denote the Dynkin indices (B.2a) of the scalar and fermion representations, respectively.

Throughout this thesis, we will consider theories with gauge group $SU(N)$ and massless hypermultiplets in a generic representation $\mathcal{R}$. In this case, replacing in (1.24) the matter content of the $\mathcal{N}=2$ supermultiplets (1.20,1.21) and using the group information summarised in Appendix (B.1), we find that β_0 takes the following form [23–26]

$$\beta_0=2N-2i_{\mathcal{R}}\ . \tag{1.25}$$

As a consequence, massless theories with matter content such that $i_{\mathcal{R}}=N$ are conformal at the quantum level. Conversely, when the β-function does not vanish classical conformal invariance is broken by quantum effects. In what follows, we will analyse *asymptotically free* theories, where $\beta_0>0$. These models are weakly coupled at high energies, while in the infrared interactions become strong. The dividing line is the *physical* [6] energy scale

$$\Lambda=\mu e^{-\frac{8\pi^2}{\beta_0 g_*^2}}\ , \tag{1.26}$$

[6] The mass scale Λ (1.26) is a physical quantity as it is invariant under the *renormalization group flow*.

generated by dimensional transmutation.

A remarkable feature of $\mathcal{N} = 2$ SYM theories is that, despite their strongly coupled nature in the infrared, their dynamics can still be captured exactly. This breakthrough was achieved in the seminal work of Seiberg and Witten [19,20], who derived the low-energy effective action of $\mathcal{N} = 2$ gauge theories by exploiting holomorphy, electric–magnetic duality and the special geometry of the moduli space of vacua. In particular, they showed that the physical information of the low-energy description is encoded in a family of Riemann surfaces, known as Seiberg–Witten curves. Subsequently, the Seiberg–Witten prepotential was derived through equivariant localization by Nekrasov [10,50], who provided a non-perturbative confirmation of the Seiberg–Witten solution.

$\mathcal{N} = 4$ super-Yang–Mills

Finally, we turn our attention to $\mathcal{N} = 4$ super-Yang–Mills, which represents the maximally supersymmetric gauge theory with *global* supersymmetry in four dimensions. These models consist of a single irreducible representation, *i.e.* the $\mathcal{N} = 4$ vector multiplet, constructed by combining one $\mathcal{N} = 2$ vector multiplet (1.20) with an adjoint $\mathcal{N} = 2$ hypermultiplet (1.21)

$$\mathcal{N} = 4 \text{ vector multiplet} = (A_\mu, \phi^m, \psi^I_\alpha) \ , \tag{1.27}$$

where we denoted with ϕ^m six real scalars ($m = 1, \dots, 6$) and with ψ^I four Weyl spinors ($I = 1, \dots, 4$). All fields are massless and transform in the adjoint representation of the gauge group. The R-symmetry group is $SU(4)$, with fermions and scalars transforming in the fundamental and in the rank two antisymmetric representation, respectively.

Unlike the $\mathcal{N} = 2$ case, where the interplay between supersymmetry and gauge dynamics still allows a non-trivial renormalization group flow and rich low-energy dynamics, $\mathcal{N} = 4$ super-Yang–Mills theories enjoy remarkable simplifications: they are perturbatively finite and conformal at the quantum level, as the β-function vanishes identically [51–54]. These unique properties make $\mathcal{N} = 4$ SYM an ideal laboratory for developing non-perturbative approaches, such as supersymmetric localization [55], integrability [11] and gauge-gravity dualities [5,6].

Chapter 2

Matrix models on S^4

In this chapter, we discuss the framework of supersymmetric localization in the context of $\mathcal{N} = 2$ super-Yang–Mills theories. More specifically, Section 2.1 introduces the general principles of this technique, which can be applied to $\mathcal{N} = 2$ theories on S^4 to reduce the computation of a broad class of protected observables to interacting matrix models. Two distinct cases will be considered: theories with a vanishing β-function, for which the resulting matrix model is well-defined and presented in Section 2.2, and theories with a non-vanishing β-function, where a suitable regularization procedure is required. The latter case will be discussed in Section 2.3.

2.1 Supersymmetric localization

Supersymmetric localization can be understood through the *deformation-invariance* approach [9, 55–57]. We consider a Lagrangian theory with a global fermionic symmetry $\mathcal{Q}$, such that $\mathcal{Q}^2$ generates a bosonic charge, and we deform the *Euclidean* path integral as follows

$$\mathcal{Z}(t) = \int \mathcal{D}[\Phi]\, \mathrm{e}^{-S[\Phi]-t\mathcal{Q}V[\Phi]} \,, \tag{2.1}$$

where t is a real parameter and V is a functional which preserves the asymptotic behaviour of the path integral and such that $\mathcal{Q}^2 V = 0$. Assuming that $\mathcal{D}[\Phi]$ is invariant under $\mathcal{Q}$, it is straightforward to show that $\mathcal{Z}(t)$ is independent of t

$$\frac{\mathrm{d}}{\mathrm{d}t}\mathcal{Z} = -\int \mathcal{D}[\Phi]\, \mathcal{Q}\Big(V[\Phi]\mathrm{e}^{-S[\Phi]-t\mathcal{Q}V[\Phi]}\Big) = 0 \,, \tag{2.2}$$

where the last equality follows from Stokes' theorem. Obviously, the same argument holds if we insert an arbitrary operator $\mathcal{O}[\Phi]$ which is annihilated by $\mathcal{Q}$.

If the bosonic part of $\mathcal{Q}V$ is semi-positive definite, we can safely take the limit $t \to \infty$, thereby constraining the original path integral to localize over the bosonic zeros Φ_0 of the *localizing* action $\mathcal{Q}V$. This is usually achieved by the following canonical choice of V

$$V = \sum_{\Psi \in \text{fermions}} \Big[(\mathcal{Q}\Psi)^\dagger \Psi + \Psi^\dagger (\mathcal{Q}\Psi)\Big] \,, \tag{2.3}$$

where the sum extends over all fermions of the theory. With this choice, the bosonic part of $\mathcal{Q}V$ is a sum of absolute squares of supersymmetry variations, and is therefore manifestly semi-positive definite.

Expanding the fields about the configurations Φ_0 as

$$\Phi = \Phi_0 + \frac{1}{\sqrt{t}}\Phi' \,, \tag{2.4}$$

we find that

$$S + t\mathcal{Q}V = S + \frac{1}{2}\frac{\delta^2(\mathcal{Q}V)}{\delta\Phi^2}\bigg|_{\Phi=\Phi_0}\Phi' + \mathcal{O}(t^{-1/2}) \ . \tag{2.5}$$

Substituting (2.5) into (2.1), the integral over Φ' becomes Gaussian and leads to

$$\mathcal{Z} = \int_{\mathcal{B}} \mathcal{D}[\Phi_0]\, \mathrm{e}^{-S[\Phi_0]} Z_{1-\text{loop}}[\Phi_0]\, Z_{\text{Inst}}[\Phi_0] \ . \tag{2.6}$$

In the previous expression, $\mathcal{B}$ denotes the space of configurations Φ_0, sometimes known as the *localization locus*, Z_{Inst} encodes possible instanton solutions of the equation $\mathcal{Q}V = 0$, while $Z_{1-\text{loop}}$ is schematically given by

$$Z_{1-\text{loop}} = \frac{\det(D_{\text{Fer}})}{\det(D_{\text{Bos}})} \ , \tag{2.7}$$

where D_{Bos} and D_{Fer} are the quadratic operators for bosonic and fermionic fluctuations, respectively. Computing (2.7) is generally challenging and requires an infrared (IR) regulator. For this reason, supersymmetric localization is usually applied on compact manifolds.

Finally, we observe that when the configurations Φ_0 are constant, the dimension of the locus $\mathcal{B}$ is finite, and the partition function (2.6) reduces to a matrix model. This is precisely what occurs when localizing $\mathcal{N} = 2$ super-Yang–Mills theories on the four-sphere S^4.

2.2 The general structure of the matrix model on S^4

We consider an $\mathcal{N} = 2$ theory with gauge group $SU(N)$ and massless hypermultiplets in an arbitrary representation $\mathcal{R}$. When these models are defined on a four-sphere of radius R, supersymmetric localization reduces the path integral describing the partition function and certain protected observables to an interacting matrix model [55]. This arises from the specific structure of the localizing action of these theories [1], which forces all fields to vanish except for the complex scalar ϕ of the $\mathcal{N} = 2$ vector multiplet and gauge field A_μ. The latter is restricted to an (anti-)instanton contribution, while the scalar ϕ reduces to a constant $N \times N$ traceless Hermitian matrix $a \in su(N)$. Upon integrating and summing over this set of critical configurations, the partition function takes the following form

$$\mathcal{Z} = \int Da\ Z(a, R, g) \ , \tag{2.8}$$

where g is the coupling constant of the theory.

In this work, we employ the so-called *full Lie algebra approach* [58], where the partition function (2.8) is obtained by integrating over the components a_b (with $b = 1, \dots, N^2 - 1$) of the matrix a with respect to a basis of fundamental $su(N)$ generators t_a [2], *i.e.* $a = a_b t^b$. In this parametrization, the integration measure is flat and takes the following form

$$Da = \prod_{b=1}^{N^2-1} \mathrm{d}a_b \ . \tag{2.9}$$

The integrand in (2.8) consists of three different factors

$$Z = Z_{\text{cl}}\, Z_{1-\text{loop}}\, |Z_{\text{Inst}}|^2 \ , \tag{2.10}$$

[1] See in particular Section 3 of [55] for more details.

[2] We summarise in Appendix B.1 our notations and conventions for the $SU(N)$ group.

where $Z_{1-\text{loop}}$ and Z_{inst} encode, respectively, the one-loop determinants and the instanton contributions, while Z_{cl} denotes the classical term of the partition function. The latter arises when we evaluate the action on S^4 at the localization locus and takes the following form [55]

$$\begin{aligned} Z_{\text{cl}}(a,g,R) &\equiv \mathrm{e}^{-S_{\text{cl}}(a,g,R)} \\ &= \mathrm{e}^{-\frac{8\pi^2 R^2}{g^2}\,\mathrm{tr}\,a^2} \end{aligned} \quad . \tag{2.11}$$

The dependence on the radius R highlights that Z_{cl} is determined by the coupling of the vector-multiplet scalar ϕ with the curvature of the four-sphere [3].

The presence of non-trivial one-loop determinants and instanton corrections is one of the distinctive features of the partition function (2.10). Nevertheless, the instanton contribution to (2.10) is irrelevant for our purposes, as we will primarily work either in perturbation theory or in the large-N limit, where $Z_{\text{Inst}} \to 1$. To see this, we expand Z_{Inst} over different instanton sectors [10]

$$Z_{\text{Inst}}(a,g,R) = \sum_{k=0}^{\infty} \mathrm{e}^{2\pi i \tau k}\, Z_k(a,R) \ , \tag{2.12}$$

where $\tau = \frac{4\pi i}{g^2} + \frac{\theta}{2\pi}$, while the functions Z_k arise from the integration over the multi-instanton (quasi)-moduli [10]. Independently of the presence of the θ-angle, which we will set to zero throughout this work, we observe that both in perturbation theory, where $g \to 0$, and in the large-N limit, where $N \to \infty$ and $\lambda = g^2 N$ remains fixed, the functions Z_k are exponentially suppressed except for $Z_{k=0} = 1$. Therefore, we can set $Z_{\text{Inst}} = 1$ in these regimes.

Let us finally turn our attention to the structure of the fluctuation determinants. According to the results derived in [55], the function $Z_{1-\text{loop}}$ receives contributions from the $\mathcal{N} = 2$ vector multiplet and from the matter sector of the theory. If the latter only involves massless hypermultiplets in an arbitrary representation $\mathcal{R}$ of the gauge group, then we find that [55]

$$Z_{1-\text{loop}} = \prod_{n=1}^{\infty} \left(\frac{\prod_{\alpha\in\Phi} R^2\,(\alpha\cdot a)^2 + n^2}{\prod_{\omega\in W(\mathcal{R})} R^2\,(\omega\cdot a)^2 + n^2} \right)^n \ , \tag{2.13}$$

where Φ denotes the root space of the Lie algebra $su(N)$, $W(\mathcal{R})$ is the weight space of the representation $\mathcal{R}$, while $\alpha\cdot a$ denotes the eigenvalue of the matrix a acting on the eigenspace of the adjoint representation corresponding to the root α. Similarly, $\omega\cdot a$ denotes the eigenvalue acting on the eigenspace of the representation $\mathcal{R}$ corresponding to weight ω.

An immediate consequence of (2.13) is that the matrix model of $\mathcal{N} = 4$ SYM does not receive one-loop contributions. Indeed, this theory is characterized by a single massless hypermultiplet in the adjoint representation, which compensates the contributions of the vector multiplet and leads to $Z_{1-\text{loop}} = 1$.

The infinite products in (2.13) are divergent and must be regularised. To do so, we replace them by [55]

$$H(z) = \prod_{n=1}^{\infty} \left(1 + \frac{z^2}{n^2}\right)^n \mathrm{e}^{-\frac{z^2}{n}} \ , \tag{2.14a}$$

$$\log H(z) = \sum_{p=1}^{\infty} (-1)^p \frac{\zeta_{2p+1}}{p+1} z^{2p+2} \ , \tag{2.14b}$$

[3] The coupling between the vector-multiplet scalar field ϕ and the curvature of the four-sphere, given by $\frac{2}{R^2}\phi^2$, is essential to preserve rigid supersymmetry [59].

where (2.14b) is valid for $z \to 0$. Going through the calculation, we find that

$$Z_{1-\text{loop}} = \mathrm{e}^{\beta_0\left(\sum_{n\geq 1}\frac{1}{n}\right)R^2\,\mathrm{tr}\,a^2}\,\frac{\prod_{\alpha\in\Phi}H(R\alpha\cdot a)}{\prod_{\omega\in W(\mathcal{R})}H(R\omega\cdot a)}\ , \tag{2.15}$$

where we recall that β_0 is the one-loop coefficient (1.25). Importantly, (2.15) is affected by a divergent [4] *a-dependent* factor that only disappears when $\beta_0 = 0$, that is when the β-function (1.25) vanishes. When $\beta_0 \neq 0$, the matrix model requires an additional regularization which we will discuss in the next section.

If we assume that the β-function vanishes but $\mathcal{R}$ is not the adjoint representation, we can express the contribution of the one-loop determinants (2.15) by a ratio of functions H (2.14)

$$Z_{1-\text{loop}} = \frac{\prod_{\alpha\in\Phi}H(\alpha\cdot a)}{\prod_{\omega\in W(\mathcal{R})}H(\omega\cdot a)}\ , \tag{2.16}$$

where we set $R = 1$ since the theory is conformal in flat space. Combining together (2.11) and (2.16), we obtain the matrix model of an $SU(N)$ $\mathcal{N} = 2$ gauge theory with massless hypermultiplets in an arbitrary representation $\mathcal{R}$ and vanishing β-function [5]

$$\begin{aligned}\mathcal{Z} &= \int Da\ \mathrm{e}^{-\mathrm{tr}\,a^2 - S_{\text{Int}}(a,g)}\\ &= \left\langle \mathrm{e}^{-S_{\text{Int}}}\right\rangle_0\ .\end{aligned} \tag{2.17}$$

In the previous expression, we neglected the instanton contribution and we used the subscript 0 to indicate that the expectation value is evaluated with the Gaussian measure

$$\begin{aligned}\int Da\ \mathrm{e}^{-\mathrm{tr}\,a^2} &= 1\ ,\\ \int Da\ \mathrm{e}^{-\mathrm{tr}\,a^2} a_b\ a_c &= \delta_{bc} \equiv \left\langle a_b a_c\right\rangle_0\ ,\end{aligned} \tag{2.18}$$

where we recall that the subscripts $b, c = 1, \ldots, N^2 - 1$ denote the components of the $su(N)$ matrix a.

The interaction potential S_{Int} of the matrix model (2.17) encodes the contribution of the fluctuation determinants and takes the following form

$$\begin{aligned}S_{\text{Int}}(a,g) &= -\log Z_{1-\text{loop}}(a,g)\\ &= \left(\mathrm{Tr}_{\mathcal{R}} - \mathrm{Tr}_{\text{Adj}}\right)\log H\left(\sqrt{\frac{g^2}{8\pi^2}}a\right)\\ &= \mathrm{Tr}'_{\mathcal{R}}\log H\left(\sqrt{\frac{g^2}{8\pi^2}}a\right)\ ,\end{aligned} \tag{2.19}$$

where we introduced the primed trace $\mathrm{Tr}'_{\mathcal{R}}$ [60]. At weak coupling, we can use (2.14b) to expand the interaction action (2.19) in powers of g

$$S_{\text{Int}}(a,g) = -\sum_{m=2}^{\infty}\left(-\frac{g^2}{8\pi^2}\right)^m\frac{\zeta_{2m-1}}{m}\,\mathrm{Tr}'_{\mathcal{R}}\,a^{2m}\ . \tag{2.20}$$

[4] The divergence arises from the pole of the Riemann function $\zeta_z = \sum_{n\geq 1}\frac{1}{m^z}$ in $z = 1$.

[5] To derive (2.17), we rescaled the integration variable as $a \to \frac{g}{2\sqrt{2}\pi}a$ to obtain a unit Gaussian term and we omitted the Jacobian of the transformation since it disappears in any properly normalized observable.

For an arbitrary representation $\mathcal{R}$, the primed trace $\mathrm{Tr}'_{\mathcal{R}}$ in (2.20) is non-vanishing and precisely describes the matter sector of the so-called *difference theory* [60, 61]. This arises when we subtract the field content of $\mathcal{N} = 4$ SYM from that of $\mathcal{N} = 2$ theories with hypermultiplets in the representation $\mathcal{R}$. This means that in perturbative field theory, the matrix model suggests that the relevant interaction contributions can be constructed by considering diagrams with matter lines in the representation $\mathcal{R}$ to which we subtract identical corrections with $\mathcal{R} = \mathrm{Adj}$.

In $\mathcal{N} = 2$ superconformal theories, the matrix model predictions have been tested at high orders in perturbation theory for various observables [60–64], confirming the effectiveness of the interaction potential in organizing Feynman diagrams. These results further support the natural expectation that, in conformal setups, the localization predictions on S^4 can be extended to the flat space and exploited to probe the dynamics of the underlying theory. This approach gives access to interesting regimes, such as the strong coupling dynamics in the large-N limit, where certain models are expected to admit dual holographic descriptions [58, 65–70].

The success of the matrix model in superconformal theories naturally raises the question of whether it can also be employed to probe non-conformal models in flat space. A natural first step in this direction consists of considering $\mathcal{N} = 2$ theories with massless hypermultiplets in an arbitrary representation $\mathcal{R}$ and non-vanishing β-function, where classical conformal symmetry is broken at the quantum level. These models bring us closer to more realistic scenarios, such as QCD, where the coupling constant runs and the low-energy dynamics involves non-perturbative effects that cannot be described within the framework of perturbation theory. However, due to a non-vanishing β-function, it is no longer obvious whether the localization predictions on S^4 extend to $\mathbb{R}^4$. We consider this problem in Chapters 5 and 6, where we show that, within a specific regime of validity, the matrix model on S^4 still captures perturbation theory in flat space at high orders. Therefore, our next goal is to introduce a regularization procedure to properly define the matrix model for theories with $\beta_0 \neq 0$.

2.3 The matrix model of $\mathcal{N} = 2$ theories with non-vanishing β-function

Let us consider an $SU(N)$ $\mathcal{N} = 2$ theory with massless hypermultiplets in a representation $\mathcal{R}$ such that the associated β-function is non-vanishing. Due to the lack of UV finiteness, the matrix model generated by supersymmetric localization on S^4 is ill-defined (2.15).

To avoid this issue, we introduce additional hypermultiplets of mass M in a representation $\widetilde{\mathcal{R}}$, such that the total matter content transforms in the direct sum

$$\widehat{\mathcal{R}} = \mathcal{R} \oplus \widetilde{\mathcal{R}} \,. \tag{2.21}$$

The key idea is to choose $\widetilde{\mathcal{R}}$ such that the corresponding β-function vanishes, *i.e.* $i_{\widehat{\mathcal{R}}} = N$. This set of massless and massive hypermultiplets defines the matter content of a new UV-finite model, denoted as the *regulating theory*, which triggers a flow from a superconformal configuration in the ultraviolet to the original asymptotically free theory in the infrared. Indeed, at energy scales much higher than M, the mass terms are negligible and the theory is effectively superconformal. In contrast, at energies much lower than M, the massive hypermultiplets decouple and can be integrated out, leaving a theory with only the original massless hypermultiplets in the representation $\mathcal{R}$. Since the regulating theory has a vanishing β-function, the corresponding matrix model on S^4 is well-defined. This strategy provides a controlled framework to regularise the matrix models of $\mathcal{N} = 2$ theories with non-vanishing β-function [23, 55].

Let us therefore consider an $SU(N)$ $\mathcal{N} = 2$ theory on S^4 with matter representation $\widehat{\mathcal{R}}$ (2.21). We denote with M the mass of the hypermultiplets in the representation $\widetilde{\mathcal{R}}$ and with g_*

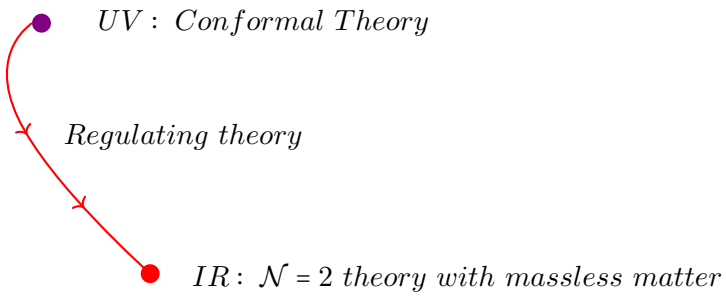

Figure 2.1: Flow triggered by a partial massive deformation of a superconformal $\mathcal{N}=2$ theory. At high energies, the deformation is irrelevant, and the theory flows to a conformal point. At low energies, the massive sector decouples, leaving a non-conformal theory with massless matter. This picture is inspired by the one employed in [71].

the coupling constant. The matrix model generated by supersymmetric localization takes the following form

$$\mathcal{Z}(M) = \int Da\ \mathrm{e}^{-\frac{8\pi^2 R^2}{g_*^2}\operatorname{tr} a^2} Z^*_{1-\text{loop}}(M)\,|Z^*_{\text{Inst}}(M)|^2\ . \tag{2.22}$$

According to [55], the function $Z^*_{1-\text{loop}}(M)$ is given by

$$Z^*_{1-\text{loop}}(M) = \prod_{n=1}^{\infty} \frac{Z_{1-\text{loop}}}{\left(\prod_{\omega\in W(\widetilde{\mathcal{R}})}\left(R^2\left(\omega\cdot a+M\right)^2+n^2\right)\left(R^2\left(\omega\cdot a-M\right)^2+n^2\right)\right)^{\frac{n}{2}}}\ , \tag{2.23}$$

where $Z_{1-\text{loop}}$ is defined in (2.15) and encodes the contribution of the massless hypermultiplets in the representation $\mathcal{R}$ and the $\mathcal{N}=2$ vector multiplet. By expressing the infinite products in terms of the H-function (2.14), the final result reads

$$Z^*_{1-\text{loop}}(M) \propto \frac{\prod_{\alpha\in\Phi} H(R\alpha\cdot a)}{\prod_{\omega\in W(\mathcal{R})} H(R\omega\cdot a)}\left(\prod_{\omega\in W(\widetilde{\mathcal{R}})} H\left(R\left(\omega\cdot a+M\right)\right)H\left(R\left(\omega\cdot a-M\right)\right)\right)^{-\frac{1}{2}}\ , \tag{2.24}$$

where the overall proportionality constant depends on M and is still divergent but, in contrast to (2.15), is *independent* of a. Consequently, any properly normalized observable is unaffected by this divergent term, and we are free to redefine the partition function by omitting it.

To derive the matrix model for $\mathcal{N}=2$ theories with massless hypermultiplets, we decouple the massive degrees of freedom by taking the low-energy limit. On the four-sphere S^4, this corresponds to $MR\to\infty$. Going through the calculation, we find that

$$\begin{aligned}\mathrm{e}^{-\frac{8\pi^2R^2}{g_*^2}\operatorname{tr}a^2} Z^*_{1-\text{loop}}(M) &= \mathrm{e}^{-\frac{8\pi^2R^2}{g_*^2}\operatorname{tr}a^2 - S^*_{\text{Int}}(M)}\\ &= \mathrm{e}^{-\frac{8\pi^2R^2}{g_*^2}\operatorname{tr}a^2 + (N-i_{\mathcal{R}})R^2\log(RM)^2\operatorname{tr}a^2 - S_{\text{Int}}+\ldots}\\ &= \mathrm{e}^{-\frac{8\pi^2}{g^2}\operatorname{tr}a^2 - S_{\text{Int}}}\ .\end{aligned} \tag{2.25}$$

In the previous expression, the logarithmically enhanced term in the second line arises from the large argument expansion of the H-function [6] (2.14), S_{Int} is the interaction potential (2.19) and

[6] The asymptotic expansion of the H-function (2.14) for large values of the argument is

$$\log H(z) = -\frac{1}{2}z^2\log z + \frac{z^2}{2}\left(1-2\gamma_E\right) + \mathcal{O}(\log z^2)\ , \tag{2.26}$$

where γ_E is the Euler constant.

we introduced

$$\frac{1}{g^2} = \frac{1}{g_*^2} - \frac{\beta_0}{16\pi^2}\log(RM)^2 \ , \tag{2.27}$$

where the colour factor β_0 is given by (1.25).

From the field theory perspective, g is known as the *running coupling constant* evaluated at the scale $1/R$. Its dependence on R is determined by one-loop exact β-function

$$\frac{1}{M}\frac{\partial g}{\partial R} = \beta(g) = -\frac{\beta_0}{16\pi^2}g^3 \ . \tag{2.28}$$

Integrating the previous expression from the reference value g_* at the scale M to g at the scale $1/R$, we reproduce (2.27). As a result, in the asymptotically free theory, g_* is no longer a constant but rather is interpreted as the *renormalized coupling* evaluated at the scale M.

The evolution equation (2.28) can be used to construct the usual strong coupling scale Λ (1.26) which separates the non-perturbative and perturbative regimes. The latter correspond to the range

$$\Lambda \ll \frac{1}{R} \ll M \ , \tag{2.29}$$

where $g \to 0$ and we can suppress the instanton contributions $Z^*_{\text{Inst}}(M)$ in (2.22). To see this, we expand again $Z^*_{\text{Inst}}(M)$ over different instanton sectors and we find that

$$\begin{aligned} Z^*_{\text{Inst}}(M) &= \sum_{k=0}^{\infty} \mathrm{e}^{-\frac{8\pi^2}{g_*^2}k} Z_k(a,R,M) \\ &= \sum_{k=0}^{\infty} \left(\frac{\Lambda}{M}\right)^{\beta_0 k} Z_k(a,R,M) \end{aligned} \tag{2.30}$$

where in the second line the exponential factor is replaced by the strong coupling scale Λ (1.26) due to dimensional transmutation. As a result, in the perturbative regime (2.29), all the contributions with $k > 0$ are suppressed, while $Z_{k=0} = 1$ and we can set $Z^*_{\text{Inst}}(M) = 1$.

Combining everything together, the *perturbative* matrix model for an $SU(N)$ asymptotically-free $\mathcal{N} = 2$ theory with massless hypermultiplets in an arbitrary representation $\mathcal{R}$ reads [23, 60]

$$\begin{aligned} \mathcal{Z}(g) &= \int Da\ \mathrm{e}^{-\operatorname{tr} a^2 - S_{\text{Int}}(a,g)} \\ &= \left\langle \mathrm{e}^{-S_{\text{Int}}} \right\rangle_0 \ , \end{aligned} \tag{2.31}$$

where we recall that the interaction action is given by (2.20).

It is interesting to observe that, in the perturbative regime (2.29), the structure of the matrix model (2.31) coincides with that of superconformal $\mathcal{N} = 2$ theories (2.17). The key difference between the conformal and non-conformal scenario is that in the latter case g is no longer a constant but rather, it evolves with the scale $1/R$ according to (2.27). Nevertheless, the similarity between the two matrix models suggests a partial restoration of conformal symmetry in the perturbative regime (2.29) and therefore a possible connection with the results in flat space. In Chapter 6, we will demonstrate this explicitly by computing two classes of observables in perturbation theory: the expectation value of supersymmetric Wilson loops and correlators of extremal operators.

Part II

Solving $\mathcal{N} = 2$ quiver theories by Tracy–Widom distributions

Chapter 3

$\mathcal{N} = 2$ quiver theories

Info: *Part of the content and figures of this chapter have been published together with G.P. Korchemsky in* [28].

3.1 Motivations

In this chapter, we begin the analysis of special superconformal $\mathcal{N} = 2$ theories known as circular quivers. These setups arise from an orbifold projection of $\mathcal{N} = 4$ SYM and provide a rich framework to study various non-perturbative aspects of $\mathcal{N} = 2$ models [65, 66, 72–82], through gauge-gravity dualities [6], integrability [11] and localization techniques [9], but also to explore ideas that remain inaccessible in realistic theories, such as deconstruction effects [83, 84].

The field content of the $\mathcal{N} = 2$ quiver theories is conveniently described by the diagram depicted in Fig. 3.1, where each node represents an $SU(N)$ vector multiplet with coupling constant g_I (with $I = 1, \dots L$), while lines connecting neighbouring nodes denote massless hypermultiplets in the bi-fundamental representation of $SU(N) \times SU(N)$. As a result, each coupling constant g_I receives contributions from $2N$ fundamental flavours and the corresponding β-function (1.23) vanishes, implying that classical conformal symmetry is preserved at the quantum level.

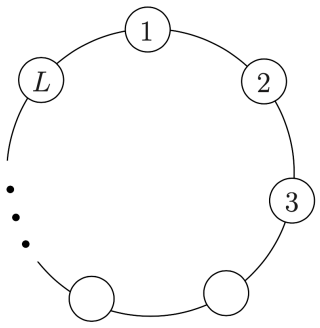

Figure 3.1: Diagrammatic representation of the circular quiver theory. Each node represents a $SU(N)$ vector multiplet, while lines connecting neighbouring nodes represent hypermultiplets in the bi-fundamental representation of $SU(N) \times SU(N)$.

The $\mathcal{N} = 2$ quiver theories are closely related to $\mathcal{N} = 4$ SYM and this connection becomes

more evident when all the L gauge couplings are equal $g_1 = \cdots = g_L = g_{\text{Y.M.}}$. In this case, the resulting model, denoted by Q_L, exhibits an additional symmetry under the cyclic shift of the nodes $I \to I + 1$, which drastically simplifies its properties. Indeed, at the leading order in the large-N limit, certain observables, such as the free energy on a four-sphere and the circular half-BPS Wilson loop, coincide with their $\mathcal{N} = 4$ counterparts for arbitrary 't Hooft coupling $\lambda = g^2_{\text{Y.M.}} N$ [69, 77, 78, 81]. Nevertheless, the two theories are not *planar* equivalent, as specific classes of protected correlation functions differ between the two models. These observables play a fundamental role in our analysis and provide an effective tool to probe the relationship among theories that exhibit different degrees of supersymmetry [65, 66, 80, 85, 86].

For our purposes, the quiver Q_L theories are particularly interesting because they are expected to exhibit novel properties in the limit $L \to \infty$ [70, 87–93]. In this regime, the nodes of the quiver diagram in Fig. 3.1 become continuously distributed along a circle, suggesting the emergence of an additional dimension. This mechanism, known as deconstruction, was originally proposed in conventional four-dimensional gauge theories [83, 84] defined on quiver diagrams analogous to that shown in Fig. 3.1. In the limit $L \to \infty$, such models remain four-dimensional at high energies, while their low-energy effective action describes a higher-dimensional gauge theory with a discretized extra dimension. The transition scale between the regimes is determined by the vacuum expectation value (v.e.v) of the link fields.

The same mechanism was later extended to $\mathcal{N} = 2$ superconformal quiver theories [94]. In this case, the fifth dimension emerges on the Higgs branch, where all chiral multiplets acquire the same vacuum expectation value and conformal symmetry is spontaneously broken. The resulting low-energy effective action describes a five-dimensional Lorentz-invariant supersymmetric gauge theory, in which the effective lattice spacing along the fifth dimension is inversely proportional to the 't Hooft coupling and to the chiral multiplet v.e.v [95–97]. In these deconstruction scenarios, the emergent higher-dimensional theories are typically strongly coupled, precluding explicit computations of observables.

The situation changes drastically in the case of $\mathcal{N} = 2$ superconformal Q_L theories, where we insist on working at the origin of the moduli space. As a result, conformal invariance is not broken and holds for an arbitrary number of nodes L, forbidding the appearance of a dimensionful lattice spacing. This indicates that if the theory exhibits higher-dimensional dynamics, its properties are expected to be different from the examples previously described. Nevertheless, the main advantage of working in these setups is that the limit $L \to \infty$ can be effectively studied by supersymmetric localization on the four-sphere, which provides complete control over both the weak and strong coupling regimes.

The remainder of this chapter is structured into four sections, which together lay the foundations for our analysis of $\mathcal{N} = 2$ quiver theories. More specifically, Section 3.2 introduces a special class of correlation functions that encodes the parameter space of the theory. These observables play the role of probes for studying the dynamics of the model and can be evaluated by supersymmetric localization on S^4. The details of the calculations are reported in Section 3.3, while in Section 3.4, we show that the planar limit of these observables can be expressed in terms of special Fredholm determinants that are closely related to the celebrated Tracy–Widom distributions. Finally, Section 3.5 describes the parameter space of these observables and the associated quiver theories, highlighting the different regimes we are interested in exploring.

3.2 Twisted correlators

We consider correlation functions of local gauge-invariant operators [65, 66]

$$O_n^I(x) = \operatorname{tr}\phi_I^n(x)\,,$$
$$\overline{O}_n^I(x) = \operatorname{tr}\bar{\phi}_I^n(x)\,, \tag{3.1}$$

where $\phi_I(x)$ and its complex conjugate $\bar{\phi}_I(x)$ are scalars fields of the I-th vector multiplet taking values in the $su(N)$ Lie algebra. These operators are conformal primaries of dimension $\Delta = n$ and annihilate supersymmetry charges (1.3) of fixed chirality, *i.e.*

$$\left[\bar{Q}, O_n^I(x)\right] = 0\ , \quad \left[Q, \bar{O}_n^I(x)\right] = 0\ . \tag{3.2}$$

As a result, $O_n^I(x)$ and its complex conjugate are half-BPS and possess a fixed chirality. Moreover, one can show that the constraint (3.2) relates the $U(1)_R$-charge r of the R-symmetry group $SU(2)_R \times U(1)_R$ to the conformal dimension Δ through the relation $\Delta = r$.

As we previously observed, the Q_L quiver theory is invariant under the cyclic shift $I \to I+1$ of the diagram nodes. This suggests to expand the operators (3.1) over Fourier modes of definite *quasimomentum* $p_\alpha = \frac{2\pi\alpha}{L}$ by the relation

$$T_{\alpha,n}(x) = \frac{1}{\sqrt{L}} \sum_{I=0}^{L-1} \mathrm{e}^{-ip_\alpha I} O_n^I(x)\,, \tag{3.3}$$

where $\alpha = 0, \dots, L-1$. The operators $T_{\alpha,n}$ are conformal primaries with scaling dimension $\Delta_\alpha = n$ and transform non-trivially under the $\mathbb{Z}_L$ group. Indeed, shifting $\phi_I \to \phi_{I+1}$, we find that

$$T_{\alpha,n}(x) \to \mathrm{e}^{\frac{2\pi i\alpha}{L}} T_{\alpha,n}(x)\,. \tag{3.4}$$

Depending on the corresponding value of the quasimomentum $p_\alpha = \frac{2\pi\alpha}{L}$, it is convenient to distinguish between *twisted* ($p_\alpha \neq 0$) and *untwisted* ($p_\alpha = 0$) conformal primary operators. The latter transform trivially under the action of the group $\mathbb{Z}_L$ and their correlation functions exhibit the same properties of the half-BPS single-trace operators in $\mathcal{N}=4$ SYM [65, 66].

Conformal symmetry dictates the structure of the two- and three-point functions of primary operators (see (1.15) and (1.16)). As a result, we can use these constraints in addition to the invariance under the $\mathbb{Z}_L$ group to construct the correlators of twisted operators (3.5), *i.e.* [1]

$$\langle T_{\alpha_1,n_1}(x_1) T^\dagger_{\alpha_2,n_2}(x_2)\rangle = G^{(2)}_{\alpha_1,n_1} \frac{\delta_{n_1,n_2}\delta(p_{\alpha_1} - p_{\alpha_2})}{|x_1 - x_2|^{2n_1}}\,, \tag{3.5a}$$

$$\langle T_{\alpha_1,n_1}(x_1) T_{\alpha_2,n_2}(x_2) T^\dagger_{\alpha_3,n_3}(x_3)\rangle = G^{(3)}_{\alpha_i,n_i} \frac{\delta_{n_1+n_2,n_3}\delta(p_{\alpha_1} + p_{\alpha_2} - p_{\alpha_3})}{|x_1 - x_3|^{2n_1}|x_2 - x_3|^{2n_2}}\ . \tag{3.5b}$$

In the previous expression, the normalization factors $G^{(2)}_{\alpha,n}$ and $G^{(3)}_{\alpha_i,n_i}$ depend on the quantum numbers n_i and p_α, the number of nodes L and the coupling constant $g_{\text{Y.M.}}$. Moreover, they carry an intrinsic dependence on the normalization of the operators which, however, can be removed by considering the structure constants (1.17), *i.e.*

$$C_{\alpha_i,n_i} = \frac{G^{(3)}_{\alpha_i,n_i}}{\sqrt{G^{(2)}_{\alpha_1,n_1} G^{(2)}_{\alpha_2,n_2} G^{(2)}_{\alpha_3,n_3}}}\ . \tag{3.6}$$

[1] The delta-functions in (3.5) fix the conservation of the quasimomentum p_α modulo 2π and arise from the requirement that the correlation functions are invariant under the action of the group $\mathbb{Z}_L$.

Although the correlation functions (3.5) are an extremely natural family of observables in quiver theories, their dual counterparts, described by the correlators of chiral operators (3.1), play an equally important role in our analysis. For this reason, we conclude this section by presenting their explicit form. In particular, applying the discrete Fourier transform (3.3) to (3.5), we find that

$$\langle O^I_n(x_1)\overline{O}^J_m(x_2)\rangle = G^{(2)}_{IJ}\frac{\delta_{nm}}{|x_1-x_2|^{2n}}\,, \tag{3.7a}$$

$$\langle O^I_{n_1}(x_1)O^J_{n_2}(x_2)\overline{O}^K_{n_3}(x_3)\rangle = G^{(3)}_{IJK}\frac{\delta_{n_1+n_2,n_3}}{|x_1-x_3|^{2n_1}|x_2-x_3|^{2n_2}}\,. \tag{3.7b}$$

Obviously, the normalization factors $G^{(2)}_{IJ}$ and $G^{(3)}_{IJK}$ are related to $G^{(2)}_{\alpha,n}$ and $G^{(3)}_{\alpha_i,n_i}$ by (3.5) and carry the dependence on the diagram sites, the number of nodes L and the gauge coupling constant $g_{\rm YM}$.

In the following sections, we will show how the matrix model generated by supersymmetric localization on S^4 allows us to naturally calculate the structure constants (3.6) and the normalization factors $G^{(2)}_{\alpha,n}$ and $G^{(3)}_{\alpha_i,n_i}$ (3.5) in the large-N limit.

3.3 The matrix model of the quiver theories in the large-N limit

In this section, we introduce the matrix model describing the Q_L quiver theory on S^4. We work in the large-N limit, where $N\to\infty$ and $\lambda = g^2_{\rm Y.M.}N$ remains fixed. Within this regime, we apply the formalism developed in [69, 70] to compute the correlation functions (3.5). We also develop a new technique to handle the normal-ordering procedure of single-trace operators as $N\to\infty$. This method allows us to reproduce the planar predictions for the structure constants (3.6) obtained in [66, 67, 82] and provides a systematic framework to include subleading $1/N$ corrections.

Using (2.17), we deduce that the partition function of the Q_L theory on S^4 is given by

$$\begin{aligned}\mathcal{Z}_{\mathsf{Q}_L} &= \int DA\exp\left(-\sum_{I=1}^{L}\left(\operatorname{tr}a_I^2 + S_{\rm Int}\left(a_I,a_{I+1}\right)\right)\right)\\ &= \left\langle\prod_{I=1}^{L}\mathrm{e}^{-S_{\rm Int}(a_I,a_{I+1})}\right\rangle_0\,,\end{aligned} \tag{3.8}$$

where the subscript 0 emphasises that the expectation value is evaluated with a Gaussian measure. Moreover, the matrices a_I are subjected to the boundary condition $a_{I+L}=a_I$, while the integration measure is given by $DA=\prod_I Da_I$ and satisfies the normalization condition (2.18).

In the large-N limit, the interaction potential $S_{\rm Int}(a_I,a_{I+1})$ takes the following form [70]

$$S_{\rm Int} = -\frac{1}{8}\sum_{i,j=2}^{\infty}C_{ij}\left(\lambda\right)\left(\mathcal{O}_i(a_I)-\mathcal{O}_i(a_{I+1})\right)\left(\mathcal{O}_j(a_I)-\mathcal{O}_j(a_{I+1})\right)\,, \tag{3.9}$$

where $\mathcal{O}_i(a_I)$ denotes the normalized single-trace operator

$$\mathcal{O}_i(a) = \operatorname{tr}\left(\frac{a}{\sqrt{N}}\right)^i\,. \tag{3.10}$$

The expansion coefficients in (3.9) are encoded in a semi-infinite matrix C_{ij} that depends on the 't Hooft coupling λ and is non-vanishing only for indices i and j with the same parity.

Introducing the notation $C_{2i,2j} \equiv C^{+}_{ij}$ and $C_{2i+1,2j+1} \equiv C^{-}_{ij}$, we find [70]

$$C^{-}_{ij}(\lambda) = 8\Big(\frac{\lambda}{8\pi^2}\Big)^{i+j+1}(-1)^{i-j+1}\zeta_{(2(i+j)+1)}\frac{\Gamma(2(i+j)+2)}{\Gamma(2i+2)\Gamma(2j+2)}\,, \tag{3.11a}$$

$$C^{+}_{ij}(\lambda) = 8\Big(\frac{\lambda}{8\pi^2}\Big)^{i+j}(-1)^{i-j+1}\zeta_{(2(i+j)-1)}\frac{\Gamma(2(i+j))}{\Gamma(2i+1)\Gamma(2j+1)}\,. \tag{3.11b}$$

Exploiting the invariance under the cyclic shift $a_I \to a_{I+1}$, we can simplify the interaction action by expanding it over Fourier modes of definite quasimomentum $p_\alpha = \frac{2\pi\alpha}{L}$, *i.e.*

$$\mathcal{O}_i(a_I) = \frac{1}{\sqrt{L}}\sum_{\alpha=0}^{L-1} e^{ip_\alpha I}\widetilde{\mathcal{O}}_{\alpha,i}\ , \tag{3.12a}$$

$$\widetilde{\mathcal{O}}_{\alpha,i} = \frac{1}{\sqrt{L}}\sum_{I=1}^{L} e^{-ip_\alpha I}\mathcal{O}_i(a_I)\ . \tag{3.12b}$$

The reality constraint $\mathcal{O}^\dagger_i(a_I) = \mathcal{O}_i(a_I)$ implies that $\widetilde{\mathcal{O}}^\dagger_{i,\alpha} = \widetilde{\mathcal{O}}_{-\alpha,i}$. Substituting (3.12) into (3.9), we finally find that $S_{\rm Int}$ becomes quadratic, *i.e.*

$$\begin{aligned}\sum_{I=1}^{L} S_{\rm Int}(a_I, a_{I+1}) &= -\frac{1}{2}\sum_{\alpha=1}^{L-1} C_{ij}(\lambda)\sin^2\frac{p_\alpha}{2}\widetilde{\mathcal{O}}_{i,\alpha}\widetilde{\mathcal{O}}_{j,-\alpha}\\ &= -\frac{1}{2}\sum_{\alpha=1}^{L-1} C_{ij}(\lambda)s_\alpha\widetilde{\mathcal{O}}_{i,\alpha}\widetilde{\mathcal{O}}_{j,-\alpha}\ ,\end{aligned} \tag{3.13}$$

where the sum over repeated indices $i,j \geq 1$ is understood and we introduced the notation $s_\alpha = \sin^2\frac{p_\alpha}{2}$. Note that in (3.9) the Fourier mode $\widetilde{\mathcal{O}}_{i,0}$ does not contribute since $s_\alpha = 0$.

Hubbard-Stratonovich linearization

Since the interaction potential (3.13) is quadratic, we can linearize it by a Hubbard-Stratonovich transformation [69, 70]

$$\exp\left(\frac{1}{2}\sum_{\alpha=1}^{L-1} C_{ij}\widetilde{\mathcal{O}}_{i,\alpha}\widetilde{\mathcal{O}}_{j,-\alpha}\right) = \int D\widetilde{J}\prod_{\alpha=1}^{L-1}\exp\left(\widetilde{J}_i(-p_\alpha)\widetilde{\mathcal{O}}_{i,\alpha} - \frac{1}{2s_\alpha}C^{-1}_{ij}\widetilde{J}_i(p_\alpha)\widetilde{J}_j(-p_\alpha)\right)\ , \tag{3.14}$$

where the integration measure is defined as follows

$$D\tilde{J} = \frac{1}{\sqrt{\det C s_1\ldots s_{L-1}}}\prod_{i,\alpha}\frac{\mathrm{d}\widetilde{J}_i(p_\alpha)}{\sqrt{2\pi}}\frac{\mathrm{d}\widetilde{J}_i(-p_\alpha)}{\sqrt{2\pi}}\ . \tag{3.15a}$$

Combining together (3.14) with (3.8), we find that the integration over the matrices a_I can be performed straightforwardly and the final result takes the following form

$$\mathcal{Z}_{\mathbf{Q}_L} = \int D\widetilde{J}\exp\left(-\sum_{\alpha=1}^{L-1}\frac{1}{2s_\alpha}C^{-1}_{ij}\widetilde{J}_i(p_\alpha)\widetilde{J}_j(-p_\alpha) + S_{\rm eff}(\widetilde{J})\right)\,, \tag{3.16}$$

where the effective action $S_{\rm eff}$ is induced by the potential (3.13) and is given by [70]

$$\begin{aligned}\exp\big(S_{\rm eff}(\widetilde{J})\big) &= \exp\left(\sum_{n=2}^{\infty}\frac{1}{n!L^{n/2-1}}G_{i_1\ldots i_n}\sum_{\alpha_1,\ldots,\alpha_n=1}^{L-1}\widetilde{J}_{i_1}(p_{\alpha_1})\ldots\widetilde{J}_{i_3}(p_{\alpha_n})\delta(p_{\alpha_1}+\ldots+p_{\alpha_n})\right)\\ &\equiv \exp\left(\sum_{n=2}^{\infty}\frac{1}{n!L^{n/2-1}}G_{i_1\ldots i_n}\widetilde{J}_{i_1}\star\ldots\star\widetilde{J}_{i_n}\right)\,.\end{aligned} \tag{3.17}$$

In the previous expression, the δ-function enforces the conservation of the quasimomentum p_α, while $G_{i_1,\dots,i_n}$ denotes a general connected correlator evaluated with a Gaussian measure, *i.e.*

$$G_{i_1,\dots,i_n} = \langle \mathcal{O}_{i_1}(a)\dots\mathcal{O}_{i_n}(a)\rangle_{0,c} \ . \tag{3.18}$$

The net effect of the transformation (3.14) is to map the partition function of the Q_L model to an effective theory in the variables $\widetilde{J}$. This description involves an infinite tower of interaction vertices, captured by the effective action S_{eff} (3.17) and proportional to the Gaussian correlators (3.18). In the large-N limit, these functions scale as (see in particular Appendix A of [69] for more details)

$$G_{i_1,\dots,i_n} = \frac{\beta_{i_1}\dots\beta_{i_n}}{N^{n-2}}\left(P_{n-3} + \frac{1}{N^2}P_n + \frac{1}{N^4}P_{n+3} + \dots\right) \ , \tag{3.19}$$

and consequently, they can naturally be interpreted as coupling constants for the effective theory (3.16). In particular, we denoted with P_K a symmetric polynomial in the variables $i_1, i_2, \dots, i_n$ of degree K [2], while the factors β_i are explicitly given by

$$\beta_{2i} \equiv \beta_i^+ = 2^{1/2-i}\frac{\Gamma(2i)}{\Gamma(i)^2} \ , \qquad \beta_{2i+1} \equiv \beta_i^- = 2^{-1-i}\frac{\Gamma(2i+2)}{\Gamma(i+2)\Gamma(i)} \ . \tag{3.20}$$

3.3.1 Matrix correlators of twisted operators

To compute the correlators (3.5), we first need to identify the matrix counterparts of the operators $T_{\alpha,i}$ (3.3). At first sight, the Fourier modes $\widetilde{\mathcal{O}}_{i,\alpha}$ (3.12b) might appear to be a natural choice. However, their two-point function violates the charge conservation and therefore cannot reproduce the correlator (3.5a). The reason is that, within the matrix model of the Q_L theory (3.8), the operators $\widetilde{\mathcal{O}}_{i,\alpha}$ (3.12b) mix with those of lower dimension.

To clarify these aspects, we consider in detail the two-point function

$$\left\langle \widetilde{\mathcal{O}}_{i_1,\alpha_1}\widetilde{\mathcal{O}}_{i_2,\alpha_2}\right\rangle = \frac{1}{\mathcal{Z}_{\mathsf{Q}_L}}\left\langle \prod_{I=1}^{L} \mathrm{e}^{-S_{\text{Int}}(a_I,a_{I+1})}\widetilde{\mathcal{O}}_{i_1,\alpha_1}\widetilde{\mathcal{O}}_{i_2,\alpha_2}\right\rangle_0 \ . \tag{3.21}$$

To systematically expand the matrix integrals in the large-N limit, we observe that $\widetilde{\mathcal{O}}_{i,\alpha}$ couples to the field $\widetilde{J}_i(-p_\alpha)$ by (3.14). As a result, we can express (3.21) as follows

$$\left\langle \widetilde{\mathcal{O}}_{i_1,\alpha_1}\widetilde{\mathcal{O}}_{i_2,\alpha_2}\right\rangle = \frac{1}{\mathcal{Z}_{\mathsf{Q}_L}}\int D\widetilde{J}\prod_{\alpha=1}^{L-1}\mathrm{e}^{-\frac{1}{2}\frac{1}{s_\alpha}C^{-1}_{ij}\widetilde{J}_i(p_\alpha)\widetilde{J}_j(-p_\alpha)}\prod_{\ell=1}^{2}\frac{\partial}{\partial\widetilde{J}_{i_\ell}(-p_{\alpha_\ell})}\bigg|_{\widetilde{J}=0}\mathrm{e}^{S_{\text{eff}}(\widetilde{J})} \ , \tag{3.22}$$

where $S_{\text{eff}}(\widetilde{J})$ is the effective action (3.17).

To proceed with the calculation, we observe that the planar correction to (3.22) is determined by contributions that do not involve the functions $G_{i_1,\dots,i_n}$ (3.18) with $n \geq 3$, since they scale as $1/N^{n-2}$. Going through the calculation, we find that

$$\left\langle \widetilde{\mathcal{O}}_{i_1,\alpha_1}\widetilde{\mathcal{O}}_{i_2,\alpha_2}\right\rangle = \delta(p_{\alpha_1}-p_{\alpha_2})G_{i_1i_2} + G_{i_1m}G_{i_2n}\left\langle \widetilde{J}_i(-p_{\alpha_1})\widetilde{J}_j(p_{\alpha_2})\right\rangle + \dots \ . \tag{3.23}$$

The expectation value in the second line of (3.23) is the two-point function of the field $\widetilde{J}_i(-p_\alpha)$, which can be evaluated by standard Feynman diagram techniques. Following [69,70], we combine

[2] In particular, for $K=-1$, we have $P_{-1} = 2/(i+j+c)$, where $c=1$ if the indices are odd and $c=0$ if they are even.

the quadratic term in the effective action S_{eff} (3.17) with that in (3.23) which involves the matrix C^{-1}, and we introduce the free propagator

$$\begin{aligned}\left\langle \widetilde{J}_i(p_\alpha)\widetilde{J}_j(p_\beta)\right\rangle_0 &= \left[s_\alpha C\left(1-s_\alpha GC\right)^{-1}\right]_{ij}\delta(p_\alpha+p_\beta)\\ &\equiv X_{ij}(s_\alpha)\delta(p_\alpha+p_\beta)\ ,\end{aligned} \tag{3.24}$$

where we recall that the matrix C is defined in (3.11), while G_{ij} is a two-point correlator in the Gaussian matrix model (3.18). Diagrammatically, we can represent (3.24) as follows

$$X_{ij}(s_\alpha) = \quad i \xrightarrow{\quad p_\alpha \quad} j \quad . \tag{3.25}$$

Using (3.25), we can construct the usual Feynman rules resulting from the effective action S_{eff} (3.17) and calculate arbitrary correlation functions. For instance, the two-point function in the second line of (3.23) admits the following diagrammatic expansion

$$\left\langle \widetilde{J}_i(-p_{\alpha_1})\widetilde{J}_j(p_{\alpha_2})\right\rangle = \quad i \xrightarrow{\quad p_{\alpha_1} \quad} j \quad + \quad i \xrightarrow{\quad p_{\alpha_1} \quad} \bullet \xrightarrow{\quad p_{\alpha_1} \quad} j \quad + \dots\ , \tag{3.26}$$

where the black dot depicts the interaction vertices arising from effective action S_{eff} (3.17).

According to the structure of the effective action S_{eff} (3.17), we observe that the second diagram in (3.26) is proportional to the Gaussian correlator G_{ijkl}, which scales as $1/N^2$ (3.19). Consequently, the planar correction to (3.26) arises from the first diagram, *i.e.* from the free propagator (3.24). This involves the Gaussian correlator G_{ij} which, in the large-N limit, scales as N^0 and takes the following form [65, 69]

$$\begin{aligned}G^-_{ij} &= \beta^-_i\beta^-_j\frac{2}{i+j+1}+\dots\ ,\\ G^+_{ij} &= \beta^+_i\beta^+_j\frac{2}{i+j}+\dots\ ,\end{aligned} \tag{3.27}$$

where the notation was introduced for $G^-_{ij}=G_{2i+1,2j+1}$ and $G^+_{ij}=G_{2i,2j}$ and we recall that the β-factors are defined in (3.20). Moreover, we can decompose these correlators as follows [3]

$$G_{ij} = (UU^T)_{ij}+\mathcal{O}(1/N^2)\ . \tag{3.29}$$

In the previous expression, U_{ij} denotes a lower triangular matrix which vanishes when its indices have different parity and its explicit form is given by [69]

$$U^-_{ij} = \frac{\sqrt{2j+1}\,\Gamma(2i+2)}{2^{i+1/2}\Gamma(i-j+1)\Gamma(i+j+2)}\ ,\qquad (U^-)^{-1}_{ji} = (-1)^{i+j}\frac{2^{i+1/2}\sqrt{2j+1}\,\Gamma(i+j+1)}{\Gamma(2i+2)\Gamma(-i+j+1)}\ , \tag{3.30a}$$

$$U^+_{ij} = \frac{\sqrt{2j}\,\Gamma(2i+1)}{2^i\Gamma(i-j+1)\Gamma(i+j+1)}\ ,\qquad (U^+)^{-1}_{ji} = (-1)^{i+j}\frac{2^i\sqrt{2j}\,\Gamma(i+j)}{\Gamma(2i+1)\Gamma(-i+j+1)}\ , \tag{3.30b}$$

[3] The matrix U in (3.29) has a simple meaning: it allows us to construct an orthonormal basis of operator $\widehat{\mathcal{O}}_i(a)$ with canonically normalized two-point function in the Gaussian ensemble, *i.e.*

$$\begin{aligned}\widehat{\mathcal{O}}_i(a) &= (U)^{-1}_{ij}\,\mathcal{O}_j(a)\ ,\\ \left\langle\widehat{\mathcal{O}}_i(a)\widehat{\mathcal{O}}_j(a)\right\rangle_{0,c} &= \delta_{ij}\ .\end{aligned} \tag{3.28}$$

where we employed the usual notation $U^{+}_{ij} \equiv U_{2i,2j}$ and $U^{-}_{ij} \equiv U_{2i+1,2j+1}$.

Substituting (3.29) into (3.24) and introducing the matrix $K = \left(U^T C U\right)$, we finally find that

$$X_{ij}(s_\alpha) = \left(U^{-,T} s_\alpha K \frac{1}{1 - s_\alpha K} U^{-1}\right)_{ij} + \mathcal{O}(1/N^2) \ . \tag{3.31}$$

Combining the previous expression with (3.23) and taking into account (3.29), we can determine the planar approximation of the two-point function (3.22), *i.e.*

$$\left\langle \widetilde{\mathcal{O}}_{i,\alpha_1} \widetilde{\mathcal{O}}^{\dagger}_{j,\alpha_2} \right\rangle = \delta(p_{\alpha_1} - p_{\alpha_2}) U_{ir} \mathsf{D}_{rs}(p_\alpha) U^T_{sj} \ , \quad \text{where} \quad \mathsf{D}_{mn}(p_\alpha) = \left(\frac{1}{1 - s_\alpha K}\right)_{mn} \tag{3.32}$$

depends on the quasimomentum p_α and on the 't Hooft coupling λ through the function s_α (3.13) and the matrix K, respectively. In what follows, we will omit the dependence on p_α of the matrix D to avoid cumbersome notations.

A remarkable property of the matrix K is that it can be expressed as a convolution of Bessel functions. Indeed, recalling that the matrices C and U are defined in (3.11) and (3.30), respectively, and vanish for indices of different parities, we find that K inherits the same structure and takes the following form [66, 69]

$$K_{ij} = \left(U^T C U\right)_{ij} = (-1)^{i+j} \sqrt{ij} \int_0^\infty \frac{\mathrm{d}t}{t} J_i(\sqrt{t}) J_j(\sqrt{t}) \chi\left(\frac{\sqrt{t}}{2\hat{\lambda}}\right) \ , \tag{3.33}$$

where the notation was introduced for

$$\hat{\lambda} = \frac{\sqrt{\lambda}}{4\pi} \ , \tag{3.34}$$

$$\chi(x) = -\frac{1}{\sinh^2 \frac{x}{2}} \ . \tag{3.35}$$

As we will shortly see, it is convenient to describe the matrix K with even and odd indices by introducing

$$(K_\ell)_{ij} = (-1)^{i+j} \sqrt{2i + \ell - 1} \sqrt{2j + \ell - 1} \int_0^\infty \frac{dt}{t} J_{2i+\ell-1}(\sqrt{t}) J_{2j+\ell-1}(\sqrt{t}) \chi\left(\frac{\sqrt{t}}{2\hat{\lambda}}\right) \ . \tag{3.36}$$

As a result, it is straightforward to show that

$$K_{2i,2j} = (K_{\ell=1})_{ij} \equiv K^{+}_{ij} \ , \qquad K_{2i+1,2j+1} = (K_{\ell=2})_{ij} \equiv K^{-}_{ij} \ . \tag{3.37}$$

Normal ordering procedure

As we previously anticipated, the two-point function (3.32) violates the charge conservation since it is not diagonal in the indices i and j. To circumvent this problem, we introduce a basis of *normal-ordered* operators. These are constructed through a Gram–Schmidt orthogonalization procedure [62, 98–100] and represent the proper matrix counterparts of the operators (3.3).

Although the Gram–Schmidt procedure is algorithmic, a closed-form expression for the normal-ordered operators, valid for arbitrary values of the parameters, is typically not available and requires a case-by-case analysis. However, in the large-N limit, the orthogonalization drastically simplifies. In fact, at leading order, $\widetilde{\mathcal{O}}_{i,\alpha}$ only receives contributions from its lower-dimensional counterparts, while composite [4] operators only contribute at the non-planar level.

[4] Here "composite" refers to products of several modes $\widetilde{\mathcal{O}}_{i,\alpha}$, such as $\widetilde{\mathcal{O}}_{i,\alpha}\widetilde{\mathcal{O}}_{j,\beta}\ldots$.

To see this explicitly, we introduce the normal-ordered basis at leading order in the large-N limit as a linear combination of the operators $\widetilde{\mathcal{O}}_{i,\alpha}$ (3.12b)

$$\mathcal{T}_{i,\alpha} = M^{(\alpha)}_{ij}\widetilde{\mathcal{O}}_{j,\alpha} + \dots \ , \tag{3.38}$$

where the coefficients $M^{(\alpha)}_{ij}$ form a lower triangular matrix that depends on λ and the sector index α, but is independent of N. Their explicit form is fixed by the orthonormality condition

$$\begin{aligned}\left\langle \mathcal{T}_{i,\alpha}\mathcal{T}^{\dagger}_{j,\beta}\right\rangle &= M^{(\alpha)}_{im}M^{(\beta)}_{jn}\left\langle \widetilde{\mathcal{O}}_{m,\alpha}\widetilde{\mathcal{O}}^{\dagger}_{n,\beta}\right\rangle + \dots \\ &= M^{(\alpha)}_{im}M^{(\beta)}_{jn}U_{mr}\mathsf{D}_{rs}U^{T}_{sn}\delta(p_\alpha - p_\beta) + \dots \\ &= V^{(\alpha)}_{im}V^{(\beta)}_{jn}\mathsf{D}_{mn}\delta(p_\alpha - p_\beta) + \dots \\ &= \delta_{ij}\delta\left(p_\alpha - p_\beta\right) \ ,\end{aligned} \tag{3.39}$$

where in the second line we substituted the correlator with its leading-order expression (3.32) and introduced the lower triangular matrix $V^{(\alpha)} = M^{(\alpha)}U$. Since U (3.30) vanishes when its indices have different parities, $V^{(\alpha)}$ inherits the same structure.

In this construction, we work with a *unitary normalization* of the operators, such that the two-point functions of the normal-ordered basis $\mathcal{T}_{i,\alpha}$ are canonically normalized. This choice is particularly convenient, as it provides a powerful framework to systematically expand the structure constants (3.6) in the large-N limit (see (3.45)).

However, since our goal is to explore the behaviour of quiver theories across their parameter space, we are also interested in determining the *un-normalized* two-point functions $G^{(2)}_{\alpha,n}$ (3.5), which exhibit a non-trivial dependence on the number of nodes L. However, computing these functions does not require a separate formalism since the same mixing coefficients that define the normalized (normal-ordered) operators (3.38) can be used to reconstruct the un-normalized correlators. At the planar level, it is straightforward to see that

$$G^{(2)}_{\alpha,i} = \left(M^{(\alpha)}_{ii}\right)^{-2} + \dots \ . \tag{3.40}$$

We will now verify that the previous expression indeed reproduces the results derived in [82,85].

The lower triangular matrix $M^{(\alpha)}$ is defined by the relation (3.39), in which it enters through the matrix $V^{(\alpha)} = M^{(\alpha)}U$, where U is defined in (3.30). To calculate (3.40), we have to determine the diagonal elements of $M^{(\alpha)}$ which, in turn, are related to the diagonal elements of $V^{(\alpha)}$ by the relation $V^{(\alpha)}_{ii} = M^{(\alpha)}_{ii}U_{ii}$.

We begin by considering the case in which V^{α} has odd indices, *i.e.* $V^{(\alpha)}_{2i+1,2j+1} \equiv V^{(\alpha),-}_{ij}$. Since this matrix is lower triangular, its diagonal elements coincide with its eigenvalues and consequently, they take the following form

$$\left(\frac{1}{V^{(\alpha),-}_{ii}}\right)^2 = \frac{\det \mathsf{D}^{-}_{(i)}}{\det \mathsf{D}^{-}_{(i-1)}} \equiv R_{\alpha,2i+1} \ . \tag{3.41}$$

where $\mathsf{D}^{-}_{ij} = \mathsf{D}_{2i+1,2j+1}$, while $\mathsf{D}^{-}_{(i)}$ denotes the $i\times i$ upper-left submatrix of D^{-}, with the convention $\mathsf{D}^{-}_{(0)} = \mathbb{I}$. As a result, we find that

$$\begin{aligned}\left(\frac{1}{M^{(\alpha),-}_{ii}}\right)^2 &= (U^{-})_{ii}\,R_{\alpha,2i+1} \\ &= \frac{2i+1}{2}R_{\alpha,2i+1} \ ,\end{aligned} \tag{3.42}$$

where $M^{(\alpha),-}_{ii} = M^{(\alpha)}_{2i+1,2i+1}$ and we obtained the last equality by the explicit form of the matrix elements $U^{-}_{ii} \equiv U_{2i+1,2i+1}$ (3.30a). The calculation of the even case yields an identical result with the replacement $2i+1 \to 2i$. Consequently, the two-point function (3.40) is simply given by

$$G^{(2)}_{\alpha,n} = \mathcal{G}_n R_{\alpha,n} + \dots \ , \qquad \text{where} \qquad \mathcal{G}_n = \frac{n}{2^n} \ , \tag{3.43}$$

in agreement with the result derived in [5] [82, 85]. Finally, using (3.17) of [85], we find that the ratio (3.41) can be expressed in terms of the matrices $K^{\pm}$ (3.37) as follows

$$R_{\alpha,2i+1} = \frac{\det\left(1 - s_\alpha K^{-}_{[i+1]}\right)}{\det\left(1 - s_\alpha K^{-}_{[i]}\right)} \ , \qquad R_{\alpha,2i} = \frac{\det\left(1 - s_\alpha K^{+}_{[i+1]}\right)}{\det\left(1 - s_\alpha K^{+}_{[i]}\right)} \ , \tag{3.44}$$

where $K^{\pm}_{[i]}$ denotes the matrix obtained by removing the first $k-1$ rows and columns from $K^{\pm}$.

Three-point functions and structure constants The advantage of working with the normalization (3.39) is that the three-point functions of normal-ordered operators (3.38) are already normalized with respect to the two-point functions. As a result, we can extract the leading planar correction to structure constants (3.6) by examining the correlator

$$\left\langle \mathcal{T}_{i_1,\alpha_1} \mathcal{T}_{i_2,\alpha_2} \mathcal{T}^{\dagger}_{i_3,\alpha_3} \right\rangle = M^{(\alpha_1)}_{i_1 m} M^{(\alpha_2)}_{i_2 n} M^{(\alpha_3)}_{i_3 p} \left\langle \widetilde{\mathcal{O}}_{m,\alpha_1} \widetilde{\mathcal{O}}_{n,\alpha_2} \widetilde{\mathcal{O}}^{\dagger}_{p,\alpha_3} \right\rangle + \dots = C_{\alpha_i, i_i} \ , \tag{3.45}$$

where we recall that the mixing coefficients $M^{(\alpha)}_{ij}$ are defined through the relation (3.38).

The calculation of the three-point correlator on the right-hand side of (3.45) is similar to (3.22). The starting point is

$$\left\langle \widetilde{\mathcal{O}}_{i_1,\alpha_1} \widetilde{\mathcal{O}}_{i_2,\alpha_2} \widetilde{\mathcal{O}}^{\dagger}_{i_3,\alpha_3} \right\rangle = \frac{1}{\mathcal{Z}_{\mathsf{Q}_L}} \int D\widetilde{J} \prod_{\alpha=1}^{L-1} \mathrm{e}^{-\frac{1}{2}\frac{1}{s_\alpha} C^{-1}_{ij} \widetilde{J}_i(p_\alpha) \widetilde{J}_j(-p_\alpha)} \prod_{\ell=1}^{2} \frac{\partial}{\partial \widetilde{J}_{i_\ell}(-p_{\alpha_\ell})} \bigg|_{\widetilde{J}=0} \mathrm{e}^{S_{\text{eff}}(\widetilde{J})} \ , \tag{3.46}$$

where we recall that the effective action $S_{\text{eff}}(\widetilde{J})$ is given by (3.17). Going through the calculation of (3.46) by using the free propagator (3.31), we find that the leading contribution in the large-N limit takes the following form

$$\begin{aligned} \left\langle \widetilde{\mathcal{O}}_{i_1,\alpha_1} \widetilde{\mathcal{O}}_{i_2,\alpha_2} \widetilde{\mathcal{O}}^{\dagger}_{i_3,\alpha_3} \right\rangle = \frac{1}{\sqrt{L}} \times \left(U_{i_1 m_1} \mathsf{D}(p_{\alpha_1})_{m_1 n_1} U^{-1}_{n_1 r_1}\right) \times \left(U_{i_2 m_2} \mathsf{D}(p_{\alpha_2})_{m_2 n_2} U^{-1}_{n_2 r_2}\right) \times \\ \times \left(U_{i_3 m_3} \mathsf{D}(p_{\alpha_3})_{m_3 n_3} U^{-1}_{n_3 r_3}\right) G_{r_1 r_2 r_3} \delta(p_{\alpha_1} + p_{\alpha_2} - p_{\alpha_3}) + \dots \ , \end{aligned} \tag{3.47}$$

where we recall that the matrices $\mathsf{D}(p_\alpha)$ and U are defined, respectively, in (3.30), while G_{ijk} is the three-point Gaussian correlator (3.18). In the large-N limit, we apply (3.19) to deduce that

$$G_{ijk} = \frac{2^{\frac{3}{2}}}{N} \beta_i \beta_j \beta_k + \mathcal{O}(1/N^3) \ , \tag{3.48}$$

where we recall that the explicit expression of the β-factors depends on the index parity and is given by (3.20). Substituting (3.48) into (3.47), we encounter the combination

$$\sqrt{2} U^{-1}_{im} \beta_m = \sqrt{i} \ . \tag{3.49}$$

[5] To be precise, in [82, 85] the function $\mathcal{G}_n$ also involves the factor N^n. In our case, we reabsorbed it into the definition of the matrix operators (3.10). Moreover, since it is independent of λ and the number of nodes L, it is irrelevant for our analysis.

Substituting the previous expression into (3.47), we find that the leading contribution to the three-point correlator takes the following form

$$\left\langle \widetilde{\mathcal{O}}_{i_1,\alpha_1}\widetilde{\mathcal{O}}_{i_2,\alpha_2}\widetilde{\mathcal{O}}^{\dagger}_{i_3,\alpha_3}\right\rangle = \frac{1}{N\sqrt{L}}\left(U_{i_1m_1}\mathsf{d}^{(\alpha_1)}_{m_1}\right)\left(U_{i_2m_2}\mathsf{d}^{(\alpha_2)}_{m_2}\right)\left(U_{i_3m_3}\mathsf{d}^{(\alpha_3)}_{m_3}\right)\delta(p_{\alpha_1}+p_{\alpha_2}-p_{\alpha_3})+\dots\,, \tag{3.50}$$

where we introduced

$$\mathsf{d}^{(\alpha)}_i = \sum_{m=2}^{\infty}\mathsf{D}^{(\alpha)}_{im}\sqrt{m}\,. \tag{3.51}$$

Finally, to obtain the structure constants (3.45), we contract (3.50) with the mixing coefficients (3.38). The final result factorizes into the product of three functions, *i.e.*

$$C_{\alpha_i,n_i} = \frac{\sqrt{n_1n_2n_3}}{\sqrt{L}N}\mathcal{V}_{\alpha_1,n_1}\mathcal{V}_{\alpha_2,n_2}\mathcal{V}_{\alpha_3,n_3}\,. \tag{3.52}$$

In the previous expression, each factor $\mathcal{V}_{\alpha_i,n_i}$ is given by

$$\mathcal{V}_{\alpha,i} = \frac{1}{\sqrt{i}}\sum_{m=2}^{\infty}V_{im}\mathsf{d}^{(\alpha)}_m\,, \tag{3.53}$$

where we recall that the matrix $V^{(\alpha)}$ was introduced in (3.39). This factorized structure matches the results derived in [66, 82, 85] and, as we will shortly see, it is connected to the two-point functions.

3.4 Relation to Fredholm determinants

In this section, we relate the results obtained by the matrix model on S^4 to a special class of determinants, also known as *generalisedd* Tracy–Widom distributions [101]. This formulation turns out to be extremely useful to study the correlation functions $G^{(2)}_{\alpha,n}$ (3.5a) and $G^{(3)}_{\alpha_i,n_i}$ (3.5b) across the parameter space of the theory.

For simplicity, we begin with discussing the two-point function $G^{(2)}_{\alpha,n}$ which, at the planar level, is explicitly given by (3.43) and involves the ratios $R_{\alpha,n}$ (3.44). These can be treated in a unified manner by employing the one-parameter matrices (3.36) as follows

$$R_{\alpha,n} = \frac{\det(1-s_\alpha K_{n+1})}{\det(1-s_\alpha K_{n-1})}\,, \tag{3.54}$$

where we recall that s_α is defined in (3.13). This function captures the dependence of $R_{\alpha,n}$ on α and L. As a result, it is straightforward to observe that the correlation functions of *untwisted* operators, *i.e.* $G^{(2)}_{\alpha=0,n}\sim R_{\alpha=0,n}$, are independent of λ [66, 82, 85] and $R_{\alpha,n}$ satisfies the relations

$$R_{\alpha,n} = R_{L-\alpha,n} = R_{-\alpha,n}\,. \tag{3.55}$$

Conversely, the dependence of (3.54) on the 't Hooft coupling λ is encoded in the matrix K_ℓ (3.36). At finite coupling, such dependence can be properly understood by relating K_ℓ to an *integrable* Bessel operator $\mathbf{K}_\ell$ [70, 102]. This acts on a smooth function f as follows

$$\mathbf{K}_\ell f(x) = \int_0^\infty dy\; K_\ell(x,y)\chi\left(\frac{\sqrt{y}}{2\hat{\lambda}}\right)f(y)\,, \tag{3.56}$$

where we recall that χ is defined in (3.35), while the kernel $K_\ell(x,y)$ is expressed in terms of the Bessel functions [28, 102]

$$K_\ell(x,y) = \sum_{i\geq 1} \psi_i(x)\psi_i(y) = \frac{\sqrt{x}J_{\ell+1}(\sqrt{x})J_\ell(\sqrt{y}) - \sqrt{y}J_{\ell+1}(\sqrt{y})J_\ell(\sqrt{x})}{2(x-y)}\,. \tag{3.57}$$

In the previous expression, $\psi_i(x)$ denotes an orthonormal basis of functions

$$\begin{aligned}\psi_i(x) &= (-1)^i\sqrt{2i+\ell-1}\,\frac{J_{2i+\ell-1}(\sqrt{x})}{\sqrt{x}}\,,\\ \langle\psi_i|\psi_j\rangle &= \int_0^\infty dx\,\psi_i(x)\psi_j(x) = \delta_{ij}\,.\end{aligned} \tag{3.58}$$

Using these relations, it is straightforward to show that $(K_\ell)_{ij} = \langle\psi_i|\mathbf{K}_\ell|\psi_j\rangle$. As a result, (3.54) can be written as a ratio of *Fredholm determinants*

$$R_{\alpha,n} = \mathrm{e}^{\mathcal{F}_{n+1}-\mathcal{F}_{n-1}}\,, \tag{3.59}$$

$$e^{\mathcal{F}_\ell} = \det(1 - s_\alpha \mathbf{K}_\ell)\,. \tag{3.60}$$

The function $\mathcal{F}_\ell$ is extremely special as we can identify it with a *generalisedd* Tracy–Widom distribution. Indeed, the determinant $\mathrm{e}^{\mathcal{F}_\ell}$ evaluated for the special symbol $\chi(x) = \theta(1-x)$ determines the probability that all the eigenvalues of a random matrix in the Laguerre ensemble fall outside the interval $[0,\hat{\lambda}^2]$ [103]. Remarkably, $\mathrm{e}^{\mathcal{F}_\ell}$ can be found in terms of a Painlevé transcendent [101, 104]. In our case, however, the symbol χ is the rapidly decreasing function (3.35) for which $\mathcal{F}_\ell$ cannot be found in closed form. However, the method of differential equations [105–110], allows us to determine the strong expansion of the determinant. Moreover, exploiting (3.60) and the properties of the Bessel functions, it is possible to show that [6] [28, 111, 112]

$$\hat{\lambda}\frac{\partial}{\partial\hat{\lambda}}\left(\mathcal{F}_{\ell+1} - \mathcal{F}_{\ell-1}\right) = 2\ell\left(\mathrm{e}^{2\mathcal{F}_\ell - \mathcal{F}_{\ell-1} - \mathcal{F}_{\ell+1}} - 1\right)\,. \tag{3.61}$$

This relation holds for arbitrary values of the parameters and symbol χ and as we will shortly see, it allows to express the structure constants (3.52) in terms of the two-point function $G^{(2)}_{\alpha,n}$.

Three-point functions Having determined the two-point function $G^{(2)}_{\alpha,n}$, we can combine its expression with the structure constants (3.6) and derive the planar correction to the three-point functions $G^{(3)}_{\alpha_i,n_i}$ (3.5b). By inverting the relation (3.6), we find that

$$G^{(3)}_{\alpha_i,n_i} = \frac{1}{\sqrt{L}N}\prod_{i=1}^{3}\sqrt{n_i G^{(2)}_{\alpha_i,n_i}}\,\mathcal{V}_{\alpha_1,n_1}\mathcal{V}_{\alpha_2,n_2}\mathcal{V}_{\alpha_3,n_3} + \dots\,, \tag{3.62}$$

where we recall that $\mathcal{V}_{\alpha,n}$ is defined in (3.53).

The function $\mathcal{V}_{\alpha,n}$ is closely related to the two-point correlator $G^{(2)}_{\alpha,n}$ (3.43). We can show this by using the constraints imposed by the normal ordering condition (3.39). To begin with, we recall that $\mathcal{V}_{\alpha,n}$ involves the function $\mathsf{d}_i^{(\alpha)}$ (3.51), which satisfies the following functional

[6] An explicit proof of the relation (3.61) can be found in Appendix A of [111].

relations (see (B.3) of [85])

$$\mathsf{d}^{(\alpha)}_{2n}\mathsf{d}^{(\alpha)}_{2m} = \sqrt{2m}\sum_{s=1}^{m-1}\sqrt{2s}\mathsf{D}^{+}_{sn}(p_\alpha) + \sqrt{2n}\sum_{s=1}^{n-1}\sqrt{2s}\mathsf{D}^{+}_{sm}(p_\alpha) + (n+m+\lambda\partial_\lambda)\,\mathsf{D}^{+}_{nm}(p_\alpha)\ , \tag{3.63a}$$

$$\mathsf{d}^{(\alpha)}_{2n+1}\mathsf{d}^{(\alpha)}_{2m+1} = \sqrt{2m+1}\sum_{s=1}^{m-1}\sqrt{2s+1}\mathsf{D}^{-}_{sn}(p_\alpha) + \sqrt{2n+1}\sum_{s=1}^{n-1}\sqrt{2s+1}\mathsf{D}^{-}_{sm}(p_\alpha) + (n+m+1+\lambda\partial_\lambda)\,\mathsf{D}^{-}_{nm}(p_\alpha)\ , \tag{3.63b}$$

$$\mathsf{d}^{(\alpha)}_{2n}\mathsf{d}^{(\alpha)}_{2m+1} = \sqrt{2m+1}\sum_{s=1}^{m}\sqrt{2s}\mathsf{D}^{+}_{sn}(p_\alpha) + \sqrt{2n}\sum_{s=1}^{n-1}\sqrt{2s+1}\mathsf{D}^{-}_{sm}(p_\alpha)\ , \tag{3.63c}$$

where we employed the usual notations $D_{2m,2n}(p_\alpha) = D^{+}_{mn}(p_\alpha)$ and $D_{2m+1,2n+1}(p_\alpha) = D^{-}_{mn}(p_\alpha)$, with $D_{mn}(p_\alpha)$ being defined in (3.32) and vanishes when its indices have different parities. For concreteness, we begin with considering the odd case and analyse the quantity

$$\begin{aligned}\mathcal{V}^2_{\alpha,2i+1} &= \frac{1}{2i+1}\left(\sum_{m=2}^{\infty}V^{(\alpha)}_{2i+1m}\mathsf{d}^{(\alpha)}_{m}\right)^2\\ &= \frac{1}{2i+1}\left(\sum_{m=1}^{\infty}V^{(\alpha),-}_{im}\mathsf{d}^{(\alpha)}_{2m+1}\right)^2\\ &= \frac{1}{2i+1}\sum_{m,n=1}^{i}V^{(\alpha),-}_{im}V^{(\alpha),-}_{in}\mathsf{d}^{(\alpha)}_{2m+1}\mathsf{d}^{(\alpha)}_{2n+1}\ ,\end{aligned} \tag{3.64}$$

where $V^{(\alpha)}_{2i+1,2j+1} = V^{(\alpha),-}_{ij}$ and we obtained the second line by recalling that $V^{(\alpha)}_{ij} = 0$ for $j > i$.

To proceed with the computation, we need the explicit form of the matrix elements $V^{(\alpha),-}_{im}$, which can be extracted from the defining condition (3.39). It is straightforward to show that

$$V^{(\alpha),-}_{im} = \frac{1}{V^{(\alpha),-}_{ii}}\left(\mathsf{D}^{-}_{(i)}\right)^{-1}_{im}(p_\alpha)\ , \tag{3.65}$$

for $i \geq m$ and we recall that $M_{(i)}$ denotes the $i\times i$ upper-left submatrix. Substituting (3.63b) into (3.64) and using the explicit form of the matrix elements $V^{(\alpha),-}_{m}$ (3.65), we find that only the derivative term survives, *i.e.*

$$\begin{aligned}\mathcal{V}^2_{\alpha,2i+1} &= \frac{1}{2i+1}\left(\sum_{m,n=1}^{i}V^{(\alpha),-}_{im}V^{(\alpha),-}_{in}\,(n+m+1+\lambda\partial_\lambda)\,\mathsf{D}^{-}_{nm}(p_\alpha)\right)\\ &= \frac{1}{2i+1}\left(\sum_{m,n=1}^{i}V^{(\alpha),-}_{im}V^{(\alpha),-}_{in}\,(2m+1+\lambda\partial_\lambda)\,\mathsf{D}^{-}_{nm}(p_\alpha)\right)\\ &= 1+\frac{1}{2i+1}\sum_{m,n=1}^{i}V^{(\alpha),-}_{im}V^{(\alpha),-}_{in}\lambda\partial_\lambda\mathsf{D}^{-}_{nm}(p_\alpha)\ ,\end{aligned} \tag{3.66}$$

where the second equality follows from the fact that D^{-} is symmetric, while in the last line we exploited the explicit form of the matrix elements $V^{(\alpha)}_{ij}$ (3.65). Similarly, the last term can be

manipulated as follows

$$\begin{aligned}\sum_{m,n=1}^{i} V_{im}^{(\alpha),-}V_{in}^{(\alpha),-}\lambda\partial_\lambda \mathsf{D}^-_{nm}(p_\alpha) &= -\sum_{m,n=1}^{i}\left(\mathsf{D}^-_{(i)}\right)_{nm}(p_\alpha)\lambda\partial_\lambda V_{im}^{(\alpha),-}V_{in}^{(\alpha),-}\\ &= -2\sum_{m,n=1}^{i} V_{in}^{(\alpha),-}\left(\mathsf{D}^-_{(i)}\right)_{nm}(p_\alpha)\lambda\partial_\lambda V_{im}^{(\alpha),-}\\ &= -2\frac{1}{V_{ii}^{(\alpha),-}}\lambda\partial_\lambda V_{ii}^{(\alpha),-}\\ &= \lambda\partial_\lambda \log\frac{1}{\left(V_{ii}^{(\alpha),-}\right)^2}\\ &= \lambda\partial_\lambda \log R_{\alpha,2i+1}\ ,\end{aligned} \tag{3.67}$$

where the last line follows from (3.41). Combining everything together, we finally find that

$$\mathcal{V}^2_{\alpha,2i+1} = 1+\frac{1}{2i+1}\lambda\partial_\lambda R_{\alpha,2i+1}\ . \tag{3.68}$$

The calculation of the even case goes along the same lines and result is given by (3.68) with the replacement $2i+1\to 2i$. As a result, the different cases can be treated in a unified manner as

$$\mathcal{V}_{\alpha,n} = \sqrt{1+\frac{1}{2n}\hat{\lambda}\frac{\partial}{\partial\hat{\lambda}}\log R_{\alpha,n}}\,. \tag{3.69}$$

Finally, we employ the Toda-like equation (3.61) to express all the relevant quantities in terms of the functions $\mathcal{F}_\ell$ (3.60), *i.e.*

$$\mathcal{V}_{\alpha,n} = \exp\left(\mathcal{F}_n-\frac{1}{2}\mathcal{F}_{n-1}-\frac{1}{2}\mathcal{F}_{n+1}\right), \tag{3.70a}$$

$$G^{(2)}_{\alpha,n} = G^{(2)}_0\exp\left(\mathcal{F}_{n+1}-\mathcal{F}_{n-1}\right), \tag{3.70b}$$

$$G^{(3)}_{\alpha_i,n_i} = \frac{G^{(3)}_0}{\sqrt{L}}\prod_{i=1}^{3}\exp\left(\mathcal{F}_{n_i}-\mathcal{F}_{n_i-1}\right). \tag{3.70c}$$

In the previous expression, we denoted with $G^{(2)}_0$ and $G^{(3)}_0$ the two- and three-point functions evaluated at $\lambda=0$. Being independent of the number of nodes L, their explicit form is not relevant to our analysis. Finally, let us note that the right-hand side of (3.70c) and (3.70b) are invariant under the interchange of any pair (α_i,n_i) and well-defined for arbitrary α_i and n_i. However, according to (3.5), we are interested in the specific case where $n_3=n_1+n_2$ and $\alpha_1+\alpha_2-\alpha_3\equiv 0\pmod L$.

3.5 The long-quiver regime as a continuum limit of a $1d$ periodic lattice

The correlation functions (3.5) depend non-trivially on different parameters: the 't Hooft coupling λ, the scaling dimension of the operators $\Delta_i=n_i$, and the number of nodes L. Crucially, the hierarchy of these parameters governs the behaviour of these observables.

To make this point concrete, we consider the two-point function $G^{(2)}_{\alpha,n} \sim R_{\alpha,n}$ (3.5a). The parameter space of this observable is spanned by (λ, a, n), with $a = \frac{\alpha}{L}$, and we can identify the following physical regimes [28]

$$\text{(i) generic operators:} \quad n \text{ finite} , \qquad a \text{ finite} , \tag{3.71}$$

$$\text{(ii) heavy operators:} \quad n \to \infty , \qquad a \text{ finite} , \tag{3.72}$$

$$\text{(iii) long-quiver limit:} \quad a \to 0 , \qquad n \text{ finite} . \tag{3.73}$$

In regime (i), the correlation functions are controlled directly by the Fredholm determinants (3.60). The weak and strong coupling limit of this regime provides the starting point for understanding the long-quiver scenario and the infinitely heavy operators. The latter arise when we send $n \to \infty$ at fixed a. In this limit, the weak-coupling corrections to the correlation functions vanish (see (4.20)), while the entire $\frac{1}{\sqrt{\lambda}}$ expansion breaks down, requiring a complete resummation to obtain a consistent result. Finally, regime (iii) is the long-quiver limit, defined by $\frac{\alpha}{L} \to 0$ at fixed n. This case is of primary interest as we expect that the theory can undergo the deconstruction mechanism and be approximated by a five-dimensional model.

3.5.1 A first look at the long-quiver limit

We can gain some intuition into the physical properties of the long-quiver limit by observing that the matrix integral (3.8) can be interpreted as the partition function of a one-dimensional periodic lattice model of length L. The nodes of the quiver diagram depicted in Fig. 3.1 correspond to the sites of this lattice, which possess $N^2 - 1$ degrees of freedom represented by the $su(N)$ matrices a_I, whose dynamics is determined by the interaction potential S_{Int} (3.9). Intuitively, for $L \to \infty$ the nodes of the quiver diagram become continuously distributed along a circle, suggesting that this regime can naturally be interpreted as the continuum limit of the discrete lattice. The crucial question is whether this continuum picture indeed corresponds to a local theory, and if so, what its properties are. It turns out that the answer depends sensitively on the ratio $\frac{\sqrt{\lambda}}{L}$.

A qualitative explanation of this result, for which we will provide an analytical proof in what follows, can be inferred from the structure of the interaction potential S_{Int} (3.9) of the matrix-model, which involves the coefficients C_{ij}. These scale as $\sim \lambda^{(i+j)/2}$ (3.11) and govern the interaction strength between two lattice sites I and J which, in turn, scales as $C^{|I-J|}$. As a result, at weak coupling and fixed L, where $\lambda \to 0$ and $\lambda \ll L$, we expect that the interaction strength rapidly decreases with node separation. Indeed, in this regime the correlation functions are exponentially suppressed as the node separation increases (see (4.19)). Viewed through the lens of the dual lattice description, this implies that the system is characterized by short-ranged interactions. In the limit $L \to \infty$, excitations propagate along the lattice with small quasimomenta p_α and the system can be *effectively* described by a one-dimensional field theory, implying that the quiver model involves a higher-dimensional dynamics. However, the emergence of the additional dimension occurs differently than in usual lattice models, where one recovers the continuum limit by sending to zero the lattice spacing. Indeed, in this context the lattice spacing is a dimensionless fixed quantity and the emergence of an additional dimension occurs through an effective description of short-ranged interactions by means of a local field theory.

At strong coupling the situation changes dramatically. Indeed, for $\sqrt{\lambda} \gg L \gg 1$ the interaction strength becomes nearly uniform across all sites. Correlation functions grow polynomially with the separation of sites (see (4.49)), and the notion of spatial ordering along the quiver diagram is lost. In this case, excitations propagate with finite quasimomentum and the

lattice collapses onto a point, while the quiver theory remains a genuinely strongly coupled four-dimensional model.

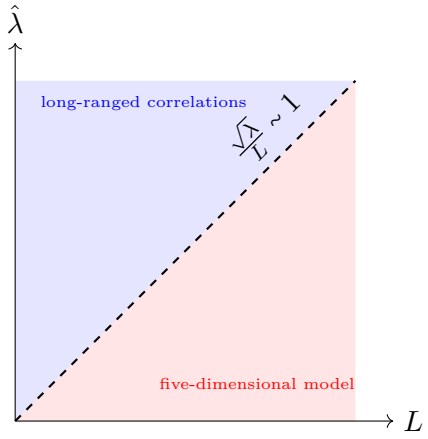

Figure 3.2: Phase diagram of the long-quiver limit in the $(L, \sqrt{\lambda})$ plane. The dashed line marks the crossover $\frac{\sqrt{\lambda}}{L} \sim 1$. For $\frac{\sqrt{\lambda}}{L} \ll 1$ (red region) interactions are short-ranged and the quiver admits a five-dimensional effective description. For $\frac{\sqrt{\lambda}}{L} \gg 1$ (blue region) interactions are long-ranged, the lattice effectively collapses, and the theory remains four-dimensional

This analysis suggests that a five-dimensional description emerges in the limit $L \to \infty$ when $\frac{\sqrt{\lambda}}{L}$ remains finite. This is equivalent to moving along the dashed line in the phase diagram depicted in Fig. 3.2. In this case, the quasimomentum p_α becomes continuous and the operators (3.3) and (3.1) are promoted to their five-dimensional counterparts, *i.e.*

$$T_{\alpha,n}(x) \;\mapsto\; T_n(x,p)\;, \qquad O_n^I(x) \;\mapsto\; O_n(x,y)\;, \tag{3.74}$$

where p is the excitation momentum and y is the emergent fifth coordinate. Of course, $O_n(x,y)$ and $T_n(x,p)$ are related by a Fourier transform and their correlation functions inherit the same structure of (3.5) and (3.7).

For instance, the correlator of two operators $O_n(x,y)$ is expected to take the following form

$$\big\langle O_n(x_1,y_1)\overline{O}_n(x_2,y_2)\big\rangle \sim \frac{G_n(y_1-y_2)}{|x_1-x_2|^{2n}}\;, \tag{3.75}$$

where $G_n(y)$ is obtained from the normalization factor $G_{IJ}^{(2)}$ (3.7) by the long-quiver limit.

From the viewpoint of the five-dimensional description, the factorization of the correlators (3.75) into a product of functions that depend separately on the four-dimensional coordinates x and y, implies that the Lorentz group is broken. Physically, this means that the four-dimensional modes remain massless, thereby preserving the conformal invariance of the Q_L theory, whereas the excitations propagating along the emergent fifth dimension become massive. This decoupling signals that the resulting five-dimensional model is intrinsically non-relativistic. The aim of the following chapter is to make these considerations quantitative by explicitly determining the function $G_n(y)$ at weak and strong coupling.

Chapter 4

Correlation functions in the long-quiver limit

Info: *Part of the content and figures of this chapter have been published together with G.P. Korchemsky in* [28].

In this chapter, we analyse the correlation functions introduced in Section 3.2 across the parameter space of the theory. The weak coupling regime is discussed in Section 4.1, while the strong coupling limits are analysed in Sections 4.2 and 4.3. Our analysis reveals the presence of deconstruction effects, where the theory exhibits an additional dimension. This manifests through a local effective field theory describing massive excitations propagating along the emergent direction. These phenomena and the properties of the effective description are analysed in Section 4.4. Finally, Section 4.5 presents the study of three-point functions at strong coupling, Section 4.6 provides a connection between our analysis and the dual holographic description of the Q_L theories, while Section 4.7 outlines some future directions that our analysis naturally hints at.

4.1 Weak coupling regimes

In this section, we compute the two-point correlation functions (3.5a) and (3.7a) at weak coupling and analyse their behaviour across the different regimes outlined in (3.71).

4.1.1 Fredholm determinants at weak coupling

We begin with considering the two-point function $G^{(2)}_{\alpha,n}$ (3.5a). In the large-N limit, the dependence of the observable on the 't Hooft coupling constant λ is encoded in the ratio of Fredholm determinants (3.40). At weak coupling, they can be approximated by an expansion in powers of the matrix K_ℓ (3.36). Changing the integration variable in (3.36) according to $t \to (2\hat{\lambda}t)^2$ and replacing the Bessel functions with their expansion around the origin, we find that [1] the ratio (3.54) takes the following form

$$R_{\alpha,n} = 1 - s_\alpha\Big(\operatorname{tr} K_{n+1} - \operatorname{tr} K_{n-1}\Big) + \mathcal{O}(\hat{\lambda}^{4n})\,, \tag{4.1}$$

[1] Note that the matrix elements scale as $(K_\ell)_{ij} = O(\hat{\lambda}^{2(\ell+i+j-1)})$(3.36) after the rescaling $t \to (2\hat{\lambda}t)^2$.

where the last term describes the subleading corrections. These are suppressed by a factor $\hat{\lambda}^{4n}$ relative to the first contribution and their structure involves products of traces with higher powers of the matrices K_ℓ.

The traces appearing at the leading order in (4.1) can be calculated by employing the definition of the matrix K_ℓ (3.36). Going through the calculation, we find that [102]

$$\operatorname{tr} K_\ell = 4\hat{\lambda}^{2(\ell+1)} \sum_{m=0}^{\infty} (-1)^{m+1} \hat{\lambda}^{2m} \frac{(2\ell+2m)!(2\ell+2m+2)!\zeta_{2\ell+2m+1}}{m![(m+\ell+1)!]^2(2\ell+m)!}\,, \tag{4.2}$$

where we recall that the symbol χ is defined in (3.35). Being combined with (4.1), the previous expression allows us to derive the perturbative expansion of (4.1), *i.e.*

$$R_{\alpha,n} = 1 - 4\hat{\lambda}^{2n} s_\alpha \binom{2n}{n} \zeta(2n-1) + 8\hat{\lambda}^{2n+2} s_\alpha \binom{2n+2}{n+1} n\zeta(2n+1) + \mathcal{O}(\hat{\lambda}^{2n+4})\,. \tag{4.3}$$

This relation coincides with the result derived in [65] by a diagrammatic calculation of the two-point function $\langle T_{\alpha,n}(x) T^\dagger{}_{\alpha,n}(0)\rangle$. In this approach, the $\mathcal{O}(\hat{\lambda}^{2n})$ term in (4.3) arises from a Feynman diagram in which n scalar lines connect the points x and 0 via an irreducible $n \to n$ transition vertex (see Section 3 of [85] for details).

The subleading corrections to (4.3) can be organised according to the power of s_α. Specifically, the terms proportional to s_α^m arise from traces of m matrices (3.36) and their contribution to (4.3) starts at order $O(\hat{\lambda}^{2mn})$. As a result, the expansion (4.3) takes the form of a double series in $\hat{\lambda}$ and s_α (3.13), *i.e.*

$$R_{\alpha,n} = 1 + \sum_{m\geq 1} \left(s_\alpha\, \hat{\lambda}^{2n}\right)^m Q_m(\hat{\lambda}^2)\,, \tag{4.4}$$

where $Q_m(\hat{\lambda}^2)$ can be expanded in powers of $\hat{\lambda}^2$, with expansion coefficients expressed as multilinear combinations of odd Riemann zeta-values of a homogeneous transcendental weight (see [106] for details). Schematically, the general structure of the expansion functions Q_m is

$$Q_m = \sum_{p\geq 0} \hat{\lambda}^{2p} \sum_{\{k\}} c_{k_1,k_2,\ldots,k_m} \zeta_{2k_1-1}\zeta_{2k_2-1}\ldots\zeta_{2k_m-1}\,, \tag{4.5}$$

where the sum goes over m positive integers $k_1 \geq k_2 \geq \ldots k_m \geq n$ satisfying the relation

$$\sum_{i=1}^{m} (2k_i - 1) = m(2n-1) + 2p\,. \tag{4.6}$$

The expansion coefficients $c_{k_1,k_2,\ldots,k_m}$ in (4.5) are rational numbers depending on p and they can be calculated by matching (4.3) with the general form (4.4) order-by-order in perturbation theory. For instance, the simplest example is the $m = 1$ case. Replacing $Q_1(\hat{\lambda}^2)$ in (4.4) with its general expression (4.5), we find that

$$c_n = -4\binom{2n}{n}, \qquad c_{n+1} = 8n\binom{2n+2}{n+1}, \qquad \ldots\,. \tag{4.7}$$

For arbitrary $m \geq 2$, the leading $\mathcal{O}(\hat{\lambda}^0)$ term in (4.5) has $k_1 = \cdots = k_m = 2n-1$ and the corresponding coefficient takes a remarkably simple form $c_{n,\ldots,n} = c_n^m$ leading to

$$Q_m = [c_n \zeta_{2n-1}]^m + \mathcal{O}(\hat{\lambda}^2)\,, \tag{4.8}$$

where c_n is given by (4.7). Substituting this relation into (4.4) and neglecting $\mathcal{O}(\hat{\lambda}^2)$ corrections to Q_m, we find that the different contributions can be resummed in terms of a geometric progression

$$R_{\alpha,n} = \frac{1}{1 - s_\alpha \hat{\lambda}^{2n} c_n \zeta_{2n-1}} + \dots \,, \tag{4.9}$$

where s_α is defined in (3.13) and encodes the dependence on the quasimomentum p_α.

A distinctive feature of (4.9) is that it develops poles for complex values of the quasimomentum p_α, in analogy to the usual one-dimensional massive Euclidean propagator

$$D(x,m) = \int \frac{\mathrm{d}p}{2\pi} \frac{\mathrm{e}^{ipx}}{p^2 + m^2} = \frac{1}{2m} \mathrm{e}^{-m|x|} \,. \tag{4.10}$$

It is however interesting to observe that the singularities of (4.9) are not present at any fixed order in the weak coupling expansion of $R_{\alpha,n}$ (4.3) but rather, they only emerge upon the resummation. In particular, the closest pole to the origin is located at $p_\alpha = \pm i\mu_n$, where $\mu_n \sim n \log(1/\lambda)$ sets the weak-coupling mass scale and grows logarithmically.

The appearance of singularities in (4.9) implies that the excitations propagating across the quiver diagram acquire non-zero masses and correlations between different sites of the lattice quiver model are suppressed as a function of their separation. This is what we anticipated in Section 3.5 and our next task is to make the analysis quantitative.

4.1.2 Correlation functions at weak coupling

The correlations between different sites of the quiver diagram depicted in Fig. 3.1 are encoded in the two-point function $G^{(2)}_{IJ}$ (3.7), which is connected to $G^{(2)}_{\alpha,n}$ (3.5a) by a discrete Fourier transform. The cyclic symmetry of the Q_L theory implies that $G^{(2)}_{IJ}$ actually depends on the separation $Y = |I - J|$ and takes the following form

$$\begin{aligned} G^{(2)}_Y &= \frac{1}{L} \sum_{\alpha=0}^{L-1} \mathrm{e}^{ip_\alpha Y} G^{(2)}_{\alpha,n} \\ &\simeq \mathcal{G}_n \sum_{\alpha=0}^{L-1} \mathrm{e}^{ip_\alpha Y} R_{\alpha,n} + \dots = \mathcal{G}_n f_Y + \dots \,, \end{aligned} \tag{4.11}$$

where in the second line we replaced $G^{(2)}_{\alpha,n}$ with its leading behaviour in the large-N limit (3.54) and introduced the function f_Y, which tacitly also depends on L and on n.

We can combine (4.3) with (4.4) to derive the perturbative expansion of the function f_Y (4.11). For instance, the first two terms look as

$$f_Y = \delta_{Y,0} + (\delta_{Y,1} - 2\delta_{Y,0} + \delta_{Y,-1})\, \hat{\lambda}^{2n} \binom{2n}{n} \zeta_{2n-1} + \mathcal{O}(\hat{\lambda}^{2n+2}) \,, \tag{4.12}$$

where the Kronecker delta-function $\delta_{Y,p}$ imposes the condition $Y = p \pmod L$ on the lattice. From a physical point of view, the three terms inside the brackets in (4.12) describe the propagation of excitations to the adjacent sites on the lattice. Similarly, the corrections in the sum (4.4) describe the propagation of excitations to the adjacent m sites and they contribute to f_Y as

$$f_Y = \delta_{Y,0} + \sum_{m \geq 1} \hat{\lambda}^{2nm} f_{m,Y} Q_m(\hat{\lambda}^2) \,. \tag{4.13}$$

In the previous expression, the partial waves $f_{m,Y}$ arise from the discrete Fourier transform of the function s^m_α (3.13), *i.e.*

$$\begin{aligned} f_{m,Y} &= \frac{1}{L}\sum_{\alpha=0}^{L-1} e^{\frac{2\pi i}{L}Y\alpha} s^m_\alpha \\ &= \sum_{\ell=-\infty}^{\infty} \frac{(-1)^{Y-\ell L}\,\Gamma(2m+1)}{4^m\Gamma(m+Y-\ell L+1)\Gamma(m-Y+\ell L+1)} \,. \end{aligned} \tag{4.14}$$

The previous expression holds for arbitrary integer Y and non-negative integers m. Moreover, the sum over ℓ ensures that $f_{m,Y}$ is periodic on the lattice, $f_{m,Y} = f_{m,Y+L}$, and satisfies the relations $f_{m,Y} = f_{m,-Y} = f_{m,L-Y}$. As a result, f_Y inherits the same structure and we can restrict the node separation Y to the interval $0 \le Y \le \frac{L}{2}$.

Combining (4.13) with (4.14) and replacing the functions $Q_m(\hat\lambda^2)$ with their perturbative expansion (4.5), we determine the function f_Y at weak coupling for arbitrary number of nodes L, and the scaling dimension of the operators, n. In particular, the leading behaviour of f_Y comes from the first term in the sum in (4.13) and takes the following form

$$f_Y = \hat\lambda^{2nY} f_{Y,Y} Q_Y(\hat\lambda^2) + \cdots = \left[\hat\lambda^{2n}\zeta_{2n-1}\binom{2n}{n}\right]^Y + \dots \,, \tag{4.15}$$

for $0 < Y \le \frac{L}{2}$. Conversely, when $Y > \frac{L}{2}$ we have $f_Y = f_{L-Y}$.

It follows from (4.15) that the correlation function decays exponentially fast with the separation Y between the two sites in the weak coupling regimes, *i.e.*

$$f_Y = e^{-\mu_n Y} \,, \qquad \mu_n = -\log\left(\hat\lambda^{2n}\zeta_{2n-1}\binom{2n}{n}\right) . \tag{4.16}$$

This relation holds for arbitrary $0 < Y \le \frac{L}{2}$ up to corrections suppressed by powers of $\hat\lambda^2$ and confirms that the parameter μ_n defines the 'mass scale' (or inverse correlation length) at weak coupling.

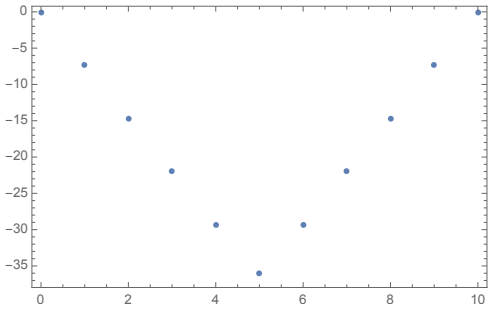

Figure 4.1: Dependence of the correlation function (4.11) on the distance between the sites $Y = |I - J|$ for $n = 2$, $\hat\lambda = 0.1$ and $L = 10$. The horizontal and vertical axis represent Y and $\log f_Y$, respectively. The correlation function is symmetric about $Y = L/2$.

To test (4.16), we set $n = 2$ and $L = 10$, and compute f_Y for $\hat\lambda = 0.1$ and integer Ys within the interval $0 \le Y \le 10$. The results are shown in Fig. 4.1 and in agreement with (4.16).

4.1.3 The long-quiver limit at weak coupling

The relation (4.15) accounts for the leading correction to f_Y at weak coupling. This poses the question of whether higher-order corrections to (4.15) alter the exponential behaviour described

in (4.16). To address this question, we consider the resummation (4.9) and calculate its discrete Fourier transform [2]

$$f_Y = \frac{1}{L}\sum_{\alpha=-L/2}^{L/2-1} \frac{e^{\frac{2\pi i\alpha}{L}Y}}{1+4\sin^2\left(\frac{\pi\alpha}{L}\right)e^{-\mu_n}}\,, \tag{4.17}$$

where μ_n is defined in (4.16). Going through the calculation, we find that this sum can be calculated in closed form

$$f_Y = e^{-\mu_n Y}\frac{\left(\frac{2}{1+\sqrt{1+4e^{-\mu_n}}}\right)^{2Y}}{\sqrt{1+4e^{-\mu_n}}\left[1-\left(\frac{2e^{-\mu_n}}{1+\sqrt{1+4e^{-\mu_n}}+2e^{-\mu_n}}\right)^{L}\right]} + (Y\to L-Y)\,, \tag{4.18}$$

where μ_n is defined in (4.16). This relation is valid for $0\le Y\le L$ and it is obtained by neglecting $\mathcal{O}(\hat\lambda^2)$ corrections in (4.9). Moreover, the two terms in (4.18) correspond to the two different paths that excitations can follow to propagate between sites I and J across the quiver diagram in Fig. 3.1 and ensure the invariance of f_Y under $Y\to L-Y$.

At weak coupling, the mass scale in (4.16) becomes large and the relation (4.18) can be expanded in powers of $e^{-\mu_n}$

$$f_Y = e^{-\mu_n Y}\left[1-2(1+Y)e^{-\mu_n}+(2+Y)(3+2Y)e^{-2\mu_n}+\mathcal{O}(e^{-3\mu_n})\right]+(Y\to L-Y)\,. \tag{4.19}$$

The first term dominates for $0<Y<\frac{L}{2}$ and the second one for $\frac{L}{2}<Y<L$. The turnover occurs at $Y=\frac{L}{2}$. Importantly, the first term in (4.19) differs from (4.16) only by the subleading corrections to f_Y, which are given by a series in $e^{-\mu_n}=\mathcal{O}(\hat\lambda^{2n})$. Since the coefficients of this series are polynomials in Y, the asymptotic behaviour of f_Y at large Y is unchanged.

As we previously remarked, the expression (4.18) holds for arbitrary conformal dimension n and consequently, it can be employed to study the *heavy-operator* regime (3.71). In particular, the dependence of (4.19) on n, enters through the mass scale μ_n (4.16). At fixed coupling and large n, this parameter scales as $\mu_n\sim n\log 4\hat\lambda^2$ and grows linearly with n. Consequently, for fixed $Y\neq 0$ the function f_Y vanishes exponentially fast at large n, *i.e.*

$$\lim_{n\to\infty} f_Y = \delta_{Y,0}\,. \tag{4.20}$$

This relation also follows immediately from (4.12).

Let us conclude the weak coupling analysis by considering the long-quiver limit $L\to\infty$. In this regime, the sum (4.17) can be approximated by an integral, suggesting that the quasi-momentum p_α becomes continuous and takes values within the first Brillouin zone $[-\pi,\pi)$. Consequently, in the continuum limit, for $L\to\infty$, and for fixed Y the relation (4.17) reduces to

$$\lim_{L\to\infty} f_Y = \int_{-\pi}^{\pi}\frac{dp}{2\pi}\frac{\mathrm{e}^{ipY}}{1+4\sin^2(p/2)\mathrm{e}^{-\mu_n}} = \mathrm{e}^{-\mu_n Y}\frac{\left(\frac{2}{1+\sqrt{1+4\mathrm{e}^{-\mu_n}}}\right)^{2Y}}{\sqrt{1+4\mathrm{e}^{-\mu_n}}}\,. \tag{4.21}$$

We verify that this relation is in a perfect agreement with (4.18).

We conclude that, in the weak coupling regime, the correlations between different sites in the quiver diagram in Fig. 3.1 decrease exponentially with site separation Y. The corresponding

[2] We use the symmetry of the sum in (4.11) under $\alpha\to L-\alpha$ to change the range of α.

mass scale (4.16) depends on the scaling dimension of the operators $\Delta = n$ and scales logarithmically with the coupling constant, $\mu_n \sim n \log 4\hat{\lambda}^2$. By combining together (4.21) and (4.19), we find that f_Y can be *effectively* described by the one-dimensional Feynman propagator (4.10)

$$\lim_{L\to\infty} f_Y \sim D(Y, \mu_n) \,, \tag{4.22}$$

with mass scale μ_n (4.16) and separation Y, which can be now continued to arbitrary real values.

Let us finally observe that the structure of (4.22) confirms the qualitative discussion we presented in Section 3.5. However, the effective description collapses to a free propagation without interactions. As we will shortly see, the strong coupling regimes possess a richer structure.

4.2 Twisted correlators at strong coupling

We now turn our attention to the strong coupling regime of the correlation functions (3.70). In this limit, it is convenient to regard the determinants in (3.54) as generalisedd Tracy–Widom distributions (3.60). Our first goal is to review the properties of these distributions in the large–λ limit and then, compute the correlation functions across the different regimes (3.71).

4.2.1 Asymptotic behaviour of the generalisedd Tracy–Widom distributions

For arbitrary values of the parameters, the strong coupling expansion of the function $\mathcal{F}_\ell$ (3.60) was determined in [69, 102, 109, 110]. In terms of the ratio $a = \frac{\alpha}{L}$ and the rescaled 't Hooft coupling $\hat{\lambda}$ (3.34), we find the following general form

$$\mathcal{F}_\ell = 4\pi\hat{\lambda}\, a(1-a) - \frac{1}{2}(2\ell-1)\log\hat{\lambda} + B_\ell + \Delta\mathcal{F}_\ell(\hat{\lambda}) \,. \tag{4.23}$$

Each successive term on the right-hand side of (4.23) is smaller than the preceding one. The constant term B_ℓ can be expressed in terms of Barnes–G functions [70] and satisfies the relation

$$B_{\ell+1} - B_\ell = \log\ell - \frac{1}{2}\log(4s_\alpha) \,, \tag{4.24}$$

while the logarithmic enhanced term $\log\hat{\lambda}$ arises from the singular behaviour of the combination $1-\chi(x)$ around the origin [113].

The function $\Delta\mathcal{F}_\ell(\hat{\lambda})$ vanishes as $\hat{\lambda}\to\infty$. It accounts for subleading terms in (4.23) of two different types: 'perturbative' corrections, proportional to powers of $1/\hat{\lambda}$, and 'non-perturbative', exponentially small contributions that are proportional to

$$\Lambda_-^2 = e^{-8\pi\hat{\lambda}a} \,, \qquad \Lambda_+^2 = e^{-8\pi\hat{\lambda}(1-a)} \,. \tag{4.25}$$

These parameters are related by the transformation $\alpha \to L-\alpha$ and satisfy the relation $\Lambda_-^2\Lambda_+^2 = e^{-8\pi\hat{\lambda}}$. The resulting expression for $\Delta\mathcal{F}_\ell(\hat{\lambda})$ takes the form of a transseries

$$\Delta\mathcal{F}_\ell(\hat{\lambda}) = \mathcal{F}_\ell^{(0,0)}(\hat{\lambda}) + \sum_{n,m} \Lambda_-^{2n}\Lambda_+^{2m}\mathcal{F}_\ell^{(n,m)}(\hat{\lambda}) \,, \tag{4.26}$$

where the coefficient functions $\mathcal{F}_\ell^{(0,0)}(\hat{\lambda})$ and $\mathcal{F}_\ell^{(n,m)}(\hat{\lambda})$ are asymptotic series in powers of $1/\hat{\lambda}$ and related to each other by transformation $\alpha \to L-\alpha$.

The first term on the right-hand side of (4.26) encodes the perturbative corrections at strong coupling

$$\begin{aligned}\mathcal{F}_\ell^{(0,0)} = & -\frac{1}{16\hat{\lambda}}(2\ell-1)(2\ell-3)I_1 - \frac{1}{64\hat{\lambda}^2}(2\ell-1)(2\ell-3)I_1^2 \\ & -\frac{1}{3072\hat{\lambda}^3}(2\ell-1)(2\ell-3)[(2\ell-5)(2\ell+1)I_2+16I_1^3] \\ & -\frac{1}{2048\hat{\lambda}^4}(2\ell-1)(2\ell-3)\left[(2\ell-5)(2\ell+1)I_1I_2+4I_1^4\right]+\mathcal{O}(1/\hat{\lambda}^5)\,,\end{aligned} \tag{4.27}$$

where the expression for the subleading terms in the previous expression can be found in [106]. To all orders in $1/\hat{\lambda}$, the expansion coefficients in (4.27) are proportional to $(2\ell-1)(2\ell-3)$ and they are given by multilinear combinations of the shape functions $I_n = I_n(a)$

$$I_n = \frac{(-1)^n}{(2\pi)^{2n-1}(2n-2)!}\left[\psi^{(2n-2)}(a)+\psi^{(2n-2)}(1-a)-2\psi^{(2n-2)}(1)\right]\,, \tag{4.28}$$

where $\psi^{(n)}(x) = (d/dx)^n\,\psi(x)$ is a derivative of Euler function $\psi(x) = (\log\Gamma(x))'$. Note that the expansion coefficients in (4.27) involve powers of I_1. All such terms depending on this function can be eliminated through the redefinition of the coupling constant

$$\hat{\lambda}' = \hat{\lambda} - \frac{1}{2}I_1(a)\,. \tag{4.29}$$

The reason why (4.26) takes the form of a transseries is that the expansion coefficients in (4.27) grow factorially at large orders [102,109,110], making the series divergent and necessitating a regularization. The non-perturbative terms in (4.26) compensate the inherent ambiguities arising from the choice of Borel resummation for the functions $\mathcal{F}_\ell^{(0,0)}(\hat{\lambda})$ and $\mathcal{F}_\ell^{(n,m)}(\hat{\lambda})$, which are related to each other by resurgence relations [114, 115]. In particular, the leading non-perturbative function in (4.26) is given by

$$\begin{aligned}\mathcal{F}_\ell^{(1,0)} = & -i(-1)^\ell\mathcal{S}(a)\Bigg[1+\frac{(2\ell-3)(2\ell-1)}{16\pi a\hat{\lambda}'}+\frac{(2\ell-5)(2\ell-3)(2\ell-1)(2\ell+1)}{512(\pi a\hat{\lambda}')^2} \\ & +\frac{(2\ell-5)(2\ell-3)(2\ell-1)(2\ell+1)((2\ell-7)(2\ell+3)+6)}{24576(\pi a\hat{\lambda}')^3} \\ & +\frac{(2\ell-5)(2\ell-3)(2\ell-1)(2\ell+1)\left((2\ell-7)^2(2\ell+3)^2+768(\pi a)^3I_2\right)}{1572864(\pi a\hat{\lambda}')^4}+\mathcal{O}(1/\hat{\lambda}^5)\Bigg],\end{aligned} \tag{4.30}$$

where the coupling $\hat{\lambda}' = \hat{\lambda}'(a)$ is defined in (4.29) and $\mathcal{S}(a)$ is the Stokes constant

$$\mathcal{S}(a) = \frac{\Gamma(1-2a)\Gamma^2(1+a)}{\Gamma(1+2a)\Gamma^2(1-a)}\,. \tag{4.31}$$

Using the transformation $a \to 1-a$ in (4.30) we can determine $\mathcal{F}_\ell^{(0,1)}$, while the explicit expressions for the subleading corrections to (4.30) can be found in [109, 110].

Correlation functions of twisted operators at strong coupling

Using the expressions for the strong coupling expansion of the function $\mathcal{F}_\ell$ (4.23), we determine the large-$\hat{\lambda}$ behaviour of $R_{\alpha,n}$ (3.54) and $\mathcal{V}_{\alpha,n}$ (3.69), *i.e.*

$$R_{\alpha,n} = \frac{(n-1)n}{4\hat{\lambda}^2 s_\alpha} \times R^{(0,0)} \left[1 + \mathrm{e}^{-8\pi\hat{\lambda}a}\, R^{(1,0)} + \mathrm{e}^{-8\pi\hat{\lambda}(1-a)}\, R^{(0,1)} + \dots\right],$$
$$\mathcal{V}_{\alpha,n} = \sqrt{\frac{n-1}{n}} \times \mathcal{V}^{(0,0)} \left[1 + \mathrm{e}^{-8\pi\hat{\lambda}a}\, \mathcal{V}^{(1,0)} + \mathrm{e}^{-8\pi\hat{\lambda}(1-a)}\, \mathcal{V}^{(0,1)} + \dots\right]. \tag{4.32}$$

In the previous expression, $R^{(0,0)}$ and $\mathcal{V}^{(0,0)}$ are connected to $\mathcal{F}_\ell^{(0,0)}$ by (3.70) and yield the leading asymptotic behaviour at large $\hat{\lambda}$, while the subleading corrections are suppressed by powers of the non-perturbative parameters $\Lambda_\pm^2$ (4.25).

The perturbative functions $R^{(0,0)}$ and $\mathcal{V}^{(0,0)}$ are given by an asymptotic series in $1/\hat{\lambda}$ with coefficients that are polynomial in $I_n(a)$. Going through the calculation, we find that

$$R^{(0,0)} = \left(\frac{\hat{\lambda}'}{\hat{\lambda}}\right)^{2(n-1)} \left[1 - \frac{(n-1)(2n-3)(2n-1)}{96\hat{\lambda}'^3} I_2(a) - \frac{3(n-1)(2n-5)(2n-3)(2n-1)(2n+1)}{10240\hat{\lambda}'^5} I_3(a) + \mathcal{O}(1/\hat{\lambda}'^6)\right],$$
$$\mathcal{V}^{(0,0)} = \left(\frac{\hat{\lambda}}{\hat{\lambda}'}\right)^{1/2} \left[1 + \frac{(2n-3)(2n-1)}{128\hat{\lambda}'^3} I_2(a) + \frac{3(2n-5)(2n-3)(2n-1)(2n+1)}{8192\hat{\lambda}'^5} I_3(a) + \mathcal{O}(1/\hat{\lambda}'^{,6})\right]. \tag{4.33}$$

Note that the expansion coefficients of the series within the brackets are polynomials in n with a degree that matches the power of $1/\hat{\lambda}'$ for $R^{(0,0)}$, while it is one degree lower for $\mathcal{V}^{(0,0)}$.

Turning our attention to the first non-perturbative contributions in (4.32), we find that their expressions are given by

$$R^{(1,0)} = i(-1)^n \mathcal{S}(a) \frac{(n-1)}{\pi a \hat{\lambda}'} \left[1 + \frac{(2n-3)(2n-1)}{16\pi a\hat{\lambda}'} + \frac{(2n-3)(2n-1)\left(4n^2-8n-1\right)}{512(\pi a\hat{\lambda}')^2} + \mathcal{O}(1/\hat{\lambda}^3)\right],$$
$$\mathcal{V}^{(1,0)} = -2i(-1)^n \mathcal{S}(a) \left[1 + \frac{4n^2-8n+5}{16\pi a\hat{\lambda}'} + \frac{(2n-3)(2n-1)\left(4n^2-8n+7\right)}{512(\pi a\hat{\lambda}')^2} + \mathcal{O}(1/\hat{\lambda}^3)\right], \tag{4.34}$$

where $\mathcal{S}(a)$ is given by (4.31) and we note that the expansion coefficients in (4.34) are polynomials in n with a degree that is twice the power of $1/\hat{\lambda}'$. The functions $R^{(0,1)}$ and $\mathcal{V}^{(0,1)}$ can be obtained from (4.34) by replacing $a \to 1-a$.

For finite $a = \frac{\alpha}{L}$, the relations (4.32) can be used to describe the functions $R_{\alpha,n}$ and $\mathcal{V}_{\alpha,n}$ at strong coupling. In this regime, the non-perturbative corrections to (4.32) are exponentially suppressed at large $\hat{\lambda}$, while they become significant in the transition region where $\hat{\lambda} = \mathcal{O}(1)$.

The situation changes significantly for small a, or equivalently, in the long-quiver limit $L \to \infty$. First, the expansion coefficients in the perturbative functions (4.33) become singular as

$a \to 0$. Second, the parameter $\Lambda_-^2 = \mathrm{e}^{-8\pi\hat{\lambda}a}$ approaches 1 in the limit $a \to 0$. Consequently, the non-perturbative corrections to (4.32) proportional to powers of Λ_-^2, become indistinguishable from the perturbative contributions. Moreover, the functions (4.34) develop $1/a$ poles, similar to their perturbative counterparts in (4.33). Therefore, determining the functions $R_{\alpha,n}$ and $\mathcal{V}_{\alpha,n}$ in the long-quiver limit $L \to \infty$ requires the resummation of an infinite series of non-perturbative contributions in (4.32). As we will shortly see, this scenario mirrors the resummation we performed in the weak coupling regime (4.9).

4.2.2 The long-quiver limit

The relations (4.32) are valid at strong coupling for arbitrary $a = \frac{\alpha}{L}$ and n. Our next goal is to examine their behaviour in the long-quiver limit $L \to \infty$, or equivalently, $a \to 0$. As follows from (4.28), the functions $I_n(a)$ diverge in this limit as

$$I_n(a) = \frac{(-1)^{n+1}}{(2\pi a)^{2n-1}} + \mathcal{O}\left(a^2\right) . \tag{4.35}$$

Substituting this relation into (4.33) and (4.34), we find that the strong coupling expansion effectively runs in powers of $1/(a\hat{\lambda})$. This suggests to consider the following double scaling limit

$$L \to \infty\,, \qquad \hat{\lambda} \to \infty\,, \qquad \xi = \frac{2\pi\alpha\hat{\lambda}}{L} = \text{fixed}\,. \tag{4.36}$$

As a non-trivial test, we verify that the expressions in (4.32) approach a finite value in this regime. In particular, the function $R_{\alpha,n}$ takes the following form

$$\widetilde{R}_{\alpha,n} = (n-1)n\,\xi^{-2}\,\widetilde{R}^{(0,0)}\left[1 + \mathrm{e}^{-2\xi}\,\widetilde{R}^{(1,0)} + \mathcal{O}(\mathrm{e}^{-4\xi})\right], \tag{4.37}$$

where we introduced a tilde to indicate that this relation only holds in the limit (4.36). Since the parameter $\Lambda_+^2 = \mathrm{e}^{-8\pi\hat{\lambda}(1-a)}$ vanishes in the limit (4.36), we find that the non-perturbative corrections to (4.37) run in powers of $\Lambda_-^2 = \mathrm{e}^{-2\xi}$ with coefficient functions expressed in terms of asymptotic series in $1/\xi$. For instance,

$$\begin{aligned}
\widetilde{R}^{(0,0)} &= 1 - \frac{(n-1)}{\xi} + \frac{1}{4\xi^2}(n-1)(2n-3) - \frac{1}{32\xi^3}(n-1)(2n-5)(2n-3) + \mathcal{O}(1/\xi^4)\,, \\
\widetilde{R}^{(1,0)} &= 2i(-1)^n(n-1)\left[\frac{1}{\xi} + \frac{1}{8\xi^2}(4n^2-8n+7) + \frac{1}{128\xi^3}(4n^2-8n+7)(4n^2-8n+11) + \mathcal{O}\left(1/\xi^4\right)\right].
\end{aligned} \tag{4.38}$$

It follows from (4.37) and (4.38) that the function $\widetilde{R}_{\alpha,n}$ has a different behaviour at small and large ξ. Indeed, at large ξ, the non-perturbative corrections in (4.37) are exponentially suppressed and the resulting expansion of $R_{\alpha,n}$ is in one-to-one correspondence with the conventional $1/\hat{\lambda}$ expansion of the AdS/CFT duality. This regime describes the correlation function (3.5a) of twisted operators (3.3) at strong coupling in a quiver theory with a large number of nodes. At small ξ, all terms inside the brackets of (4.37) become equally important, requiring the resummation of an infinite series of non-perturbative corrections to find $R_{\alpha,n}$ in this limit.

Resummation in the long-quiver limit

The resummation of (4.37) in the small-ξ limit can be performed by observing that the functions (4.32) can be found in a closed form for arbitrary ξ. The key observation is that, in the dual lattice model description of the quiver theory, the limit (4.36) corresponds to describe excitations that propagate across the quiver diagram with vanishing quasimomentum p_α (3.12b). As a result, we can simplify the integral representation of the matrix (3.36) by replacing the symbol $\chi(x)$ (3.35) by its leading behaviour at large $\hat{\lambda}$ [28, 70], *i.e.*

$$s_\alpha \chi\left(\frac{\sqrt{t}}{2\hat{\lambda}}\right) \to -\frac{(2\xi)^2}{t}\,, \tag{4.39}$$

where we used (3.35) and took the limit (4.36). Applying this transformation to (3.36), the matrix K_ℓ becomes tridiagonal and its Fredholm determinant (3.60) is given by [70]

$$\widetilde{\mathcal{F}}_\ell = \log\left(\Gamma(\ell)\,\xi^{1-\ell}\,\mathrm{I}_{\ell-1}(2\xi)\right)\,, \tag{4.40}$$

where $\mathrm{I}_{\ell-1}(2\xi)$ is a modified Bessel function of the first kind. Finally, we substitute (4.40) into (3.70) and we find that

$$\begin{aligned}\widetilde{R}_{\alpha,n} &= (n-1)n\,\frac{\mathrm{I}_n(2\xi)}{\xi^2\mathrm{I}_{n-2}(2\xi)}\,,\\ \widetilde{\mathcal{V}}_{\alpha,n} &= \sqrt{\frac{n-1}{n}}\left[\frac{\mathrm{I}_{n-1}^2(2\xi)}{\mathrm{I}_{n-2}(2\xi)\mathrm{I}_n(2\xi)}\right]^{1/2}.\end{aligned} \tag{4.41}$$

These relations hold in the double scaling limit (4.36) for arbitrary ξ. The dependence of the functions (4.41) on ξ is shown in Fig. 4.2. At large ξ, they behave differently, while for small ξ they approach the same value.

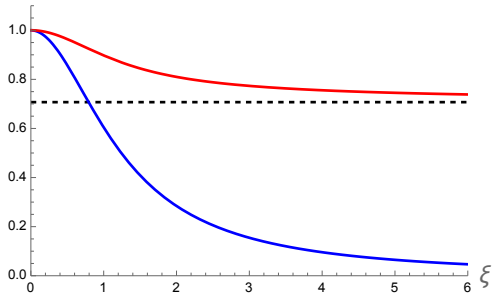

Figure 4.2: The dependence of the functions $\widetilde{R}_{\alpha,n}$ (blue curve) and $\widetilde{\mathcal{V}}_{\alpha,n}$ (red curve) defined in (4.41) on ξ for $n = 2$. The dashed line indicates the limiting value of $\widetilde{\mathcal{V}}_{\alpha,n}$ for $\xi \to \infty$.

Replacing the Bessel functions in (4.41) by their asymptotic behaviour at infinity, we verified that the expansion of $\widetilde{R}_{\alpha,n}$ at large ξ is in agreement with (4.37) and (4.38). Similarly, the large-ξ expansion of $\widetilde{\mathcal{V}}_{\alpha,n}$ coincides with (4.32) in the limit (4.36).

At small ξ, or equivalently for $L \gg \hat{\lambda}$, we find from (4.41)

$$\begin{aligned}\widetilde{R}_{\alpha,n} &= 1 - \frac{2\xi^2}{(n-1)(n+1)} + \frac{(5n+1)\xi^4}{(n-1)^2 n(n+1)(n+2)} + \mathcal{O}(\xi^6)\,,\\ \widetilde{\mathcal{V}}_{\alpha,n} &= 1 - \frac{\xi^2}{(n-1)n(n+1)} + \frac{3(2n+1)\xi^4}{2(n-1)^2 n(n+1)^2(n+2)} + \mathcal{O}(\xi^6)\,.\end{aligned} \tag{4.42}$$

It is interesting to note that, although this relation was derived in the strong coupling regime, the asymptotic behaviour of the functions $\widetilde{R}_{\alpha,n}$ and $\widetilde{\mathcal{V}}_{\alpha,n}$ as $\xi \to 0$ closely resembles the weak coupling expansion (4.3). This universality arises because, in both regimes, the coupling constant is much smaller than the quiver length. Consequently, for $L \gg \hat{\lambda}$, the correlation functions (4.11) are expected to exhibit the same exponential behaviour (4.16) with respect to the distance between sites, regardless of the value of the coupling constant. We explicitly demonstrate this in the next section and calculate the mass scale $\mu_n(\hat{\lambda})$ in the strong coupling regime.

4.2.3 Heavy operators limit

Following the analysis of the weak-coupling regime, we discuss the heavy-operator limit $n \gg 1$ (3.71) before entering the analysis of the correlations in the long-quiver limit.

To begin with, we observe from (4.33) that, at large n, the strong coupling expansion of the perturbative functions $R^{(0,0)}$ and $\mathcal{V}^{(0,0)}$ runs in powers of $\frac{n}{\hat{\lambda}}$. As a result, we find it convenient to consider the double scaling limit

$$n \to \infty\,, \qquad \hat{\lambda} \to \infty\,, \qquad \hat{n} = \frac{n}{2\hat{\lambda}} = \text{fixed}\,. \tag{4.43}$$

It follows from (4.32) that for finite $a = \frac{\alpha}{L}$ the non-perturbative corrections vanish in this limit and the functions $R_{\alpha,n}$ and $\mathcal{V}_{\alpha,n}$ only receive perturbative contributions. In particular, we use (4.32) and (4.33) to obtain in the limit (4.43)

$$\log \hat{R}_{\alpha,n} = 2\log \hat{n} - \log s_\alpha - 2\hat{n} I_1(a) - \frac{1}{3}\hat{n}^3 I_2(a) + \mathcal{O}(\hat{n}^5)\,, \tag{4.44}$$

where the hat on the left-hand side indicates that this relation holds in the regime (4.43).

The subleading terms in (4.44) involve odd powers of $\hat{n}$ accompanied by functions $I_k(a)$ defined in (4.28). Following [106], we can show that the series in (4.44) admits the following compact integral representation

$$\begin{aligned}\log \hat{R}_{n,\alpha} &= -\frac{2\hat{n}}{\pi}\int_{\hat{n}}^{\infty} \frac{dz}{z}\frac{\log(1 - s_\alpha \chi(z))}{\sqrt{z^2 - \hat{n}^2}} + \mathcal{O}(1/\hat{\lambda}) \\ &= -\frac{2\hat{n}}{\pi}\int_{\hat{n}}^{\infty} \frac{dz}{z\sqrt{z^2 - \hat{n}^2}} \log\left(\frac{\cosh z - \cos(2\pi a)}{\cosh z - 1}\right) + \mathcal{O}(1/\hat{\lambda})\,,\end{aligned} \tag{4.45}$$

where we replaced $\chi(z)$ and s_α by their expressions (3.35) and (3.13). The corresponding expression for the function $\hat{\mathcal{V}}_{n,\alpha}(\hat{\lambda})$ can be obtained by the relation (3.69), *i.e.*

$$\hat{\mathcal{V}}_{\alpha,n} = 1 - \frac{1}{2\pi\hat{\lambda}}\int_{\hat{n}}^{\infty} \frac{dz}{\sqrt{z^2 - \hat{n}^2}} \frac{\sin^2(\pi a)\coth(z/2)}{\cosh z - \cos(2\pi a)} + \mathcal{O}(1/\hat{\lambda}^2)\,. \tag{4.46}$$

We stress that the previous expressions are valid up to corrections that vanish in the limit (4.43).

The relations (4.45) and (4.46) hold in the limit (4.43) for arbitrary $a = \frac{\alpha}{L}$. For $a = \frac{1}{2}$, or equivalently $s_\alpha = 1$, the relation (4.45) coincides with the result derived in [102]. For $a = 0$ both functions coincide with their value in a free theory, $\hat{R}_{0,n} = \hat{\mathcal{V}}_{0,n} = 1$, in agreement with the properties of untwisted operators.

Let us conclude the analysis by examining the behaviour of the functions (4.45) and (4.46) in the limit $L \to \infty$. This regime is closely related to the long-quiver limit (4.36). We therefore expect that the relations (4.45) and (4.46) have to match (4.41) upon appropriate identification of the parameters. To observe this agreement, it is important to note that (4.41) was derived

at large coupling $\hat{\lambda}$ with n kept fixed. To reconcile this with the regime specified in (4.43), we consider n to be large but much smaller than $\hat{\lambda}$. This corresponds to the limit of small $\hat{n}$ in (4.43), where the dominant contribution to (4.45) and (4.46) comes from integration around $z = \hat{n}$. We find at small $a = \frac{\alpha}{L}$

$$\begin{aligned}\hat{R}_{n,\alpha} &= \left[\frac{2}{1+\sqrt{1+4\xi^2/n^2}}\right]^2, \\ \hat{\mathcal{V}}_{\alpha,n} &= \left[\frac{n-1}{n}+\frac{1}{n\sqrt{1+4\xi^2/n^2}}\right]^{1/2},\end{aligned} \tag{4.47}$$

where ξ is defined in (4.36). This relation holds for $1 \ll n \ll \hat{\lambda}$ and $a \ll 1$ with fixed ratio $\frac{\xi}{n} = 2\pi a\frac{\hat{\lambda}}{n}$.

It is straightforward to verify that the expansion of (4.47) for small and large $\frac{\xi}{n}$ aligns with the relations (4.42) and (4.38), respectively, up to subleading corrections suppressed by powers of $\frac{1}{n}$ and $\frac{1}{\xi}$. For arbitrary $\xi = \mathcal{O}(n)$ and large n, the equivalence of the relations (4.41) and (4.47) can be established by the asymptotic behaviour of the Bessel functions in (4.41) at large order.

4.3 Correlations at strong coupling

We now turn our attention to the strong coupling behaviour of correlations between different nodes of the lattice model in the long-quiver limit. According to (4.11), these correlations are encoded in the function f_Y, which is given by the sum of $R_{\alpha,n}$ over possible values of the quasimomentum p_α. In particular, $R_{\alpha=0,n}$ is protected, while for $1 \le \alpha \le L-1$ the ratio $R_{\alpha,n}$ admits the strong coupling expansion (4.32). Substituting $R_{\alpha,n}$ in (4.11) with its leading behaviour at strong coupling (4.32), we get

$$f_Y = \frac{1}{L}+\frac{1}{L}\sum_{\alpha=1}^{L-1} e^{\frac{2\pi i\alpha}{L}Y}\frac{(n-1)n}{4\hat{\lambda}^2 s_\alpha}+\mathcal{O}(1/\hat{\lambda}^3), \tag{4.48}$$

where the first term on the right-hand side comes from $\alpha = 0$.

Replacing s_α with its definition (3.13), we find that at large L the sum (4.48) receives the dominant contribution from $\alpha \ll L$ and $(L-\alpha) \ll L$. Going through the calculation, we find

$$f_Y = \frac{1}{L}+\frac{(n-1)nL}{4\hat{\lambda}^2}\left[\frac{1}{3}-\frac{2Y(L-Y)}{L^2}\right]+\mathcal{O}(1/\hat{\lambda}^3). \tag{4.49}$$

We observe that, at large $\hat{\lambda}$ and L, the second term on the right-hand side behaves as $\mathcal{O}(L/\hat{\lambda}^2)$. Furthermore, taking into account (4.32), we find from the original definition of the function f_Y (4.11) that the subleading corrections to (4.49) scale as $\mathcal{O}(L^k/\hat{\lambda}^{k+1})$. Consequently, the strong coupling expansion (4.49) is well-defined for $L < \hat{\lambda}$. In this regime, (4.49) reveals that correlations between different sites of the lattice grow polynomially with their separation Y. This means that all the sites of the lattice model are equally correlated and interactions are not short-ranged. As a result, we do not expect the emergence of an additional dimension.

In the opposite limit, for $L > \hat{\lambda}$, the non-perturbative corrections in (4.32) become comparable to the $1/\hat{\lambda}$ contributions and the strong coupling expansion diverges. Computing the function

f_Y for $L > \hat{\lambda}$ requires a resummation of the series (4.49) to all orders in $1/\hat{\lambda}$. To start with, we use (3.55) to rewrite the sum in (4.11) in a more symmetric form

$$f_Y = \frac{1}{L} \sum_{\alpha=-L/2}^{L/2-1} \mathrm{e}^{\frac{2\pi i \alpha}{L} Y} R_{\alpha,n}(\hat{\lambda}) \,. \tag{4.50}$$

At large $\hat{\lambda}$ and L, the dominant contribution to the sum comes from small $\frac{\alpha}{L}$. In this region, the function $R_{\alpha,n}$ can be replaced by its asymptotic expression (4.41) in the limit (4.36), *i.e.*

$$f_Y = \frac{(n-1)n}{\hat{\lambda}^2 L} \sum_{\alpha=-L/2}^{L/2-1} \mathrm{e}^{ip_\alpha Y} \frac{\mathrm{I}_n(2\hat{\lambda}p_\alpha)}{p_\alpha^2 \, \mathrm{I}_{n-2}(2\hat{\lambda}p_\alpha)} \,, \tag{4.51}$$

where the sum runs over possible values of the quasimomentum in the first Brillouin zone $-\pi \le p_\alpha < \pi$. To be precise, the sum should be restricted to $|\frac{\alpha}{L}| \ll 1$, which corresponds to $|p_\alpha| \ll 1$. However, at large $\hat{\lambda}$, the contribution from $p_\alpha = \mathcal{O}(1)$ to (4.51) is suppressed by a factor of $1/\hat{\lambda}^2$ compared to contribution from small p_α and consequently, it does not affect the leading behaviour of (4.51).

The relation (4.51) holds for large $\hat{\lambda}$ and L with their ratio $\frac{L}{\hat{\lambda}}$ held fixed. Consequently, it can be used to interpolate between $L \gg \hat{\lambda}$ and $L \ll \hat{\lambda}$. In the latter case, by isolating the $\alpha = 0$ term in the sum (4.51) and replacing the ratio of the Bessel functions for $\alpha \neq 0$ with their expansion at large argument, we arrive at (4.49). Conversely, for $L \gg \hat{\lambda}$, the sum in (4.51) becomes independent of L and can be approximated by an integral over the quasimomentum

$$f_Y = \frac{(n-1)n}{\hat{\lambda}^2} \int_{-\pi}^{\pi} \frac{dp}{2\pi} \mathrm{e}^{ipY} \frac{\mathrm{I}_n(2\hat{\lambda}p)}{p^2 \, \mathrm{I}_{n-2}(2\hat{\lambda}p)} \,. \tag{4.52}$$

This relation is valid at strong coupling for $\hat{\lambda} \ll L$ as $L \to \infty$.

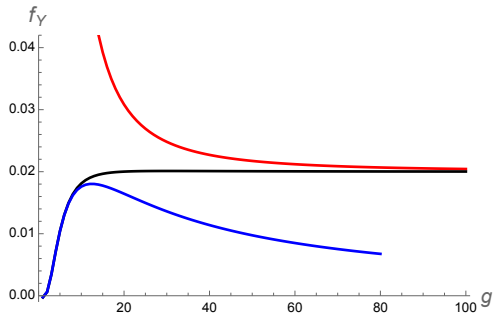

Figure 4.3: The dependence of the function f_Y (black line) defined in (4.51) on the coupling constant $1 \le \hat{\lambda} \le 100$ for $L = 50$, $Y = 10$ and $n = 2$. The red and blue lines represent its asymptotic expressions for $\hat{\lambda} \gg L$ and $\hat{\lambda} \ll L$ given by (4.49) and (4.52), respectively.

The dependence of the function (4.51) on the coupling constant is shown in Fig. 4.3. We observe that it agrees with the asymptotic expressions (4.49) and (4.52) for $\hat{\lambda} \gg L$ and $\hat{\lambda} \ll L$, respectively.

4.3.1 Correlations in the long-quiver limit

We showed in Sect. 4.1 that the function f_Y decreases exponentially with the distance Y (4.51) at weak coupling. Moreover, in the long-quiver limit, it collapses to a free one-dimensional

massive propagator $D(y,\mu_n)$ (4.22). This behaviour of the function f_Y is intimately related to the fact that $\hat{\lambda} \ll L$.

At strong coupling, the situation changes drastically. Indeed, our analysis emphasises that the behaviour of f_Y crucially depends on the ratio $\frac{L}{\hat{\lambda}}$. For $L \ll \hat{\lambda}$, the function f_Y is described by (4.49). It depends on the quiver length L and its leading $\mathcal{O}(1/\hat{\lambda}^2)$ correction displays polynomial dependence on Y. This implies that correlations in the lattice model spread uniformly and the quiver theory remains a strongly coupled four-dimensional model. Conversely, for $L \gg \hat{\lambda}$, we apply (4.52) and change the integration variable $p \to p/(2\hat{\lambda})$ to find at large $\hat{\lambda}$

$$f_Y = \frac{2(n-1)n}{\hat{\lambda}} \int_{-\infty}^{\infty} \frac{dp}{2\pi} e^{ipy} \frac{\mathrm{I}_n(p)}{p^2\,\mathrm{I}_{n-2}(p)}\,, \tag{4.53}$$

where $y = Y/(2\hat{\lambda})$ is kept fixed in the large–$\hat{\lambda}$ limit.

The relation (4.53) should be compared with the analogous result (4.21) in the weak coupling regime. In both cases, the leading large-Y behaviour of the integral over p is determined by the singularity of the integrand closest to the origin. At weak coupling, this singularity arises from a pole at $p = i\mu_n$, where μ_n is the weak coupling mass scale (4.16). At strong coupling, the singularities originate from the zeros of $\mathrm{I}_{n-2}(p)$ in the integrand of (4.53). They are located along the imaginary axis at $p = im_k$, where m_k is the k-th zero of the Bessel function $J_{n-2}(x)$

$$J_{n-2}(m_k) = 0\,, \qquad (k = 1, 2, \dots)\,. \tag{4.54}$$

To avoid clutter, we do not display the dependence of m_k on n.

To calculate the integral (4.53), it is convenient to express the ratio of Bessel functions in terms of an infinite sum over poles at $p = \pm i m_k$

$$\frac{\mathrm{I}_n(p)}{p^2\mathrm{I}_{n-2}(p)} = \sum_{k=1}^{\infty} \frac{4(n-1)}{m_k^2\left(p^2+m_k^2\right)}\,. \tag{4.55}$$

Each term on the right-hand side contains the factor of $(p^2+m_k^2)^{-1}$, describing a one-dimensional Euclidean propagator (4.10) of a particle with momentum p and mass m_k. Substituting (4.55) into (4.53) and closing the integration contour in the upper half-plane, we find for $y > 0$

$$f_Y = \frac{4n(n-1)^2}{\hat{\lambda}} \sum_{k=1}^{\infty} \frac{e^{-ym_k}}{m_k^3}\,. \tag{4.56}$$

At large y, the sum is dominated by the term involving the minimal mass m_1, *i.e.*

$$f_Y \sim e^{-ym_1} = e^{-Y\frac{m_1}{2\hat{\lambda}}}\,. \tag{4.57}$$

Remarkably, this relation exhibits the same exponential dependence on the distance between the nodes Y as in the weak coupling regime (4.16). According to (4.57), the corresponding mass scale μ_n at strong coupling is given by

$$\mu_n = \frac{m_1}{2\hat{\lambda}}\,, \tag{4.58}$$

which decreases as $\hat{\lambda} \to \infty$.

The function (4.56) describes the correlation function (4.11) of two operators inserted at different nodes $Y = |I - J|$ in the limit $L \gg \hat{\lambda} \gg 1$. Viewed through the lens of the quiver lattice model, the exponential suppression of correlations (4.57) at large separations Y indicates

the presence of short-ranged interactions, with correlation length $1/\mu_n = \mathcal{O}(\hat{\lambda})$. This result is in agreement with the findings of [70] and suggests the emergence of an additional dimension through a local description of these interactions.

Before turning our attention to this aspect, we examine the relation (4.56) in the limit (4.43), where the scaling dimensions of the operators in (4.11) become large. The dependence on n enters the sum (4.56) through the zeros of the Bessel function (4.54). In the limit of large n, the zeros of the Bessel functions $J_{n-2}(x)$ have the following properties. The minimal zero m_1 is given by (see [116], Eq. (10.21.32))

$$m_1 = n + c\, n^{1/3} + \mathcal{O}(n^0)\,, \tag{4.59}$$

where c is a real positive number, while the remaining zeros approach a nearly uniform distribution with a spacing of approximately π. Taking these properties into account we get from (4.56)

$$f_Y = \frac{4}{\hat{\lambda}} e^{-yn} + \cdots = \frac{4}{\hat{\lambda}} e^{-Y\frac{n}{2\hat{\lambda}}} + \dots\,, \tag{4.60}$$

where the dots denote subleading corrections suppressed by powers of $1/n$ and e^{-y}. The corresponding mass scale (4.58) approaches a finite value in the limit (4.43)

$$\mu_n = \frac{n}{2\hat{\lambda}} = \hat{n}\,. \tag{4.61}$$

Thus, for the operators with large scaling dimension the correlation length $1/\mu_n$ remains finite at strong coupling.

4.4 Constructing a five-dimensional theory

In the previous sections, we computed the correlation f_Y (4.11) between two different nodes of the quiver diagram in Fig. 3.1 across the different regimes (3.71). We determined the dependence of f_Y on the node separation Y and showed that in the long-quiver limit $L \to \infty$, f_Y approaches a finite value both at weak- and strong-coupling. This suggests that f_Y can be interpreted as a correlation function in a one-dimensional field theory, which arises as an effective description of the lattice model when $L \to \infty$. Our final goal is to identify the properties of this theory.

At weak coupling, where $\lambda \to 0$, f_Y reduces to a massive free propagator on the real line (4.22). This means that the lattice model is essentially described by a free model at the leading order of the long-quiver limit. Moreover, combining (4.22) with (4.11), we can identify the function $G_n(y)$ (3.75) at weak coupling, *i.e.*

$$G_n(y) \sim \mathcal{G}_n D(y, \mu_n)\,, \tag{4.62}$$

where $\mathcal{G}_n$ is the colour factor introduced in (3.54), $D(x,m)$ is the massive one-dimensional Feynman propagator defined in (4.10), while μ_n is the weak-coupling mass scale (4.16).

The situation changes drastically at strong coupling, where the two-point function f_Y is given by a linear combination of one-dimensional free propagators (4.56). This structure suggests to introduce a spectral density

$$\rho_n(\mu^2) = \frac{4(n-1)}{\mu^2} \sum_{k=1}^{\infty} \delta(\mu^2 - m_k^2)\,, \tag{4.63}$$

where the sum runs over zeros of the Bessel function (4.54). Moreover, by examining the leading asymptotic behaviour on both sides of (4.55) for $p \to \infty$, we find that ρ_n is properly normalized

$$\int_0^\infty d\mu^2 \rho_n(\mu^2) = 1\,. \tag{4.64}$$

As a result, the two-point function f_Y (4.56) takes the form of a *Källén-Lehmann representation* [117]

$$f_n(y) = \frac{2n(n-1)}{\hat{\lambda}} \int_0^\infty d\mu^2 \rho_n(\mu^2) D(y,\mu)\,, \tag{4.65}$$

where the masses of the excited states are identified with the zero of the Bessel functions (4.54). As a result, at strong coupling the effective description is interacting and by substituting the previous relation into (3.75), we determine the function $G_n(y)$, *i.e.*

$$G_n(y) \sim \int_0^\infty d\mu^2 \rho_n(\mu^2) D(y,\mu)\,. \tag{4.66}$$

4.5 Three-point functions

So far our discussion was restricted to the two-point functions (4.11). We observed that in the long-quiver limit, these observables behave differently at weak and strong coupling. In the latter case, we showed that the effective theory describing the lattice model as $L \to \infty$ is interacting and we determined the spectrum of excitations. To gain some further intuition into the interaction structures of this effective field theory, we extend analysis to the three-point function (3.7b) in the long-quiver limit at strong coupling.

Applying the discrete Fourier transform (3.3) to each operator in (3.5b), we obtain the following representation for the three-point function in the long-quiver limit

$$\left\langle O_{n_1}(x_1,y_1) O_{n_2}(x_2,y_2) \bar{O}_{n_3}(x_3,y_3) \right\rangle = \mathcal{G}_{n_1 n_2 n_3} \frac{\sqrt{n_1 n_2 n_3}}{N} \frac{f_{\mathbf{n}}(y_1,y_2,y_3)}{|x_1-x_3|^{2n_1}|x_2-x_3|^{2n_2}}\,. \tag{4.67}$$

The normalization factor $\mathcal{G}_{n_1 n_2 n_3} = \delta_{n_1+n_2,n_3}\sqrt{\mathcal{G}_{n_1}\mathcal{G}_{n_2}\mathcal{G}_{n_3}}$, where $\mathcal{G}_n$ is defined in (3.54), is non-vanishing only when $n_3 = n_1 + n_2$, while the function $f_{\mathbf{n}}(y_1,y_2,y_3)$ depends on the separations between the operators $y_{ij} = y_i - y_j$ and their scaling dimensions $\mathbf{n} = (n_1,n_2,n_3)$. In particular, $f_{\mathbf{n}}$ arises from the long-quiver limit of (3.70c), *i.e.*

$$f_{\mathbf{n}}(y_1,y_2,y_3) = \frac{1}{L^2} \sum_{\alpha_1,\alpha_2=0}^{L-1} \mathrm{e}^{\frac{2\pi i}{L}(\alpha_1 Y_{13} + \alpha_2 Y_{23})} \prod_{i=1}^{3} \mathrm{e}^{\mathcal{F}_{n_i} - \mathcal{F}_{n_i-1}}\,, \tag{4.68}$$

where we keep fixed $Y_{ij} = I_i - I_j = 2\hat{\lambda}(y_i - y_j)$, and we recall that $\mathcal{F}_{n_i}$ (3.60) depends on the quasimomenta $p_i = 2\pi\frac{\alpha_i}{L}$ through the function s_α (3.13). Following the approach we developed for the two-point functions, we can replace the sums in (4.68) by integrals over a continuum variable p as follows

$$f_{\mathbf{n}}(y_1,y_2,y_3) = \int_{-\infty}^{\infty} dy_0\, G_{n_1}(y_1-y_0) G_{n_2}(y_2-y_0) G_{n_3}(y_3-y_0)\,. \tag{4.69}$$

The function $G_n(y)$ is given by a Fourier integral

$$G_n(y) = \int_{-\pi}^{\pi} \frac{dp}{2\pi} \mathrm{e}^{ipY} e^{\widetilde{\mathcal{F}}_n - \widetilde{\mathcal{F}}_{n-1}} = \frac{n-1}{\hat{\lambda}} \int_{-\infty}^{\infty} \frac{dp}{2\pi} \mathrm{e}^{ipy} \frac{\mathrm{I}_{n-1}(p)}{p\,\mathrm{I}_{n-2}(p)}\,, \tag{4.70}$$

where in the second relation we replaced $\widetilde{\mathcal{F}}_n$ with its expression (4.40), changed the integration variable as $p \to p/(2\hat{\lambda})$ and took the limit of large $\hat{\lambda}$. The integral in (4.70) is similar to that in (4.53) and it can be evaluated in the same manner. We use the properties of the Bessel function to replace in (4.70)

$$\frac{\mathrm{I}_{n-1}(p)}{p\mathrm{I}_{n-2}(p)} = \sum_{k\geq 1} \frac{2}{p^2+m_k^2}\,, \tag{4.71}$$

where the sum runs over zeros of the Bessel function (4.54). In this way, we obtain the following representation of the function (4.70)

$$\begin{aligned} G_n(y) &= \frac{n-1}{\hat{\lambda}} \sum_{k=1}^{\infty} \frac{e^{-m_k|y|}}{m_k} \\ &= \frac{1}{2\hat{\lambda}} \int_0^{\infty} d\mu\, \mu^2\, \rho_n(\mu^2) D(y,\mu)\,, \end{aligned} \tag{4.72}$$

where the spectral density ρ_n is given by (4.63), while $D(x,m)$ is the usual massive propagator on the real line (4.10). Similar to (4.57), the leading behaviour of $G_n(y)$ at large y is determined by the minimal zero m_1 of the Bessel function (4.54)

$$G_n(y) \sim \frac{n-1}{\hat{\lambda}\nu_n} \mathrm{e}^{-\nu_n|y|}\,, \tag{4.73}$$

where $\nu_n = m_1$ depends on n (see (4.59)). Substituting this relation into (4.69) we find that the three-point function (4.69) rapidly decreases for $y_1 \gg y_2, y_3$ as follows

$$f_{\mathbf{n}}(y_1,y_2,y_3) \sim \mathrm{e}^{-\nu\, y_1}\,, \tag{4.74}$$

where $\nu = \min(\nu_{n_1}, \nu_{n_2}+\nu_{n_3})$.

The relations (4.73) and (4.74) are in agreement with our expectations that, due to a finite mass of excitations propagating in the fifth dimension, the correlation functions should be exponentially decreasing functions of the separations of the operators.

4.6 Dual holographic description

The $\mathcal{N}=2$ quiver theories under examination admit a dual holographic description in terms of an $\mathrm{AdS}_5 \times S^5$ geometry [118,119]. We now want to compare the results of our analysis at strong coupling with those previously obtained using the AdS/CFT correspondence.

The correlation functions (3.5) are holographically described by the dynamics of fields propagating in the AdS space [6]. The effective action for the supergravity modes dual to the operators $T_{\alpha,n}(x)$ (3.3) was derived in [66,82,119,120]. Using this effective action, the two- and three-point correlation functions (3.5) were computed in [66] in terms of effective Witten diagrams. The resulting expression for the OPE coefficients (3.52) obtained in the AdS/CFT approach is [3]

$$C_{\alpha_i,n_i} = \frac{\sqrt{(n_1-1)(n_2-1)(n_3-1)}}{\sqrt{L}N} + O(1/\hat{\lambda})\,, \tag{4.75}$$

[3] Strictly speaking, this relation only holds for the twisted operators with $\alpha_i \neq 0$. For the untwisted operators with $\alpha_i = 0$ one has to replace $\sqrt{n_i-1} \to \sqrt{n_i}$ in (4.75).

where the last term describes the subleading correction coming from the stringy modes. This relation aligns with the analogous result (3.52), derived from localization, after replacing the functions $\mathcal{V}_{\alpha_i,n_i}$ (3.69) with their leading behaviour at strong coupling (4.32).

An important question is whether (4.75) provides a good approximation for the OPE coefficients at strong coupling. We observe that the leading term in (4.75) is independent of the quasimomenta $p_{\alpha_i} = 2\pi\alpha_i/L$ of the operators. This dependence arises when we account for the subleading corrections to (4.75) in $1/\hat{\lambda}$. We demonstrated in the previous sections that for small values of the quasimomenta, or equivalently in the large L limit, these corrections run in powers of $1/(\hat{\lambda}p_\alpha)$. As a result, for $L \gg \lambda$, the subleading corrections become comparable with the leading term in (4.75), thus invalidating the strong coupling expansion of C_{α_i,n_i}.

Applying (4.41), we find that the structure constants (3.52) are given in the long-quiver limit by

$$C_3 = \frac{\sqrt{(n_1-1)(n_2-1)(n_3-1)}}{\sqrt{L}N}\prod_{i=1}^{3}\left[\frac{I_{n-1}^2(2\xi_i)}{I_{n-2}(2\xi_i)I_n(2\xi_i)}\right]^{1/2}, \tag{4.76}$$

where $\xi_i = 2\pi\alpha_i\hat{\lambda}/L$. As we previously explained, the last factor in this relation takes into account both perturbative corrections in $1/\hat{\lambda}$ as well as non-perturbative exponentially small contributions.

The relation (4.75) corresponds to the limit of (4.76) when all ξ_i are sent to infinity. Another interesting feature of the relation (4.76) is that for $\alpha_i \to 0$ (or equivalently $\xi_i \to 0$) it correctly reproduces the OPE coefficient for the untwisted operators

$$\lim_{\alpha_i\to 0} C_3 = \frac{\sqrt{n_1n_2n_3}}{\sqrt{L}N}\,. \tag{4.77}$$

In the dual holographic description, the last factor in (4.76) should arise from the effective action of the Kaluza-Klein (KK) mode η_{α_i,n_i} dual to the operators $T_{\alpha_i,n_i}(x)$ (3.3). We can use the results of the previous sections to construct this action.

In the long-quiver limit, the Q_L theory living at the boundary of the AdS_5 becomes effectively five-dimensional. This suggests to interpret the quasimomentum p_α carried by the conformal primary operator as a momentum in the fifth dimension $T_{\alpha_i,n_i} \to T_{n_i}(p_{\alpha_i})$. Consequently, the KK modes also carry this momentum $\eta_{\alpha_i,n_i} \to \eta_{n_i}(p_{\alpha_i})$ and their effective action depends on p_{α_i}.

Due to the factorized dependence of the two- and three-point correlation functions on the quasimomentum and the space-time coordinates of operators, the dynamics of the KK modes in the fifth dimension is decoupled from the one in AdS_5. This allows us to neglect the dependence of $T_n(p)$ and $\eta_n(p)$ on the AdS coordinates and concentrate on their dependence on p. The resulting effective action of the KK modes takes the form

$$S_{\text{eff}} = S_{\text{bdry}} + S^{(2)} + S^{(3)} + \dots\,. \tag{4.78}$$

The first term describes the coupling of the local operators with the KK modes at the boundary of the AdS space

$$S_{\text{bdry}} = \sum_n \int \frac{dp}{2\pi}\left[\bar{\eta}_n(p)T_n(-p) + \bar{T}_n(p)\eta_n(-p)\right]. \tag{4.79}$$

The two additional terms in (4.78) are quadratic and cubic in the KK modes, respectively. Their general form, consistent with the conservation of $U(1)$ charge and momentum along the fifth

dimension, is given by

$$S^{(2)} = \sum_n \int \frac{dp}{2\pi} S(p)\eta_n(p)\bar{\eta}_n(-p)\,, \tag{4.80a}$$

$$S^{(3)} = \sum_{n_i} \int \prod_{i=1}^{3} \frac{dp_i}{2\pi} S(p_1,p_2,p_3)\eta_{n_1}(p_1)\eta_{n_2}(p_2)\bar{\eta}_{n_3}(p_3)\delta_{n_1+n_2,n_3}\delta(p_1+p_2+p_3) + \text{c.c.}\,, \tag{4.80b}$$

where the dependence of $S(p)$ and $S(p_1,p_2,p_3)$ on the charges n_i is tacitly assumed. We would like to emphasise that these relations hold for small values of the momenta p_i.

The $S-$functions in (4.80) can be determined by comparing the correlators $\langle 0|T_{n_1}(p_1)T^\dagger_{n_2}(p_2)|0\rangle$ and $\langle 0|T_{n_1}(p_1)T_{n_2}(p_2)T^\dagger_{n_3}(p_3)|0\rangle$ computed within the effective theory (4.78) with their expressions predicted by the localization in the long-quiver limit. This procedure yields

$$S(p) = \omega^2 N^2 L \frac{(n-1)\mathrm{I}_n(2\hat{\lambda}p)}{(\hat{\lambda}p)^2\,\mathrm{I}_{n-2}(2\hat{\lambda}p)}\,, \tag{4.81a}$$

$$S(p_1,p_2,p_3) = \omega^3 N^2 L \prod_{i=1}^{3} \frac{(n_i-1)\mathrm{I}_{n_i-1}(2\hat{\lambda}p_i)}{\hat{\lambda}p_i\,\mathrm{I}_{n_i-2}(2\hat{\lambda}p_i)}\,, \tag{4.81b}$$

where ω is a normalization factor. The OPE coefficients (4.76) are given by

$$C_3 = \frac{S(p_1,p_2,p_3)}{\sqrt{S(p_1)S(p_2)S(p_3)}}\,. \tag{4.82}$$

We recall that the untwisted operators carry vanishing momenta along fifth dimension. The effective action of the corresponding KK modes $\eta_n(0)$ should be independent of the coupling constant. Indeed, we verify that for $p_i \to 0$ both relations in (4.81) cease to depend on g and C_3 coincides with its value (4.77) in a free theory. For nonzero p and $g \to \infty$ the function $S(0,p,-p)$ coincides (up to a normalization factor) with the analogous function defining the cubic term in the effective action proportional to $\eta_{0,n_1}\eta_{\alpha,n_2}\bar{\eta}_{-\alpha,n_3}$ and involving one untwisted and two twisted KK modes carrying small quasimomentum $p_\alpha = 2\pi\alpha/L$ (see (5.64) in [66]).

4.7 Discussions and Future Directions

In this second part of the thesis, we analysed a special class of superconformal $\mathcal{N} = 2$ theories, known as quiver models. Our purpose was to employ these setups as protected playgrounds for exploring physical effects that remain elusive in more realistic scenarios. The primary example we considered in our analysis is the limit of long-quiver, where the theory is expected to undergo the deconstruction mechanism [94] and behaves as a higher-dimensional model.

We revisit this mechanism by investigating protected correlation functions (3.5) of chiral primary half-BPS operators. Using supersymmetric localization, these observables can be expressed as matrix integrals which, in the planar limit, reduce to Fredholm determinants of semi-infinite matrices (3.36). This powerful representation, which is closely related to the celebrated Tracy–Widom distributions [104], allowed us to investigate the properties of the correlation functions across the parameter space of the theory.

We analysed the correlation functions at weak and strong coupling, and in various limits of the number of nodes and the operator scaling dimensions. We showed that their properties are naturally interpreted in terms of a one-dimensional lattice model (3.8) defined on the quiver diagram (Fig. 3.1). The emergence of a fifth dimension in the long-quiver limit, understood

as the continuum limit of this lattice model, crucially depends on the hierarchy between the 't Hooft coupling λ and the number of nodes L. A fifth dimension arises only in the regime $L \gg \sqrt{\lambda}$, where interactions in the lattice model become short-ranged and can be described by an effective local field theory. This involves massive degrees of freedom which remain, however, decoupled from the four-dimensional ones. Consequently, for $L \gg \sqrt{\lambda}$ the quiver theory behaves as a five-dimensional model in which Lorentz invariance is broken.

At weak coupling, the two-point correlation functions have a well-defined scaling behaviour in the limit $L \to \infty$. They decay exponentially fast with the node separation and the characteristic mass scale grows logarithmically with λ. This scaling is consistent with the propagation of massive particles along the emergent fifth dimension. In this case, the effective description collapses to a free field theory as the interaction strength between the diagram nodes goes to zero.

At strong coupling, the semi-classical AdS/CFT expansion of the correlation functions diverges as $L \to \infty$. By including both perturbative corrections in $1/\sqrt{\lambda}$ and an infinite tower of non-perturbative, exponentially suppressed contributions, we derived a remarkably simple expression for the observables in the long-quiver limit. These exhibit an exponential behaviour with the node separation which is analogous to that of the weak coupling regime. In this case, however, the effective description is interacting and possesses a well-defined spectrum of masses which are in one-to-one correspondence with the zeros of Bessel functions.

Our analysis poses the natural question of whether the behaviour in the long-quiver limit is preserved at the non-planar level. To address this question, the method developed in Section 3.3 to calculate the observable at the planar level can provide an efficient approach to systematically include the non-planar corrections. For the free energy and expectation value of circular Wilson loops this was done in [69, 70, 81]. Determining these observables at the non-planar level can shed new light on the holographic description of the emergent five-dimensional theory describing quiver models in the deconstruction limit.

Part III

Probing non-conformal $\mathcal{N} = 2$ gauge theories by localization

Chapter 5

Localization predictions in non-conformal theories

Info: *Part of the content and figures of this chapter have been published together with M. Billo', L. Griguolo and A. Lerda in* [23–26].

5.1 Motivations

In the previous chapters, we applied supersymmetric localization on the four-sphere S^4 to study special $\mathcal{N} = 2$ superconformal models. In this case, conformal invariance ensures that the observables computed on the sphere can be naturally related to their flat-space counterparts. This correspondence allows us to exploit the matrix model derived from localization to explore regions of the parameter space that are otherwise inaccessible by standard perturbative techniques.

In four-dimensional superconformal $\mathcal{N} = 2$ and $\mathcal{N} = 4$ super-Yang–Mills theories, the correspondence between matrix models on the sphere and flat-space dynamics has been extensively explored for a wide range of observables, including BPS Wilson loops [27, 55, 121–123], families of BPS local operators [58, 62, 63, 80, 124–128], and Bremsstrahlung functions [75, 129–132].

The remarkable effectiveness of the matrix model description in these conformal settings naturally raises the question of whether supersymmetric localization predictions on S^4 retain a physical meaning in flat space when we move beyond conformal setups.

When the theory involves dimensionful parameters, such as a mass term in $\mathcal{N} = 2^*$ models or a scale generated by dimensional transmutation, the properties of the theory at short and long distances change, and we generally expect a mismatch between the results in flat space and on the sphere. In particular, in massive theories, observables on $\mathbb{S}^4$ exhibit a dependence on both the mass scale and the radius through their product, which is usually different from the flat-space counterparts. This scenario was analysed in [133], where the authors studied the half-BPS Wilson loop in $\mathcal{N} = 2^*$ SYM and found that two-loop perturbative computations on $\mathbb{S}^4$ match the matrix model predictions, whereas the analogous flat-space calculation exhibits a distinct behaviour.

While a mass deformation explicitly breaks conformal symmetry, in theories with massless matter and a non-vanishing β-function, the breaking occurs dynamically at the quantum level. Nevertheless, as we showed in Section 2.3, supersymmetric localization on S^4 remains applicable and maps the expectation values of protected operators to a matrix model whose effective coupling depends on the radius of the sphere through the one-loop exact running coupling

g (2.27). This mirrors the usual structure of flat-space renormalization, naturally leading to the question of whether the two descriptions remain connected despite conformal symmetry breaking.

In this final part of the thesis, we address this question by studying localizable observables in $\mathcal{N} = 2$ SYM theories with gauge group $SU(N)$ and massless hypermultiplets in a generic representation $\mathcal{R}$. Within this framework, we focus on two classes of observables: correlators of multi-trace chiral operators and the expectation value of half-BPS Wilson loops. On the four-sphere, supersymmetric localization maps these quantities to the matrix model (2.31) discussed in Section 2.3. Our analysis demonstrates that, within a specific regime of validity, the flat-space computations of these observables at high orders in perturbation theory precisely match the matrix model predictions, establishing a non-trivial bridge between supersymmetric localization on S^4 and flat-space dynamics beyond the conformal domain.

The remainder of this chapter is organised as follows. In Section 5.2, we introduce the observables under consideration, namely, the half-BPS Wilson loops and the chiral correlators, and in Section 5.4 we present their evaluation within the matrix model framework on S^4.

5.2 Supersymmetric Wilson loops and chiral operators

The high-energy behaviour of non-Abelian gauge theories, such as QCD, is well understood within the framework of perturbation theory through the mechanism of asymptotic freedom. In this regime, dynamical quarks are treated as light degrees of freedom in the action and the theory can be probed perturbatively. At low energies, however, these models exhibit confinement: quarks cannot freely propagate and only appear as bound states.

An efficient approach to probe the strongly coupled regimes of non-Abelian gauge theories consists of introducing external heavy quarks, which are no longer dynamical but are kept at a fixed distance in time. The physical observable that naturally encodes their interaction potential $\mathcal{V}_{q\bar{q}}(r)$ is the expectation value of the *Wilson loop*.

Originally introduced in [134], this operator captures the phase factor acquired by an external quark moving along a closed path. In non-Abelian theories, it provides one of the most general non-local (gauge-invariant) observables, and it is defined as the holonomy of the connection $A_\mu(x) = A^a_\mu(x) T^a_{\boldsymbol{\mathcal{R}}}$

$$W = \frac{1}{\dim \boldsymbol{\mathcal{R}}} \mathrm{Tr}_{\boldsymbol{\mathcal{R}}}\, \mathcal{P} \exp\left\{ \mathrm{i} g_{\text{Y.M.}} \int_C \mathrm{d}\tau\, A^\mu(x(\tau)) \dot{x}_\mu(\tau) \right\} . \tag{5.1}$$

Here, $g_{\text{Y.M.}}$ is the gauge coupling constant, $\dim \boldsymbol{\mathcal{R}}$ denotes the dimension of the representation $\boldsymbol{\mathcal{R}}$, and C is a closed curve parametrized by the coordinates $x^\mu(\tau)$. Moreover, $\mathcal{P}$ denotes the *path-ordering* symbol, which accounts for the non-commutativity of the gauge-algebra valued matrices $A_\mu(x(\tau))$ and acts as

$$\mathcal{P} \prod_{i=1}^{n} A_\mu(x(\tau_i)) = A_\mu(x(\tau_1))\, A_\mu(x(\tau_2)) \dots A_\mu(x(\tau_n)) \theta(\tau_{12}) \dots \theta(\tau_{n-1,n}) + \dots \ , \tag{5.2}$$

where $\theta(x)$ is the Heaviside step function and $\tau_{ij} = \tau_i - \tau_j$. The path-ordering operator $\mathcal{P}$ is required to define the non-Abelian holonomy consistently, while the trace over the representation $\boldsymbol{\mathcal{R}}$ ensures gauge invariance of W.

One of the reasons why the expectation value of the Wilson loop (5.1) is extremely important in gauge theories is that it can be interpreted as an order parameter for confinement. To see this, we consider a rectangular Wilson loop in Euclidean space with temporal extent T and

spatial separation r, which describes a quark-antiquark ($q\bar{q}$) pair created at $t = 0$ and held fixed at distance r (see Fig. 5.1). In this setup, one can show that

$$\langle W \rangle \simeq \mathrm{e}^{-T\mathcal{V}_{q\bar{q}}(r)} \ , \tag{5.3}$$

where $\mathcal{V}_{q\bar{q}}(r)$ is the static potential of the quark pair at distance r in the limit $T \to \infty$. In the confining phase, the potential grows linearly with the distance, $\mathcal{V}_{q\bar{q}}(r) \sim r$, meaning that quarks cannot be separated by a finite amount of energy. Conversely, in the deconfined (or Coulomb-like) phase, the behaviour is similar to electrodynamics, with $\mathcal{V}_{q\bar{q}}(r) \sim 1/r$. These two regimes translate into distinct behaviours of (5.3): in the confined phase the observable follows an area law, depending on $A = rT$, while in the deconfined phase it scales as $k = T/r$. Accordingly,

$$\begin{aligned} &\lim_{r\to\infty} \langle W \rangle \sim \mathrm{e}^{-A} \to 0 \ , \quad \text{confined phase,} \\ &\lim_{r\to\infty} \langle W \rangle \sim \mathrm{e}^{-k} \neq 0 \ , \quad \text{unconfined phase.} \end{aligned} \tag{5.4}$$

This illustrates why the Wilson loop expectation value serves as an order parameter for confinement.

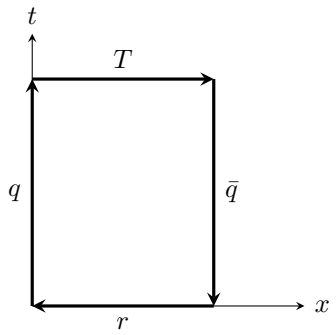

Figure 5.1: Rectangular Wilson loop in the (x, t) plane.

5.2.1 Supersymmetric Wilson loops

In supersymmetric gauge theories, one can construct generalisedd versions of the Wilson loop (5.1) that preserve part of the underlying supersymmetry. This idea, originally developed by Maldacena in the context of the AdS/CFT correspondence [5, 6], consists of modifying the operator (5.1) by introducing additional couplings to the scalar fields of the vector multiplet.

In $\mathcal{N} = 4$ super-Yang–Mills theory, the resulting operator, known as the Maldacena–Wilson loop, takes the following form [135]

$$W_{\mathcal{N}=4} \ = \ \frac{1}{\dim \boldsymbol{\mathcal{R}}} \operatorname{Tr}_{\boldsymbol{\mathcal{R}}} \mathcal{P} \exp\left(g_{\text{Y.M.}} \oint_C d\tau \left(\mathrm{i}\dot{x}^\mu(\tau) A_\mu(x(\tau)) + |\dot{x}(\tau)|\, n^u \phi_u(x(\tau)) \right) \right) , \tag{5.5}$$

where $g_{\text{Y.M.}}$ is the gauge coupling constant, n^u (with $u = 1, \dots, 6$) is a unit vector in the internal space of scalar fields, and C is a closed contour parametrized by $x^\mu(\tau)$.

Under supersymmetry transformations, the variation of the gauge term in (5.5) can be compensated by the scalar coupling. This mechanism imposes non-trivial constraints on the contour C and on the choice of the vector n^u, determining the preserved fraction of supercharges. For example, if C is a straight line or a circle in $\mathbb{R}^4$ and n^u is constant, the operator (5.5) preserves half of the global supersymmetry. More general contours usually preserve smaller fractions of

supersymmetry and were systematically classified in [136–138], revealing a rich interplay between geometry and supersymmetry.

In this section, we focus on $\mathcal{N}=2$ super-Yang–Mills theories, where only two real scalars from the vector multiplet are available to couple to the Wilson loop and the general construction reduces to (5.5) with $u=1,2$, *i.e.*

$$W_{\mathcal{N}=2} = \frac{\mathrm{Tr}_{\boldsymbol{\mathcal{R}}}}{\dim \boldsymbol{\mathcal{R}}} \mathcal{P}\exp\left(g_{\text{Y.M.}} \oint_C d\tau \left(\mathrm{i}\dot{x}^\mu(\tau) A_\mu(x(\tau)) + |\dot{x}(\tau)| \left(n_1(\tau)\phi_1(x(\tau)) + n_2(\tau)\phi_2(x\tau)\right)\right)\right). \tag{5.6}$$

Despite the lower amount of supersymmetry than the $\mathcal{N}=4$ case, one can still construct half- and quarter-BPS Wilson loops: the former are associated with straight lines or circles, whereas the latter correspond to special contours lying on a two-sphere S^2 [27, 61].

For our purposes, the half-BPS circular Wilson loop serves as an effective probe to examine the dynamics of $\mathcal{N}=2$ theories. Its expectation value is a non-trivial function of the theory parameters and, remarkably, can be computed exactly through supersymmetric localization on S^4 [55]. This makes it a natural candidate for testing the relation between localization results on S^4 and standard field-theory techniques in flat space beyond conformal settings.

In general $SU(N)$ $\mathcal{N}=2$ SYM theories defined in Euclidean space, the half-BPS circular Wilson loop in the fundamental representation is given by

$$W = \frac{1}{N}\mathrm{tr}\ \mathcal{P}\exp\left\{g_B \int_C \mathrm{d}\tau \left[\mathrm{i}A^\mu(x(\tau))\dot{x}_\mu(\tau) + \frac{R}{\sqrt{2}}\left(\bar{\phi}(x(\tau)) + \phi(x(\tau))\right)\right]\right\}, \tag{5.7}$$

where g_B is the *bare* coupling constant, while tr denotes the trace in the fundamental representation. Moreover, the gauge field A_μ and the complex scalar ϕ are integrated over a circle C of radius R, canonically parametrized by

$$x^\mu(\tau) = R(\cos\tau, \sin\tau, 0, 0)\ , \quad \text{with} \quad 0 \le \tau < 2\pi\ . \tag{5.8}$$

In theories with a non-vanishing β-function, conformal invariance is broken at the quantum level, making the agreement between the flat-space predictions and those on the four-sphere S^4 no longer automatic. Nevertheless, the half-BPS circular Wilson loop can still be consistently defined on both manifolds. In particular, to apply supersymmetric localization on S^4, the operator must be placed on a maximal circle of S^4 [55]. This requirement fixes the configuration in flat space, where we consider a circular loop of radius R such that, under stereographic projection, is mapped to the equator of S^4. As a result, the radii in the two geometries coincide (see Fig. 5.2), providing a clear and natural geometric bridge between flat space and the sphere.

5.3 Chiral and anti-chiral correlators

The second class of observables we consider are the correlation functions of gauge-invariant *multi-trace* operators

$$O_{\vec{n}}(x) = \prod_{i=1}^{\ell} g_B^{n_i}\, \mathrm{tr}\,\phi^{n_i}(x)\ , \tag{5.9}$$

where ϕ denotes the complex scalar field in the vector multiplet, g_B is the bare coupling, and the integers n_i are collectively encoded in $\vec{n} = (n_1, n_2, \ldots, n_\ell)$. These operators belong to the chiral ring of the theory, whose structure is protected by supersymmetry.

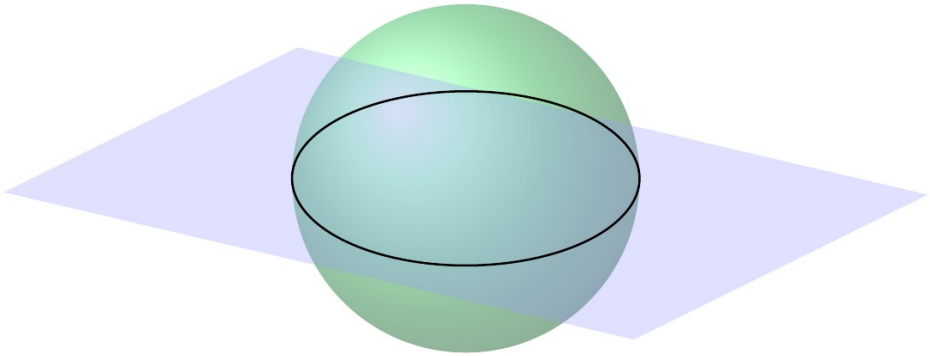

Figure 5.2: Relation between the circular Wilson loop defined on $\mathbb{R}^4$ and its counterpart on S^4. A circle of radius R in flat space is mapped to the equator of S^4, which is the configuration required by supersymmetric localization.

The operator $O_{\vec{n}}(x)$ preserves half of the supercharges, as it arises from a composition of chiral single-trace operators (3.1), and possesses a bare scaling dimension

$$n = \sum_{i=1}^{\ell} n_i \ , \tag{5.10}$$

together with a $U(1)$ charge which, in our conventions, coincides with n.

Since the scalar $\phi(x)$ takes values in the gauge algebra $su(N)$, it can be expressed as a linear combination of generators [1] T^a (with $a = 1, \dots, N^2 - 1$), *i.e.* $\phi(x) = \phi^a(x) T^a$. Consequently, $O_{\vec{n}}(x)$ can be expanded as

$$O_{\vec{n}}(x) = g_B^n \, R_{\vec{n}}^{a_1 \dots a_n} \, \phi^{a_1}(x) \dots \phi^{a_n}(x) \ , \tag{5.11}$$

where $R_{\vec{n}}^{a_1 \dots a_n}$ is an $SU(N)$ completely symmetric tensor defined as

$$R_{\vec{n}}^{a_1 \dots a_n} = \mathrm{tr}\, T^{(a_1} \dots T^{a_{n_1}} \ \mathrm{tr}\, T^{a_{n_1+1}} \dots T^{a_{n_1+n_2}} \ \dots \ \mathrm{tr}\, T^{a_{n_1+\dots+n_{\ell-1}+1}} \dots T^{a_n)} \ . \tag{5.12}$$

By replacing ϕ with its complex conjugate $\overline{\phi}$ in (5.9), one obtains the anti-chiral operators $\overline{O}_{\vec{n}}$, characterized by the same scaling dimension of $O_{\vec{n}}(x)$ but negative $U(1)$-charge.

The object of interest is the two-point correlator $\langle O_{\vec{n}}(x) \, \overline{O}_{\vec{m}}(0) \rangle$. In $\mathcal{N} = 2$ superconformal theories, the operator $O_{\vec{n}}(x)$ is a conformal primary. This implies that the kinematic structure of the two-point function is fixed by conformal symmetry (1.15), *i.e.*

$$\langle O_{\vec{n}}(x) \, \overline{O}_{\vec{m}}(0) \rangle = \frac{G_{\vec{n},\vec{m}}}{(4\pi^2 x^2)^n} \, \delta_{nm} \ , \tag{5.13}$$

where the normalization factor $G_{\vec{n},\vec{m}}$ is a non-trivial function of the gauge coupling and of the rank of the gauge group N. In these setups, $G_{\vec{n},\vec{m}}$ can be computed from the partition function on S^4 with insertions of chiral and anti-chiral operators at the north and south poles, respectively; supersymmetric localization reduces this observable to a matrix model [62, 98–100, 139–143].

[1] Our conventions for the generators of $su(N)$ are outlined in Appendix B.1

By contrast, in theories with non-vanishing β-function, conformal invariance is broken at the quantum level. As a result, $G_{\vec{n},\vec{m}}$ acquires a dependence on the separation x^2 through the running coupling, which signals the presence of anomalous dimensions [26, 144]. Nevertheless, the matrix model on S^4 can still be employed to compute $G_{\vec{n},\vec{m}}$, provided that the chiral and anti-chiral operators (5.9) are inserted at antipodal points on S^4 [98, 143]. This requirement sets the scale of the observable and provides the geometric connection between the description in flat space and that on S^4. More concretely, the operator separation in flat space $|x|$ is related to the radius R of S^4 by the relation (see Fig. 5.3)

$$|x| = 2R \ . \tag{5.14}$$

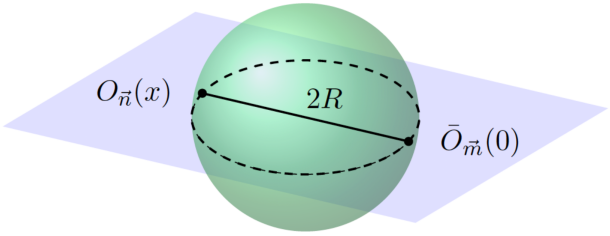

Figure 5.3: A three-dimensional representation of the relation between operators at antipodal points on the sphere are related to those in flat space by a separation $|x| = 2R$.

In the following, we will provide a detailed analysis of the supersymmetric Wilson loop and the correlator (5.13) both in flat space and on the four-sphere. Working in $\mathcal{N} = 2$ theories with non-vanishing β-function, we will show a non-trivial agreement at high orders in perturbation theory between the predictions in the two descriptions.

5.4 Localization predictions

In this section, we analyse the vacuum expectation value of the half-BPS Wilson loop (5.7) and the two-point function $G_{\vec{n},\vec{m}}$ (5.13) using the matrix model generated by supersymmetric localization on S^4. We consider $\mathcal{N} = 2$ SYM theories with massless hypermultiplets in an arbitrary representation $\mathcal{R}$ and non-vanishing β-function, for which the matrix model was extensively discussed in Section 2.3. Although our analysis is completely general, we sometimes focus on theories with N_f fundamental, N_s symmetric and N_a anti-symmetric flavours, where the matter representation $\mathcal{R}$ takes the following form

$$\widehat{\mathcal{R}} = N_f \, \square \oplus N_s \, \square\square \oplus N_a \, \begin{smallmatrix}\square\\\square\end{smallmatrix} \ . \tag{5.15}$$

The corresponding one-loop coefficient β_0 (1.25) of the β-function can be calculated by applying the group information outlined in Appendix B.1 and is given by

$$\begin{aligned} \hat{\beta}_0 &= 2N - 2i_{\widehat{\mathcal{R}}} \\ &= 2N - N_f - N_a(N-2) - N_s(N+2) \ . \end{aligned} \tag{5.16}$$

5.4.1 Supersymmetric Wilson loop

We begin with considering the vacuum expectation value of the half-BPS circular Wilson loop on S^4. Defining the operator (5.7) on the equator of a four-dimensional sphere S^4 of radius R, supersymmetric localization maps the observable to a matrix model [55].

In the $\mathcal{N}=2$ theories under examination, the observable can be written as follows [2] [23, 24]

$$\begin{aligned} W(g) &= \frac{1}{\mathcal{Z}} \int Da\, \mathrm{e}^{-\operatorname{tr} a^2 - S_{\text{Int}}(a,g)}\, \mathcal{W}(a,g) \\ &= \frac{1}{\mathcal{Z}} \int Da\, \mathrm{e}^{-\operatorname{tr} a^2 - S_{\text{Int}}(a,g)} \left(\frac{1}{N} \operatorname{tr} \exp\left(\frac{ag}{\sqrt{2}} \right) \right) , \end{aligned} \tag{5.17}$$

where $\mathcal{Z}$ is the partition function (2.31), g is the *running coupling constant* (2.27), while tr denotes the fundamental trace of $su(N)$.

At weak coupling, we can expand the matrix integral (5.17) in powers of the interaction action $S_{\text{Int}}(a,g)$ (2.20) and reduce the calculation to a set of expectation values evaluated with a Gaussian measure, *i.e.*

$$\begin{aligned} W(g) &= W_0(g) - \langle \mathcal{W}(a,g)\, S_{\text{Int}}(a,g) \rangle_{0,c} + \dots \\ &= W_0(g) + \left(\frac{g^2}{8\pi^2} \right)^2 \frac{\zeta_3}{2} \langle \mathcal{W}(a,g)\, \operatorname{Tr}'_{\mathcal{R}}\, a^4 \rangle_{0,c} + \dots , \end{aligned} \tag{5.18}$$

where to obtain the second line we replaced the interaction action S_{Int} with its perturbative expansion (2.20). Moreover, we denoted with a subscript c the connected part of the correlator and with W_0 the expectation value of the half-BPS Wilson loop in the free matrix model or, equivalently, in $\mathcal{N}=4$ SYM. By employing the recursive relations of [62], we find that

$$\begin{aligned} W_0 &= \int Da\, \mathrm{e}^{-\operatorname{tr} a^2}\, \mathcal{W}(a,g) \\ &= 1 + \frac{g^2 C_F}{4} + \frac{g^4 C_F (2N^2-3)}{192N} + \frac{g^6 C_F (N^4 - 3N^2 + 3)}{4608 N^2} + \dots , \end{aligned} \tag{5.19}$$

where $C_F = (N^2-1)/2N$ is the fundamental Casimir. Crucially, W_0 can be expressed in terms of the first generalisedd Laguerre polynomials of N^2-1 [121, 122]

$$W_0 = \frac{1}{N} L^1_{N-1}\left(-\frac{g^2}{4} \right) \exp\left(\frac{g^2}{8} \left(1 - \frac{1}{N} \right) \right) . \tag{5.20}$$

As we will shortly see, each contribution in (5.19) corresponds to a *ladder-like* corrections in perturbative field theory [3]. These contributions are associated with Feynman diagrams that only involve the *free propagations* of the gauge field A_μ and the scalar ϕ on the Wilson loop contour (5.7). Remarkably, this implies that the observable does not receive quantum corrections in $\mathcal{N}=4$ SYM [121, 122].

Turning our attention to the contributions of the interaction action (5.18), we note that these become evident only at three loops, *i.e.*

$$\begin{aligned} \left(\frac{g^2}{8\pi^2} \right)^2 \frac{\zeta_3}{2} \langle \mathcal{W}(a,g)\, \operatorname{Tr}'_{\mathcal{R}}\, a^4 \rangle_{0,c} &= \left(\frac{g^2}{8\pi^2} \right)^2 \frac{\zeta_3}{2} \frac{g^2}{4N} \langle \operatorname{tr} a^2\, \operatorname{Tr}'_{\mathcal{R}}\, a^4 \rangle_{0,c} + \mathcal{O}(g^8) \\ &= \frac{g^6 \zeta_3 C_F}{2^9 \pi^4} \left(12 \left(C_{\mathcal{R}} i_{\mathcal{R}} - N^2 \right) + N \beta_0 \right) + \mathcal{O}(g^8) , \end{aligned} \tag{5.21}$$

where β_0 is defined in (1.25), while $i_{\mathcal{R}}$ and $C_{\mathcal{R}}$ are, respectively, the Dynkin index and the quadratic Casimir of the representation $\mathcal{R}$ (see (B.2)). Moreover, to obtain the second line of (5.21), we evaluated the correlator by Wick's theorem with the basic contraction (2.18).

[2] In (5.17), we suppressed the instanton contributions as we work in the perturbative regime (2.29).

[3] See (6.11) and (6.19) for explicit examples of ladder-like diagrams.

Combining together (5.21) and (5.19), we derive the three-loop prediction of the matrix model for the circular half-BPS Wilson loop [24, 25], *i.e.*

$$W(g) = W_0(g) + \frac{g^6 \zeta_3 C_F}{2^9 \pi^4} \left(12 \left(C_{\mathcal{R}} i_{\mathcal{R}} - N^2\right) + N\beta_0\right) + \mathcal{O}(g^8) \ . \tag{5.22}$$

The structure of the term proportional to ζ_3 in (5.22) consists of two contributions. The first one involves the combination $C_{\mathcal{R}} i_{\mathcal{R}} - N^2$ and was originally reproduced in superconformal models defined in Euclidean space by standard perturbative techniques in [60, 61]. Conversely, the term involving the coefficient β_0 (1.25) of the β-function is a distinctive feature of non-conformal theories, and its presence makes the agreement with flat-space results highly non-trivial.

Finally, we stress that (5.22) is valid only within the perturbative regime (2.29). Beyond this limit, the observable receives power-like corrections of the form $C_n (\Lambda R)^n$, where Λ is the strong coupling scale (1.26). Since these terms are *infrared* contributions [4], we expect that they take a different form on the sphere and in flat space.

5.4.2 Chiral correlators

We now turn our attention to the calculation of the two-point correlator $G_{\vec{n},\vec{m}}$ (5.13). In order to compute this observable on S^4, we need to identify the matrix counterparts of the chiral operators $O_{\vec{n}}(x)$ (5.9). As we already observed in Section 3, this identification requires us to apply a Gram-Schmidt procedure on the basis of operators

$$O_{\vec{n}}(a) = \prod_{i=1}^{\ell} g^{n_i} \operatorname{tr} a^{n_i} \ . \tag{5.23}$$

This procedure leads us to a normal-ordered basis, in which each element is orthogonal to those of lower dimension. To maintain the analysis completely general, we can keep the orthogonalization implicit and represent the normal ordered version of the operator (5.9) as follows

$$\begin{aligned} \mathcal{O}_{\vec{n}}(a) &= :O_{\vec{n}}(a): \\ &= :\prod_{i=1}^{\ell} g^{n_i} \operatorname{tr} a^{n_i}: \\ &= g^n \, R_{\vec{n}}^{a_1 \dots a_n} \, :a^{a_1} \dots a^{a_n}: \ , \end{aligned} \tag{5.24}$$

where the fully symmetric R tensor is defined as in (5.12), while g is the *running coupling constant* (2.27). The use of colons stresses that $\mathcal{O}_{\vec{n}}(a)$ is orthogonal to the operators of lower dimensions.

In the $\mathcal{N} = 2$ SYM theory under examination, the correlator (5.9) on S^4 can be represented by the following matrix integral [26]

$$G_{\vec{n},\vec{m}} = \frac{1}{\mathcal{Z}} \int Da \ \mathrm{e}^{-\operatorname{tr} a^2 - S_{\mathrm{Int}}(a,g)} \mathcal{O}_{\vec{n}}(a) \mathcal{O}_{\vec{m}}(a) \ , \tag{5.25}$$

where we did not include the contribution of the instantons as we are working in the perturbative regime (2.29) and we recall that $\mathcal{Z}$ is given by (2.31).

At weak coupling, we can evaluate (5.25) by following the approach employed for the Wilson loop. We expand the integrand in powers of the interaction action and we find that

[4] In certain models, such as $\mathcal{N} = 2^*$ or the massive deformation of conformal $\mathcal{N} = 2$ SQCD, the coefficients C_n were calculated by the matrix model on S^4 [71]. Let us note that the instantons, which we neglected in our analysis, also contribute to the observable by power-like corrections.

$$\begin{aligned} G_{\vec{n},\vec{m}} &= \big\langle \mathcal{O}_{\vec{n}}(a)\,\mathcal{O}_{\vec{m}}(a)\big\rangle_0 - \big\langle \mathcal{O}_{\vec{n}}(a)\,\mathcal{O}_{\vec{m}}(a)\,S_{\rm Int}(a,g)\big\rangle_{0,c} + \dots \\ &= \big\langle \mathcal{O}_{\vec{n}}(a)\,\mathcal{O}_{\vec{m}}(a)\big\rangle_0 + \Big(\frac{g^2}{8\pi^2}\Big)^2 \frac{\zeta_3}{2}\,\big\langle \mathcal{O}_{\vec{n}}(a)\,\mathcal{O}_{\vec{m}}(a)\,\mathrm{Tr}'_{\mathcal{R}}\,a^4\big\rangle_{0,c} + \dots \ , \end{aligned} \tag{5.26}$$

where to obtain the second line we replaced the interaction action with its perturbative expansion (2.20) and we employed the subscript c to denote the connected part of the correlator.

The first contribution on the right-hand side of (5.26) is the chiral correlator in the free matrix model. It can be computed by Wick's theorem and the contraction (2.18), *i.e.*

$$\big\langle \mathcal{O}_{\vec{n}}(a)\,\mathcal{O}_{\vec{m}}(a)\big\rangle_0 = g^{2n}\,n!\,R_{\vec{n}}^{a_1\dots a_n}\,R_{\vec{m}}^{a_1\dots a_n} \equiv g^{2n}\,G^{(0)}_{\vec{n},\vec{m}} \ . \tag{5.27}$$

In the previous expression, the factor of $n!$ counts the different ways in which the n indices of the two symmetric tensors $R_{\vec{n}}$ and $R_{\vec{m}}$ can be contracted. Notice that the vectors $\vec{n}$ and $\vec{m}$ can be different, but the sum of their components must be equal because of $U(1)$ charge conservation. For future reference, we provide a few explicit values of $G^{(0)}_{\vec{n},\vec{m}}$ for operators of low dimensions

$$G^{(0)}_{2,2} = \frac{N^2-1}{2} \ , \quad G^{(0)}_{3,3} = \frac{3(N^2-1)(N^2-4)}{8N} \ , \quad G^{(0)}_{(2,2),(2,2)} = \frac{N^4-1}{2} \tag{5.28a}$$

$$G^{(0)}_{4,(2,2)} = \frac{(N^2-1)(2N^2-3)}{2N} \ , \quad G^{(0)}_{4,4} = \frac{(N^2-1)(N^4-6N^2+18)}{4N^2} \ . \tag{5.28b}$$

The expressions of $G^{(0)}_{\vec{n},\vec{m}}$ for higher dimensional operators can be calculated straightforwardly using the fusion/fission identities presented in [62].

Let us now consider the interacting part in (5.26) proportional to ζ_3. The calculation of this connected correlator is more involved than (5.21). Therefore, we find it convenient to adopt a diagrammatic approach to highlight the nature of the different contributions. We depict the quartic vertex as

$$\mathrm{Tr}'_{\mathcal{R}}\,a^4 \quad \leftrightarrow \quad \text{  } \ , \tag{5.29}$$

while the operator $\mathcal{O}_{\vec{m}}(a)$ is represented by a black dot with m lines. Computing all possible Wick's contractions then corresponds to connecting the lines between the vertex and the operators with the free propagator (2.18). However, it is important to recall that self-contractions between lines belonging to the same operators $\mathcal{O}_{\vec{n}}(a)$ are forbidden, as they are normal ordered (5.24). Conversely, the quartic vertex (5.29) it is not normal ordered and admits self-contractions. Going through the calculation, we find that the final result is given by the sum of two diagrams

$\mathcal{O}_{\vec{n}}(a)$ 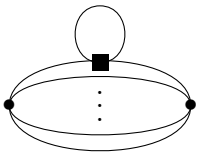 $\mathcal{O}_{\vec{m}}(a)$ $= g^{2n}\,12n\,n!\,\widehat{C}_s^{a_1b_1dd}\,R_{\vec{n}}^{a_1c_1\dots c_{n-1}}\,R_{\vec{m}}^{b_1c_1\dots c_{n-1}}$, (5.30a)

$\mathcal{O}_{\vec{n}}(a)$ 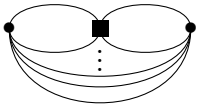 $\mathcal{O}_{\vec{m}}(a)$ $= g^{2n}\,6n(n-1)\,n!\,\widehat{C}_s^{a_1a_2b_1b_2}\,R_{\vec{n}}^{a_1a_2c_1\dots c_{n-2}}\,R_{\vec{m}}^{b_1b_2c_1\dots c_{n-2}}$. (5.30b)

In the previous expression, the notation was introduced for

$$\widehat{C}_s^{abcd} = \frac{1}{6}\Big(\widehat{C}^{abcd} + \widehat{C}^{acdb} + \widehat{C}^{adbc} + \widehat{C}^{abdc} + \widehat{C}^{acbd} + \widehat{C}^{adcb}\Big) \ , \tag{5.31a}$$

$$\widehat{C}^{abcd} = \big(\mathrm{Tr}_{\mathcal{R}}\, T^a T^b T^c T^c - \mathrm{Tr}_{\mathrm{Adj}}\, T^a T^b T^c T^c\big) \ . \tag{5.31b}$$

The overall coefficients on the right-hand side of the diagrams in (5.30) correspond to the symmetry factors arising from the different ways of contracting the operators with the vertex (5.31a). For instance, the factor $12nn!$ corresponds to $2\binom{4}{2}$ ways of selecting an ordered pair of indices in the tensor $\widehat{C}_s$ (5.31a), n ways of connecting one index of $R_{\vec{n}}$ (5.12) with $\widehat{C}_s$, n ways of connecting one index of $R_{\vec{m}}$ with $\widehat{C}_s$ and $(n-1)!$ ways of contracting the remaining indices of $R_{\vec{n}}$ and $R_{\vec{m}}$ with each other. The coefficient $6n(n-1)$ follows from similar arguments.

Combining together (5.30a) and (5.30b), we find

$$\begin{aligned}\big\langle \mathcal{O}_{\vec{n}}(a)\, \mathcal{O}_{\vec{m}}(a)\ \mathrm{Tr}'_{\mathcal{R}}\, a^4\big\rangle_0^c = 6g^{2n}\Big[&2n\, n!\, \widehat{C}_s^{a_1 b_1 d d}\ R_{\vec{n}}^{a_1 c_1 \dots c_{n-1}}\, R_{\vec{m}}^{b_1 c_1 \dots c_{n-1}} \\ &+ n(n-1)\, n!\, \widehat{C}_s^{a_1 a_2 b_1 b_2}\ R_{\vec{n}}^{a_1 a_2 c_1 \dots c_{n-2}}\, R_{\vec{m}}^{b_1 b_2 c_1 \dots c_{n-2}}\Big] \ .\end{aligned} \tag{5.32}$$

The contributions appearing in the previous expression can be further simplified by employing the following relations that we will prove in Appendix B.2

$$2n\, n!\, \widehat{C}_s^{a_1 b_1 d d}\ R_{\vec{n}}^{a_1 c_1 \dots c_{n-1}}\, R_{\vec{m}}^{b_1 c_1 \dots c_{n-1}} = 2n\Big(C_{\mathcal{R}}\, i_{\mathcal{R}} - N^2 + \frac{N\beta_0}{12}\Big)\, G^{(0)}_{\vec{n},\vec{m}} \ , \tag{5.33a}$$

$$n(n-1)\, n!\, \widehat{C}_s^{a_1 a_2 b_1 b_2}\ R_{\vec{n}}^{a_1 a_2 c_1 \dots c_{n-2}}\, R_{\vec{m}}^{b_1 b_2 c_1 \dots c_{n-2}} = \widehat{\mathcal{G}}_{\vec{n},\vec{m}} - n\,\frac{N\beta_0}{6}\, G^{(0)}_{\vec{n},\vec{m}} \ , \tag{5.33b}$$

where $G^{(0)}_{\vec{n},\vec{m}}$ is the tree-level coefficient we introduced in (5.27), while $\widehat{\mathcal{G}}_{\vec{n},\vec{m}}$ is given by

$$\widehat{\mathcal{G}}_{\vec{n},\vec{m}} = n(n-1)n!\widehat{C}^{a_1 a_2 b_1 b_2} R_{\vec{n}}^{a_1 a_2 c_1, \dots, c_{n-2}} R_{\vec{m}}^{a_1 a_2 c_1, \dots, c_{n-2}} \ . \tag{5.34}$$

Combining together (5.33) with (5.32), we find that the terms proportional to $N\beta_0$ cancel each other and the final result takes the following form

$$\begin{aligned} G_{\vec{n},\vec{m}} &= g^{2n}\, G^{(0)}_{\vec{n},\vec{m}} + g^{2n}\Big(\frac{g^2}{8\pi^2}\Big)^2 3\,\zeta_3\Big[2n\big(C_{\mathcal{R}}\, i_{\mathcal{R}} - N^2\big)\, G^{(0)}_{\vec{n},\vec{m}} + \widehat{\mathcal{G}}_{\vec{n},\vec{m}}\Big] \\ &= g^{2n}\, G^{(0)}_{\vec{n},\vec{m}}\left[1 + \Big(\frac{g^2}{8\pi^2}\Big)^2 3\zeta_3\, \mathcal{C}^{(2)}_{\vec{n},\vec{m}} + \mathcal{O}(g^6)\right] , \end{aligned} \tag{5.35}$$

where

$$\mathcal{C}^{(2)}_{\vec{n},\vec{m}} = 2n\,\big(C_{\mathcal{R}}\, i_{\mathcal{R}} - N^2\big) + \frac{\widehat{\mathcal{G}}_{\vec{n},\vec{m}}}{G^{(0)}_{\vec{n},\vec{m}}} \ . \tag{5.36}$$

As we already remarked in the case of the supersymmetric Wilson loop, the prediction (5.35) is valid within the perturbative regime (2.29). By relaxing this condition, the observable receives additional non-perturbative *infrared* corrections of the form $C_n\,(\Lambda R)^n$ that we expect to be different in flat space and on the sphere.

Chapter 6

Chiral correlators and BPS Wilson loop in perturbation theory

Info: *Part of the content and figures of this chapter have been published together with M. Billo', L. Griguolo and A. Lerda in* [23–26].

In this chapter, we turn our attention to the calculation of the chiral correlators and the expectation value of the half-BPS Wilson loop in flat space. We provide a detailed analysis of the half-BPS Wilson loop in Section 6.1, while the chiral correlators are considered in Section 6.2.

6.1 Half-BPS circular Wilson loops in perturbation theory

We now turn our attention to the calculation of the half-BPS circular Wilson loop (5.7) in flat space by standard perturbative approaches. Before turning our attention to the calculation of the observable, we present the Euclidean actions for $SU(N)$ $\mathcal{N}=2$ SYM theories with massless hypermultiplets in arbitrary representation $\mathcal{R}$.

Let us recall that the $\mathcal{N}=2$ vector multiplet (1.20) consists of one gauge field and one complex scalar, denoted as A_μ and ϕ respectively, along with their fermionic partners ψ and λ, known in this context as the *gauginos*. In Euclidean space, the dynamics of this supermultiplet is described by the following gauge-fixed action [24]

$$\begin{aligned} S_0^{\text{gauge}} &= \int \mathrm{d}^4x\ \mathrm{Tr}\Big[-\frac{1}{2}F_{\mu\nu}F^{\mu\nu} - 2\mathrm{i}\lambda\sigma^\mu D_\mu\bar\lambda - 2\mathrm{i}\psi\sigma^\mu D_\mu\bar\psi - 2D_\mu\bar\phi D^\mu\phi - 2\partial_\mu\bar c D^\mu c\Big]\,, \\ S_{\text{int}} &= \int \mathrm{d}^4x\ \mathrm{Tr}\Big[2\mathrm{i}g_B\sqrt{2}\Big(\bar\phi\big\{\lambda^\alpha,\psi_\alpha\big\} - \phi\big\{\bar\psi_{\dot\alpha},\bar\lambda^{\dot\alpha}\big\}\Big) - \xi(\partial_\mu A^\mu)^2 - g_B^2\big[\phi,\bar\phi\big]^2\Big]\,, \end{aligned} \tag{6.1}$$

where the intertwining matrix σ^μ is defined in (A.6), while c denotes the ghost field. Let us note that with these conventions the actions are negative-definite and consequently, they appear as e^S in the path integral. The field-strength and the adjoint covariant derivatives are given by

$$F_{\mu\nu} = \partial_\mu A_\nu - \partial_\nu A_\mu - \mathrm{i}g_B[A_\mu,A_\nu]\,, \quad D_\mu = \partial_\mu - \mathrm{i}g_B[A_\mu,\bullet]\,. \tag{6.2}$$

In the $\mathcal{N}=2$ language matter sits in the hypermultiplets (1.21). The field content of this supermultiplet consists of two complex scalars, denoted as q and $\tilde q$, along with their fermionic

partners η and $\tilde{\eta}$. In particular, q and η transform in the representation $\mathcal{R}$, while the $\tilde{q}$ and $\tilde{\eta}$ in the conjugate one, *i.e.* $\mathcal{R}^*$. The spacetime dynamics of these fields is encoded in the actions

$$\begin{aligned} S_0^Q &= \int \mathrm{d}^4x \Big[- D_\mu \bar{q} D^\mu q - \mathrm{i}\bar{\eta}\bar{\sigma}^\mu D_\mu \eta - D_\mu \tilde{q} D^\mu \bar{\tilde{q}} - \mathrm{i}\tilde{\eta}\sigma^\mu D_\mu \bar{\tilde{\eta}} \Big] , \\ S_{\text{int}}^Q &= \int \mathrm{d}^4x \Big[\mathrm{i}\sqrt{2} g_B \Big(\tilde{q}\bar{\lambda}\bar{\tilde{\eta}} - \tilde{\eta}\lambda\bar{\tilde{q}} \Big) + \mathrm{i}\sqrt{2} g_B \Big(\bar{\eta}\bar{\phi}\bar{\tilde{\eta}} - \tilde{\eta}\phi\eta \Big) + \mathrm{i}\sqrt{2} g_B \Big(\bar{\eta}\bar{\psi}\bar{\tilde{q}} - \tilde{q}\psi\eta \Big) , \\ &\qquad + \mathrm{i}\sqrt{2} g_B \Big(\bar{q}\bar{\psi}\bar{\tilde{\eta}} - \tilde{\eta}\psi q \Big) + \mathrm{i}\sqrt{2} g_B \Big(\bar{q}\lambda\eta - \bar{\eta}\bar{\lambda} q \Big) - g_B^2 V(\phi, \tilde{q}, q) \Big] , \end{aligned} \tag{6.3}$$

where $V(\phi, \tilde{q}, q)$ is the scalar potential describing quartic interactions

$$\begin{aligned} V = {} & \tilde{q}\{\phi, \bar{\phi}\}\bar{\tilde{q}} + \bar{q}\{\bar{\phi}, \phi\} q - (\tilde{q} T^a_{\mathcal{R}} \bar{\tilde{q}})\, (\bar{q} T^a_{\mathcal{R}} q) + 2\, (\bar{q} T^a_{\mathcal{R}} \bar{\tilde{q}})\, (\tilde{q} T^a_{\mathcal{R}} q) \\ & + \frac{1}{2}\, (\bar{q} T^a_{\mathcal{R}} q)\, (\bar{q} T^a_{\mathcal{R}} q) + \frac{1}{2}\, (\tilde{q} T^a_{\mathcal{R}} \bar{\tilde{q}})\, (\tilde{q} T^a_{\mathcal{R}} \bar{\tilde{q}}) \ . \end{aligned} \tag{6.4}$$

In the previous expressions, $T^a_{\mathcal{R}}$ denotes the generators of the Lie algebra $su(n)$ in the representation $\mathcal{R}$ of the gauge group. The covariant derivative for a field transforming in this representation is defined as

$$D_\mu = \partial_\mu - \mathrm{i} g_B A^a_\mu T^a_{\mathcal{R}} \ . \tag{6.5}$$

Organizing perturbation theory We begin by observing that, in theories with non-vanishing β-function, the expectation value of the half-BPS circular Wilson loop (5.7) receives ultraviolet-divergent contributions. To regularise these singularities while preserving the extended supersymmetry, we dimensionally reduce the theory from four to $d = 4 - 2\epsilon$ dimensions [121]. In this scheme, the gauge field A_μ is a d-dimensional vector, while the real scalars generated by the reduction are denoted by A_i, with $i = 1, \ldots, 2\epsilon$. Since the bare coupling constant g_B is dimensionless only when $d = 4$, this regularization scheme breaks classical conformal symmetry, implying that the dimensionally regularised observable can only depend on the radius of the supersymmetric Wilson loop R by the combination

$$\hat{g}_B = R^\epsilon g_B \ . \tag{6.6}$$

Perturbatively, we expand the expectation value of the half-BPS Wilson loop (5.7) as follows

$$\big\langle W \big\rangle \equiv \mathcal{W} = \mathcal{W}_1 + \mathcal{W}_2 + \mathcal{W}_4 + \mathcal{W}_6 + \mathcal{O}(\hat{g}_B^8) \ , \tag{6.7}$$

where the quantities $\mathcal{W}_{2k}$ are proportional to $\hat{g}_B^{2k}$ (6.6) and can be organised as follows

$$\mathcal{W}_{2k} = \mathcal{W}_{2k}^{\ell.\ell.} + \mathcal{W}_{2k}^{\text{v.m.}} + \mathcal{W}_{2k}^{\mathcal{R}} \ . \tag{6.8}$$

The first two contributions capture, respectively, the *ladder-like* diagrams, in which the gauge field A_μ and the scalar field ϕ freely propagate on the Wilson loop contour, and the interaction corrections involving internal vertices and lines of the vector multiplet only. These contributions are in common with the $\mathcal{N} = 4$ theory. By contrast, $\mathcal{W}_{2k}^{\mathcal{R}}$ denotes the diagrams with internal lines associated with the matter hypermultiplets in the representation $\mathcal{R}$.

In $\mathcal{N} = 4$ SYM, where matter transforms in the adjoint representation, only the ladder-like diagrams contribute to the expectation value of the Wilson loop in the limit $d \to 4$ [121, 122]. This means that the interaction contributions have to satisfy the general identity

$$\mathcal{W}_{2k}^{\text{v.m.}} = -\mathcal{W}_{2k}^{\text{Adj}} + \delta\mathcal{W}_{2k}^{\text{v.m.}} \ , \tag{6.9}$$

where $\delta\mathcal{W}_{2k}^{\text{v.m.}}$ denotes an evanescent correction: it vanishes for $d = 4$ and can be expanded in power series of $\epsilon = (4-d)/2$. As we will discuss in Section 6.1.4, upon renormalization, the ultraviolet poles of the bare coupling constant $\hat{g}_B$ can interfere with these evanescent terms, producing finite higher-loop corrections. In particular, the renormalized expectation value at three loops receives non-trivial contributions from the evanescent corrections $\delta\mathcal{W}_4^{\text{v.m.}}$.

Substituting (6.9) into (6.8), we find that

$$\mathcal{W}_{2k} = \mathcal{W}_{2k}^{\ell.\ell.} + \mathcal{W}'_{2k} + \delta\mathcal{W}_{2k}^{\text{v.m.}} \ , \quad \text{where} \quad \mathcal{W}'_{2k} \equiv \mathcal{W}_{2k}^{\mathcal{R}} - \mathcal{W}_{2k}^{\text{Adj}} \ . \tag{6.10}$$

By definition, the interaction term $\mathcal{W}'_{2k}$ is constructed by subtracting from $\mathcal{W}_{2k}^{\mathcal{R}}$ analogous corrections with $\mathcal{R} = \text{Adj}$ and consequently, it precisely encodes the *difference-theory* contributions predicted by interaction potential (2.19) of the matrix model.

6.1.1 One- and two-loop corrections

At order $\hat{g}_B^2$, the expectation value of the half-BPS Wilson loop only involves the following ladder-like contributions

$\mathcal{W}_2^{\ell.\ell.} =$ 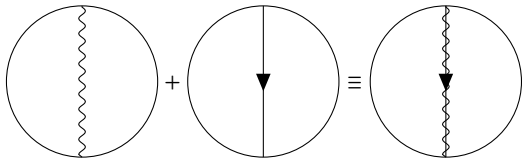 , (6.11)

where we depicted with a straight and wiggly line the tree-level propagators of the adjoint scalar and of the gauge-field, respectively. In d dimensions, we find that [1]

$$\begin{aligned} \left\langle \phi^a(x_1)\bar{\phi}^b(x_2)\right\rangle_0 &= \delta^{ab}\Delta(x_{12}) \ , \\ \left\langle A_\mu^a(x_1)A_\nu^b(x_2)\right\rangle_0 &= \delta_{\mu\nu}\delta^{ab}\Delta(x_{12}) \ , \end{aligned} \tag{6.12}$$

where we introduced the notation $x_{12} \equiv x_1 - x_2$, while the function $\Delta(x_{12})$ is given by [2]

$$\Delta(x_{12}) = \frac{\Gamma(1-\epsilon)}{4\pi^{2-\epsilon}\left(x_{12}^2\right)^{1-\epsilon}} \ . \tag{6.13}$$

Expanding the Wilson loop (5.7) at order g_B^2, and employing the free Wick contractions (6.12), we obtain the following representation for the diagrams (6.11)

$$\begin{aligned} \mathcal{W}_2^{\ell.\ell.} &= \frac{g_B^2 C_F}{2}\oint \mathrm{d}^2\tau \left(R^2 - \dot{x}_1\cdot\dot{x}_2\right)\Delta(x_{12}) \\ &= \frac{g_B^2 C_F}{2}\oint \mathrm{d}^2\tau\hat{\Delta}(x_{12}) \ . \end{aligned} \tag{6.14}$$

In the second line of the previous expression, we introduced the *effective (tree-level) propagator* $\hat{\Delta}(x_{12})$, which can be expressed in terms of trigonometric functions by employing the parametrization (5.8), *i.e.*

$$\hat{\Delta}(x_{12}) = \frac{\Gamma(1-\epsilon)}{8\pi^{2-\epsilon}}\left(4R^2\sin^2\left(\frac{\tau_{12}}{2}\right)\right)^{\epsilon} \ . \tag{6.15}$$

[1] We perform the calculations in the Feynman gauge.

[2] This corresponds to the $s = 1$ case in (C.14), since in momentum space the tree-level propagator is simply $1/p^2$.

Substituting (6.15) into (6.14), we can perform the integration over the contour by (6.23b). The final result takes the following form

$$\mathcal{W}_2^{\ell.\ell.} = \hat{g}_B^2 C_F B_1 \ , \tag{6.16}$$

$$B_n(\epsilon) = \frac{\Gamma^n(1-\epsilon)}{8\pi^{-n\epsilon}} \frac{\sec(n\epsilon)\Gamma(-n\epsilon)}{\Gamma(1+n\epsilon)\Gamma(-2n\epsilon)} \ . \tag{6.17}$$

As we will shortly see, diagrams dressed with higher-loop corrections to the propagators can be expressed in terms of the function $B_n(\epsilon)$ with $n > 1$.

6.1.2 Two-loop corrections

At two loops, the expectation value of the supersymmetric Wilson loop receives contributions from the following class of diagrams

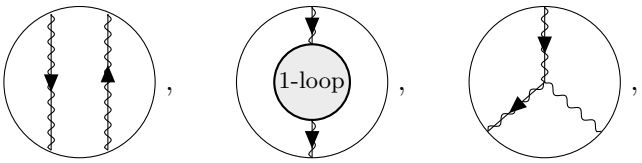

(6.18)

which we will analyse in turn.

Ladder-like diagrams Expanding the Wilson loop operator (5.7) at order g_B^4 and employing the tree-level propagators of the adjoint scalar and gauge field (6.12), we find that the two-loop ladder-like diagrams can be expressed as follows

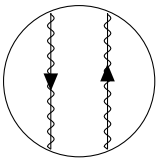

$$= \frac{g_B^4}{N} \oint_{\mathcal{D}} \mathrm{d}^4\tau \left(C^{aabb} \left(\widehat{\Delta}(x_{12})\widehat{\Delta}(x_{34}) + \widehat{\Delta}(x_{14})\widehat{\Delta}(x_{23}) \right) + C^{abab} \widehat{\Delta}(x_{13})\widehat{\Delta}(x_{24}) \right) , \tag{6.19}$$

where the domain of integration $\mathcal{D}$ denotes the ordered region $\tau_1 > \tau_2 > \tau_3 > \tau_4$, the effective propagator $\widehat{\Delta}(x)$ is defined in (6.15) and we introduced the $SU(N)$ tensor

$$C^{abcd} = \mathrm{tr}\, T^a T^b T^c T^d \ . \tag{6.20}$$

Using the non-Abelian exponentiation of the Wilson loop [145,146], we find that (6.19) takes the following form

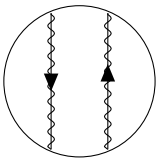

$$= \frac{1}{2} \left(\mathcal{W}_2^{\ell.\ell.} \right)^2 + \frac{\hat{g}_B^4}{2N} \mathrm{tr} \left(\left[T^b, T^a \right] \right)^2 \oint_{\mathcal{D}} \mathrm{d}^4\tau \widehat{\Delta}(x_{13})\widehat{\Delta}(x_{24}) \ , \tag{6.21}$$

where $\mathcal{W}_2^{\ell.\ell}$ is the one-loop ladder-like contribution (6.16), while the second term in (6.21) defines the so-called *maximally non-Abelian part* of the diagram. This involves the trigonometric integral

$$\int_{\mathcal{D}} \mathrm{d}^4\tau \left(4 \sin^2 \frac{\tau_{13}}{2} \right)^{2-d/2} \left(4 \sin^2 \frac{\tau_{24}}{2} \right)^{2-d/2} \ , \tag{6.22}$$

which arises when we replace the effective propagators $\widehat{\Delta}(x)$ (6.15) with their explicit form and employ the coordinate parametrization (5.8). The nested integration in (6.22) can be performed in arbitrary dimension d by the Fourier expansion of the real even function $1/\sin^{2\alpha}\left(\frac{x}{2}\right)$ [147], *i.e.*

$$\frac{1}{\left(4\sin^2\frac{x}{2}\right)^{\alpha}} = \frac{1}{2}a_0(\alpha) + \sum_{n=1}^{\infty} a_n(\alpha)\cos nx \ , \tag{6.23a}$$

$$a_n(\alpha) = \frac{\sec(\pi\alpha)\Gamma(n+\alpha)}{\Gamma(2\alpha)\Gamma(1-\alpha+n)} \ . \tag{6.23b}$$

Applying the identities (6.23) to the calculation of (6.22), we find that the nested integration becomes elementary and (6.21) assumes a remarkably simple form

$$\mathcal{W}_4^{\ell.\ell.} = \hat{g}_B^4 \frac{C_F(2N^2-3)}{12N} B_1^2 - \epsilon \hat{g}_B^4 \frac{C_F N \zeta_3}{16\pi^2} + \mathcal{O}(\epsilon)^2 \ , \tag{6.24}$$

where the function $B_1(x)$ (6.17) emerges from the ladder-like correction $\mathcal{W}_2^{\ell.\ell.}$ (6.16), while the term proportional to ζ_3 arises from the maximally non-Abelian part of the diagram.

Interacting diagrams We now turn our attention to the interacting diagrams in (6.18), starting from the contribution that involves internal virtual corrections to the propagators.

In the Feynman gauge, the expectation based on supersymmetry is that the one-loop propagators of the gauge field A_μ and the adjoint scalar ϕ coincide up to spacetime indices. Indeed, the detailed analysis of these corrections, reported in Appendix C, shows that

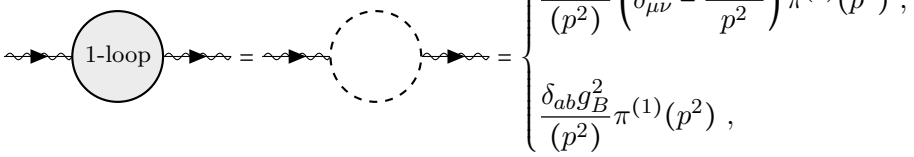

$$\begin{cases} \dfrac{\delta_{ab} g_B^2}{(p^2)} \left(\delta_{\mu\nu} - \dfrac{p_\mu p_\nu}{p^2}\right) \pi^{(1)}(p^2) \ , \\ \dfrac{\delta_{ab} g_B^2}{(p^2)} \pi^{(1)}(p^2) \ , \end{cases} \tag{6.25}$$

where the one-loop polarization operator $\pi^{(1)}(p^2)$ takes the following form

$$\pi^{(1)}(p^2) = -2i_{\mathcal{R}} g_B^2 \frac{1}{p^{2\epsilon}} \frac{\Gamma(\epsilon)}{(4\pi)^{2-\epsilon}} \frac{\Gamma^2(1-\epsilon)}{\Gamma(2-2\epsilon)} \ . \tag{6.26}$$

The previous expression only depends on the matter content of the theory through the Dynkin index $i_{\mathcal{R}}$ of the representation $\mathcal{R}$. This result is emphasised in (6.25) by the dashed lines, which signal that only matter fields run in the virtual loop.

Substituting (6.25) into the second diagram in (6.18), we find that

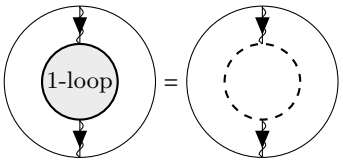

(6.27)

Since the *bubble-like* contribution (6.27) is the only two-loop diagram with internal lines in the representation $\mathcal{R}$ we denoted it by $\mathcal{W}_4^{\mathcal{R}}$ according to the decomposition (6.8).

Before analysing (6.27) in detail, we consider the third class of diagrams in (6.18), *i.e.*

$\mathcal{W}_4^{\text{v.m.}} =$ 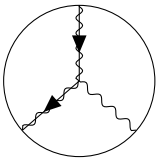 . (6.28)

The correction $\mathcal{W}_4^{\text{v.m.}}$ only involves internal interactions associated with the $\mathcal{N}=2$ vector multiplet and consequently, it is in common with $\mathcal{N}=4$ SYM. In this theory, the diagrams (6.28) were originally studied in [121], where it was shown that

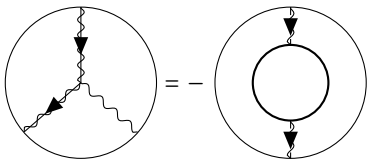 $+\,\delta\mathcal{W}_4^{\text{v.m.}} = -\mathcal{W}_4^{\text{Adj}} + \delta\mathcal{W}_4^{\text{v.m.}}$. (6.29)

In the previous expression, the internal bubble denotes the one-loop corrections to the adjoint scalar and gauge field propagator in $\mathcal{N}=4$ SYM, where we have a single adjoint hypermultiplet. Consequently, this class of corrections can be deduced by (6.25) with $\mathcal{R}=\text{Adj}$.

Let us observe that (6.29) provides a concrete realization of the relation (6.9) at two loops with the evanescent correction $\delta\mathcal{W}_4^{\text{v.m.}}$ that takes the following form [121]

$$\delta\mathcal{W}_4^{\text{v.m.}} = \epsilon\,\frac{\hat{g}_B^4 C_F N\Gamma(1-2\epsilon)}{(2\pi)^{-2\epsilon}128\pi^4}\int_0^1 \mathrm{d}F(\alpha\beta\gamma)^{-\epsilon}\oint \mathrm{d}^3\tau\;\varepsilon(\tau)\;\frac{\sin\tau_{13}}{Q^{1-2\epsilon}} + \mathcal{O}(\epsilon)^2\ . \tag{6.30}$$

In the previous expression, the notation was introduced for

$$Q = \alpha\beta(1-\cos\tau_{12}) + \beta\gamma(1-\cos\tau_{23}) + \gamma\alpha(1-\cos\tau_{13})\ , \tag{6.31}$$

$$\mathrm{d}F = \mathrm{d}\alpha\,\mathrm{d}\beta\,\mathrm{d}\gamma\,\delta(1-\alpha-\beta-\gamma)\ , \tag{6.32}$$

$$\varepsilon(\tau) = \theta(\tau_{12})\theta(\tau_{23}) - \theta(\tau_{13})\theta(\tau_{32}) + \text{ permutations}\ . \tag{6.33}$$

The path-ordered integral in (6.30) is completely regular in the limit $\epsilon\to 0$ and is evaluated in Appendix C.4.1. Using (C.148), we find that

$$\int_0^1 \mathrm{d}F\;(\alpha\beta\gamma)^{-\epsilon}\oint \mathrm{d}^3\tau\;\varepsilon(\tau)\frac{\sin\tau_{13}}{Q^{1-2\epsilon}} = -16\pi^2\,\zeta_3 + \mathcal{O}(\epsilon)\ . \tag{6.34}$$

Substituting this expression into (6.30) and expanding the prefactor about $\epsilon\to 0$, we finally arrive at the following result

$$\delta\mathcal{W}_4^{\text{v.m.}} = -\epsilon\frac{\hat{g}_B^4 C_F N\zeta_3}{8\pi^2} + \mathcal{O}(\epsilon)^2\ . \tag{6.35}$$

Finally, we discuss the bubble-like contributions in (6.27) and (6.29). By combining together these corrections, we find that they take the form of difference-theory diagrams, *i.e.*

$\mathcal{W}_4' = \mathcal{W}_4^{\mathcal{R}} - \mathcal{W}_4^{\text{Adj}} =$ 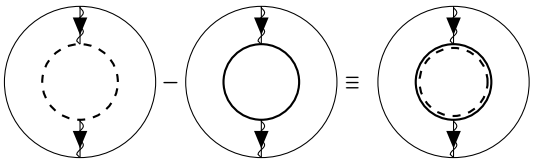 . (6.36)

This class of diagrams naturally arises from subtracting the corrections of the $\mathcal{N}=4$ theory from those of $\mathcal{N}=2$ SYM, and precisely describes the content of the interaction potential of the matrix model (2.20). Consequently, one might expect that it provides a complete description of the two-loop interaction contributions. However, this is not the case as it does not account for corrections (6.28) which give rise to the evanescent term (6.35). In theories with a non-vanishing β-function, such contributions become relevant: they interfere with the ultraviolet poles of the bare coupling and yield finite effects at higher orders, whereas in superconformal setups they can be safely neglected.

The contribution (6.36) involves the one-loop propagators of the adjoint scalar and gauge field propagator in the difference-theory approach. The explicit form of such corrections is obtained by subtracting from (6.25) an identical contribution with $\mathcal{R}=\text{Adj}$, namely

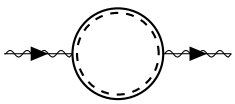

$$= \begin{cases} \dfrac{\delta_{ab} g_B^2}{(p^2)} \left(\delta_{\mu\nu} - \dfrac{p_\mu p_\nu}{p^2} \right) \Pi^{(1)}(p^2) \ , \\ \\ \dfrac{\delta_{ab} g_B^2}{(p^2)} \Pi^{(1)}(p^2) \ . \end{cases} \tag{6.37}$$

In the previous expression, we denoted by $\Pi^{(2)}$ the one-loop polarization operator in the difference-theory approach, *i.e.*

$$\Pi^{(1)}(p^2) = \beta_0 g_B^2 \frac{1}{p^{2\epsilon}} \frac{\Gamma(\epsilon)}{(4\pi)^{2-\epsilon}} \frac{\Gamma^2(1-\epsilon)}{\Gamma(2-2\epsilon)} \ , \tag{6.38}$$

which depends on the coefficient β_0 (1.25) of the β-function and consequently, it vanishes in superconformal models. Switching to configuration space by (C.14) and expanding the Wilson loop (5.7) at order g_B^2, we finally find that [3]

$$\mathcal{W}_4' = \frac{g_B^2 C_F}{2} \oint \mathrm{d}^2\tau \, \hat{\Delta}^{(1)}(x_{12}) \ . \tag{6.39}$$

In the previous expression, we introduced the one-loop effective propagator on the Wilson loop contour

$$\begin{aligned} \hat{\Delta}^{(1)}(x_{12}) &= \frac{g_B^2 \beta_0}{2^7 \pi^{4-2\epsilon}} \frac{\Gamma^2(1-\epsilon)}{\epsilon(1-2\epsilon)} \left(x_{12}^2\right)^{2\epsilon} \\ &= \frac{g_B^2 \beta_0}{2^7 \pi^{4-2\epsilon}} \frac{\Gamma^2(1-\epsilon)}{\epsilon(1-2\epsilon)} \left(4R^2 \sin^2\left(\frac{\tau_{12}}{2}\right)\right)^{2\epsilon} \ , \end{aligned} \tag{6.40}$$

where to obtain the second line we employed the parametrization (5.8). Performing the integration over the contour by (6.23), we finally arrive at the following result

$$\mathcal{W}_4' = \hat{g}_B^4 C_F \, P_2 \, B_2 \ , \quad \text{where} \quad P_2(\epsilon) = \frac{\beta_0}{16\pi^2 \epsilon(1-2\epsilon)} \tag{6.41}$$

captures the ultraviolet pole of the diagram and we recall that B_2 is given by (6.17). Since P_2 involves the coefficient β_0 (1.25), it vanishes in superconformal theories.

Combining together the relations we derived in this subsection, we find that the two-loop corrections to the observable can be written as follows

$$\mathcal{W}_4 = \hat{g}_B^4 \frac{C_F(2N^2-3)}{12N} B_1^2 + \hat{g}_B^4 C_F \, P_2 \, B_2 - \epsilon \hat{g}_B^4 \frac{3 C_F N \zeta_3}{16\pi^2} + \mathcal{O}(\epsilon)^2 \ . \tag{6.42}$$

[3] Let us note that the one-loop correction to the gluon propagator (6.25) involves the tensor structure $p_\mu p_\nu$. In the bubble-like contribution (6.36), this is contracted with the tangent vectors $\dot{x}_1^\mu \dot{x}_2^\nu$ and, upon Fourier transform, gives rise to total derivatives integrated over a closed path. These contributions obviously vanish.

6.1.3 Three-loop corrections

The calculation of the three-loop diagrams is significantly more involved and technical than its two-loop counterpart. However, the logical steps are identical except for the fact that we do not have to calculate the evanescent corrections since they contribute to four loops. This means that we can apply (6.10) to cast the three-loop corrections as follows

$$\mathcal{W}_6 = \mathcal{W}_6^{\ell.\ell.}\big|_{\epsilon=0} + \mathcal{W}_6' + \mathcal{O}(\epsilon) \ . \tag{6.43}$$

The ladder-like diagrams $\mathcal{W}_6^{\ell.\ell.}$ in $d = 4$ dimensions are captured by (5.19), *i.e.*

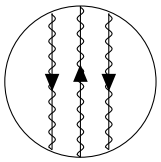

$$= \frac{\hat{g}_B^6 C_F (N^4 - 3N^2 + 3)}{4608 N^2} + \mathcal{O}(\epsilon) \ , \tag{6.44}$$

while the three-loop interaction contributions are encoded in the difference-theory term $\mathcal{W}_6' = \mathcal{W}_6^{\mathcal{R}} - \mathcal{W}_6^{\text{Adj}}$. This consists of the following diagrams

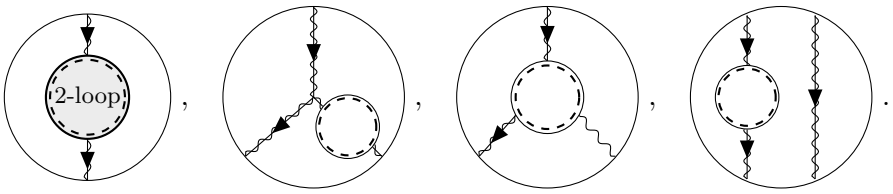

(6.45)

To facilitate the analysis, we organise these corrections in three families of diagrams according to the number of insertions on the Wilson loop contour.

Diagrams with two insertions We begin by considering the first contribution in (6.45). This diagram is a single-exchange correction dressed with the two-loop corrections to the adjoint scalar and gauge field propagator in the difference-theory approach. The relevant self-energies are extensively discussed in Appendix C.1.2, while here we only present the final result. In momentum space, it follows from (C.35a) and (C.35b) that

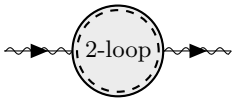

$$= \begin{cases} \dfrac{\delta_{ab} g_B^2}{(p^2)^2} \left(\delta_{\mu\nu} - \dfrac{p_\mu p_\nu}{p^2} \right) \Pi^{(2)}(p^2) \ , \\ \\ \dfrac{\delta_{ab} g_B^2}{(p^2)^2} \Pi^{(2)}(p^2) \ , \end{cases} \tag{6.46}$$

where $\Pi^{(2)}(p^2)$ is the two-loop polarization operator. According to (C.36) and (C.44), the polarization operator takes the following form

$$\Pi^{(2)}(p^2) = \sum_{i=1}^{4} f_i^{(2)}(\epsilon) \left(p^2\right)^{1-2\epsilon} \ , \tag{6.47}$$

where we denoted with $f_i^{(2)}(\epsilon)$ a set of meromorphic functions of the analytical continuation parameter ϵ, which are explicitly given by (C.45) and depend on the matter representation $\mathcal{R}$.

Switching to configuration space by (C.14) and expanding the Wilson loop operator (5.7) at order g_B^2, we find that

$$\mathcal{W}'_{6(2)} = \quad = \frac{g_B^2 C_F}{2} \oint \mathrm{d}^2\tau \, \hat{\Delta}^{(2)}(x_{12}) \ , \tag{6.48}$$

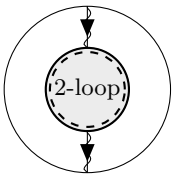

where, in analogy to the corrections (6.14) and (6.36), we defined a two-loop effective propagator on the Wilson loop contour

$$\begin{aligned} \hat{\Delta}^{(2)}(x_{12}) &= \sum_{i=1}^{4} f_i^{(2)}(\epsilon) \, \frac{g_B^4 \Gamma(1-3\epsilon)}{2^{3+4\epsilon}\pi^{2-\epsilon}\Gamma(1+2\epsilon)} \frac{1}{\left(x_{12}^2\right)^{-3\epsilon}} \ , \\ &= \sum_{i=1}^{4} f_i^{(2)}(\epsilon) \, \frac{g_B^4 \Gamma(1-3\epsilon)}{2^{3+4\epsilon}\pi^{2-\epsilon}\Gamma(1+2\epsilon)} \frac{1}{\left(4R^2 \sin^2 \frac{\tau_{12}}{2}\right)^{-3\epsilon}} \ , \end{aligned} \tag{6.49}$$

where to obtain the second equality we employed the parametrization (5.8). Substituting (6.49) into (6.48) and performing the integration over the contour by (6.23), we find that

$$\mathcal{W}'_{6(2)} = \hat{g}_B^6 \sum_{i=1}^{4} F_i^{(2)} \ , \tag{6.50}$$

$$F_i^{(2)} = f_i^{(2)}(\epsilon) \frac{C_F \Gamma(1-3\epsilon)}{2^{3+4\epsilon}\pi^{-\epsilon}\Gamma(1+2\epsilon)} \frac{\sec(3\epsilon)\,\Gamma(-3\epsilon)}{\Gamma(-6\epsilon)\Gamma(1-3\epsilon)} \ . \tag{6.51}$$

Finally, by replacing the functions $f_i^{(2)}(\epsilon)$ with their explicit form (C.45), we obtain

$$\begin{aligned} F_1^{(2)} &= -\frac{C_F \, i_{\mathcal{R}}}{8\pi^2} \frac{P_2 B_3}{\epsilon(1-2\epsilon)} + \mathcal{O}(\epsilon) \ , \\ F_2^{(2)} &= -\frac{C_F \, N}{16\pi^2} \frac{P_2 B_3}{\epsilon(1-3\epsilon)} \ , \\ F_3^{(2)} &= \frac{C_F \, N}{32\pi^2} \frac{P_2 B_3}{\epsilon(1+\epsilon)} \ , \\ F_4^{(2)} &= \frac{\mathcal{C}'_4}{N} \frac{3\zeta_3}{(4\pi)^4} + \mathcal{O}(\epsilon) \ , \end{aligned} \tag{6.52}$$

where we recall that the functions $B_n(\epsilon)$ and $P_2(\epsilon)$ are defined in (6.17) and (6.41), respectively, while $\mathcal{C}'_4$ is a colour factor which depends on the Dynkin index $i_{\mathcal{R}}$ (B.2a) and the quadratic Casimir $C_{\mathcal{R}}$ (B.2b) of the representation $\mathcal{R}$ as

$$\mathcal{C}'_4 = 2NC_F \left(C_{\mathcal{R}} i_{\mathcal{R}} - \frac{N i_{\mathcal{R}}}{2} - \frac{N^2}{2} \right) \ . \tag{6.53}$$

Diagrams with three insertions We now turn our attention to the three-loop diagrams with three insertions on the Wilson loop contour *i.e.*

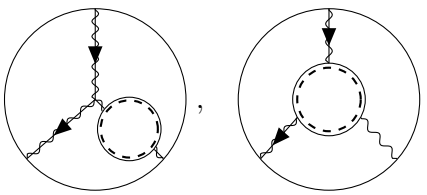

(6.54)

The first contribution describes the *reducible corrections* to the pure-gauge and gauge-scalar vertex. It arises when we dress the internal lines of the diagram (6.28) with the one-loop correction to the propagators of the adjoint scalar and gauge field in the difference-theory approach (C.28). The analysis of these diagrams is described in Appendix C.2 and closely resembles that presented in [121] for the analogous one-loop corrections (6.29). The calculation shows that

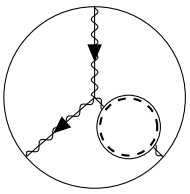

$$= -\hat{g}_B^6 \left(2F_2^{(2)} + 2F_3^{(2)} + \frac{N}{i_{\mathcal{R}}} F_1^{(2)} + 9\frac{\beta_0 C_F N}{2^8\pi^4}\zeta_3 \right) + \dots \ , \tag{6.55}$$

where we recall that the functions $F_i^{(2)}$ are defined in (6.52) and describe single-exchange contributions at three loops (6.48). It is interesting to observe that the structure of (6.55) mirrors (6.29). In that case, however, the term proportional to ζ_3 involves an evanescent factor which, according to (6.30), is generated by an integration over the contour. Conversely, in (6.55) the ζ_3 term is finite. The reason is that the diagrams (6.55) naturally come with an ultraviolet pole associated with the one-loop self-energy which compensates the evanescent ζ_3-like factor generated by integration over the contour. This interference effect leaves a finite result.

The second class of diagrams in (6.54) describes the *irreducible corrections* to the pure-gauge and gauge-scalar vertex in the difference method. These corrections are one of the novelties of this analysis and are evaluated in Appendix C.3. The complexity of the calculation arises from the structure of the internal interactions, which involves the famous triangle-like integrals [148]. These have to be integrated over a *path-ordered* contour in arbitrary dimension d due to the presence of UV singularities. Although the computations are extremely technical, the final result is remarkably simple, *i.e.*

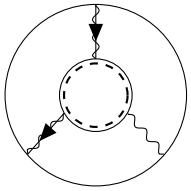

$$= \hat{g}_B^6 F_2^{(2)} + \hat{g}_B^6 \frac{5 C_F N \beta_0 \zeta_3}{2^8\pi^4} + \dots \ . \tag{6.56}$$

The structure of the result is extremely similar to (6.55) and the meaning of the different contributions is analogous as well.

By combining together (6.55) and (6.56), we finally find that

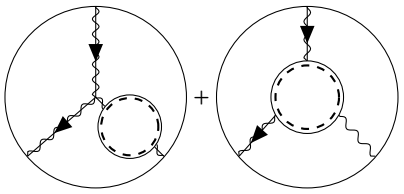

$$= \hat{g}_B^6 \left(\frac{N}{i_{\mathcal{R}}} F_1^{(2)} - F_2^{(2)} - 2F_3^{(2)} - \frac{C_F N \beta_0}{2^6\pi^4}\zeta_3 \right) + \mathcal{O}(\epsilon) \ . \tag{6.57}$$

Diagrams with four insertions Finally, we consider the three-loop corrections in (6.45) that involve four insertions on the Wilson loop contour. This class of contributions is obtained by dressing the internal lines of the two-loop ladder-like diagrams (6.19) with the one-loop correction to the adjoint scalar and gauge field propagator in the difference approach (C.28). The intermediate steps of the calculation are reported in Appendix C.4, where we show that

(C.133)

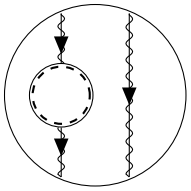

$$= \hat{g}_B^6 \left(F_3^{(2)} + \frac{C_F(2N^2-3)}{6N} B_1(\epsilon) B_2 P_2 - C_F N \frac{3\zeta_3\beta_0}{2^8\pi^4} \right) + \mathcal{O}(\epsilon) \ , \tag{6.58}$$

where we recall that $F_3^{(2)}$ is the three-loop bubble-like contribution defined in (6.52).

6.1.4 Renormalization

Combining together (6.50), (6.57) and (6.58), we observe partial cancellations between the bubble-like contributions $F_i^{(2)}$ (6.52) and the three-loop correction (6.43) takes the following form

$$\mathcal{W}_6' = \hat{g}_B^6 C_F \left(P_2^2 B_3 + \frac{2N^2-3}{6N} B_1 B_2 P_2 - N \frac{7\zeta_3\beta_0}{2^8\pi^4} + \frac{\mathcal{C}_4'}{N} \frac{3\zeta_3}{2^8\pi^4 C_F} \right) + \mathcal{O}(\epsilon) \ , \tag{6.59}$$

where we recall that the functions $B_n(\epsilon)$ and $P_2(\epsilon)$ are defined, respectively, in (6.17) and (6.41), while the colour factor $\mathcal{C}_4'$ is given by (6.53). Being combined with the one-loop (6.14) and two-loop corrections (6.42), the previous expression allows us to derive the dimensionally regularised observable at three-loop accuracy

$$\begin{aligned} \mathcal{W} = 1 &+ \hat{g}_B^2 C_F B_1 + \hat{g}_B^4 C_F \left(\frac{2N^2-3}{12N} B_1^2 + P_2 B_2 - \epsilon N \frac{3\zeta_3}{16\pi^2} \right) \\ &+ \hat{g}_B^6 C_F \left(\frac{N^4-3N^2+3}{4608N^2} + \frac{2N^2-3}{6N} B_1 B_2 P_2 + P_2^2 B_3 - N \frac{7\zeta_3\beta_0}{2^8\pi^4} + \frac{3\zeta_3\mathcal{C}_4'}{2^8\pi^4 N C_F} \right) \ , \end{aligned} \tag{6.60}$$

where we suppressed terms of order $\mathcal{O}(\epsilon)$ as they are irrelevant for our analysis.

The expectation value of the supersymmetric Wilson loop (6.60) develops both simple and double poles in the $\epsilon \to 0$ limit, through its dependence on $P_2(\epsilon)$ and $P_2^2(\epsilon)$ (6.41). Since the operator is defined over a smooth curve, the singularities must be reabsorbed by the charge renormalization [149–151] which, in terms of $\hat{g}_B = g_B R^\epsilon$, is given by [4]

$$\hat{g_B} = g_* \left(RM \, \mathrm{e}^{-\frac{1}{2}(2+\gamma+\log\pi)} \right)^\epsilon Z_{g_*} \equiv \left(R\overline{M} \right)^\epsilon Z_{g_*} \ , \tag{6.61}$$

where γ is the Euler-Mascheroni constant, g_* is the renormalized coupling evaluated at the renormalization scale M, namely the mass scale used to regularise the matrix model on S^4, while $Z_{g_*}(\epsilon)$ encodes the so-called subtraction terms. These can be easily calculated by employing the explicit expression of the β-function (1.25). We find that [23, 24, 144]

$$\begin{aligned} Z_{g_*}(\epsilon) &= \exp\left(- \int_0^{g_*} \frac{\mathrm{d}t}{t} \frac{(\epsilon t + \beta(t))}{\beta(t)} \right) \\ &= \left(1 + \frac{\beta_0 g_*^2}{16\pi^2\epsilon} \right)^{-\frac{1}{2}} = 1 - \frac{\beta_0 g_*^2}{32\pi^2\epsilon} + \dots \ . \end{aligned} \tag{6.62}$$

[4] In (6.61), we included the exponential factor $\mathrm{e}^{-\frac{1}{2}(2+\gamma+\log\pi)}$ to remove scheme-dependent contributions.

The renormalized Wilson loop average is obtained by replacing in (6.60) the bare coupling $\hat{g}_B$ with the renormalized one g_* and taking the limit $\epsilon \to 0$, *i.e.*

$$W_* = \lim_{\epsilon\to 0} \mathcal{W}(g_B)\Big|_{\hat{g}_B=g_*\left(R\bar{M}\right)^{\epsilon} Z_{g_*}} \,. \tag{6.63}$$

As a result, the overall dependence on the renormalization scale M vanishes and W_* satisfies a Callan-Symanzik equation [23]. This constrains the dependence of the observable on M, g_* and R, making these parameters appear in the running coupling constant g (2.27).

To see this more explicitly, we begin by examining the terms

$$\hat{g}_B^2 C_F \left(B_1 + \hat{g}_B^2 P_2 B_2 + \hat{g}_B^4 P_2^2 B_3\right) \,. \tag{6.64}$$

To proceed with the computation, we use (6.17) and (6.41) to expand the functions $B_n(\epsilon)$ and $P_2(\epsilon)$ in the limit $\epsilon \to 0$ and we replace the bare coupling constant in (6.64) with the renormalized one (6.61). Using the explicit expression for the subtraction terms $Z_{g_*}(\epsilon)$ (6.62), we find that the final result is finite in four dimensions and takes the following form

$$\begin{aligned}
&\lim_{\epsilon\to 0}\ \hat{g}_B^2\Big(B_1 + \hat{g}_B^2 P_2 B_2 + \hat{g}_B^4 P_2^2 B_3\Big)\Big|_{\hat{g}_B=g_*\left(R\bar{M}\right)^{\epsilon} Z_{g_*}} \\
&\qquad = \frac{g_*^2}{4}\left(1 - \beta_0 g_*^2 \log M^2R^2 + \beta_0^2 g_*^4\left(\left(\log M^2R^2\right)^2 + \frac{\pi^2}{3}\right)\right) + \mathcal{O}(g_*^8) \\
&\qquad = \frac{g^2}{4} + \mathcal{O}(g^8) + \mathcal{O}(\log^0 RM) \,,
\end{aligned} \tag{6.65}$$

where we recall that β_0 is the one-loop coefficient (1.25) of the β-function, while g is the running coupling constant (2.27). To obtain the last equality, we exploited the fact that the radius of the Wilson loop, identified with the radius of S^4 under the stereographic projection (see Fig. 5.2), has to satisfy the condition (2.29). As a result, the logarithmic contributions $\log RM$, associated with the short-distance behaviour of the theory, grow and dominate over the constant term of order $\mathcal{O}(\log^0 RM)$ in the second line of (6.65). To keep the perturbative expansion under control, these logarithmic corrections must be resummed into the running coupling g, as predicted by the Callan-Symanzik equations [23].

Repeating the calculation for the divergent terms proportional to the colour factor $(2N^2-3)$ in (6.60), we find that

$$\lim_{\epsilon\to 0}\ \hat{g}_B^4\left(B_1^2 + 2\hat{g}_B^2 B_1 B_2 P_2\right)\Big|_{\hat{g}_B=g_*\left(R\bar{M}\right)^{\epsilon} Z_{g_*}} = \frac{g^4}{16} + \mathcal{O}(g^8) \,. \tag{6.66}$$

As we anticipated, the result is free of divergences and all the singularities were reabsorbed via the charge renormalization (6.62). Finally, we consider the regular corrections in (6.60). These are proportional to ζ_3 and contribute to the renormalized observable as follows

$$\lim_{\epsilon\to 0}\ \hat{g}_B^4\left(\hat{g}_B^2\frac{\mathcal{C}_4'}{N}\frac{3\zeta_3}{2^8\pi^4} - \frac{C_F N\zeta_3}{16\pi^2}\left(3\epsilon + 7\frac{\beta_0}{16\pi^2}\hat{g}_B^2\right)\right)\Bigg|_{\hat{g}_B=g_*\left(R\bar{M}\right)^{\epsilon} Z_{g_*}} = -g^6\beta_0\frac{C_F N\zeta_3}{2^8\pi^4} + g^6\frac{\mathcal{C}_4'}{N}\frac{3\zeta_3}{2^8\pi^4} \,. \tag{6.67}$$

Crucially, the term proportional to β_0 arises from an interference effect between the evanescent contribution 3ϵ and the ultraviolet poles of the bare coupling encoded in the subtraction terms (6.62). Importantly, the interference is only sensitive to the short-distance properties of the

theory, as it involves ultraviolet poles, and consequently, we expect that the contributions to the observable associated with these effects take the same form in flat space and on the sphere. Indeed, collecting all the results we derived in this subsection, we find that the renormalized observable within the regime (2.29) is given by

$$\begin{aligned} W_* &= W_0 + g^6 \frac{\mathcal{C}_4'}{N} \frac{3\zeta_3}{2^8\pi^4} - g^6 C_F N \beta_0 \frac{\zeta_3}{2^8\pi^4} + \mathcal{O}(g^8) \\ &= W_0(g) + \frac{g^6 \zeta_3 C_F}{2^9\pi^4} \left(12\left(C_{\mathcal{R}} i_{\mathcal{R}} - N^2\right) + N\beta_0\right) + \dots \ , \end{aligned} \tag{6.68}$$

where W_0 was introduced in (5.19) and to obtain the second line we replaced the colour factor $\mathcal{C}_4'$ with its explicit form (6.53). As anticipated, (6.68) *precisely matches* the three-loop prediction of localization (5.22) *within* the perturbative regime (2.29). Although restricted to this range, the agreement of the calculation in flat space (6.68) with the results on S^4 provides a non-trivial extension of the localization results beyond the usual conformal settings.

6.2 Chiral correlators in perturbation theory

We now turn our attention to the calculation of the two-point function (6.80) in flat space. For this class of observables, we can employ the $\mathcal{N} = 1$ superfield formalism [5] [30, 60, 62, 152–155] to simplify the analysis.

In this approach, the adjoint scalar field $\phi(x)$ of the $\mathcal{N} = 2$ vector multiplet corresponds to the lowest component of an adjoint $\mathcal{N} = 1$ chiral superfield Φ, *i.e.*

$$\phi(x) = \Phi(x, \theta, \bar{\theta})\Big|_{\theta=\bar{\theta}=0} \ , \tag{6.69}$$

where θ and $\bar{\theta}$ are complex-valued Grassmann coordinates. Similarly, the complex conjugate scalar $\bar{\phi}(x)$ sits in an anti-chiral adjoint superfield, *i.e.*

$$\bar{\phi}(x) = \Phi^\dagger(x, \theta, \bar{\theta})\Big|_{\theta=\bar{\theta}=0} \ . \tag{6.70}$$

The dynamics of an $SU(N)$ $\mathcal{N} = 2$ vector multiplet (1.20) can be described through the $\mathcal{N} = 1$ formalism by combining together an $\mathcal{N} = 1$ vector and an adjoint $\mathcal{N} = 1$ chiral superfield. In Euclidean space, the gauge-fixed action takes the following form [6]

$$\begin{aligned} S_{\text{gauge}} = \frac{1}{8g_B^2}\left(\int d^4x\, d^2\theta\, \text{tr}\left(W^\alpha W_\alpha\right) + \text{h.c.}\right) + 2\int d^4x\, d^2\theta\, d^2\bar{\theta}\ \text{tr}\left(\text{e}^{-2g_B V}\, \Phi^\dagger\, \text{e}^{2g_B V}\, \Phi\right) \\ - \frac{\xi}{4}\int d^4x\, d^2\theta\, d^2\bar{\theta}\ \text{tr}\left(\bar{D}^2 V\, D^2 V\right) \ , \end{aligned} \tag{6.71}$$

where W_α is the chiral superfield-strength of V, namely

$$W_\alpha = -\frac{1}{4}\bar{D}^2\left(\text{e}^{-2gV} D_\alpha\, \text{e}^{2gV}\right) \ , \tag{6.72}$$

[5] Note that the superfield formalism cannot be applied to the perturbative calculation of the supersymmetric Wilson loops (5.7), as it is not manifestly expressed in terms of fundamental superfields.

[6] We summarise in Section A.1 our convention for the integration of Grassmann variables.

with

$$D_\alpha = +\frac{\partial}{\partial\theta^\alpha} + \mathrm{i}\,\sigma^\mu_{\alpha\dot\alpha}\bar\theta^{\dot\alpha}\partial_\mu\ , \qquad \bar D_{\dot\alpha} = -\frac{\partial}{\partial\bar\theta^{\dot\alpha}} - \mathrm{i}\,\theta^\alpha\sigma^\mu_{\alpha\dot\alpha}\partial_\mu\ . \tag{6.73}$$

The last term in (6.71) implements the gauge fixing, with $\xi = 1$ corresponding to the Feynman gauge[7]. With our conventions, the action S_{gauge}, as well as the matter actions we will shortly describe, are negative-definite and consequently, they appear in the path integral as $\mathrm{e}^{S_{\text{gauge}}}$.

Expanding the superfields on a basis of fundamental generators t^a of $SU(N)$ as $V = V^a t_a$ and $\Phi = \Phi^a t_a$, we find that the action (6.71) up to second order in V with $\xi = 1$ becomes

$$S_{\text{gauge}} = \int d^4x\, d^2\theta\, d^2\bar\theta \Big(- V^a \,\Box\, V^a + \Phi^{\dagger a}\Phi^a + 2\mathrm{i} g_B f^{abc}\,\Phi^{\dagger a} V^b \Phi^c - 2 g_B^2 f^{abe} f^{ecd}\,\Phi^{\dagger a} V^b V^c \Phi^d + \cdots \Big)\ , \tag{6.74}$$

where f^{abc} are the structure constants of $SU(N)$ (B.1).

In the $\mathcal{N} = 1$ language, the dynamics of an $\mathcal{N} = 2$ massless hypermultiplet in an arbitrary representation $\mathcal{R}$ of the gauge group consists of two chiral multiplets Q and $\tilde Q$ transforming in the representation $\mathcal{R}$ and in the conjugate $\mathcal{R}^*$, respectively, together with their anti-chiral partners $Q^\dagger$ and $\tilde Q^\dagger$. The action for these massless hypermultiplets is

$$S_Q = \int d^4x\, d^2\theta\, d^2\bar\theta \left(Q^\dagger\, \mathrm{e}^{2 g_B V} Q + \widetilde{Q}\, \mathrm{e}^{-2 g_B V} \widetilde{Q}^\dagger \right) + \left(\mathrm{i}\sqrt{2} g_B \int d^4x\, d^2\theta\, \widetilde{Q}\Phi Q + \text{h.c.} \right)\ , \tag{6.75}$$

which, up to second order in V, explicitly reads

$$\begin{aligned} S_Q = \int d^4x\, d^2\theta\, d^2\bar\theta \Big(& Q^\dagger_u Q_u + 2 g_B\, Q^\dagger_u V^a T^a_{uv}\, Q_v + 2 g_B^2\, Q^\dagger_u V^a T^a_{uw} V^b T^b_{wv} Q_v \\ & + \widetilde{Q}_u \widetilde{Q}^\dagger_u - 2 g_B \widetilde{Q}_u V^a T^a_{uv} \widetilde{Q}^\dagger_v + 2 g_B^2\, \widetilde{Q}_u V^a T^a_{uw} V^b T^b_{wv} \widetilde{Q}^\dagger_v + \cdots \\ & + \mathrm{i}\sqrt{2} g_B\, \widetilde{Q}_u \Phi^a T^a_{uv} Q_v\, \bar\theta^2 - \mathrm{i}\sqrt{2} g_B\, Q^\dagger_u \Phi^{\dagger a} T^a_{uv} \widetilde{Q}^\dagger_v\, \theta^2 \Big)\ . \end{aligned} \tag{6.76}$$

In the previous expression, u and v are the indices of the representation $\mathcal{R}$, *i.e.* $u, v = 1, \ldots, \dim \mathcal{R}$.

In the $\mathcal{N} = 1$ superfield formalism, we regularise Feynman diagrams in superspace by first integrating over the Grassmann-valued coordinates in four dimensions and subsequently, continuing the resulting momentum integrals to $d = 4 - 2\epsilon$ dimensions [60, 62, 144, 156]. Most of the diagrams we will consider in what follows were originally calculated in [144], where the authors studied the correlators (6.80) in non-conformal $\mathcal{N} = 2$ SQCD. Here we generalised those results to theories with massless matter in an arbitrary representation $\mathcal{R}$, by including novel classes of diagrams that were not considered in [60].

Before entering the analysis of the chiral correlator (6.80), we report the explicit expression for the propagators in superspace. These are a straightforward generalization of those considered in ordinary spacetime and can be extracted from the actions (6.74) and (6.75). For instance, the free propagators of the $\mathcal{N} = 1$ vector and $\mathcal{N} = 1$ chiral superfield take the following form

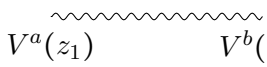

$$= -\frac{\delta_{ab}}{2}\theta_{12}^2\bar\theta_{12}^2\Delta(x_{12})\ , \tag{6.77a}$$

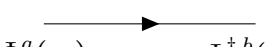

$$= \delta_{ab}\boldsymbol{\Delta}(z_1, z_2)\ , \tag{6.77b}$$

[7] While in general the gauge choice (*i.e.* different values of ξ in (6.71)) is a matter of taste, in a supersymmetric field theory the choice of the Fermi-Feynman gauge ($\xi = 1$) is obligatory, since otherwise the auxiliary field in the vector multiplet with zero canonical dimension has a logarithmic propagator. Note that S_{gauge} should contain also a ghost contribution, which however is not relevant for our calculations, and thus we omit it.

where $\Delta(x)$ is defined in (6.13) and we introduced

$$\begin{aligned}\mathbf{\Delta}(z_i, z_j) &= \mathrm{e}^{\mathrm{i}(\theta_i\sigma\bar{\theta}_i+\theta_j\sigma\bar{\theta}_j-2\,\theta_i\sigma\bar{\theta}_j)\cdot\partial_{x_i}}\int\frac{\mathrm{d}^d p}{(2\pi)^d}\frac{e^{\mathrm{i}p\cdot x}}{(p^2)}\\ &= \mathrm{e}^{\mathrm{i}(\theta_i\sigma\bar{\theta}_i+\theta_j\sigma\bar{\theta}_j-2\,\theta_i\sigma\bar{\theta}_j)\cdot\partial_{x_i}}\Delta(x_{ij})\ .\end{aligned} \tag{6.78}$$

In the previous expression, we introduced the notation $z_i = (x^\mu, \theta_i, \bar{\theta}_i)$, the intertwining matrix σ is explicitly given by (A.6), while to obtain the second equality we performed the integration over p and expressed the result in terms of the massless propagator $\Delta(x)$ (6.13).

Analogously, the Feynman propagators for the $\mathcal{N}=1$ matter superfields are given by

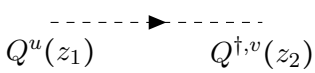

$$= \delta_{uv}\mathbf{\Delta}(z_1, z_2)\ , \tag{6.79a}$$

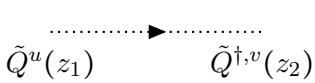

$$= \delta_{uv}\mathbf{\Delta}(z_1, z_2)\ . \tag{6.79b}$$

Organizing perturbation theory In theories with a non-vanishing β-function, the (dimensionally regularised) correlator (6.80) takes the following form [144]

$$\left\langle O_{\vec{n}}(x)\,\overline{O}_{\vec{m}}(0)\right\rangle = G_{\vec{n},\vec{m}}(g_B, x, \epsilon)\,\Delta^n(x)\,\delta_{nm}\ , \tag{6.80}$$

where $\Delta(x)$ is the massless scalar propagator in $d = 4-2\epsilon$ dimensions (6.13), while the function $G_{\vec{n},\vec{m}}$ depends non-trivially on the spacetime separation of the operator, signalling the presence of anomalous dimensions. In perturbation theory, it can be expanded in powers of g_B as follows

$$G_{\vec{n},\vec{m}}(g_B, x, \epsilon) = g_B^{2n}\,G^{(0)}_{\vec{n},\vec{m}}\Big[1+\sum_{k=1}^{\infty} g_B^{2k}\,\mathcal{G}^{(k)}_{\vec{n},\vec{m}}(x,\epsilon)\Big]\ , \tag{6.81}$$

where we factorized the tree-level contribution $G^{(0)}_{\vec{n},\vec{m}}$ (5.27) while $\mathcal{G}^{(k)}_{\vec{n},\vec{m}}$ denotes the corrections at k loops. When the notation is not ambiguous, we will omit the dependence on $\vec{n}$ and $\vec{m}$.

Following the approach developed in Section 6.1 for the supersymmetric Wilson loop, we decompose the loop corrections $\mathcal{G}^{(k)}$ as

$$\mathcal{G}^{(k)} = \mathcal{G}^{(k)}_{\mathcal{R}} + \mathcal{G}^{(k)}_{\text{v.m.}}\ , \tag{6.82}$$

where $\mathcal{G}^{(k)}_{\mathcal{R}}$ and $\mathcal{G}^{(k)}_{\text{v.m.}}$ capture, respectively, the diagrams with internal hypermultiplet lines in the representation $\mathcal{R}$ and those involving vector-multiplet lines only. Of course, the decomposition (6.82) also holds for $\mathcal{N}=4$ SYM, which can be seen as an $\mathcal{N}=2$ theory with an adjoint hypermultiplet. This means that in the maximally supersymmetric model we can write (6.8) with $\mathcal{R} = \text{Adj}$. On the other hand, it is well-known that in $\mathcal{N}=4$ SYM the loop corrections to the correlator (6.80) identically vanish in $d=4$ and consequently, we must have

$$\mathcal{G}^{(k)}_{\text{v.m.}} = -\mathcal{G}^{(k)}_{\text{Adj}} + \delta'\mathcal{G}^{(k)}\ , \tag{6.83}$$

where $\mathcal{G}^{(k)}_{\text{Adj}}$ captures all the corrections with internal hypermultiplet lines in the adjoint representation, while the second term is an evanescent correction in four dimensions.

In a generic $\mathcal{N}=2$ gauge theory, the contribution arising from the $\mathcal{N}=2$ vector multiplet $\mathcal{G}^{(k)}_{\text{v.m.}}$ is in common with $\mathcal{N}=4$ SYM and consequently, we find that

$$\mathcal{G}^{(k)} = \mathcal{G}^{(k)}_{\mathcal{R}} - \mathcal{G}^{(k)}_{\text{Adj}} + \delta'\mathcal{G}^{(k)} \equiv \mathcal{G}'^{(k)} + \delta'\mathcal{G}^{(k)}\ , \tag{6.84}$$

where $\mathcal{G}'^{(k)}$ encodes the usual *difference-theory* corrections, analogous to those encountered in the analysis of the supersymmetric Wilson loop.

For non-conformal $\mathcal{N}=2$ SQCD, the functions $\mathcal{G}'^{(k)}$ were computed in [144] for $k=1,2$, while the evanescent corrections $\delta'\mathcal{G}^{(k)}$ are a novelty. In what follows, we generalised the calculations of [144] to an arbitrary matter representation $\mathcal{R}$, and show that, by including interference effects between the evanescent contributions and the UV poles of the bare coupling, the renormalized correlators perfectly match the localization predictions up to two loops.

6.2.1 Tree-level

At tree-level, we find a unique diagram which can be simply computed by using the free propagator of the adjoint scalar field (6.12). Going through the calculation, we obtain

$$\left\langle O_{\vec{n}}(x)\,\overline{O}_{\vec{m}}(0)\right\rangle\Big|_{\text{tree}} = \quad x \quad 0 \quad = g_B^{2n}\,G^{(0)}_{\vec{n},\vec{m}}\,\Delta^n(x,\epsilon)\,\delta_{nm}\ , \tag{6.85}$$

where we recall that $G^{(0)}_{\vec{n},\vec{m}}$ is given by (5.27). The previous expression encodes tree-level correction to the correlator (6.80), which is regular in four dimensions and matches the structure of (6.81).

6.2.2 One-loop corrections

At one-loop accuracy ($k=1$), the two-point function (6.80) receives contributions from the following classes of diagrams

$$x \quad 0 \ , \qquad x \quad 0 \ , \qquad x \quad 0 \ , \tag{6.86}$$

where the internal interactions involve the propagation of *virtual* $\mathcal{N}=1$ superfields. More precisely, the dashed and dotted lines represent, respectively, the $\mathcal{N}=1$ chiral superfields in the representation $\mathcal{R}$ and $\mathcal{R}^*$, which give rise to the $\mathcal{N}=2$ matter hypermultiplets, while the wavy line denotes the propagation of the $\mathcal{N}=1$ vector multiplet (1.19) sitting inside the $\mathcal{N}=2$ vector multiplet (1.20). In terms of the decomposition (6.8), the first diagram accounts for $\mathcal{G}^{(1)}_{\mathcal{R}}$, while the second and third diagram yield $\mathcal{G}^{(1)}_{\text{v.m.}}$.

We can conveniently combine together the first two contributions in (6.86) and represent their sum as

$$x \quad v_{2,1} \quad 0 \ , \tag{6.87}$$

where the grey bubble stands for the one-loop correction to the propagator of the adjoint scalar. Thus, our task is to evaluate diagrams dressed with a one-loop scalar self-energy and with an internal vector exchange.

Diagrams with a one-loop correction to the propagators The one-loop correction to the scalar propagator in the $\mathcal{N}=1$ superfield formalism receives contributions from the following diagrams

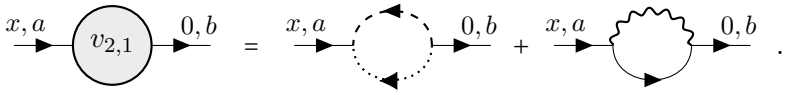

(6.88)

To simplify the calculation, we observe that in the $\mathcal{N}=1$ superfield formalism the total one-loop correction to the scalar propagator $\mathcal{N}=4$ SYM identically vanishes in *any dimension* [8]. As a result, we can write

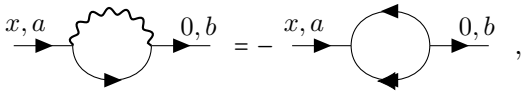

(6.89)

where the loop on the right-hand side is associated with the hypermultiplet in the adjoint representation. Substituting the previous expression into (6.88), we find that

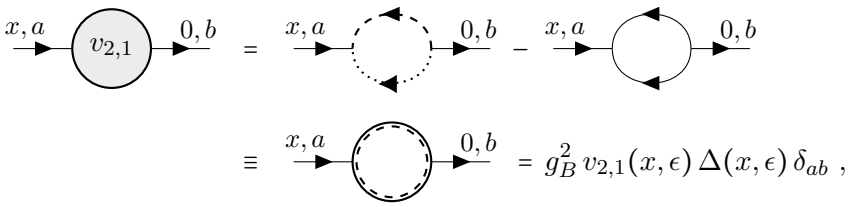

(6.90)

where we employed the familiar double dashed/continuous line to emphasise that this combination of diagrams is a difference-theory contribution and defined

$$v_{2,1}(x,\epsilon) = \beta_0 \frac{(\pi x^2)^\epsilon}{8\pi^2} \frac{\Gamma(1-\epsilon)}{2\epsilon(1-2\epsilon)} \,, \tag{6.91}$$

where β_0 is the β-function coefficient (1.25). This function exhibits a UV divergence, associated with the pole in ϵ, and vanishes in superconformal models where $\beta_0 = 0$.

Using (6.90), it is straightforward to find that

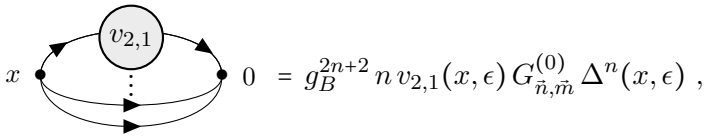

(6.92)

where n is the symmetry factor corresponding to the insertion of the bubble in each of the n propagators. According to the decomposition (6.84), we have

$$\mathcal{G}'^{(1)}_{\tilde{n},\tilde{m}}(x,\epsilon) = n\, v_{2,1}(x,\epsilon) \,, \tag{6.93}$$

since (6.92) is a pure difference-theory contribution.

[8] This is a peculiar feature of the $\mathcal{N}=1$ superfield formalism, which maintains manifest supersymmetry. In contrast, working in the Wess-Zumino gauge, as we did in Appendix C, the propagator of the adjoint scalar field receives non-trivial contributions from the matter sector. These different results are expected as propagators are not gauge-invariant quantities. For a more advanced analysis of these effects we refer to [157–161]

Diagrams with internal vector lines We finally turn our attention to the rightmost diagram in (6.86). Since this correction was not considered in [60], we present a detailed derivation of the calculation.

To begin with, we consider the building block diagram

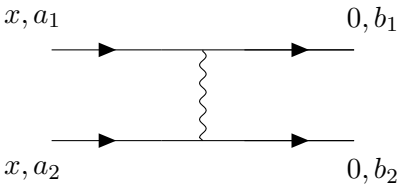

$$\equiv \Sigma^{a_1 a_2 b_1 b_2}(x) \ , \tag{6.94}$$

which arises from the cubic interaction $\Phi^\dagger V \Phi$ of the pure-gauge action (6.74). In particular, by employing the propagators in superspace (6.77), we find that

$$\begin{aligned}\Sigma^{a_1 a_2 b_1 b_2} &= -N g_B^2 \, C^{a_1 a_2 b_1 b_2} \int \mathrm{d}z_3 \mathrm{d}z_4 \, \theta_{34}^2 \, \bar\theta_{34}^2 \, \mathbf{\Delta}(z_3, z_4) \mathbf{\Delta}(x, z_3) \mathbf{\Delta}(x, z_4) \mathbf{\Delta}(z_3, 0) \mathbf{\Delta}(z_4, 0) \\ &\equiv g_B^2 \, C^{a_1 a_2 b_1 b_2} \, \Sigma(x) \ ,\end{aligned} \tag{6.95}$$

where the functions $\mathbf{\Delta}(z_i, z_j)$ are defined in (6.78), the integration measure $\mathrm{d}z$ is given by $\mathrm{d}z_i = \mathrm{d}^4 x_i \, \mathrm{d}^2\theta_i \, \mathrm{d}^2\bar\theta_i$, while the colour structure of the diagram is encoded in the $SU(N)$ tensor

$$C^{a_1 a_2 b_1 b_2} = -\frac{1}{N} f^{a_1 b_1 c} f^{a_2 b_2 c} \ . \tag{6.96}$$

To proceed with the calculation of (6.95), we replace the functions $\mathbf{\Delta}(z_i, z_j)$ with their integral representation in momentum space (6.78) and we obtain

$$\begin{aligned}\Sigma &= -N \int \mathrm{d}^2\theta_4 \, \mathrm{d}^2\bar\theta_4^2 \int \frac{\mathrm{d}^d p}{(2\pi)^d} \frac{\mathrm{d}^d k}{(2\pi)^d} \frac{\mathrm{d}^d \ell}{(2\pi)^d} \frac{\mathrm{e}^{-2\theta_4 p \bar\theta_4} \, \mathrm{e}^{\mathrm{i}px}}{\ell^2 \, k^2 \, (\ell - k)^2 \, (k + p)^2 \, (\ell + p)^2} \\ &= N \int \frac{\mathrm{d}^d p}{(2\pi)^d} \frac{\mathrm{d}^d k}{(2\pi)^d} \frac{\mathrm{d}^d \ell}{(2\pi)^d} \frac{p^2 \, \mathrm{e}^{\mathrm{i}px}}{\ell^2 \, k^2 \, (\ell - k)^2 \, (k + p)^2 \, (\ell + p)^2} \ ,\end{aligned} \tag{6.97}$$

where to obtain the second line we integrated over the Grassmann variables θ_4 and $\bar\theta_4$ by Taylor expanding the exponential factor. The resulting integrations over the momenta k and ℓ are considered in Section C.1. In particular, using (C.12) and (C.13), we finally find that [9]

$$\Sigma(x) = e_{2,1}(x, \epsilon) \, \Delta^2(x, \epsilon) \quad \text{with} \quad e_{2,1}(x, \epsilon) = \frac{3N \, \zeta_3 \, \epsilon \, (x^2)^\epsilon \, \Gamma(2 - 3\epsilon)}{4^{1+2\epsilon} \, \pi^{2+\epsilon} \, \Gamma(1 - \epsilon)^2 \, \Gamma(1 + 2\epsilon)} \ . \tag{6.98}$$

Combining together (6.98) with (6.94) and exploiting the fusion/fission rules of $SU(N)$ to compute the colour factor of the corresponding correlator as explained in [144] [10], we obtain

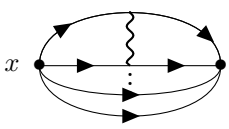

$$= -g_B^{2n+2} \, n \, e_{2,1}(x, \epsilon) \, G^{(0)}_{\vec n, \vec m} \, \Delta^n(x, \epsilon) \ . \tag{6.99}$$

[9] We checked that the expansion around $\epsilon \to 0$ in (6.98) coincides with the result reported in [162].
[10] See in particular Eqs. (2.36)–(2.39) of [144].

This is an explicit realization of an evanescent contribution and thus, according to (6.84), we can write

$$\delta' \mathcal{G}^{(1)}_{\vec{n},\vec{m}}(x,\epsilon) = -n\, e_{2,1}(x,\epsilon) \ . \tag{6.100}$$

Combining together (6.93) and (6.100), we find that the total one-loop result is given by

$$\mathcal{G}^{(1)}_{\vec{n},\vec{m}}(x,\epsilon) = \mathcal{G}'^{(1)}_{\vec{n},\vec{m}}(x,\epsilon) + \delta' \mathcal{G}^{(1)}_{\vec{n},\vec{m}}(x,\epsilon) = n\big[v_{2,1}(x,\epsilon) - e_{2,1}(x,\epsilon)\big] \ . \tag{6.101}$$

The previous expression confirms that, up to evanescent terms, the one-loop corrections are encoded in the difference-theory term $\mathcal{G}'^{(1)}_{\vec{n},\vec{m}}$ given in (6.93). At two loops, we exploit this fact to reduce the number of diagrams we have to compute.

6.2.3 Two loops

We now consider the two-loop contributions ($k = 2$). Since we are interested in computing correlators up to order g_B^{2n+4}, we can focus on the difference-theory terms and discard the two-loop evanescent parts which only affect the result at order g_B^{2n+6}. Most of the difference-theory diagrams at this order were already computed in [144] for the non-conformal $\mathcal{N} = 2$ SQCD. In what follows, we will generalised these results to a generic representation $\mathcal{R}$, including the one-loop evanescent factor $e_{2,1}(x,\epsilon)$ that was not considered in [144].

Diagrams with one-loop propagators At two loops, the correlator (6.80) receives contributions from diagrams in which lines are dressed with the one-loop self-energy (6.90). We find two distinct classes of corrections. The first one takes the following form

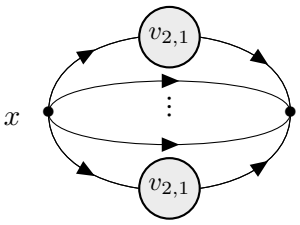

$$= g_B^{2n+4}\, \frac{n(n-1)}{2}\, v_{2,1}^2(x,\epsilon)\, G^{(0)}_{\vec{n},\vec{m}}\, \Delta^n(x,\epsilon) \ , \tag{6.102}$$

where the symmetry factor $\frac{n(n-1)}{2}$ encodes the combinatorics of the possible bubble insertions, while the second class of corrections is described by

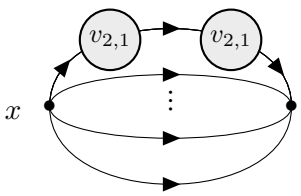

$$= g_B^{2n+4}\, n\, v_{2,1}^2(x,\epsilon)\, G^{(0)}_{\vec{n},\vec{m}}\, \Delta^n(x,\epsilon) \ . \tag{6.103}$$

Diagrams with two-loop corrections to the propagators The two-loop correction to the scalar propagator is described by the following diagrams evaluated in [144]

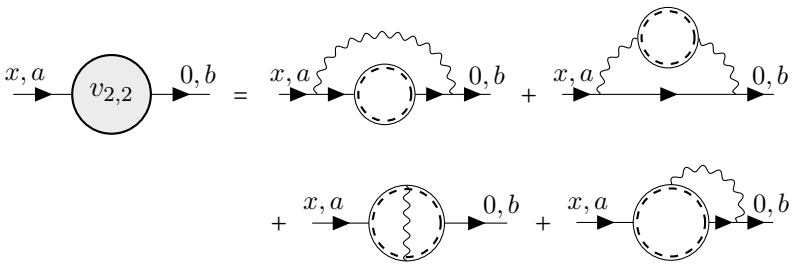

$$= g_B^4\, v_{2,2}(x,\epsilon)\, \Delta(x,\epsilon)\, \delta^{ab} \ , \tag{6.104}$$

where

$$v_{2,2}(x,\epsilon) = \frac{(\pi x^2)^{2\epsilon}}{(8\pi^2)^2}\left[6\,\zeta_3\Big(C_{\mathcal{R}}\, i_{\mathcal{R}} - N^2 + \frac{N\beta_0}{4}\Big) + \frac{N\beta_0\,\Gamma^2(1-\epsilon)}{4\epsilon^2\,(1-2\epsilon)(1+\epsilon)}\right] + \mathcal{O}(\epsilon)\ . \tag{6.105}$$

In the previous expression, $C_{\mathcal{R}}$ denotes the quadratic Casimir of the representation $\mathcal{R}$ (B.2b). For the specific matter representation (5.15), the overall coefficient of ζ_3 inside the square brackets becomes

$$-3\left(\frac{N_f}{2N} + \frac{N_a(N-2)(4+2N-N^2)}{2N} + \frac{N_s(N+2)(4-2N-N^2)}{2N} + N^2\right)\ , \tag{6.106}$$

which reduces to the one given in [144] for SQCD. Notice that the term in (6.105) proportional to ζ_3 is regular when $\epsilon \to 0$, while the second term proportional to $N\beta_0$ exhibits a double pole in ϵ. Using this result, it is immediate to find that

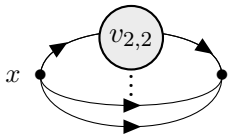

$$= g_B^{2n+4}\, n\, v_{2,2}(x,\epsilon)\, G^{(0)}_{\vec{n},\vec{m}}\, \Delta^n(x,\epsilon)\ , \tag{6.107}$$

where n is the symmetry factor of the diagram.

Diagrams with internal vector lines and one-loop self-energies At two loops, the correlator (6.80) receives contributions also from diagrams involving vector-multiplet propagation and a single self-energy (6.90). These contributions can be organised into two distinct families according to the insertion of the self-energy. For instance, when dressing with the one-loop correction (6.90) the lines of the diagram (6.94), we obtain the contributions originally analysed

in [144], namely

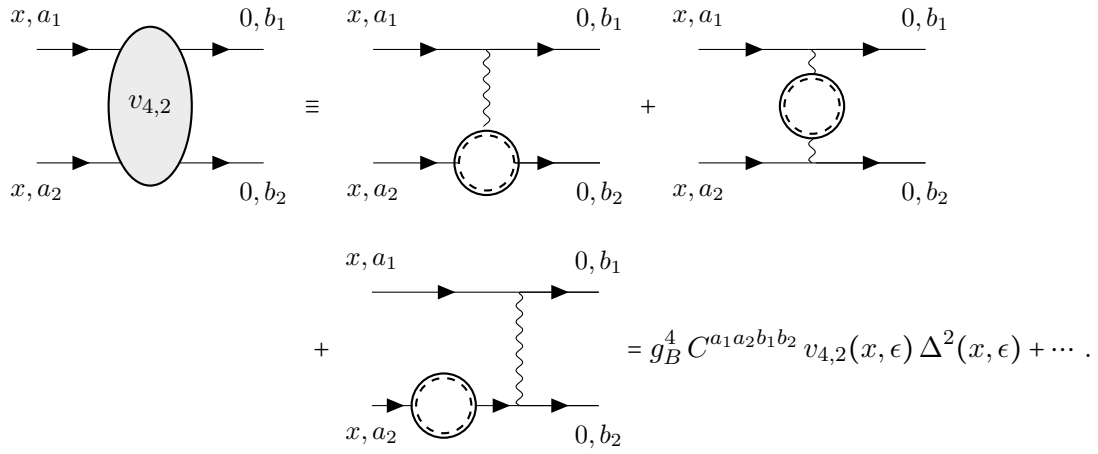

(6.108)

Here, the colour tensor is defined in (6.96) and the function $v_{4,2}(x,\epsilon)$ is given by [11]

$$v_{4,2}(x,\epsilon) = \frac{(\pi x^2)^{2\epsilon}}{(8\pi^2)^2} N\beta_0 \left[\frac{21\,\zeta_3}{2} + \frac{\Gamma^2(1-\epsilon)}{4\epsilon^2\,(1-2\epsilon)(1+\epsilon)}\right] + \mathcal{O}(\epsilon)\ . \tag{6.109}$$

Finally, the ellipses on right-hand side of (6.108) stand for terms that are anti-symmetric in (a_1,a_2) and (b_1,b_2). Since they do not contribute when this sub-diagram is inserted in a chiral/anti-chiral correlator, they can be neglected. Using this result and the fusion/fission identities of $SU(N)$ to compute the overall colour factor, we find

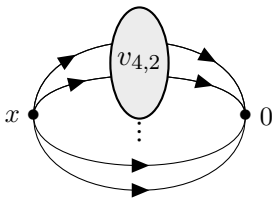

$$= -g_B^{2n+4}\, n\, v_{4,2}(x,\epsilon)\, G^{(0)}_{\vec{n},\vec{m}}\, \Delta^n(x,\epsilon)\ . \tag{6.110}$$

The second class of contributions arises from diagrams where the one-loop correction is inserted in one of the scalar propagators that are not involved in the vector exchange, *i.e.*

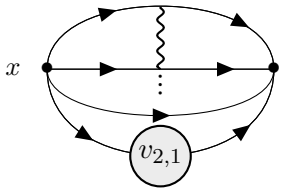

$$= -g_B^{2n+4}\, n(n-2)\, v_{2,1}(x,\epsilon)\, e_{2,1}(x,\epsilon)\, G^{(0)}_{\vec{n},\vec{m}}\, \Delta^n(x,\epsilon)\ . \tag{6.111}$$

The overall symmetry factor can be explained as follows. The sign and the coefficient n are analogous to those appearing in the vector-exchange diagram at one loop (6.99), while the factor of $(n-2)$ arises from the possibilities of inserting the one-loop self-energy in each of the $(n-2)$ remaining propagators. Importantly, the function appearing in (6.111) is finite in the limit $\epsilon \to 0$, since the pole of $v_{2,1}(x,\epsilon)$ (6.90) is compensated by the evanescent term $e_{2,1}(x,\epsilon)$ (6.98). Therefore, this contribution is regular at this order.

[11] In [144] this function is denoted by $v^{(A)}_{4,2}(x,\epsilon)$ and contains also a factor of g_B^4 which instead here we have explicitly put in front of the whole amplitude.

Diagram with a scalar box The last two-loop correction to the correlator (6.80) we have to consider corresponds to diagrams with an internal loop of hypermultiplets in the difference theory [62, 144]. The basic building block is

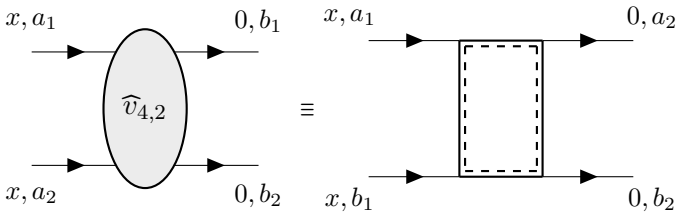

$$= g_B^4\, \widehat{C}^{a_1 a_2 b_1 b_2}\, \widehat{v}_{4,2}(x,\epsilon)\, \Delta^2(x,\epsilon)\ , \tag{6.112}$$

where we recall that the tensor $\widehat{C}^{a_1 a_2 b_1 b_2}$ is defined in (5.31b), while the function $\widehat{v}_{4,2}(x,\epsilon)$ is [12]

$$\widehat{v}_{4,2}(x,\epsilon) = \frac{(\pi x^2)^{2\epsilon}}{(8\pi^2)^2}\, 3\,\zeta_3 + \mathcal{O}(\epsilon)\ . \tag{6.113}$$

Inserting this diagram in the two-point correlator, we find

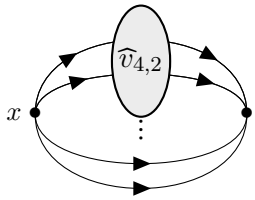

$$= g_B^{2n+4}\, \widehat{v}_{4,2}(x,\epsilon)\, \widehat{\mathcal{G}}_{\vec{n},\vec{m}}\, \Delta^n(x,\epsilon)\ , \tag{6.114}$$

where we recall that $\widehat{\mathcal{G}}_{\vec{n},\vec{m}}$ is defined in (5.34).

Combining all two-loop contributions together, we obtain

$$\begin{aligned}\mathcal{G}^{(2)}_{\vec{n},\vec{m}}(x,\epsilon) = {}& \frac{n(n+1)}{2}\, v_{2,1}^2(x,\epsilon) + n\big[v_{2,2}(x,\epsilon) - v_{4,2}(x,\epsilon)\big] \\ & - n(n-2)\, v_{2,1}(x,\epsilon)\, e_{2,1}(x,\epsilon) + \widehat{v}_{4,2}(x,\epsilon)\, \frac{\widehat{\mathcal{G}}_{\vec{n},\vec{m}}}{G^{(0)}_{\vec{n},\vec{m}}} + \mathcal{O}(\epsilon)\ .\end{aligned} \tag{6.115}$$

These terms define the difference-theory part $\mathcal{G}'^{(2)}$, while the $\mathcal{O}(\epsilon)$ term is the two-loop evanescent contribution $\delta'\mathcal{G}^{(2)}$. Since this is relevant only at the next perturbative order, its explicit expression is not needed. Note that the combination $[v_{2,2}(x,\epsilon) - v_{4,2}(x,\epsilon)]$ is finite when $\epsilon \to 0$, as it follows from (6.105) and (6.109). This means that the UV singularities are entirely encoded in the one-loop function $v_{2,1}(x,\epsilon)$, as expected from the one-loop exactness of the β-function.

6.2.4 Renormalized correlators

Collecting all contributions up to two loops, we find that the correlator (6.80) is given by

$$\begin{aligned}G_{\vec{n},\vec{m}}(g_B,x,\epsilon) = G^{(0)}_{\vec{n},\vec{m}} \Bigg[& \frac{g_B^{2n}}{\big(1 - g_B^2\, v_{2,1}(x,\epsilon)\big)^n} - g_B^{2n+2}\, n\, e_{2,1}(x,\epsilon) \\ & + g_B^{2n+4}\, n\big[v_{2,2}(x,\epsilon) - v_{4,2}(x,\epsilon)\big] - g_B^{2n+4}\, n\,(n-2)\, v_{2,1}(x,\epsilon)\, e_{2,1}(x,\epsilon) \\ & + g_B^{2n+4}\, \widehat{v}_{4,2}(x,\epsilon)\, \frac{\widehat{\mathcal{G}}_{\vec{n},\vec{m}}}{G^{(0)}_{\vec{n},\vec{m}}} \Bigg] + \mathcal{O}(g_B^{2n+6})\ .\end{aligned} \tag{6.116}$$

[12] In [144], the function $\widehat{v}_{4,2}(x,\epsilon)$, originally computed in [62], is denoted by $v^{(B)}_{4,2}$ and contains also a factor of g_B^4.

In the previous expression, the terms proportional to g_B^{2n+4} are finite in the limit $\epsilon \to 0$, while the UV singularities are captured by the geometric progression

$$\frac{1}{\big(1 - g_B^2\, v_{2,1}(x,\epsilon)\big)^n} = 1 + n\, g_B^2\, v_{2,1}(x,\epsilon) + \frac{1}{2} n(n+1)\, g_B^4\, v_{2,1}(x,\epsilon)^2 + \dots \ . \tag{6.117}$$

To remove these divergences, we follow the procedure outlined in Section 6.1.4 for the supersymmetric Wilson loop case. We introduce the renormalized coupling constant g_* according to (6.61) and we define the renormalized correlator $G^*_{\vec{n},\vec{m}}$ as [13]

$$G^*_{\vec{n},\vec{m}} = \lim_{\epsilon\to 0} G_{\vec{n},\vec{m}}(g_B, x, \epsilon)\Big|_{g_B = g_*\, \overline{M}^\epsilon\, Z_{g_*}} \ , \tag{6.118}$$

where we recall that Z_{g_*} is defined in (6.62), while $\overline{M} = M e^{-\frac{1}{2}(2+\gamma+\log\pi)}$, with M being the mass scale we employed to regularise the matrix model on S^4.

Going through the calculation, we find that the ϵ-poles of Z_{g_*} (6.62) precisely remove those appearing in (6.117), leading to a finite result in $d = 4$. Indeed, we find that

$$\lim_{\epsilon\to 0} \frac{g_B^{2n}}{\big(1 - g_B^2\, v_{2,1}(x,\epsilon)\big)^n}\bigg|_{g_B = g_*\, \bar{\mu}^\epsilon\, Z_{g_*}} = \left(\frac{g_*^2}{1 - g_*^2 \frac{\beta_0}{16\pi^2} \log(M^2 x^2)}\right)^n \equiv g_x^{2n} \ , \tag{6.119}$$

where g_x defines the running coupling evaluated at the energy scale $1/|x|$. Furthermore, using (6.98) one can show that

$$\lim_{\epsilon\to 0} g_B^{2n+2}\, n\, e_{2,1}(x,\epsilon)\Big|_{g_B = g_*\, \bar{\mu}^\epsilon\, Z_{g_*}} = -g_x^{2n+4}\, \frac{3N\zeta_3\beta_0}{64\pi^4}\, n(n+1) + \mathcal{O}\big(g_x^{2n+6}\big) \ . \tag{6.120}$$

Here we explicitly see that the one-loop evanescent contribution $e_{2,1}$ (6.98), upon renormalization, produces a finite term at two loops. Finally, as already anticipated, the remaining contributions in (6.116) are regular in the limit $\epsilon \to 0$. So for them we can safely set $\epsilon = 0$ and replace the bare coupling with the running one g_x (6.119) and we find that

$$\lim_{\epsilon\to 0} g_B^{2n+4}\ v_{2,1}(x,\epsilon)\, e_{2,1}(x,\epsilon)\Big|_{g_B = g_*\, \overline{M}^\epsilon\, Z_{g_*}} = g_x^{2n+4}\, \frac{3N\zeta_3\beta_0}{64\pi^4} + \mathcal{O}\big(g_x^{2n+6}\big) \ . \tag{6.121}$$

The two contributions (6.120) and (6.121), produced by the evanescent function $e_{2,1}$, are new with respect to the analysis of [144]. Being combined with the other corrections, they allow us to determine the renormalized correlator (6.118) at two loops, *i.e.*

$$G^*_{\vec{n},\vec{m}} = g_x^{2n}\, G^{(0)}_{\vec{n},\vec{m}} \left[1 + \left(\frac{g_x^2}{8\pi^2}\right)^2 3\zeta_3\, \mathcal{C}^{(2)}_{\vec{n},\vec{m}} + \mathcal{O}(g_x^6)\right] , \tag{6.122}$$

where

$$\mathcal{C}^{(2)}_{\vec{n},\vec{m}} = 2n\left(C_{\mathcal{R}}\, i_{\mathcal{R}} - N^2\right) + \frac{\widehat{\mathcal{G}}_{\vec{n},\vec{m}}}{G^{(0)}_{\vec{n},\vec{m}}} \ , \tag{6.123}$$

with $\widehat{\mathcal{G}}_{\vec{n},\vec{m}}$ defined in (5.34). We would like to remark that in (6.122) there is a hidden dependence on x since the running coupling g is evaluated at the scale $|x|$. Of course, in conformal theories, where $\beta_0 = 0$ and the coupling does not run, this dependence is absent.

[13] For composite operators a separate renormalization function is in general required. The reason why in our case we can reabsorb all singularities with the subtraction terms Z_{g_*} (6.62) is because the operators $O_{\vec{n}}$ have an overall factor of g_B^n as one can see from (5.9).

Finally, to connect the results in flat space with those on the four-sphere S^4, we recall that the operator separation $|x|$ is related to the radius R of S^4 by the relation $|x| = 2R$ (see Fig. 5.3). Using this information and taking into account the perturbative regime (2.29), we find that

$$g_x^2 = g^2 + \mathcal{O}(\log^0(RM)) \ , \tag{6.124}$$

where we recall that g is the running coupling constant evaluated at the scale $1/R$ (2.27). Substituting (6.124) into (6.122), we find that the final results coincide with the matrix model predictions (5.35). As in the Wilson loop case, the agreement is strictly limited to the perturbative regime (2.29). As we already remarked several times along the discussion, outside this range the observable receives additional *infrared* corrections of the form $C_n\,(\Lambda R)^n$, with Λ being the strong coupling scale (1.26), that we expect to be different in flat space and on the sphere.

For completeness and to facilitate the comparison with existing results in the literature, we provide the explicit expressions of the renormalized correlator (6.122) for the lowest dimensional operators when the representation $\mathcal{R}$ is (5.15). Evaluating $\widehat{\mathcal{G}}_{\vec{n},\vec{m}}$ (5.34) and using the results in (5.28a), we obtain

$$\begin{aligned} G^*_{2,2} = g^4\,\frac{N^2-1}{2}\Bigg\{1+\Big(\frac{g^2}{8\pi^2}\Big)^2\,\frac{3\zeta_3}{2N}\Big[N_f(2N^2-3)-10N^3 \\ +N_a(N-2)(5N^2-6N-12)+N_s(N+2)(5N^2+6N-12)\Big]+\mathcal{O}(g^6)\Bigg\}\ , \end{aligned} \tag{6.125a}$$

$$\begin{aligned} G^*_{3,3} = g^6\,\frac{3(N^2-1)(N^2-4)}{8N}\Bigg\{1+\Big(\frac{g^2}{8\pi^2}\Big)^2\,\frac{9\zeta_3}{2N}\Big[N_f(N^2-3)-4N^3 \\ +2N_a(N^3-4N^2+12)+2N_s(N^3+4N^2-12)\Big]+\mathcal{O}(g^6)\Bigg\}\ . \end{aligned} \tag{6.125b}$$

6.3 Discussions and Future Directions

In this third part of the thesis, we have addressed the question of whether and to what extent supersymmetric localization on the four-sphere can be extended beyond the usual conformal setups in flat space. We focused on $\mathcal{N}=2$ super-Yang–Mills theories with massless hypermultiplets and a non-vanishing β-function, where classical conformal symmetry is dynamically broken at the quantum level.

Within this framework, we evaluated two classes of observables: the expectation value of the half-BPS Wilson loop (5.7) and the correlation functions of chiral operators (6.80). Our analysis shows that, within the specific regime of validity (2.29), the ζ_3-like contributions arising from the interaction potential of the matrix model on the four-sphere S^4 precisely reproduce the perturbative results obtained in flat space.

From the field-theoretic perspective, this agreement originates from interference effects between the ultraviolet pole of the bare coupling and certain evanescent terms. The corresponding contributions to the observables are sensitive only to the short-distance structure of the theory, thereby explaining this highly non-trivial matching between localization and perturbative computations.

Based on these consistency checks, we can conjecture that the localization matrix model correctly captures protected observables within the regime specified by (2.29) even in $\mathcal{N}=2$ SYM theories with massless matter and a non-zero β-function. This opens the door to using the

matrix model as a tool for deriving new non-trivial results in such theories. We mention two of them below.

Higher order diagrammatic computations: Computations in the matrix model are less intricate than in field theory and we can probe higher perturbative orders without much effort. For instance, in the diagrammatic approach, we can take into account the sextic vertex in the interaction action (2.20), namely

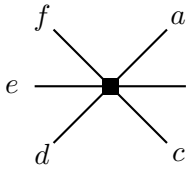

$$= \left(\frac{g^2}{8\pi^2}\right)^3 \frac{\zeta_5}{3}\, \widehat{C}_s^{abcdef} \,, \tag{6.126}$$

where $\widehat{C}_s^{abcdef} = \mathrm{Tr}'\left(T^{(a}T^bT^cT^dT^eT^{f)}\right)$ is a completely symmetric tensor of rank six that generaliseds the one in (5.31a). This diagram can be used to predict the ζ_5-like contributions to the observables. For instance, in the case of the chiral two-point function $\langle \mathcal{O}_{\vec{n}}(a)\, \mathcal{O}_{\vec{m}}(a)\rangle$ we find that the matrix model predicts the following corrections

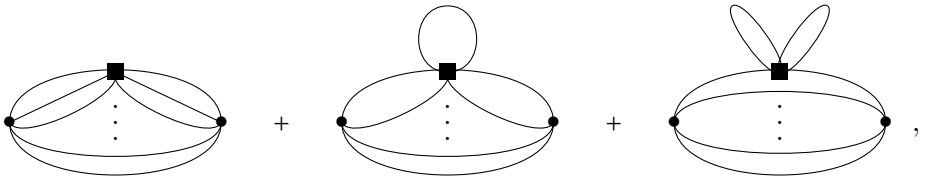

(6.127)

where we recall that black dots represent the two operators $\mathcal{O}_{\vec{n}}$ and $\mathcal{O}_{\vec{m}}$. Keeping track of the combinatorics of the Wick contractions in the three diagrams, we find

$$\begin{aligned}\left(\frac{g^2}{8\pi^2}\right)^3 \zeta_5\, n! \Bigg[& \frac{20}{3} n(n-1)(n-2)\, R_{\vec{n}}^{a_1a_2a_3c_1\ldots c_{n-3}}\, R_{\vec{m}}^{b_1b_2b_3c_1\ldots c_{n-3}}\, \widehat{C}_s^{a_1a_2a_3b_1b_2b_3} \\ & + 30n(n-1)\, R_{\vec{n}}^{a_1a_2c_1\ldots c_{n-2}}\, R_{\vec{m}}^{b_1b_2c_1\ldots c_{n-2}}\, \widehat{C}_s^{a_1a_2b_1b_2dd} \\ & + 30n\, R_{\vec{n}}^{a_1c_1\ldots c_{n-1}}\, R_{\vec{m}}^{b_1c_1\ldots c_{n-1}}\, \widehat{C}_s^{a_1b_1ddee} \Bigg] .\end{aligned} \tag{6.128}$$

This matrix model prediction could possibly be checked against direct Feynman diagram computations in the superfield formalism for which a computerized approach suitable for this kind of correlators has been proposed in [155]. It is however rather difficult to push Feynman diagram computations at even higher orders, while it is straightforward to extend the calculation by the matrix-model approach.

Specializing the tensors $R_{\vec{n}}$ and $R_{\vec{m}}$, and evaluating the tensor $\widehat{C}_s$ for a given matter representation $\mathcal{R}$, we can easily derive explicit results. For instance, if we consider the low dimensional operators $\mathcal{O}_2$ and $\mathcal{O}_3$ in SQCD with N_f flavors (and $N_a = N_s = 0$), from (6.125a), (6.125b) and the above formula (6.128), we get

$$\begin{aligned}G_{2,2} = g^4\, \frac{N^2-1}{2} \Bigg\{ & 1 + \left(\frac{g^2}{8\pi^2}\right)^2 \frac{3\zeta_3}{2N} \left[N_f(2N^2-3) - 10N^3\right] \\ & - \left(\frac{g^2}{8\pi^2}\right)^3 \frac{5\zeta_5}{N^2} \left[N_f(N^4 - 3N^2 + 3) - 14N^5\right] + O(g^8) \Bigg\}\end{aligned} \tag{6.129}$$

and

$$G_{3,3} = g^6\,\frac{3(N^2-1)(N^2-4)}{8N}\left\{1+\Big(\frac{g^2}{8\pi^2}\Big)^2\,\frac{9\zeta_3}{2N}\left[N_f(N^2-3)-4N^3\right]\right.$$
$$\left.-\Big(\frac{g^2}{8\pi^2}\Big)^3\,\frac{5\zeta_5}{4N^2}\left[N_f(6N^4-31N^2+53)-56N^5\right]+O(g^8)\right\}. \tag{6.130}$$

For the dimension 4 operators, we have

$$G^*_{4,4} = g^8\,\frac{(N^2-1)(N^4-6N^2+18)}{4N^2}\left\{1+\Big(\frac{g^2}{8\pi^2}\Big)^2\,\frac{6\,\zeta_3}{N(N^4-6N^2+18)}\times\right.$$
$$\times\Big[N_f\,(N^6-8N^4+45N^2-81)-4N^7+12N^5-54N^3$$
$$+N_a\,(N-2)(2N^6-4N^5-14N^4+36N^3+99N^2-162N-324)$$
$$\left.+N_s\,(N+2)(2N^6+4N^5-14N^4-36N^3+99N^2+162N-324)\Big]+\mathcal{O}(g^6)\right\}, \tag{6.131}$$

$$G^*_{4,(2,2)} = g^8\,\frac{(N^2-1)(2N^2-3)}{2N}\left\{1+\Big(\frac{g^2}{8\pi^2}\Big)^2\,\frac{3\,\zeta_3}{N(2N^2-3)}\times\right.$$
$$\times\Big[N_f\,(5N^4-18N^2+27)+18N^3-22N^5$$
$$+N_a\,(N-2)(11N^4-18N^3-45N^2+54N+108)$$
$$\left.+N_s\,(N+2)(11N^4+18N^3-45N^2-54N+108)\Big]+\mathcal{O}(g^6)\right\}, \tag{6.132}$$

$$G^*_{(2,2),(2,2)} = g^8\,\frac{(N^4-1)}{2}\left\{1+\Big(\frac{g^2}{8\pi^2}\Big)^2\,\frac{3\,\zeta_3(N^2+3)}{N(N^2+1)}\times\right.$$
$$\times\Big[N_f\,(2N^2-3)-10N^3+N_a\,(N-2)(5N^2-6N-12)$$
$$\left.+N_s\,(N+2)(5N^2+6N-12)\Big]+\mathcal{O}(g^6)\right\}. \tag{6.133}$$

For the dimension 5 operators, we have

$$G^*_{5,5} = g^{10}\,\frac{5(N^2-1)(N^2-4)(N^4+24)}{32N^3}\left\{1+\Big(\frac{g^2}{8\pi^2}\Big)^2\,\frac{15\,\zeta_3}{2N(N^4+24)}\times\right.$$
$$\times\Big[N_f\,(N^6+N^4+24N^2-144)-4N^7-24N^5-48N^3$$
$$+N_a\,(2N^7-8N^6+12N^5-8N^4+24N^3-192N^2+1152)$$
$$\left.+N_s\,(2N^7+8N^6+12N^5+8N^4+24N^3+192N^2-1152)\Big]+\mathcal{O}(g^6)\right\}, \tag{6.134}$$

$$G^*_{5,(3,2)} = g^{10}\,\frac{15(N^2-1)(N^2-2)(N^2-2)}{16N^2}\left\{1+\Big(\frac{g^2}{8\pi^2}\Big)^2\,\frac{3\,\zeta_3}{N(N^2-2)}\times\right.$$
$$\times\Big[N_f\,(N^4-14N^2+30)+10N^3-12N^5$$
$$+N_a\,(6N^5-24N^4-5N^3+112N^2-240)$$
$$\left.+N_s\,(6N^5+24N^4-5N^3-112N^2+240)\Big]+\mathcal{O}(g^6)\right\}, \tag{6.135}$$

$$G^{*}_{(3,2),(3,2)} = g^{10}\,\frac{3(N^2-1)(N^2-4)(N^2+5)}{16N}\left\{1+\left(\frac{g^2}{8\pi^2}\right)^2\frac{3\,\zeta_3}{2N(N^2+5)}\times\right.$$
$$\times\Big[N_f\,(5N^4+37N^2-150)-22N^5-194N^3$$
$$+N_a\,(11N^5-40N^4+97N^3-296N^2+1200)$$
$$\left.+N_s\,(11N^5+40N^4+97N^3+296N^2-1200)\Big]+\mathcal{O}(g^6)\right\}. \tag{6.136}$$

Large-N and strong coupling analysis: The matrix-model description leads, for certain classes of conformal $\mathcal{N}=2$ theories, to powerful results in the large-N 't Hooft limit in which the coupling $\lambda = g^2N$ is kept fixed while N tends to infinity [58,72,77,100,108,139,140,163–167]. In these cases, the λ-perturbative expansion of correlators involving single-trace operators can be resummed and even continued to strong coupling, allowing us to compare the result with dual holographic descriptions [65–67,82]. In the light of our analysis, it is natural to pose the question of whether such strong-coupling results can be extended to some classes of theories with non-vanishing β-function. Let us note that in the 't Hooft limit the coupling g must be sent to zero in order to keep λ constant when $N\to\infty$. The scale $1/R$ must therefore satisfy (2.29), meaning that we can neglect the instanton contributions and consider just the perturbative interaction action as we did here. This is a very interesting direction since it could lead to new insights into the holographic description of theories with a non-vanishing β-function.

Part IV

Conclusions

Chapter 7

Conclusions and outlook

Conclusions

In this thesis, we presented several results regarding $\mathcal{N} = 2$ supersymmetric gauge theories in four dimensions, encompassing both conformal and non-conformal models. The extended, though not maximal, supersymmetry of these theories allows for non-trivial low-energy dynamics while still admitting powerful non-perturbative techniques, such as gauge-gravity dualities, integrability, and supersymmetric localization. As a result, $\mathcal{N} = 2$ models serve as powerful theoretical laboratories where we can explore phenomena that are otherwise inaccessible in realistic settings.

This general philosophy guided the analyses developed in Chapters 3 and 4, where we investigated a particular class of superconformal $SU(N)$ $\mathcal{N} = 2$ quiver theories, known as the Q_L models. These arise from an orbifold projection of $SU(NL)$ $\mathcal{N} = 4$ super-Yang–Mills theory and provide a rich framework for probing non-perturbative aspects of $\mathcal{N} = 2$ dynamics. In particular, in the limit $L \to \infty$, these setups are expected to exhibit novel properties through the *deconstruction mechanism*, which makes emerge an additional dimension from lower-dimensional dynamics and was originally studied in ordinary Yang–Mills theories [83,84]. In this context, the emergent higher-dimensional dynamics involves strong interactions, preventing explicit computations of physical observables. Conversely, in the Q_L models the situation changes drastically: by exploiting conformal invariance and supersymmetric localization on the four-sphere S^4, we computed protected correlation functions that act as probes to investigate the theory across its parameter space. These observables can be mapped via localization to finite-dimensional matrix integrals which, in the planar limit, reduces to special *Fredholm determinants* closely related to the celebrated *Tracy–Widom distributions* [101]. The determinant formalism allows the study of observables at both weak and strong coupling, providing access to the deconstruction limit. We performed a quantitative analysis of these regimes and showed that when $L \gg \sqrt{\lambda}$, where λ is the 't Hooft coupling, the Q_L theory effectively behaves as a five-dimensional model. The emergent dimension manifests through the propagation of massive excitations, interpretable within a local effective field theory. At weak coupling, this effective theory is free, while at strong coupling it becomes interacting, exhibiting a mass spectrum which is described by the zeros of Bessel functions. These results hold within the planar approximation, and it remains an open question whether such behaviour persists beyond it. Extending the formalism of Chapter 4 to incorporate non-planar corrections to two- and three-point functions would not only provide a systematic approach to these higher-order effects, but also offer valuable insights into the nature of the dual description in the long-quiver limit.

The remarkable effectiveness of supersymmetric localization in conformal theories, where the results on S^4 automatically connect to flat-space dynamics, naturally raises the question of

whether this technique retains physical meaning in non-conformal settings. Indeed, conformal invariance represents a very special symmetry, absent in realistic contexts such as Quantum Chromodynamics. Understanding to what extent the localization framework survives away from conformality therefore becomes a physically meaningful challenge.

This motivated the second part of the thesis, where we considered $\mathcal{N} = 2$ supersymmetric Yang–Mills theories with massless hypermultiplets and a non-vanishing β-function. In these models, classical conformal symmetry is broken at the quantum level through the mechanism of *dimensional transmutation*. Nevertheless, the theory remains supersymmetric and can still be consistently defined on S^4, allowing the application of localization methods.

Within this framework, we analysed two classes of observables: the expectation value of the half-BPS Wilson loop, and the correlation functions of chiral operators. On the four-sphere, localization maps these observables to the same class of matrix models that describe conformal theories, but now with an interaction potential depending on a running coupling constant that evolves with the radius of the sphere. The central question addressed in this part of the work was whether the results extracted from the S^4 matrix model continue to capture the physical content of the corresponding flat-space quantities, despite the absence of conformal symmetry.

To answer this, we performed a detailed comparison between the matrix model predictions and explicit perturbative computations in flat space for the aforementioned observables. Remarkably, within a specific perturbative regime associated with the short-distance properties of the theory, we found precise agreement between the two approaches. In particular, the ζ_3-like terms emerging from the matrix model's interaction potential on S^4 reproduce exactly the perturbative contributions computed in flat space. In field theory, these terms arise from interferences between the ultraviolet poles of the bare coupling and certain evanescent terms emerging from dimensional regularization. Their matching with localization results provides a highly non-trivial check of the consistency of this framework beyond the conformal domain and it is natural to exploit this technique to study the 't Hooft limit at strong coupling in theories with non-vanishing β-function, which can shed new light on possible holographic descriptions.

Part V

Appendices

Appendix A

Conventions on spinors and Grassmann variables

A.1 Spinors in four dimensions

In four-dimensional Euclidean space, the rotation group is $SO(4)$, while the spin group is $Spin(4) \simeq SU(2)_\alpha \otimes SU(2)_{\dot\alpha}$. We denote by ψ a chiral spinor of components ψ_α, where $\alpha = 1, 2$, and by $\bar\psi$ an anti-chiral spinor of components $\bar\psi^{\dot\alpha}$, with $\dot\alpha = 1, 2$. The spinor indices are raised and lowered by following rules

$$\psi^\alpha = \epsilon^{\alpha\beta}\,\psi_\beta \ , \quad \psi_\alpha = \epsilon_{\alpha\beta}\,\psi^\beta \ , \quad \bar\psi^{\dot\alpha} = \epsilon^{\dot\alpha\dot\beta}\,\bar\psi_{\dot\beta} \ , \quad \bar\psi_{\dot\alpha} = \epsilon_{\dot\alpha\dot\beta}\,\bar\psi^{\dot\beta} \ , \tag{A.1}$$

where

$$\epsilon^{12} = \epsilon^{\dot1\dot2} = \epsilon_{21} = \epsilon_{\dot2\dot1} = 1 \ . \tag{A.2}$$

Using the ϵ-symbol (A.2), we can construct $SO(4)$ invariants by contracting chiral/anti-chiral spinors as follows

$$(\psi\chi) \equiv \psi^\alpha\,\chi_\alpha = \epsilon^{\alpha\beta}\,\psi_\beta\,\chi_\alpha = \psi^\alpha\,\chi^\beta\,\epsilon_{\alpha\beta} \ , \tag{A.3}$$

$$(\bar\psi\bar\chi) \equiv \bar\psi_{\dot\alpha}\,\bar\chi^{\dot\alpha} = \epsilon_{\dot\alpha\dot\beta}\,\bar\psi^{\dot\beta}\,\bar\chi^{\dot\alpha} = \bar\psi_{\dot\alpha}\,\bar\chi_{\dot\beta}\,\epsilon^{\dot\alpha\dot\beta} \ . \tag{A.4}$$

In contrast to their Minkowskian counterparts, chiral and anti-chiral spinors are independent in Euclidean spacetime as they satisfy a *pseudoreality* condition

$$(\psi_\alpha)^\dagger = \psi^\alpha \ . \tag{A.5}$$

Nevertheless, the two copies of $SU(2)$ are intertwined by the matrices $(\bar\sigma^\mu)^{\dot\alpha\alpha}$ and $(\sigma^\mu)_{\alpha\dot\beta}$

$$\sigma^\mu = (\vec\tau, -\mathrm{i}\mathbb{I}) \ , \qquad \bar\sigma^\mu = (-\vec\tau, -\mathrm{i}\mathbb{I}) \ , \tag{A.6}$$

where $\vec\tau$ denotes the ordinary Pauli matrices. Furthermore, it is straightforward to show that the following relations hold

$$(\bar\sigma^\mu)^{\dot\alpha\alpha} = \epsilon^{\dot\alpha\dot\beta}\epsilon^{\alpha\beta}(\sigma^\mu)_{\beta\dot\beta} \ , \tag{A.7}$$

$$\sigma^\mu\bar\sigma^\nu + \sigma^\nu\bar\sigma^\mu = -2\delta^{\mu\nu}\mathbb{I} \ , \tag{A.8}$$

$$\bar\sigma^\mu\sigma^\nu + \bar\sigma^\nu\sigma^\mu = -2\delta^{\mu\nu}\mathbb{I} \ . \tag{A.9}$$

Finally, by employing the Clifford algebra (A.7), we find that

$$\operatorname{Tr}\sigma^{\mu}\bar{\sigma}^{\nu} = -2\delta^{\mu\nu} \ , \tag{A.10}$$

$$\operatorname{tr}(\bar{\sigma}^{\mu}\sigma^{\nu}\bar{\sigma}^{\rho}\sigma^{\sigma}) = 2\big(\delta^{\mu\nu}\delta^{\rho\sigma} - \delta^{\mu\rho}\delta^{\nu\sigma} + \delta^{\mu\sigma}\delta^{\nu\rho} + \epsilon^{\mu\nu\rho\sigma}\big) \ ,$$

$$\operatorname{tr}(\sigma^{\mu}\bar{\sigma}^{\nu}\sigma^{\rho}\bar{\sigma}^{\sigma}) = 2\big(\delta^{\mu\nu}\delta^{\rho\sigma} - \delta^{\mu\rho}\delta^{\nu\sigma} + \delta^{\mu\sigma}\delta^{\nu\rho} - \epsilon^{\mu\nu\rho\sigma}\big) \ , \tag{A.11}$$

$$\bar{\sigma}^{\mu}\sigma^{\nu}\bar{\sigma}^{\rho} = -\delta^{\mu\nu}\bar{\sigma}^{\rho} + \delta^{\mu\rho}\bar{\sigma}^{\nu} - \delta^{\nu\rho}\bar{\sigma}^{\mu} - \epsilon^{\mu\nu\rho\alpha}\bar{\sigma}_{\alpha} \ ,$$

where we normalize $\epsilon^{1234} = \epsilon_{1234} = 1$.

A.2 Grassmann integration formulæ and spinor derivatives

The basic integration formulæ for Grassmann variables are

$$\int d^2\theta\,\theta^2 = 1 \ , \quad \int d^2\bar{\theta}\,\bar{\theta}^2 = 1 \ , \tag{A.12}$$

where $\theta^{\alpha}\theta_{\alpha}$ and $\bar{\theta}_{\dot{\alpha}}\bar{\theta}^{\dot{\alpha}}$. As a result, θ^2 and $\bar{\theta}^2$ act as fermionic δ-functions. In particular, writing $\theta_{ij} = \theta_i - \theta_j$, we have

$$\theta_{ij}^2 = \delta^2(\theta_{ij}) \ , \quad \bar{\theta}_{ij}^2 = \delta^2(\bar{\theta}_{ij}) \ . \tag{A.13}$$

For spinor derivatives we use the notation $\partial_{\alpha} \equiv \dfrac{\partial}{\partial\theta^{\alpha}}$ and $\bar{\partial}_{\dot{\alpha}} \equiv \dfrac{\partial}{\partial\bar{\theta}^{\dot{\alpha}}}$. Using (A.3), it is straightforward to prove that

$$\begin{aligned} &\partial_{\alpha}\,\theta^2 = 2\,\theta_{\alpha} \ , \quad \partial\partial\,\theta^2 = -4 \\ &\bar{\partial}_{\dot{\alpha}}\,\bar{\theta}^2 = -2\,\bar{\theta}_{\dot{\alpha}} \ , \quad \bar{\partial}\bar{\partial}\,\bar{\theta}^2 = -4 \ . \end{aligned} \tag{A.14}$$

The covariant spinor derivatives are defined as

$$D_{\alpha} = \partial_{\alpha} + \mathrm{i}\,(\sigma^{\mu})_{\alpha\dot{\alpha}}\,\bar{\theta}^{\dot{\alpha}}\,\partial_{\mu} \ , \tag{A.15}$$

$$\bar{D}_{\dot{\alpha}} = -\bar{\partial}_{\dot{\alpha}} - \mathrm{i}\,\theta^{\alpha}\,(\sigma^{\mu})_{\alpha\dot{\alpha}}\,\partial_{\mu} \ , \tag{A.16}$$

where the matrix σ^{μ} is defined in (A.6).

Appendix B

Group Theory conventions

B.1 The Lie algebra $su(N)$

In this section, we summarise the relevant notations and conventions for the Lie algebra $su(N)$. This is spanned by a set of (Hermitian) generators T^a, with $a = 1, \dots N^2 - 1$, satisfying the relation

$$\left[T^a, T^b\right] = \mathrm{i} f^{abc} T^c \ , \tag{B.1}$$

where the coefficients f^{abc} are completely antisymmetric and go under the name of *structure constants*. In a generic representation $\mathcal{R}$, we define the Dynkin index $i_{\mathcal{R}}$ and the quadratic Casimir $C_{\mathcal{R}}$ as follows

$$\mathrm{Tr}_{\mathcal{R}}\, T^a T^b = i_{\mathcal{R}} \delta_{ab} \ , \tag{B.2a}$$

$$T^a_{\mathcal{R}} T^a_{\mathcal{R}} = C_{\mathcal{R}} \mathbb{I} \ . \tag{B.2b}$$

Combining together (B.2a) and (B.2b), we find the following relation

$$C_{\mathcal{R}} = \frac{N^2 - 1}{d_{\mathcal{R}}} i_{\mathcal{R}} \ , \tag{B.3}$$

where $d_{\mathcal{R}}$ is the dimension of the representation $\mathcal{R}$.

In the fundamental representation ($\mathcal{R} = F$), we denote the generators as t_a and we normalize them in such a way that $i_F = 1/2$. For the anti-fundamental and adjoint representation, we use the notation $\bar{t}^a$ and T^a_{Adj}, respectively. These matrices satisfy

$$\bar{t}^a = -t^{a,T} \ , \tag{B.4}$$

$$\left(T^a_{\mathrm{Adj}}\right)_{bc} = \mathrm{i} f^{abc} \ , \tag{B.5}$$

where T denotes the transpose matrix and we recall that f^{abc} are the structure constants (B.1).

We summarise in table B.1 the relevant group information for the adjoint ($\mathcal{R} = \mathrm{Adj}$), symmetric ($\mathcal{R} = \square\square$) and the antisymmetric $\left(\mathcal{R} = \begin{smallmatrix}\square\\\square\end{smallmatrix}\right)$ representation of $SU(N)$.

B.2 Identities for colour factors

In this appendix, we prove the relations (5.33). We begin with considering the amplitude

$$\mathcal{A}_{\vec{n},\vec{m}} = 2n\, n!\, \widehat{C}_s^{a_1 b_1 d\, d}\, R_{\vec{n}}^{a_1 c_1 \dots c_{n-1}}\, R_{\vec{m}}^{b_1 c_1 \dots c_{n-1}} \ , \tag{B.6}$$

Representation $\mathcal{R}$	$d_{\mathcal{R}}$	$i_{\mathcal{R}}$
$\square$	N	$1/2$
Adj	N^2-1	N
$\square\square$	$N(N+1)/2$	$(N+2)/2$
$\begin{smallmatrix}\square\\\square\end{smallmatrix}$	$N(N-1)/2$	$(N-2)/2$

Table B.1: Relevant group information for different representations of $SU(N)$.

which coincides with (5.30a) up to an overall factor of $6\,g^{2n}$. Taking into account the definition (5.31a) of the symmetric tensor $\widehat{C}_s$ we find

$$\mathcal{A}_{\vec{n},\vec{m}} = \frac{2n\,n!}{3}\Big[\,\mathrm{Tr}'_{\mathcal{R}}\,T^{a_1}T^{b_1}T^dT^d + \mathrm{Tr}'_{\mathcal{R}}\,T^{a_1}T^dT^{b_1}T^d + \mathrm{Tr}'\,T^{b_1}T^{a_1}T^dT^d\Big]R^{a_1c_1\ldots c_{n-1}}_{\vec{n}}\,R^{b_1c_1\ldots c_{n-1}}_{\vec{m}}\,, \tag{B.7}$$

where we recall that the primed trace is given by $\mathrm{Tr}'_{\mathcal{R}} = \mathrm{Tr}_{\mathcal{R}} - \mathrm{Tr}_{\mathrm{Adj}}$. Recalling the definition of the quadratic Casimir (B.2b) and of the Dynkin index (B.2a), the first primed trace in (B.7) can be replaced by

$$\mathrm{Tr}'_{\mathcal{R}}\,T^aT^bT^dT^d = \big(C_{\mathcal{R}}\,i_{\mathcal{R}} - N^2\big)\,\delta^{ab}\,, \tag{B.8}$$

where we used $C_{\mathrm{Adj}} = i_{\mathrm{Adj}} = N$. By similar manipulations and employing (B.1), the second primed trace (B.7) takes the following form

$$\mathrm{Tr}'_{\mathcal{R}}\,T^{a_1}T^dT^{b_1}T^d = \mathrm{Tr}'_{\mathcal{R}}\,T^{a_1}T^{b_1}T^dT^d + \mathrm{i}\,f^{db_1c}\,\mathrm{Tr}'_{\mathcal{R}}\,T^{a_1}T^cT^d\,, \tag{B.9}$$

where f^{db_1c} are the structure constants (B.1). The previous expression can be further manipulated by observing the following decomposition

$$\mathrm{Tr}'_{\mathcal{R}}\,T^aT^bT^c = \mathrm{i}\,\frac{(i_{\mathcal{R}}-N)}{2}\,f^{abc} + x'\,d^{abc} = -\mathrm{i}\,\frac{\beta_0}{4}\,f^{abc} + x'\,d^{abc}\,, \tag{B.10}$$

where d^{abc} is fully symmetric, we used $\beta_0 = 2(N - i_{\mathcal{R}})$, x' is a group factor whose explicit expression is not relevant. As a result, we find that (B.9) can be written as follows

$$\mathrm{Tr}'_{\mathcal{R}}\,T^{a_1}T^dT^{b_1}T^d = \mathrm{Tr}'_{\mathcal{R}}\,T^{a_1}T^{b_1}T^dT^d + \frac{\beta_0}{4}\,f^{db_1c}f^{a_1cd} = \Big[C_{\mathcal{R}}\,i_{\mathcal{R}} - N^2 + \frac{N\beta_0}{4}\Big]\,\delta^{a_1b_1}\,, \tag{B.11}$$

where we observed that $f^{abc}f^{abd} = N\,\delta^{cd}$. Combining everything together, we find that the amplitude (B.7) coincides with the identity (5.33a). Indeed, we apply (5.27) to find that

$$\begin{aligned}\mathcal{A}_{\vec{n},\vec{m}} &= \frac{2n\,n!}{3}\Big[3\big(C_{\mathcal{R}}\,i_{\mathcal{R}} - N^2\big) + \frac{N\beta_0}{4}\Big]\,\delta^{a_1b_1}\,R^{a_1c_1\ldots c_{n-1}}_{\vec{n}}\,R^{b_1c_1\ldots c_{n-1}}_{\vec{m}} \\ &= 2n\,\Big(C_{\mathcal{R}}\,i_{\mathcal{R}} - N^2 + \frac{N\beta_0}{12}\Big)\,G^{(0)}_{\vec{n},\vec{m}}\,.\end{aligned} \tag{B.12}$$

We now turn our attention to the amplitude

$$\mathcal{B}_{\vec{n},\vec{m}} = n(n-1)\,n!\,\widehat{C}_s^{a_1a_2b_1b_2}\;R^{a_1a_2c_1\ldots c_{n-2}}_{\vec{n}}\,R^{b_1b_2c_1\ldots c_{n-2}}_{\vec{m}}\,, \tag{B.13}$$

which coincides with (5.30b), up to an overall factor of $6\,g^{2n}$. Using (5.31a), we express $\mathcal{B}_{\vec{n},\vec{m}}$ as follows

$$\mathcal{B}_{\vec{n},\vec{m}} = \frac{n(n-1)\,n!}{3}\Big[\widehat{C}^{a_1a_2b_1b_2} + 2\,\mathrm{Tr}'_{\mathcal{R}}\,T^{a_1}T^{a_2}T^{b_1}T^{b_2}\Big]R_{\vec{n}}^{a_1a_2c_1\ldots c_{n-2}}\,R_{\vec{m}}^{b_1b_2c_1\ldots c_{n-2}}\,. \tag{B.14}$$

The second primed trace in the previous expression can be manipulated as follows

$$\begin{aligned}\mathrm{Tr}'_{\mathcal{R}}\,T^{a_1}T^{a_2}T^{b_1}T^{b_2} &= \mathrm{Tr}'_{\mathcal{R}}\,T^{a_1}T^{b_1}T^{a_2}T^{b_2} + \mathrm{i}f^{a_2b_1c}\,\mathrm{Tr}'_{\mathcal{R}}\,T^{a_1}T^{c}T^{b_2}\\ &= \widehat{C}^{a_1a_2b_1b_2} - \frac{\beta_0}{4}\,f^{a_2b_1c}f^{a_1cb_2} + \mathrm{i}\,x'f^{a_2b_1c}d^{a_1cb_2}\\ &= \widehat{C}^{a_1a_2b_1b_2} + \frac{N\beta_0}{4}\,C^{a_1a_2b_1b_2} + \mathrm{i}\,x'f^{a_2b_1c}d^{a_1cb_2}\ ,\end{aligned} \tag{B.15}$$

where we recall that C^{abcd} is defined in (5.31b). We note that the part proportional to x' can be discarded since it gives rise to structures that are anti-symmetric in (a_1,a_2) and (b_1,b_2) and consequently, it vanishes when contracted with the symmetric tensors $R_{\vec{n}}$ and $R_{\vec{m}}$. Using the identity (B.15), we obtain

$$\begin{aligned}\mathcal{B}_{\vec{n},\vec{m}} &= \frac{n(n-1)\,n!}{3}\Big[3\,\widehat{C}^{a_1a_2b_1b_2} + \frac{N\beta_0}{2}\,C^{a_1a_2b_1b_2}\Big]R_{\vec{n}}^{a_1a_2c_1\ldots c_{n-2}}\,R_{\vec{m}}^{b_1b_2c_1\ldots c_{n-2}}\\ &= n(n-1)\,n!\,\widehat{C}^{a_1a_2b_1b_2}\;R_{\vec{n}}^{a_1a_2c_1\ldots c_{n-2}}\,R_{\vec{m}}^{b_1b_2c_1\ldots c_{n-2}}\\ &\quad + \frac{N\beta_0}{6}\,n(n-1)\,n!\,C^{a_1a_2b_1b_2}\;R_{\vec{n}}^{a_1a_2c_1\ldots c_{n-2}}\,R_{\vec{m}}^{b_1b_2c_1\ldots c_{n-2}}\ .\end{aligned} \tag{B.16}$$

The term proportional to $\widehat{C}$ is exactly $\widehat{\mathcal{G}}_{\vec{n},\vec{m}}$ defined in (5.34), while the term proportional to C can be evaluated using the fusion/fission identities as described in [144] and provides us with

$$n(n-1)\,n!\,C^{a_1a_2b_1b_2}\;R_{\vec{n}}^{a_1a_2c_1\ldots c_{n-2}}\,R_{\vec{m}}^{b_1b_2c_1\ldots c_{n-2}} = -n\,G^{(0)}_{\vec{n},\vec{m}}\ . \tag{B.17}$$

Therefore, collecting all terms we have

$$\mathcal{B}_{\vec{n},\vec{m}} = \widehat{\mathcal{G}}_{\vec{n},\vec{m}} - n\,\frac{N\beta_0}{6}\,G^{(0)}_{\vec{n},\vec{m}} \tag{B.18}$$

which is the relation written in (5.33b).

Appendix C

Supersymmetric Wilson loop in perturbation theory

In this appendix, we provide a detailed analysis of the perturbative corrections to the expectation value of the half-BPS Wilson loop (5.7). We work in $SU(N)$ $\mathcal{N}=2$ SYM theories with massless hypermultiplets in an arbitrary representation $\mathcal{R}$ and non-vanishing β-function. The actions of these theories in Euclidean space are reported in Section 6.1.

Before entering the details of analysis, we consider the explicit expression for the Feynman propagators, starting from the $\mathcal{N}=2$ vector multiplet. The dynamics of these fields is described by the gauge-fixed action (6.1). In the Feynman gauge, *i.e.* $\xi=1$, the tree-level propagator of the adjoint scalar ϕ and of the gauge field A_μ are identical up to spacetime indices. We have

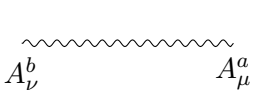

$$= \frac{\delta^{ab}}{p^2}\delta_{\mu\nu} \ , \qquad$$

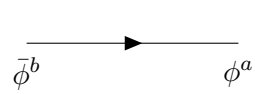

$$= \frac{\delta^{ab}}{p^2} \ . \tag{C.1}$$

On the other hand, the tree-level propagators of the two *gauginos* λ and ψ exhibit a more complicated structure. Here we consider in detail the relevant expressions for the Weyl spinor λ but analogous results hold for ψ. We have two relevant Wick contractions, *i.e.*

$$\left\langle \lambda^a_\alpha(x)\bar{\lambda}^b_{\dot\alpha}(y)\right\rangle_0 \ , \qquad \left\langle \bar{\lambda}^{\dot\alpha}_b(y)\lambda^\alpha_a(x)\right\rangle_0 \ . \tag{C.2}$$

In our conventions, the arrow associated with the particle flow always goes from the dotted index to the undotted one. As a result, in momentum space we represent the first contraction as follows

$$\left\langle \lambda^a_\alpha(x)\bar{\lambda}^b_{\dot\alpha}(y)\right\rangle_0 \quad \leftrightarrow \quad$$

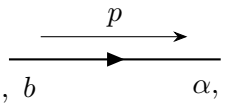

$$= \frac{\delta^{ab}\sigma_{\alpha\dot\alpha}\cdot p}{p^2} \ , \tag{C.3}$$

where $\sigma_{\alpha\dot\alpha}\cdot p = \sigma^\mu_{\alpha\dot\alpha}\, p_\mu$, with $\sigma^\mu_{\alpha\dot\alpha}$ defined in (A.6). The tree-level propagator with raised indices in (C.2) is obtained from the previous expression by employing the ϵ-tensor and following the rule (A.1). We find

$$\left\langle \bar{\lambda}^{\dot\alpha}_b(y)\lambda^\alpha_a(x)\right\rangle_0 \quad \leftrightarrow \quad$$

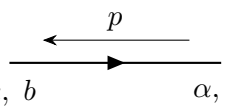

$$= \frac{\delta^{ab}\bar\sigma^{\dot\alpha\alpha}\cdot p}{p^2} \ . \tag{C.4}$$

The propagators associated with the spacetime fields of the massless hypermultiplets in the representation $\mathcal{R}$ have a similar structure. For the complex scalars q and $\tilde{q}$ we have

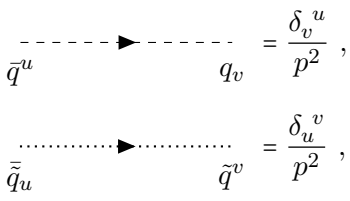

(C.5)

where $u, v = 1, \ldots, \dim \mathcal{R}$, while for the fermions η and $\tilde{\eta}$ we find

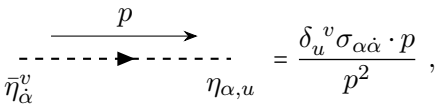

(C.6)

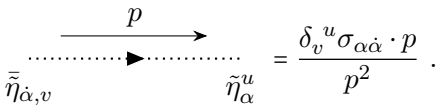

(C.7)

The propagators with raised indices are analogous to those presented in (C.4).

C.1 Perturbative corrections to the propagators

In this subsection, we focus on the one- and two-loop corrections to the propagators. We will work in momentum space and follow the formalism of [168], which we briefly review below.

In Euclidean space, the basis one-loop integral is

$$G(n_1, n_2) = \int \frac{\mathrm{d}^d k}{(2\pi)^d} \frac{1}{(k^2)^{n_1}((k+p)^2)^{n_2}} = (p^2)^{d/2-n_1-n_2} \widetilde{G}(n_1, n_2) \ , \tag{C.8}$$

where d is the spacetime dimension, the overall dependence on external momentum p^2 follows from dimensional analysis, while $\widetilde{G}(n_1, n_2)$ is a function of d and of the integers n_1 and n_2 [1]. Going through the calculation of (C.8), we find that it can be expressed in terms of Euler gamma functions as follows

$$\widetilde{G}(n_1, n_2) = \frac{\Gamma(n_1 + n_1 - d/2)}{(4\pi)^{d/2}\Gamma(n_1)\Gamma(n_2)} \frac{\Gamma(d/2 - n_1)\Gamma(d/2 - n_2)}{\Gamma(d - n_1 - n_2)} \ , \tag{C.9}$$

At two-loop accuracy, the basis integral we consider is [61, 168]

$$\begin{aligned} G(n_1, n_2, n_3, n_4, n_5) &= \int \frac{\mathrm{d}^d k}{(2\pi)^d} \frac{\mathrm{d}^d l}{(2\pi)^d} \frac{1}{((k+p)^2)^{n_1}((l+p)^2)^{n_2}(k^2)^{n_3}(l^2)^{n_4}((l-k)^2)^{n_5}} \\ &= (p^2)^{d-\Sigma n_i} \widetilde{G}(n_1, n_2, n_3, n_4, n_5) \ , \end{aligned}$$

where n_i are integers. We note that (C.10) is symmetric under the interchanges $(1 \leftrightarrow 2, 3 \leftrightarrow 4)$ and $(1 \leftrightarrow 3, 2 \leftrightarrow 4)$. Moreover, when one of the parameters n_i vanishes, (C.10) reduces to a product of one-loop integrals (C.8). In particular, we will use the identities

$$\widetilde{G}(n_1, n_2, n_3, n_4, 0) = \widetilde{G}(n_1, n_3)\widetilde{G}(n_2, n_4) \ , \tag{C.10}$$

$$\widetilde{G}(0, n_2, n_3, n_4, n_5) = \widetilde{G}(n_3, n_5)\widetilde{G}(n_2, n_3 + n_4 + n_5 - d/2) \ , \tag{C.11}$$

[1] Let us note that when $n_1 \leq 0$ or $n_2 \leq 0$ (C.8) vanishes.

which can be derived by repeated applications of (C.8). When all the indices n_i in (C.10) are equal to one, it is possible to show that (see Section 5.1 of [168])

$$G(d) \equiv G(1,1,1,1,1) = \frac{2G(1,1)}{d-4}\left(G(2,1) - \left(p^2\right)^{2-d/2} G(2,3-d/2)\right) . \tag{C.12}$$

Using (C.8), it is straightforward to prove that the previous expression is regular in the limit $d \to 4$ and is proportional to ζ_3

$$G(d) = (p^2)^{d-5}\widetilde{G}(d) = \frac{6\zeta_3}{(4\pi)^4 p^2} + \mathcal{O}(d-4) . \tag{C.13}$$

Finally, we switch to configuration space by the Fourier transform

$$D(x,s) \equiv \int \frac{\mathrm{d}^d p}{(2\pi)^d} \frac{e^{\mathrm{i}p\cdot x}}{(p^2)^s} = \frac{\Gamma(d/2-s)}{4^s \pi^{d/2}\Gamma(s)} \frac{1}{(x^2)^{d/2-s}} . \tag{C.14}$$

The tree-level propagators in configuration space are given by $\Delta(x) = D(x,1)$.

C.1.1 One-loop corrections to the propagators

In this subsection, we analyse the one-loop corrections to the propagators entering the computation of the supersymmetric Wilson loop. We recall that ultraviolet divergent diagrams are regularised by dimensionally reducing the theory from four to $d = 4 - 2\epsilon$ dimensions [121]. In this scheme, the gauge field A_μ is a d-dimensional vector, while the real scalars generated by the reduction are denoted by A_i, with $i = 1, \ldots, 4-d$. Unless explicitly stated otherwise, we shall work in the Feynman gauge.

One-loop corrections to the scalar and gluon propagator

We begin by considering the corrections to the propagators of the adjoint scalar ϕ and the gauge field A_μ. Gauge invariance dictates that these corrections must take the following form

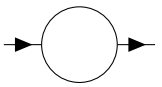

$$= \frac{\delta^{ab} g_B^2}{(p^2)^2} \pi_S^{(1)}(p^2) , \tag{C.15}$$

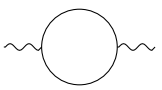

$$= \frac{\delta^{ab} g_B^2}{(p^2)^2} \left(\delta_{\mu\nu} - \frac{p_\mu p_\nu}{p^2}\right) \pi_G^{(1)}(p^2) , \tag{C.16}$$

where $\pi_G^{(1)}$ and $\pi_S^{(1)}$ denote the gluon and scalar polarization, respectively. The expectation based on supersymmetry is that

$$\pi_G^{(1)} = \pi_S^{(1)} \equiv \pi^{(1)} . \tag{C.17}$$

We will now verify this identity explicitly by considering the relevant diagrams separately.

The scalar polarization The relevant Feynman diagrams contributing to the scalar polarization $\pi_S^{(1)}(p^2)$ can be deduced from the explicit form of actions (6.1) and (6.3). We find three contributions

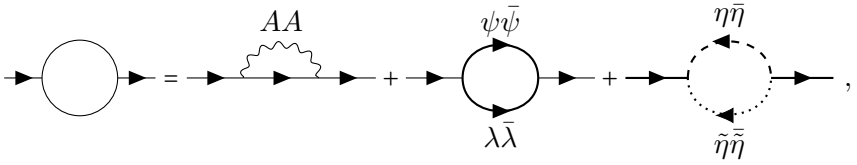

, (C.18)

where we recall that ψ and λ denote the two gauginos of the $\mathcal{N}=2$ vector multiplet, while η and $\tilde{\eta}$ are the Weyl fermions associated with the massless hypermultiplets in the representation $\mathcal{R}$. Going through the calculation, we obtain

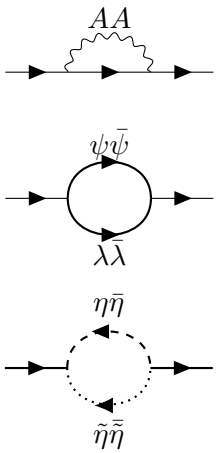

$$= \frac{g_B^2\delta^{ab}N}{(4\pi)^{d/2}}\frac{\Gamma(d/2)\Gamma(2-d/2)\Gamma(d/2-1)}{\Gamma(d)p^{6-d}}4(d-1)\ ,$$
$$= -\frac{g_B^2\delta^{ab}N}{(4\pi)^{d/2}}\frac{\Gamma(d/2)\Gamma(2-d/2)\Gamma(d/2-1)}{\Gamma(d)p^{6-d}}4(d-1)\ , \tag{C.19}$$
$$= -i_{\mathcal{R}}\frac{g_B^2\delta^{ab}}{(4\pi)^{d/2}}\frac{\Gamma(d/2)\Gamma(2-d/2)\Gamma(d/2-1)}{\Gamma(d)p^{6-d}}4(d-1)\ ,$$

where we recall $i_{\mathcal{R}}$ is the Dynkin index of the representation $\mathcal{R}$ (B.2a). Note that the first two-diagrams cancel each other out and consequently, the one-loop scalar polarization $\pi_S^{(1)}$ (C.15) only receives corrections from the matter sector of the theory. Expressing the last diagram in (C.19) by the basis integral (C.8), we find that

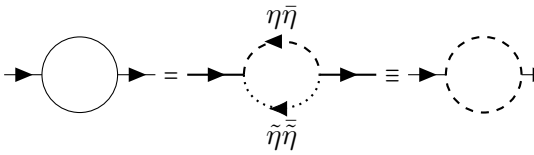

$$= -2\frac{\delta_{ab}g_B^2}{p^2}i_{\mathcal{R}}G(1,1)\ . \tag{C.20}$$

The gluon polarization The calculation of the gluon $\pi_G^{(1)}$ goes along the same lines. In particular, the $\mathcal{N}=2$ vector multiplet contributes to $\pi_G^{(1)}$ through: the gauge and ghost fields

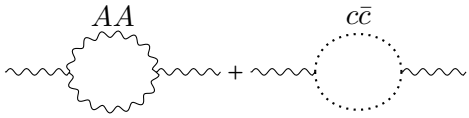

$$= \frac{g^2\delta^{ab}N}{(4\pi)^{d/2}}\frac{\Gamma(d/2)\Gamma(2-d/2)\Gamma(d/2-1)}{\Gamma(d)}(3d-2)\frac{P_{\mu\nu}}{p^{6-d}}\ , \tag{C.21}$$

one complex and $4-d$ real adjoint scalar fields [2]

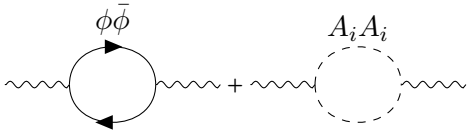

$$= \frac{g^2\delta^{ab}N}{(4\pi)^{d/2}}\frac{\Gamma(d/2)\Gamma(2-d/2)\Gamma(d/2-1)}{\Gamma(d)}(d-6)\frac{P_{\mu\nu}}{p^{6-d}}\ , \tag{C.22}$$

and two gauginos λ and ψ

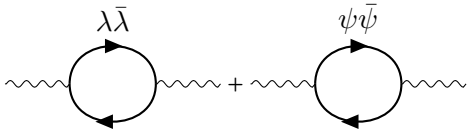

$$= \frac{g^2\delta^{ab}N}{(4\pi)^{d/2}}\frac{\Gamma(d/2)\Gamma(2-d/2)\Gamma(d/2-1)}{\Gamma(d)}(8-4d)\frac{P_{\mu\nu}}{p^{6-d}}\ . \tag{C.23}$$

[2] These scalars result from dimensional reduction.

In the previous expression, we denoted with $P_{\mu\nu} = \delta_{\mu\nu} - p_\mu p_\nu/p^2$ the transverse projector, which ensures that each correction is gauge invariant. Moreover, combining together (C.21), (C.22), and (C.23), we find that they cancel each other out, as in the scalar case (C.19).

Finally, we consider the diagrams resulting from the matter sector. We find that the polarization $\pi_G^{(1)}$ (C.16) receives contributions from the fermions through the diagrams

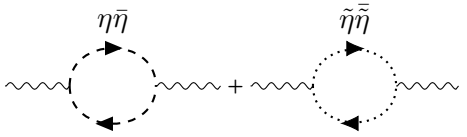

$$= \frac{g^2\delta^{ab}4i_{\mathcal{R}}}{(4\pi)^{d/2}}\frac{\Gamma(d/2)\Gamma(2-d/2)\Gamma(d/2-1)}{\Gamma(d)}(2-d)\frac{P_{\mu\nu}}{p^{6-d}} \ , \tag{C.24}$$

and from the scalars q and $\tilde{q}$

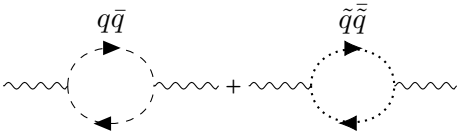

$$= -4\frac{g^2\delta^{ab}i_{\mathcal{R}}}{(4\pi)^{d/2}}\frac{\Gamma(d/2)\Gamma(2-d/2)\Gamma(d/2-1)}{\Gamma(d)}\frac{P_{\mu\nu}}{p^{6-d}} \ . \tag{C.25}$$

Combining together (C.24) and (C.25), we finally arrive at the following result

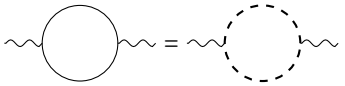

$$= -2i_{\mathcal{R}}\frac{\delta_{ab}g_B^2}{(p^2)}\left(\delta_{\mu\nu} - \frac{p_\mu p_\nu}{p^2}\right)G(1,1) \ . \tag{C.26}$$

The previous expression coincides with (C.20) up to the transverse projector $P_{\mu\nu}$, confirming the expectation based on supersymmetry (C.17), and leads to the following expression for the polarization operator

$$\pi^{(1)}(p^2) = -2i_{\mathcal{R}}g_B^2\frac{\Gamma(2-d/2)}{(4\pi)^{d/2}}\frac{\Gamma(d/2-1)\Gamma(d/2-1)}{\Gamma(d-2)}(p^2)^{d/2-2} \ , \tag{C.27}$$

where we recall that $i_{\mathcal{R}}$ is the Dynkin index of the representation $\mathcal{R}$ (B.2a).

Using (C.20) and (C.26), we can easily derive the one-loop corrections to the propagators in the difference-theory method. Subtracting off the contributions of $\mathcal{N} = 4$ SYM, where the hypermultiplets transform in the adjoint representation, we find that

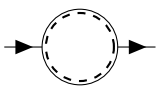

$$= \delta_{ab}\frac{g_B^2\Pi^{(1)}(p^2)}{(p^2)^2} \ , \tag{C.28a}$$

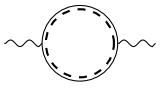

$$= \delta_{ab}\left(\delta_{\mu\nu} - \frac{p_\mu p_\nu}{p^2}\right)\frac{g_B^2\Pi^{(1)}(p^2)}{(p^2)^2} \ , \tag{C.28b}$$

where we employed a double dashed/continuous line to emphasise that the diagram is constructed by using the difference method. Moreover, the polarization operator $\Pi^{(1)}$ is given by

$$\begin{aligned} \Pi^{(1)}(p^2) &= f^{(1)}(d)(p^2)^{d/2-1} \ , \\ f^{(1)}(d) &= \beta_0\widetilde{G}(1,1) \ , \end{aligned} \tag{C.29}$$

where $\widetilde{G}(1,1)$ is defined in (C.8), while β_0 is the one-loop coefficient (1.25) of the β-function. Finally, by applying the Fourier transform (C.14) to the corrections (C.28), we switch to configuration space. For the scalar propagator, we find the following result

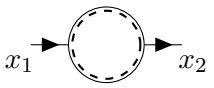

$$= f^{(1)}(d)g_B^2\,D(x_{12},3-d/2) \equiv \Delta^{(1)}(x_{12}) \ . \tag{C.30}$$

Repeating the same calculation for the correction (C.28b), we obtain

$$\begin{aligned} x_1 \sim\!\bigcirc\!\sim x_2 &= g_B^2 f^{(1)}(d)\ \left(\delta_{\mu\nu} D(x_{12}, 3-d/2) - \partial_{1,\mu}\partial_{2,\nu} D(x_{12}, 4-d/2)\right) \\ &\equiv \delta_{\mu\nu}\Delta^{(1)}(x_{12}) - \partial_{1,\mu}\partial_{2,\nu}\Delta^{(1),\mathrm{g}}(x_{12})\ . \end{aligned} \tag{C.31}$$

By gauge invariance, we expect that all the Wilson loop diagrams which involve the gauge-like term $\partial_{1,\mu}\partial_{2,\nu}\Delta^{(1),\mathrm{g}}(x_{12})$ do not contribute to the final results and in the following, we will verify this property explicitly.

One-loop corrections to the fermion propagators

We conclude this subsection by considering the one-loop corrections to the fermion propagators. These corrections are essential to determine the two-loop scalar propagator, which will be considered in the following subsection.

We begin with the one-loop corrections to the propagators of the gaugino ψ. The relevant Feynman diagrams are

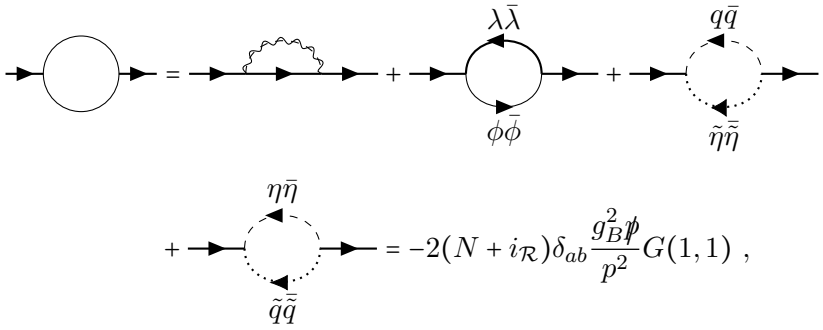

$$= -2(N + i_{\mathcal{R}})\delta_{ab}\frac{g_B^2 \not{p}}{p^2} G(1,1)\ , \tag{C.32}$$

where $\not{p} \equiv p_\mu \sigma^\mu$, with σ^μ given by (A.6). Moreover, the virtual emission in the first diagram, depicted by a wiggly/dashed line, arises from the interaction of the fermion ψ with the gauge field A_μ and with the real scalars A_i generated by dimensional reduction.

Going through the calculations of the corrections to the propagator of the gaugino λ, we find that they coincide with (C.32). This result is expected as these fields belong to the same supermultiplet. Moreover, we can use (C.32) to deduce the one-loop correction to the fermion propagators in the difference method

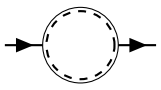

$$= 2(N - i_{\mathcal{R}})\delta_{ab}\frac{g_B^2 \not{p}}{p^2} G(1,1)\ , \tag{C.33}$$

where we employed the graphical notation of (C.28).

Finally, we consider the corrections to the propagators of the matter fermions η and $\tilde{\eta}$. For instance, the relevant Feynman diagrams contributing to η are given by

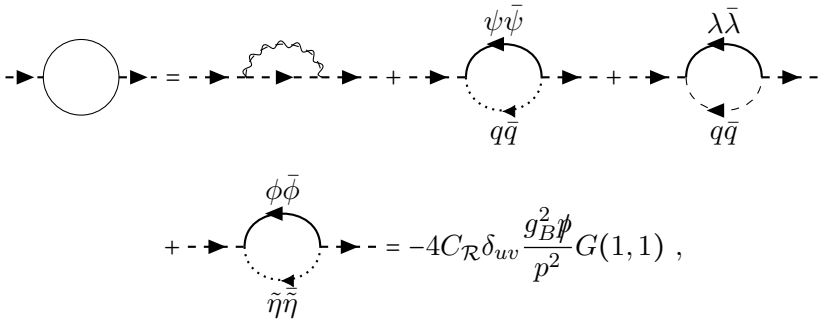

$$= -4C_{\mathcal{R}}\delta_{uv}\frac{g_B^2 \not{p}}{p^2} G(1,1)\ , \tag{C.34}$$

where $u, v = 1, \dots, \dim \mathcal{R}$ and we recall that $C_{\mathcal{R}}$ is the quadratic Casimir (B.2b). Going through the calculations of the corrections to the propagators of $\tilde{\eta}$ we find that they coincide with (C.34), as expected from supersymmetry.

C.1.2 Two-loop corrections to the propagators

At three loops, the expectation value of the supersymmetric Wilson loop receives contributions from diagrams involving the two-loop corrections to the propagators of the adjoint scalar and gauge field in the *difference-theory approach* [3] (6.48). The expectation based on supersymmetry is that these corrections coincide up to spacetime indices [4], as we already observed at one loop (see (C.28a) and (C.28b)). Therefore, we can assume that

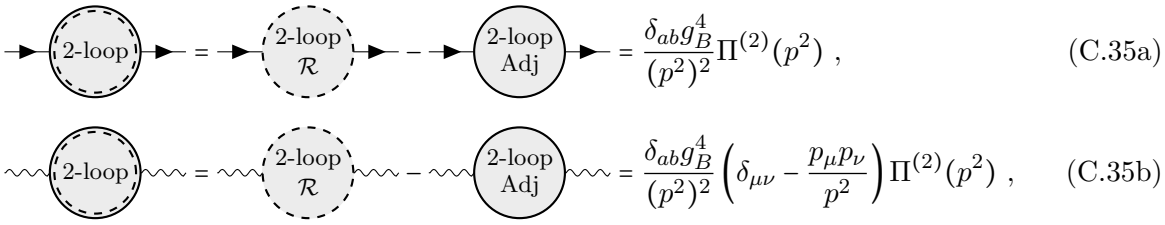

$$= \frac{\delta_{ab} g_B^4}{(p^2)^2} \Pi^{(2)}(p^2) \ , \tag{C.35a}$$

$$= \frac{\delta_{ab} g_B^4}{(p^2)^2} \left(\delta_{\mu\nu} - \frac{p_\mu p_\nu}{p^2} \right) \Pi^{(2)}(p^2) \ , \tag{C.35b}$$

and determine the two-loop polarization operator $\Pi^{(2)}(p^2)$ by considering (C.35a). In (C.35a) and (C.35b), the diagrams labelled by $\mathcal{R}$ capture all the two-loop corrections in which the scalar ϕ (or the gluon) interacts with matter fields in the representation $\mathcal{R}$, while those labelled by Adj denote the same corrections with $\mathcal{R} = \text{Adj}$.

By simple dimensional arguments, we deduce that the polarization operator can be written as follows

$$\Pi^{(2)}(p^2) = (p^2)^{d-3} f^{(2)}(d) \ , \tag{C.36}$$

where $f^{(2)}(d)$ depends on the spacetime dimension d and includes colour factors. To avoid cumbersome expressions, we will express the different diagrams that enter (C.35a) by the basis integrals (C.8) and (C.10), and we will directly provide their contributions to $f^{(2)}(d)$ by omitting the overall prefactor $g_B^4 \delta_{ab}/(p^2)^{5-d}$.

We find that the two-loop scalar polarization $\Pi^{(2)}(p^2)$ involves both reducible and irreducible diagrams. The former are simply given by

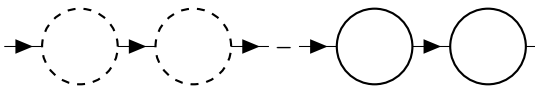

$$= 4(i_{\mathcal{R}}^2 - N^2) \widetilde{G}(1,1)^2 \ , \tag{C.37}$$

where we used (C.20). Conversely, the irreducible contributions can be grouped into two classes of corrections. The first one arises when we dress the internal lines of the diagrams in (C.18)

[3] Let us recall that in this scheme we consider diagrams with internal lines in the representation $\mathcal{R}$ and we subtract identical contributions with $\mathcal{R} = \text{Adj}$.

[4] An explicit test of this property at two-loop accuracy can be found in [61], where the authors studied the 1/2 BPS Wilson loop in superconformal $\mathcal{N} = 2$ QCD.

with proper one-loop self-energies, *i.e.*

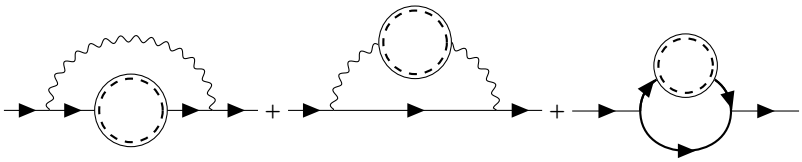

$$= 2N(N - i_{\mathcal{R}})\left(5\widetilde{G}(0,1,1,0,1) - \widetilde{G}(0,1,1,2,1)\right) , \tag{C.38}$$

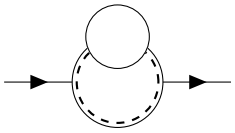

$$= 16\left(C_{\mathcal{R}} i_{\mathcal{R}} - N^2\right)\left(\widetilde{G}(0,1,1,1,1) - \widetilde{G}(0,1,1,0,1)\right) . \tag{C.39}$$

In (C.38), the internal dashed/continuous bubbles denote, respectively, the one-loop correction to the propagators of the adjoint scalar, gauge field and gaugino in the difference-theory method (see, respectively, (C.28a), (C.28b) and (C.33)). Similarly, the correction (C.39) is obtained by dressing the matter loop in (C.20) with the one-loop correction (C.34) and subtracting the contribution of $\mathcal{N} = 4$ SYM.

The second class of irreducible corrections emerges from pure two-loop diagrams, *i.e.*

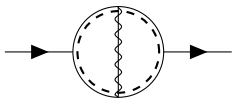

$$= \frac{2\mathcal{C}'_4}{NC_F}\Big(\widetilde{G}(d) - \widetilde{G}(1,0,1,1,1) + 2\widetilde{G}(0,1,1,0,1)\Big) , \tag{C.40}$$

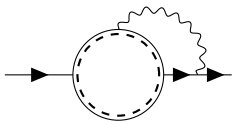

$$= -4N(i_{\mathcal{R}} - N)\left(\widetilde{G}(0,1,1,1,1) - \widetilde{G}(1,1)^2\right) , \tag{C.41}$$

$$= 4N(i_{\mathcal{R}} - N)\left(4\widetilde{G}(0,1,1,0,1) - 2\widetilde{G}(1,1)^2\right) , \tag{C.42}$$

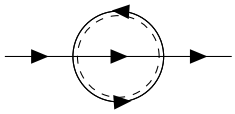

$$= \left(8(C_{\mathcal{R}} i_{\mathcal{R}} - N^2) - 2N(i_{\mathcal{R}} - N)\right)\widetilde{G}(0,1,1,0,1) , \tag{C.43}$$

where we recall that the colour factor $\mathcal{C}'_4$ in (C.40) is defined in (6.53). In (C.40), we employed a double wiggly/continuous line to depict the propagation of the gauge field A_μ and the $4-d$ real scalars arising from dimensional reduction. Similarly, the diagrams in (C.42) are constructed from Yukawa-like vertices, where the adjoint scalar ϕ interacts with the matter fermions (depicted by a *thick dashed* line), the two gauginos (shown as a thick *continuous* line), and the matter scalars (represented by a *thin dashed* line).

Combining together the results we derived in this subsection, we can express $f^{(2)}(d)$ (C.36) as the sum of four different terms

$$f^{(2)}(d) = f_1^{(2)}(d) + f_2^{(2)}(d) + f_3^{(2)}(d) + f_4^{(2)}(d) . \tag{C.44}$$

Recalling the explicit definition of the coefficient β_0 (1.25), we finally find that

$$\begin{aligned}
f_1^{(2)}(d) &= -2\,\beta_0\, i_{\mathcal{R}}\, \widetilde{G}(1,1)^2 , \\
f_2^{(2)}(d) &= -2\,\beta_0\, N\, \widetilde{G}(0,1,1,1,1) , \\
f_3^{(2)}(d) &= -\,\beta_0\, N\, \widetilde{G}(0,1,1,2,1) , \\
f_4^{(2)}(d) &= \frac{2\mathcal{C}'_4}{NC_F}\, \widetilde{G}(d) ,
\end{aligned} \tag{C.45}$$

where we recall that the dimensionless $\widetilde{G}$-functions are defined in Section C.1

Finally, we switch to configuration space by employing (C.14). We find that the two-loop corrections to the propagator of the scalar ϕ take the following form

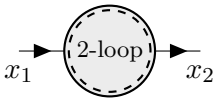

$$= g_B^4 f^{(2)}(d)\, D(x_{12}, 5-d) \equiv \Delta^{(2)}(x_{12}) \ . \tag{C.46}$$

Conversely, the gluon propagator involves two terms

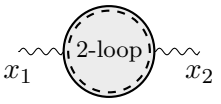

$$\begin{aligned} &= g_B^4 f^{(2)}(d)\ \left(\delta_{\mu\nu} D(x_{12}, 5-d) - \partial_{1,\mu}\partial_{2,\nu} D(x_{12}, 6-d)\right) \\ &\equiv \delta_{\mu\nu}\Delta^{(2)}(x_{12}) - \partial_{1,\mu}\partial_{2,\nu}\Delta^{(2),\mathrm{g}}(x_{12}) \ . \end{aligned} \tag{C.47}$$

Note that the gauge-like term $\partial_{1,\mu}\partial_{2,\nu}\Delta^{(2),\mathrm{g}}(x_{12})$ is completely irrelevant when inserted in the single-exchange correction (6.48), as it provides total derivatives integrated over a closed path.

C.2 Mercedes-like diagrams

We now turn our attention to the *Mercedes-like* correction

$\boldsymbol{\mathcal{M}} \equiv$ 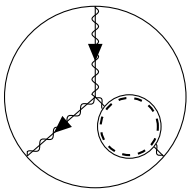 , (C.48)

where the internal bubble denotes the one-loop correction (C.28) to the propagator of the adjoint scalar and gauge field in the difference-theory approach.

By expanding the Wilson loop operator (5.7) at order g_B^3, we obtain the following representation for (C.48)

$$\boldsymbol{\mathcal{M}} = \oint \mathrm{d}^3\tau \left(\frac{(\mathrm{i}g_B)^3}{3!N} \left\langle \mathrm{tr}\, \mathcal{P}\mathcal{A}(\tau_1)\mathcal{A}(\tau_2)\mathcal{A}(\tau_3) \right\rangle_{\boldsymbol{\mathcal{M}}} + \frac{\mathrm{i}g_B^3 R^2}{2N} \left\langle \mathrm{tr}\, \mathcal{P}\mathcal{A}(\tau_1)\Phi(\tau_2)\bar{\Phi}(\tau_3) \right\rangle_{\boldsymbol{\mathcal{M}}} \right) , \tag{C.49}$$

where we introduced the notation $\mathcal{A}_i \equiv \dot{x}^\mu(\tau_i) A_\mu^a(x(\tau_i)) T^a$ and $\Phi_i \equiv \phi^a(x(\tau_i)) T^a$ and we recall that $\mathcal{P}$ denotes the path-ordering operator (5.2). In the previous expression, we used the subscript $\boldsymbol{\mathcal{M}}$ to indicate that only the reducible contributions to the internal vertices of (C.48) are retained when we evaluate the correlators.

Before entering the calculation of (C.48), we recall that the one-loop correction to the gauge-field propagator (C.31) consists of two different tensor structures. One of them is the gauge-like term $\partial_{1,\mu}\partial_{2,\nu}\Delta^{(2),\mathrm{g}}(x_{12})$, while the second one involves the metric $\delta_{\mu\nu}$. Within the Mercedes-like diagrams (C.48) these structures behave differently and consequently, we find it convenient to separate them. To do so, we represent (C.31) as follows

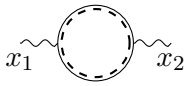

$$\begin{aligned} &= \delta_{ab}\delta_{\mu\nu}\Delta^{(1)}(x_{12}) + \delta_{ab}\partial_{1,\mu}\partial_{1,\nu}\Delta^{(1),\mathrm{g}}_{\mu\nu}(x_{12}) \\ &\equiv \quad \text{  } \quad + \quad \text{ 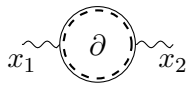 } \ , \end{aligned} \tag{C.50}$$

where we recall that $\Delta^{(1)}(x)$ and $\Delta^{(1),g}(x)$ are defined in (C.30) and (C.31) respectively.

Exploiting (C.50), we can express (C.48) as

$$\boldsymbol{\mathcal{M}} = \boldsymbol{\mathcal{M}}_1 + \boldsymbol{\mathcal{M}}_2 \ , \tag{C.51}$$

$\boldsymbol{\mathcal{M}}_1 \equiv$ 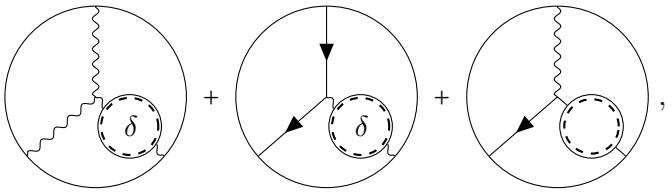 , (C.52)

$\boldsymbol{\mathcal{M}}_2 \equiv$ 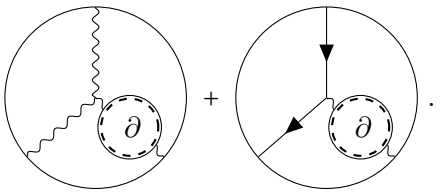 . (C.53)

Computing $\boldsymbol{\mathcal{M}}_1$

The explicit form of the diagrams contributing to $\boldsymbol{\mathcal{M}}_1$ (C.52) can be deduced by interaction vertices

$$S_{\text{gs}} = g_B \int \mathrm{d}^d\omega f^{abc} \left(\partial_\mu \bar{\phi}_b A^\mu_a \phi_c - \bar{\phi}_b A^\mu_a \partial_\mu \phi_c\right)(\omega) \ , \tag{C.54}$$

$$S_{\text{gg}} = g_B \int \mathrm{d}^d\omega f^{acb} \left(\partial_\mu A_{\nu,c} A^\mu_a A^b_\nu\right)(\omega) \ , \tag{C.55}$$

emerging from the action of pure $\mathcal{N} = 2$ super-Yang–Mills (6.1).

Substituting (C.54) into (C.49) and isolating the Wick contractions which involve the one-loop correction to the scalar propagator $\delta_{ab}\Delta^{(1)}(x)$ (C.30) and the tensor structure $\delta_{\mu\nu}\Delta^{(1)}(x)$, we obtain

$$\boldsymbol{\mathcal{M}}_1 = -\frac{g_B^4 C_F N}{2} \oint \mathrm{d}^3\tau \varepsilon(\tau) \ (R^2 - \dot{x}_1 \cdot \dot{x}_3)\,(\dot{x}_2 \cdot \partial_{x_1}) \int \mathrm{d}^d\omega \sum_{i=1}^{3} \prod_{j\neq i} \Delta^{(1)}(x_{i\omega})\Delta(x_{j\omega}) \ , \tag{C.56}$$

where $x_{i\omega} \equiv x_i - \omega$, while the tree-level propagator $\Delta(x)$ and the path-ordering symbol $\varepsilon(\tau)$ are defined in (6.13) and (6.33), respectively.

To proceed with the calculation, we replace the propagators $\Delta(x)$ and $\Delta^{(1)}(x)$ (C.30) by their explicit forms and we integrate over ω by means of usual Feynman parameters. The final result can be written as follows

$$\boldsymbol{\mathcal{M}}_1 = A_d \int_0^1 \mathrm{d}\mathcal{F} \oint \mathrm{d}^3\tau \varepsilon(\tau) \ \frac{(1-\cos(\tau_{13}))(\alpha(1-\alpha)\sin(\tau_{12}) - \alpha\gamma\sin(\tau_{32}))}{Q^{3d/2-4}} \ , \tag{C.57}$$

where we recall that Q is defined in (6.31) and the notation was introduced for [5]

$$\mathrm{d}\mathcal{F} = \mathrm{d}\alpha\mathrm{d}\beta\mathrm{d}\gamma\delta(1-\alpha-\beta-\gamma)(\alpha\beta\gamma)^{d/2-2}\left(\alpha^{d/2-2} + \beta^{d/2-2} + \gamma^{d/2-2}\right) \ , \tag{C.58}$$

$$A_d = -\frac{\hat{g}_B^6 C_F N \beta_0 \ \Gamma(3d/2-4)\Gamma^2(d/2-1)}{(d/2-2)\Gamma(d-2) \ \pi^{3d/2} 2^{3d/2+6}} \ . \tag{C.59}$$

[5] Recall that $\hat{g}_B = g_B R^{2-d/2}$.

We note that A_d exhibits a pole in four dimensions and depends on the coefficient β_0 (1.25) of the β-function. This means that in superconformal theories the previous expression vanishes.

To perform the contour integration in (C.57), we employ the identities [121, 169]

$$\oint \mathrm{d}^3\tau \frac{\partial}{\partial\tau_1}\left(\frac{\epsilon(\tau)(1-\cos\tau_{13})}{Q^{3d/2-5}}\right) = 0 \ , \tag{C.60}$$

$$\partial_{\tau_1}\varepsilon(\tau) - 2\Big(\delta(\tau_{12}) - \delta(\tau_{13})\Big) = 0 \ . \tag{C.61}$$

The advantage of these relations is that they allow us to reduce $\boldsymbol{\mathcal{M}}_1$ (C.56) to a linear combination of bubble-like contributions (6.52), analogous to those arising from the single-exchange contributions dressed with the two-loop correction (6.48). To see this, we insert (C.60) into (C.57) and exploit the fact that $\mathrm{d}\mathcal{F}$ (C.58) is fully symmetric. As a result, we can relabel the variables τ_i while keeping Q (6.31) unchanged and find that

$$\begin{aligned}\boldsymbol{\mathcal{M}}_1 &= \frac{2A_d}{3d/2-5}\int_0^1 \mathrm{d}\mathcal{F}\oint \mathrm{d}^2\tau \frac{(1-\cos\tau_{23})^{6-3d/2}}{(\gamma(1-\gamma))^{3d/2-5}} - A_d\left(\frac{3d-12}{3d-10}\right)\int_0^1 \mathrm{d}\mathcal{F}\oint \mathrm{d}^3\tau\frac{\varepsilon(\tau)\sin\tau_{13}}{Q^{3d/2-5}} \\ &= -\hat{g}_N^6\left(2F_2^{(2)} + \frac{N}{i_{\mathcal{R}}}F_1^{(2)} + \frac{\hat{g}_B^6\beta_0 C_F N 9\zeta_3}{2^8\pi^4}\right) \ ,\end{aligned} \tag{C.62}$$

where $F_1^{(2)}$ and $F_2^{(2)}$ are the (UV divergent) bubble-like contributions (6.52) which arise from the integration over the measure $\mathrm{d}\mathcal{F}$ (C.58) in the first term of the previous expression. Conversely, by applying the master integral (6.34) to the second term in the first line of (C.62), we find the ζ_3-like term. This is finite in four dimensions as it results from an interference effect between the ultraviolet pole of the amplitude A_d (C.59) and the evanescent term $(3d-12)$.

Computing $\boldsymbol{\mathcal{M}}_2$

Finally, we discuss the correction $\boldsymbol{\mathcal{M}}_2$ (C.53).

We begin with considering the diagrams involving three gauge fields. Inserting the pure-gauge vertex (C.54) into the first correlator of (C.49) and decorating the Wick contractions with the tensor $\partial_{1,\mu}\partial_{2,\nu}\Delta^{(2),\mathrm{g}}(x_{12})$ (C.50) we arrive at the following representation

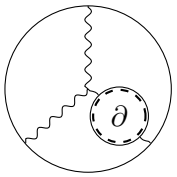

$$= \frac{g_B^4 C_F N}{2}\oint \mathrm{d}^3\tau\varepsilon(\tau)\int \mathrm{d}^d\omega\frac{\mathrm{d}}{\mathrm{d}\tau_1}\Big(\mathcal{O}(x_j)\Delta(x_{3\omega})\Delta(x_{2\omega})\Delta^{(1),\mathrm{g}}(x_{1\omega})\Big) \ , \tag{C.63}$$

where $\mathcal{O}(x_j)$ denotes the following differential operator

$$\mathcal{O}(x_j) = \Big[\,(\dot{x}_3\cdot\partial_1)\,(\partial_1-\partial_3)\cdot\dot{x}_2 + (\dot{x}_2\cdot\dot{x}_3)\,(\partial_3\cdot\partial_1)\,\Big] \ . \tag{C.64}$$

The diagrams involving both the adjoint scalars and the gauge field possess a similar structure. Indeed, inserting (C.55) into the second correlator of (C.49), and decorating the Wick contraction of the gauge field with the tensor $\partial_{1,\mu}\partial_{1,\nu}\Delta^{(1),\mathrm{g}}(x_{1\omega})$, we find

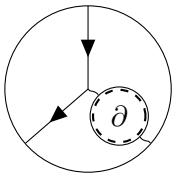

$$= -\frac{g_B^4 C_F R^2 N}{2}\oint \mathrm{d}^3\tau\varepsilon(\tau)\ \frac{\mathrm{d}}{\mathrm{d}\tau_1}\partial_3\cdot\partial_1\Big(\Delta(x_{3\omega})\Delta(x_{2\omega})\Delta^{(1),\mathrm{g}}(x_{1\omega})\Big) . \tag{C.65}$$

By combining together (C.63) and (C.65) and neglecting terms which provide total derivatives integrated over closed paths, we obtain the following result

$$\begin{aligned}\boldsymbol{\mathcal{M}}_2 &= \frac{g_B^4 C_F N}{2} \oint \mathrm{d}^3\tau\varepsilon(\tau)\left(\dot{x}_2\cdot\dot{x}_3 - R^2\right)\frac{\mathrm{d}}{\mathrm{d}\tau_1}\partial_3\cdot\partial_1 \int \mathrm{d}^d\omega\Delta(x_{2\omega})\Delta(x_{3\omega})\Delta^{(1),\mathrm{g}}(x_{1\omega}) \\ &= g_B^4 C_F N \oint \mathrm{d}^3\tau(\delta(\tau_{12})-\delta(\tau_{13}))\left(R^2 - \dot{x}_2\cdot\dot{x}_3\right)\partial_3\cdot\partial_1 \int \mathrm{d}^d\omega\Delta(x_{2\omega})\Delta(x_{3\omega})\Delta^{(1),\mathrm{g}}(x_{1\omega}) \\ &= -2\hat{g}_B^6 F_3^{(2)} \ ,\end{aligned} \tag{C.66}$$

where $F_3^{(2)}$ denotes the bubble-like contribution (6.52) and we obtained the second line by using the identity (C.61).

Combining (C.66) with (C.62), we find that the Mercedes-like diagrams (C.48) take the following form

$$\boldsymbol{\mathcal{M}} = \boldsymbol{\mathcal{M}}_1 + \boldsymbol{\mathcal{M}}_2 = -\hat{g}_B^6\left(2F_2^{(2)} + 2F_3^{(2)} + \frac{N}{i_{\mathcal{R}}}F_1^{(2)} + 9\frac{\beta_0\hat{g}_B^6 C_F N}{2^8\pi^4}\zeta_3\right) + \dots \ , \tag{C.67}$$

where the ellipses stand for evanescent corrections that contribute to higher orders in perturbation theory.

C.3 Lifesaver diagrams

We now examine in detail the *lifesaver-like* diagrams

$\boldsymbol{\mathcal{L}} =$ 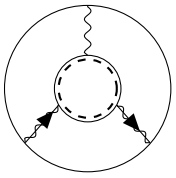 , (C.68)

where the internal bubble captures the one-loop irreducible corrections to the gauge-scalar and pure-gauge vertex in the difference-theory approach.

To simplify the initial stages of the analysis, we find it convenient to express (C.68) as the sum of two terms

$$\boldsymbol{\mathcal{L}} = \boldsymbol{\mathcal{L}}_g + \boldsymbol{\mathcal{L}}_{gs} \ , \tag{C.69}$$

where $\boldsymbol{\mathcal{L}}_g$ denotes the corrections that solely depend on the gauge field A_μ, while $\boldsymbol{\mathcal{L}}_{gs}$ captures those involving the adjoint scalar ϕ. To determine $\boldsymbol{\mathcal{L}}_g$ and $\boldsymbol{\mathcal{L}}_{gs}$, we expand the Wilson loop at order g_B^3 and we find that

$$\boldsymbol{\mathcal{L}}_g = \left(\frac{(\mathrm{i}g_B)^3}{3!N}\right)\left(\oint \mathrm{d}^3\tau\left\langle \mathrm{tr}\,\mathcal{P}\mathcal{A}(\tau_1)\mathcal{A}(\tau_2)\mathcal{A}(\tau_3)\right\rangle_{\boldsymbol{\mathcal{L}}}\right) \ , \tag{C.70}$$

$$\boldsymbol{\mathcal{L}}_{gs} = \left(\frac{\mathrm{i}g_B^3 R^2}{2N}\right)\left(\oint \mathrm{d}^3\tau\left\langle \mathrm{tr}\,\mathcal{P}\mathcal{A}(\tau_1)\Phi(\tau_2)\bar{\Phi}(\tau_3)\right\rangle_{\boldsymbol{\mathcal{L}}}\right) \ , \tag{C.71}$$

where the subscript $\boldsymbol{\mathcal{L}}$ indicates that only the irreducible corrections to the internal vertices of (C.48) are retained when we evaluate the correlators.

The irreducible corrections to gauge-scalar vertex Our first goal is to determine the explicit form of the correlator in (C.71). To do so, we have to identify the relevant Feynman diagrams that contribute to the irreducible correction to the gauge-scalar vertex in the difference-theory approach. Using the actions of the matter sector (6.3), we find that

$$\left\langle A_a^\mu(x_1)\phi^b(x_2)\bar{\phi}^c(x_3)\right\rangle_{\boldsymbol{\mathcal{L}}} =$$

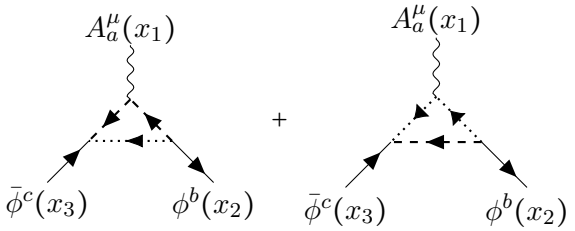

$$- (\mathcal{R} = \text{Adj}) \tag{C.72}$$

$$= f_{abc}\left(\mathcal{S}_1^\mu(x_i) + \mathcal{S}_2^\mu(x_i)\right) .$$

In the previous expression, f_{abc} are the structure constants of $SU(N)$ (B.1) and we defined

$$\mathcal{S}_1^\mu(x_i) = (2\mathrm{i}g_B^3)(i_{\mathcal{R}} - N)\int \mathrm{d}P \int \frac{\mathrm{d}^d k}{(2\pi)^d}\frac{p_2^\mu k^2 - p_3^\mu(k-p_1)^2}{k^2(k-p_1)^2(k+p_3)^2} , \tag{C.73a}$$

$$\mathcal{S}_2^\mu(x_i) = (2\mathrm{i}g_B^3)(i_{\mathcal{R}} - N)\int \mathrm{d}P \int \frac{\mathrm{d}^d k}{(2\pi)^d}\frac{p_1^2(k+p_3)^\mu - p_3^2(k-p_1)^\mu - p_2^2 k^\mu}{k^2(k-p_1)^2(k+p_3)^2} , \tag{C.73b}$$

where $\mathrm{d}P$ denotes the integration measure over the external momenta p_i

$$\mathrm{d}P = \prod_{i=1}^{3}\frac{\mathrm{d}^d p_i}{(2\pi)^d}\frac{e^{-\mathrm{i}p_i\cdot x_i}}{p_i^2}(2\pi)^d\delta^d\left(\Sigma_j\ p_j\right) . \tag{C.74}$$

The functions $\mathcal{S}_1^\mu$ (C.73a) and $\mathcal{S}_2^\mu$ (C.73b) display distinct behaviours in the limit $d \to 4$. Indeed, $\mathcal{S}_1^\mu$ can be evaluated in terms of usual gamma functions by (C.8) and develops a UV $1/(d-4)$ pole as $d \to 4$, whereas $\mathcal{S}_2^\mu(x_i)$ reduces to a combination of *triangle-like* integrals [148], which are regular in four dimensions.

The different behaviour of the functions (C.73) $d \to 4$ suggests that they contribute to the observable in a different manner and consequently, it is convenient to express $\boldsymbol{\mathcal{L}}_{gs}$ as

$$\boldsymbol{\mathcal{L}}_{gs} = \boldsymbol{\mathcal{L}}_{gs}^{(1)} + \boldsymbol{\mathcal{L}}_{gs}^{(2)} , \tag{C.75a}$$

$$\boldsymbol{\mathcal{L}}_{gs}^{(1)} = -\frac{g_B^3 R^2}{4} N C_F \oint \mathrm{d}^3\tau\varepsilon(\tau)\left(\dot{x}_1\cdot\mathcal{S}_1\right) , \tag{C.75b}$$

$$\boldsymbol{\mathcal{L}}_{gs}^{(2)} = -\frac{g_B^3 R^2}{4} N C_F \oint \mathrm{d}^3\tau\varepsilon(\tau)\left(\dot{x}_1\cdot\mathcal{S}_2\right) . \tag{C.75c}$$

Replacing $\mathcal{S}_1^\mu$ with its integral representation (C.73a), we find that the loop integration over the momentum k can be evaluated in terms of (C.8), while the Fourier transform (C.74) can be expressed by the functions $\Delta^{(1)}(x)$ and $\Delta(x)$ defined, respectively, in (C.30) and (6.13). The final result takes the following form

$$\boldsymbol{\mathcal{L}}_{gs}^{(1)} = \mathcal{A}^{(1)} R^2 \oint \mathrm{d}^3\tau\varepsilon(\tau)\left(\dot{x}_2\cdot\partial_1\right)\int \mathrm{d}^d\omega\Delta^{(1)}(x_{1\omega})\Delta(x_{2\omega})\Delta(x_{3\omega}) . \tag{C.76}$$

Similarly, the calculation of $\boldsymbol{\mathcal{L}}_{gs}^{(2)}$ leads to

$$\boldsymbol{\mathcal{L}}_{gs}^{(2)} = \mathcal{A}^{(2)} \oint \mathrm{d}^3\tau\varepsilon(\tau)\int \mathrm{d}P\left(-\mathrm{i}p_2^2\right)\int \frac{\mathrm{d}^d k}{(2\pi)^2}\frac{R^2\left(2k\cdot\dot{x}_1 - k\cdot\dot{x}_2\right)}{k^2(k+p_1)^2(k-p_3)^2} , \tag{C.77}$$

where we employed the explicit form of the function $\mathcal{S}_2^\mu$ (C.73b) and exploited the antisymmetry of the ε-symbol (6.33). Moreover, the notation was introduced for the amplitudes

$$\mathcal{A}^{(1)} = \frac{C_F N g_B^4}{2} \,, \tag{C.78}$$

$$\mathcal{A}^{(2)} = -\frac{\beta_0}{4} C_F N g_B^6 \,. \tag{C.79}$$

The one-loop corrections to pure-gauge vertex Our second goal is to evaluate the correlator in (C.70), which encodes the one-loop irreducible corrections to the pure-gauge vertex in the difference-theory approach. The Feynman diagrams contributing to this correlator arise from both matter scalars and fermions, which we treat separately.

Using the action (6.3), we find that the matter scalars contribute to the pure-gauge vertex via the following diagrams

$\mathcal{S}^{abc}_{\mu\nu\rho}(x_i) =$ 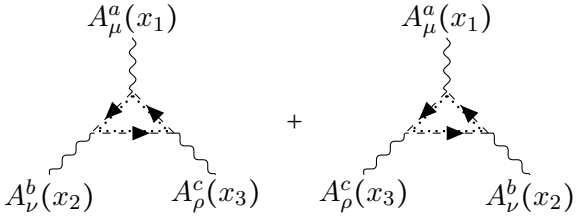 $- \ (\mathcal{R} = \mathrm{Adj})$

(C.80)

$$= 2\mathrm{i} g_B^3 f^{abc} (N - i_{\mathcal{R}}) \int \mathrm{d}P \int \frac{\mathrm{d}^d k}{(2\pi)^d} \frac{(2k+p_1)_\mu (2k+p_1-p_3)_\mu (2k-p_3)_\rho}{k^2 (k+p_1)^2 (k-p_3)^2} \,,$$

where the dashed and dotted lines denote the scalar q and $\tilde{q}$, respectively.

The matter fermions contribute to the correlator in (C.70) via the following diagrams

$\mathcal{F}^{abc}_{\mu\nu\rho}(x_i) =$ 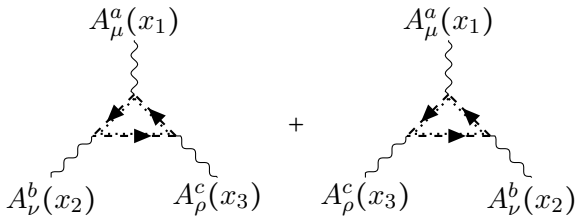 $- \ (\mathcal{R} = \mathrm{Adj})$

(C.81)

$$= \mathrm{i} g_B^3 f^{abc} (N - i_{\mathcal{R}}) \int \mathrm{d}P \int \frac{\mathrm{d}^d k}{(2\pi)^d} \frac{\left(\mathrm{Tr}\, \bar{\sigma}_\mu \not{k} \bar{\sigma}_\rho (\not{k} - \not{p}_3) \bar{\sigma}_\nu (\not{k} + \not{p}_1)\right)}{k^2 (k+p_1)^2 (k-p_3)^2}$$

$$+ \mathrm{i} g_B^3 f^{abc} (N - i_{\mathcal{R}}) \int \mathrm{d}P \int \frac{\mathrm{d}^d k}{(2\pi)^d} \frac{\left(\mathrm{Tr}\, \bar{\sigma}_\rho \not{k} \bar{\sigma}_\mu (\not{k} + \not{p}_1) \bar{\sigma}_\nu (\not{k} - \not{p}_3)\right)}{k^2 (k+p_1)^2 (k-p_3)^2} \,,$$

where the dashed and dotted lines denote the fermion η and $\tilde{\eta}$, respectively. Employing the identities in (A.11), we can simplify the traces in (C.81) and obtain [6]

$$\mathcal{F}^{abc}_{\mu\nu\rho}(x_i) = -\mathcal{S}^{abc}_{\mu\nu\rho}(x_i) + f^{abc} \left(\mathcal{G}^{(1)}_{\mu\nu\rho}(x_i) + \mathcal{G}^{(2)}_{\mu\nu\rho}(x_i) \right) \,, \tag{C.82}$$

where $\mathcal{S}^{abc}_{\mu\nu\rho}(x_i)$ is the correction to the pure-gauge vertex resulting from the matter scalars (C.80), while $\mathcal{G}^{(1)}_{\mu\nu\rho}$ and $\mathcal{G}^{(2)}_{\mu\nu\rho}$ are the counterparts of the functions $\mathcal{S}_1^\mu$ and $\mathcal{S}_2^\mu$ (C.73). As we will

[6] To arrive at (C.82), we neglected terms that, when integrated over the Wilson loop contour in (C.70), provides total derivatives.

shortly see, they exhibit the same behaviour in the limit $d \to 4$ and are related to (C.73) by supersymmetry. In particular, $\mathcal{G}^{(1)}_{\mu\nu\rho}$ takes the following form

$$\mathcal{G}^{(1)}_{\mu\nu\rho}(x_i) = -2ig_B^3(i_{\mathcal{R}} - N)\int \mathrm{d}P \int \frac{\mathrm{d}^d k}{(2\pi)^d}\Bigg[\frac{\delta_{\mu\nu}\left(k^2 p_{2,\rho} - p_{1,\rho}(k-p_3)^2\right)}{k^2(k+p_1)^2(k-p_3)^2} + \frac{\delta_{\mu\rho}\left(p_{1,\nu}(k-p_3)^2 - p_{3,\nu}(k+p_1)^2\right)}{k^2(k+p_1)^2(k-p_3)^2} + \frac{\delta_{\nu\rho}\left(p_{3,\mu}(k+p_1)^2 - p_{2,\mu}k^2\right)}{k^2(k+p_1)^2(k-p_3)^2}\Bigg] . \tag{C.83}$$

Integrating over large loop momentum k, (C.83) develops a UV pole, in close analogy to $\mathcal{S}_1^\mu$ (C.73a), while $\mathcal{G}^{(2)}_{\mu\nu\rho}(x_i)$ reduces to a combination of *triangle-like* integrals [148], *i.e.*

$$\mathcal{G}^{(2)}_{\mu\nu\rho}(x_i) = 2ig_B^3(i_{\mathcal{R}} - N)\int \mathrm{d}P \int \frac{\mathrm{d}^d k}{(2\pi)^d}\Bigg[\frac{\delta_{\mu\nu}\left(p_1^2(k-p_3)_\rho + p_2^2 k_\rho - p_3^2(k+p_1)_\rho\right)}{k^2(k+p_1)^2(k-p_3)^2} + \frac{\delta_{\mu\rho}\left(p_3^2(k+p_1)_\nu - p_2^2 k_\nu + p_1^2(k-p_3)_\nu\right)}{k^2(k+p_1)^2(k-p_3)^2} - \frac{\delta_{\nu\rho}\left(p_1^2(k-p_3)_\mu - p_2^2 k_\mu - p_3^2(k+p_1)_\mu\right)}{k^2(k+p_1)^2(k-p_3)^2}\Bigg] . \tag{C.84}$$

Combining together (C.82) with (C.80), we observe a partial cancellation between the bosonic and fermionic degrees of freedom, as expected in supersymmetric theories, and we find that the correlator in (C.70) is given by

$$\left\langle A^a_\mu(x_1)A^b_\nu(x_2)A^c_\rho(x_3)\right\rangle_{\mathcal{L}} = f^{abc}\left(\mathcal{G}^{(1)}_{\mu\nu\rho}(x_i) + \mathcal{G}^{(2)}_{\mu\nu\rho}(x_i)\right) . \tag{C.85}$$

Following the analysis of the gauge-scalar vertex (C.75), we substitute (C.85) into (C.70) and we express the result as follows

$$\boldsymbol{\mathcal{L}}_g = \boldsymbol{\mathcal{L}}_g^{(1)} + \boldsymbol{\mathcal{L}}_g^{(2)} , \tag{C.86a}$$

$$\boldsymbol{\mathcal{L}}_g^{(1)} = \frac{g_B^3}{12} N C_F \oint \mathrm{d}^3\tau\varepsilon(\tau)\left(\dot{x}_1^\mu \dot{x}_2^\nu \dot{x}_3^\rho\right)\mathcal{G}^{(1)}_{\mu\nu\rho} , \tag{C.86b}$$

$$\boldsymbol{\mathcal{L}}_g^{(2)} = \frac{g_B^3}{12} N C_F \oint \mathrm{d}^3\tau\varepsilon(\tau)\left(\dot{x}_1^\mu \dot{x}_2^\nu \dot{x}_3^\rho\right)\mathcal{G}^{(2)}_{\mu\nu\rho} . \tag{C.86c}$$

Replacing $\mathcal{G}^{(1)}_{\mu\nu\rho}$ with its integral representation (C.83), we find that the loop integration over the momentum k reduces to the basis integral (C.8), while the Fourier transform (C.74) can be expressed by the functions $\Delta^{(1)}(x)$ and $\Delta(x)$ defined, respectively, in (C.30) and (6.13). The final result takes the following form

$$\boldsymbol{\mathcal{L}}_g^{(1)} = \mathcal{A}^{(1)} \oint \mathrm{d}^3\tau\varepsilon(\tau)\left(-\dot{x}_1\cdot\dot{x}_3\right)\left(\dot{x}_2\cdot\partial_1\right)\int \mathrm{d}^d\omega\Delta^{(1)}(x_{1\omega})\Delta(x_{2\omega})\Delta(x_{3\omega}) , \tag{C.87}$$

where $\mathcal{A}^{(1)}$ is defined in (C.78). We emphasise that (C.87) has the same structure of (C.76), up to the replacement $R^2 \to -\dot{x}_i\cdot\dot{x}_j$. This can be regarded as a supersymmetry relation between the two different classes of corrections and justifies the decomposition (C.86).

Analogously, we find the following expression for $\boldsymbol{\mathcal{L}}_g^{(2)}$

$$\boldsymbol{\mathcal{L}}_g^{(2)} = \mathcal{A}^{(2)} \oint \mathrm{d}^3\tau\varepsilon(\tau)\int \mathrm{d}P\left(\mathrm{i}p_2^2\right)\int \frac{\mathrm{d}^d k}{(2\pi)^d}\frac{(2k\cdot\dot{x}_1)(\dot{x}_2\cdot\dot{x}_3) - (k\cdot\dot{x}_2)(\dot{x}_1\cdot\dot{x}_3)}{k^2(k+p_1)^2(k-p_3)^2} , \tag{C.88}$$

where the coefficient $\mathcal{A}^{(2)}$ is defined in (C.79). As we already observed for $\boldsymbol{\mathcal{L}}_g^{(1)}$, the contribution $\boldsymbol{\mathcal{L}}_g^{(2)}$ is related to $\boldsymbol{\mathcal{L}}_{gs}^{(2)}$ (C.77) by the relation $R^2 \to -\dot{x}_i\cdot\dot{x}_j$.

Summary of the results Using the results we derived above, we can construct the integral representations for the lifesaver-like diagrams (C.68). We have

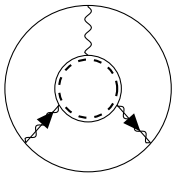

$$\overset{(C.69)}{=} \boldsymbol{\mathcal{L}}_g + \boldsymbol{\mathcal{L}}_{gs} \tag{C.89}$$

$$\overset{(C.75,C.86)}{=} \left(\boldsymbol{\mathcal{L}}_g^{(1)} + \boldsymbol{\mathcal{L}}_{gs}^{(1)}\right) + \left(\boldsymbol{\mathcal{L}}_g^{(2)} + \boldsymbol{\mathcal{L}}_{gs}^{(2)}\right) \equiv \left(\boldsymbol{\mathcal{L}}^{(1)} + \boldsymbol{\mathcal{L}}^{(2)}\right) .$$

In the previous expression, we grouped the different contributions into two terms in such a way that $\boldsymbol{\mathcal{L}}^{(1)}$ and $\boldsymbol{\mathcal{L}}^{(2)}$ naturally involve the combination $R^2 \to -\dot{x}_i \cdot \dot{x}_j$, *i.e.*

$$\boldsymbol{\mathcal{L}}^{(1)} = \mathcal{A}^{(1)} \oint \mathrm{d}^3\tau \varepsilon(\tau) \left(R^2 - \dot{x}_1 \cdot \dot{x}_3\right) \dot{x}_2 \cdot \partial_1 \int \mathrm{d}^d\omega \Delta^{(1)}(x_{1\omega})\Delta(x_{2\omega})\Delta(x_{3\omega}) \ , \tag{C.90a}$$

$$\boldsymbol{\mathcal{L}}^{(2)} = \mathcal{A}^{(2)} \oint \mathrm{d}^3\tau \varepsilon(\tau) \int \mathrm{d}P\left(\mathrm{i}p_2^2\right) \int \frac{\mathrm{d}^d k}{(2\pi)^d} \frac{(2k\cdot\dot{x}_1)\left(\dot{x}_2\cdot\dot{x}_3 - R^2\right) - (k\cdot\dot{x}_2)\left(\dot{x}_1\cdot\dot{x}_3 - R^2\right)}{k^2(k+p_1)^2(k-p_3)^2} \ . \tag{C.90b}$$

Our next goal is to develop a technique to calculate these two functions.

C.3.0.1 Computing $\mathcal{L}^{(1)}$

Let us begin by considering the calculation of $\boldsymbol{\mathcal{L}}^{(1)}$ (C.90a). Integrating over ω, we obtain

$$\boldsymbol{\mathcal{L}}^{(1)} = -A_d \int_0^1 \mathrm{d}F \left(\alpha^2\beta\gamma\right)^{d/2-2} \oint \mathrm{d}^3\tau \frac{\varepsilon(\tau)\ (1-\cos\tau_{13})\left(\alpha(1-\alpha)\sin\tau_{12} + \alpha\gamma\sin\tau_{23}\right)}{Q^{3d/2-4}} \ , \tag{C.91}$$

where $\mathrm{d}F$ is the usual measure over the unit cube (6.32), while Q is defined in (6.31). The previous expression is divergent in the limit $d \to 4$, as it involves the amplitude A_d (C.59). Moreover, its structure is extremely similar to the correction $\boldsymbol{\mathcal{M}}^{(1)}$ (C.56) and consequently, we can integrate over the contour by similar manipulations. We apply (C.60) and we obtain

$$\begin{aligned}\boldsymbol{\mathcal{L}}^{(1)} = {} & A_d \frac{2}{5-3d/2} \int_0^1 \mathrm{d}F \left(\alpha^2\beta\gamma\right)^{d/2-2} \oint \mathrm{d}^2\tau \frac{(1-\cos\tau_{23})^{6-3d/2}}{(\gamma(1-\gamma))^{3d/2-5}} \\ & + A_d \frac{6-3d/2}{5-3d/2} \int_0^1 \mathrm{d}F \left(\alpha^2\beta\gamma\right)^{d/2-2} \oint \mathrm{d}^3\tau \frac{\varepsilon(\tau)\sin\tau_{13}}{Q^{3d/2-5}} - \delta\boldsymbol{\mathcal{L}}^{(1)} \ ,\end{aligned} \tag{C.92}$$

where

$$\delta\boldsymbol{\mathcal{L}}^{(1)} = A_d \int_0^1 \mathrm{d}F \left(\alpha^{d-4}(\beta\gamma)^{d/2-1} - \beta^{d-3}\alpha^{d/2-2}\gamma^{d/2-1}\right) \oint \mathrm{d}^3\tau\varepsilon(\tau) \frac{(1-\cos\tau_{23})\sin\tau_{13}}{Q^{3d/2-4}} \ . \tag{C.93}$$

Comparing (C.92) with (C.62), we observe that the term $\delta\boldsymbol{\mathcal{L}}^{(1)}$ is a novelty. It arises because the integrand in (C.90a) is not fully symmetric in the exchange of the coordinates x_i. However, we now show that (C.93) vanishes in four dimensions, and consequently, it is irrelevant for the three-loop analysis. To see this, we replace $Q^{3d/2-4}$ (6.31) with a two-fold Mellin-Barnes integral via (C.140) and we find that

$$\frac{1}{Q^{3d/2-4}} = \frac{2^{4-3d/2}}{\Gamma(3d/2-4)} \int \frac{\mathrm{d}u\mathrm{d}v}{(2\pi\mathrm{i})^2} \frac{\Gamma(3d/2-4+u+v)\Gamma(-u)\Gamma(-v)\left(\beta\gamma\sin^2\frac{\tau_{23}}{2}\right)^u}{\left(\alpha\beta\sin^2\frac{\tau_{12}}{2}\right)^{3d/2-4+u+v}\left(\alpha\gamma\sin^2\frac{\tau_{13}}{2}\right)^{-v}} \ , \tag{C.94}$$

where the integration contour runs parallel to the imaginary axis and separates the increasing and decreasing poles of the gamma function. Substituting the previous expression into (C.93), we integrate over the Wilson loop contour via (C.139) and we obtain

$$\begin{aligned}\delta\boldsymbol{\mathcal{L}}^{(1)} &= A_d \int \frac{\mathrm{d}u\mathrm{d}v}{(2\pi\mathrm{i})^2} \frac{\Gamma(3d/2-4+u+v)\Gamma(-u)\Gamma(-v)\Gamma(d/2+u+v)}{2^{3d/2-5}\Gamma(3d/2-4)\Gamma(5-d)} \\ &\times \mathcal{J}(4-3d/2-u-v,u+1,v)\Big(\Gamma(1-d/2-u)\Gamma(4-d-v)-\Gamma(2-d/2-v)\Gamma(3-d-u)\Big)\,,\end{aligned} \tag{C.95}$$

where $\mathcal{J}(x,y,z)$ is defined in (C.139). Expanding the integrand around $d=4$ and using the explicit expression for the amplitude A_d (C.59), it is straightforward to verify

$$\delta\boldsymbol{\mathcal{L}}^{(1)} = \mathcal{O}(d-4)\,. \tag{C.96}$$

As a result, we can neglect this contribtuon for the three-loop analysis.

Finally, we consider the first two terms in (C.92). Performing the integration over the Feynman parameters and applying the master integral (6.34), we find that

$$\boldsymbol{\mathcal{L}}^{(1)} = \hat{g}_B^6 F_2^{(2)} + \hat{g}_B^6 \frac{3C_F N\beta_0\zeta_3}{2^8\pi^4} + \mathcal{O}(d-4)\,, \tag{C.97}$$

where $\hat{g}_B^6 = R^{2-d/2}g_B$ and we recall that $F_2^{(2)}$ is the bubble-like contribution (6.52).

C.3.0.2 Computing $\mathcal{L}^{(2)}$

The calculation of the correction $\boldsymbol{\mathcal{L}}^{(2)}$ (C.90b) is way more complicated. To begin with, we integrate over the internal momentum k by introducing the usual Feynman parameters for the propagators and we find that

$$\boldsymbol{\mathcal{L}}^{(2)} = 2\mathcal{A}^{(2)}\frac{\mathrm{i}\Gamma(3-d/2)}{(4\pi)^{d/2}}\oint \mathrm{d}^3\tau\varepsilon(\tau)(R^2-\dot{x}_1\cdot\dot{x}_3)\int \mathrm{d}P\mathrm{d}X \frac{p_3^2\,(z\dot{x}_2\cdot p_2 - x\dot{x}_2\cdot p_1)+zp_2^2\;\dot{x}_2\cdot p_3}{\big(xyp_1^2+zyp_2^2+zxp_3^2\big)^{3-d/2}}\,, \tag{C.98}$$

with $\mathrm{d}X$ denoting the usual measure over the unit cube (6.32). The previous expression involves the quantity $p_2\cdot\dot{x}_2$ which, upon integration over the external momenta $\mathrm{d}P$ (C.74), yields a total derivative with respect to the variable τ_2. As a result, the contour integration of this contribution is technically simpler to treat. For this reason, we decompose (C.98) as the sum of two terms

$$\boldsymbol{\mathcal{L}}^{(2)} = \boldsymbol{\mathcal{L}}_1^{(2)} + \boldsymbol{\mathcal{L}}_2^{(2)}\,, \tag{C.99a}$$

$$\boldsymbol{\mathcal{L}}_1^{(2)} = 2\mathcal{A}^{(2)}\frac{\mathrm{i}\Gamma(3-d/2)}{(4\pi)^{d/2}}\oint \mathrm{d}^3\tau\varepsilon(\tau)(R^2-\dot{x}_1\cdot\dot{x}_3)\int \mathrm{d}P\int_0^1 \mathrm{d}X \frac{p_3^2\,(z\dot{x}_2\cdot p_2)}{M^{3-d/2}}\,, \tag{C.99b}$$

$$\boldsymbol{\mathcal{L}}_2^{(2)} = 2\mathcal{A}^{(2)}\frac{\mathrm{i}\Gamma(3-d/2)}{(4\pi)^{d/2}}\oint \mathrm{d}^3\tau\varepsilon(\tau)(R^2-\dot{x}_1\cdot\dot{x}_3)\int \mathrm{d}P\int_0^1 \mathrm{d}X \frac{zp_2^2\,(\dot{x}_2\cdot p_3)-p_3^2x(\dot{x}_2\cdot p_1)}{M^{3-d/2}}\,, \tag{C.99c}$$

where M is given by

$$M = xyp_1^2+zyp_2^2+zxp_3^2\,. \tag{C.100}$$

Computing $\mathcal{L}_1^{(2)}$ As we already observed, the calculation of (C.99b) is technically simpler as the combination $p_2 \cdot \dot{x}_2$ becomes a total derivative upon integration over $\mathrm{d}P$ (C.74). Indeed, by relabelling $\tau_1 \leftrightarrow \tau_2$ and recalling that $\varepsilon(\tau)$ (6.33) is antisymmetric, we find that

$$\begin{aligned}\mathcal{L}_1^{(2)} &= 2\mathcal{A}^{(2)} \frac{\Gamma(3-d/2)}{(4\pi)^{d/2}} \oint \mathrm{d}^3\tau \varepsilon(\tau)(R^2 - \dot{x}_2 \cdot \dot{x}_3) \frac{\mathrm{d}}{\mathrm{d}\tau_1} \int \mathrm{d}P \int_0^1 \mathrm{d}X \frac{x p_3^2}{M^{3-d/2}} \\ &= 4\mathcal{A}^{(2)} \frac{\Gamma(3-d/2)}{(4\pi)^{d/2}} \oint \mathrm{d}^3\tau \left(\delta(\tau_{13}) - \delta(\tau_{12})\right)(R^2 - \dot{x}_2 \cdot \dot{x}_3) \int \mathrm{d}P \int_0^1 \mathrm{d}X \frac{x p_3^2}{M^{3-d/2}} ,\end{aligned} \tag{C.101}$$

where we obtained the second line via integration by parts and (C.61). To perform the Fourier transform $\mathrm{d}P$ (C.74), we apply (C.146) to represent M (C.100) by a two-fold Mellin-Barnes integral

$$\frac{\Gamma(3-d/2)}{M^{3-d/2}} = \int \frac{\mathrm{d}u\mathrm{d}v}{(2\pi\mathrm{i})^2} \frac{\Gamma(3-d/2+u+v)\Gamma(-u)\Gamma(-v)}{x^{3-d/2+u} y^{3-d/2+v} z^{-u-v}} \frac{(p_2^2)^u (p_3^2)^v}{(p_1^2)^{3-d/2+u+v}} , \tag{C.102}$$

where the integration contour separates the increasing and decreasing poles of the Γ-functions. Substituting the previous expression into (C.101) and sequentially performing the integration over the Feynman parameters and the momenta $\mathrm{d}P$ (C.74), we find that

$$\mathcal{L}_1^{(2)} = \mathcal{A}^{(2)} \frac{\Gamma(3d/2-5)\left(\mathcal{M}^{(ii)}(d) - \mathcal{M}^{(i)}(d)\right)}{4^4 \pi^{3d/2} \Gamma(d-2)\Gamma(5-d)} \oint \frac{R^2 - \dot{x}_2 \cdot \dot{x}_3}{\left(x_{23}^2\right)^{3d/2-5}} . \tag{C.103}$$

where the amplitudes

$$\mathcal{M}^{(i)} = \int \frac{\mathrm{d}u\mathrm{d}v}{(2\pi\mathrm{i})^2} \frac{\Gamma(d-4-u-v)\Gamma(d/2-1+u)\Gamma(5-d+v)\Gamma(-v)\Gamma(1+u+v)}{u(d/2-3-u-v)\Gamma(3d/2-5-v)[\Gamma(d/2-2-v)\Gamma(d/2-1-u)]^{-1}} , \tag{C.104a}$$

$$\mathcal{M}^{(ii)} = \int \frac{\mathrm{d}u\mathrm{d}v}{(2\pi\mathrm{i})^2} \frac{\Gamma(-u)\Gamma(4-d+u)\Gamma(1+u+v)\Gamma(d/2-1-u)\Gamma(d/2-2-v)}{\Gamma(3d/2-4-u)(3-d/2+u+v)[\Gamma(d-4-u-v)\Gamma(d/2+v)]^{-1}} . \tag{C.104b}$$

It is interesting to note that $\mathcal{M}^{(i)}$ and $\mathcal{M}^{(ii)}$ exhibit different behaviours when $d \to 4$. On the one hand, (C.104b) becomes singular in four dimensions, due to the product $\Gamma(-u)\Gamma(4-d+u)$. Indeed, in the limit $d \to 4$, the first increasing and the first decreasing pole of the gamma functions cannot be separated. This gives rise to a *pinching* effect, which manifests as $1/(d-4)$ pole. On the other hand, (C.104a) is perfectly finite in four dimensions and for future reference, we provide its expansion around $d = 4$

$$\mathcal{M}^{(i)}(d) = \int_{\delta-\mathrm{i}\infty}^{\delta+\mathrm{i}\infty} \frac{\mathrm{d}u\mathrm{d}v}{(2\pi\mathrm{i})^2} \frac{\pi^3 \csc(\pi u)\csc(\pi v)\csc(\pi(u+v))}{v(u+v+1)} + \ldots = 2\zeta_3 + \ldots , \tag{C.105}$$

where $\delta \in (-1, 0)$ represents the real part of the variables u and v. As we will shortly see, similar quantities will also arise from the integral $\mathcal{L}_2^{(2)}$ (C.99c).

Computing $\mathcal{L}_2^{(2)}$ The calculation of (C.99c) goes along the same lines. We replace $M^{3-d/2}$ (C.100) with its Mellin-Barnes representation (C.102) and we perform the integration over the external momenta p_i (C.74) in terms of the generalisedd propagators (C.14). The final result

can be written as an integration contour analogous to (C.91) weighted by functions in Mellin space that depends on the Feynman parameters α, β and γ, *i.e.*

$$\boldsymbol{\mathcal{L}}_2^{(2)} = \frac{\mathcal{A}^{(2)}\Gamma(3d/2-4)R^{12-3d}}{\Gamma(d-2)2^9\pi^{3d/2}2^{3d/2-5}}\int \mathrm{d}\mathcal{M}\oint \mathrm{d}^3\tau \frac{\varepsilon(\tau)(\cos\tau_{13}-1)\left(\alpha(1-\alpha)\sin\tau_{12}+\alpha\gamma\sin\tau_{23}\right)}{Q^{3d/2-4}} \,. \tag{C.106}$$

In the previous expression, Q is defined in (6.31), while $\mathrm{d}\mathcal{M}$ is given by

$$\mathrm{d}\mathcal{M} = \frac{\mathrm{d}u\,\mathrm{d}v}{(2\pi\mathrm{i})^2}\mathrm{d}F\;\alpha^{d-5-u-v}\beta^{d/2-2+u}\gamma^{d/2-2+v}\Big(\tilde{f}(u,v)\gamma+\tilde{f}(v,u)\beta\Big)\,, \tag{C.107}$$

$$\tilde{f}(u,v) = -\frac{\Gamma(d/2-1-v)\Gamma(d/2-2-u)\Gamma(1+u+v)}{u(3-d/2+u+v)}\,, \tag{C.108}$$

where $\mathrm{d}F$ denotes the usual measure over the unit cube (6.32). Importantly, $\mathrm{d}\mathcal{M}$ is symmetric under the simultaneous exchange of $\beta \leftrightarrow \gamma$ and $u \leftrightarrow v$.

As we anticipated, the structure of (C.106) is analogous to (C.91) and we can integrate over the Wilson loop contour by the identity (C.60). We find that

$$\begin{aligned}\boldsymbol{\mathcal{L}}_2^{(2)} =& -\mathcal{A}^{(2)}\frac{\Gamma(3d/2-4)R^{12-3d}}{\Gamma(d-2)2^9\pi^{3d/2}2^{3d/2-5}}\int \mathrm{d}\mathcal{M}\left(\frac{2}{3d/2-5}\oint \mathrm{d}^2\tau\frac{(1-\cos\tau_{12})^{6-3d/2}}{[\gamma(1-\gamma)]^{3d/2-5}}\right)\\ &-\mathcal{A}^{(2)}\frac{\Gamma(3d/2-4)R^{12-3d}}{\Gamma(d-2)2^9\pi^{3d/2}2^{3d/2-5}}\frac{3(2-d/2)}{3d/2-5}\int \mathrm{d}\mathcal{M}\oint \mathrm{d}^3\tau\varepsilon(\tau)\frac{\sin\tau_{13}}{Q^{3d/2-5}} - \delta\boldsymbol{\mathcal{L}}_2^{(2)}\,,\end{aligned} \tag{C.109}$$

where

$$\delta\boldsymbol{\mathcal{L}}_2^{(2)} = \mathcal{A}^{(2)}\frac{\Gamma(3d/2-4)R^{12-3d}}{\Gamma(d-2)2^9\pi^{3d/2}2^{3d/2-5}}\int \mathrm{d}\mathcal{M}\mathcal{T}^{(2)}(\alpha,\beta,\gamma)\,, \tag{C.110a}$$

$$\mathcal{T}^{(2)}(\alpha,\beta,\gamma) = \oint \mathrm{d}^3\tau\varepsilon(\tau)\frac{\beta\gamma\sin\tau_{13}(1-\cos\tau_{23})+\alpha\gamma\sin\tau_{23}(1-\cos\tau_{13})}{Q^{3d/2-4}}\,. \tag{C.110b}$$

The first term in the second line of (C.109) is proportional to $(d-4)$: it vanishes in the limit $d\to 4$ since the path-ordered integral is regular and consequently, it can be neglected for the three-loop analysis. Actually, as we will shortly see, also $\delta\boldsymbol{\mathcal{L}}_2^{(2)}$ is of order $(d-4)$ and consequently, we can write

$$\begin{aligned}\boldsymbol{\mathcal{L}}_2^{(2)} =& -\mathcal{A}^{(2)}\frac{\Gamma(3d/2-4)R^{12-3d}}{\Gamma(d-2)2^9\pi^{3d/2}2^{3d/2-5}}\int \mathrm{d}\mathcal{M}\left(\frac{2}{3d/2-5}\oint \mathrm{d}^2\tau\frac{(1-\cos\tau_{12})^{6-3d/2}}{[\gamma(1-\gamma)]^{3d/2-5}}\right)+\mathcal{O}(d-4)\\ =& -\mathcal{A}^{(2)}\frac{\Gamma(3d/2-5)\left(\mathcal{M}^{(ii)}(d)+\mathcal{M}^{(i)}(d)\right)}{4^4\pi^{3d/2}\Gamma(d-2)\Gamma(5-d)}\oint \mathrm{d}^2\tau\frac{R^2-\dot{x}_2\cdot\dot{x}_3}{(x_{23}^2)^{3d/2-5}}+\mathcal{O}(d-4)\,,\end{aligned} \tag{C.111}$$

where to obtain the second line we performed the integration by employing the explicit form of the measure $\mathrm{d}\mathcal{M}$ (C.107), and we recall that $\mathcal{M}^{(i)}(d)$ and $\mathcal{M}^{(ii)}(d)$ are given by (C.104).

Finally, combining (C.111) with (C.103), we find that

$$\begin{aligned}\boldsymbol{\mathcal{L}}^{(2)} &\overset{(C.99a)}{=} \boldsymbol{\mathcal{L}}_1^{(2)}+\boldsymbol{\mathcal{L}}_2^{(2)}\\ &\overset{(C.103,C.111)}{=} -\frac{\mathcal{A}^{(2)}\Gamma(3d/2-5)\mathcal{M}^{(i)}(d)}{2^7\pi^{3d/2}\Gamma(d-2)\Gamma(5-d)}\oint \mathrm{d}^2\tau\frac{R^2-\dot{x}_2\cdot\dot{x}_3}{(x_{23}^2)^{3d/2-5}}+\mathcal{O}(d-4)\\ &= \beta_0\frac{C_F N\hat{g}_B^6\zeta_3}{2^7\pi^4}+\mathcal{O}(d-4)\,,\end{aligned} \tag{C.112}$$

where we obtained the last equality by expanding the amplitude $\mathcal{M}^{(i)}(d)$ around $d=4$ through (C.105) and recalling the definition of $\mathcal{A}^{(2)}$ (C.79). Remarkably, when combining together (C.103) and (C.111), the divergent amplitudes $\mathcal{M}^{(ii)}$ (C.104b) cancel each other out, leaving a finite result.

Evanescent integrals We conclude the analysis by explicitly showing that $\delta\boldsymbol{\mathcal{L}}_2^{(2)}$ (C.110) is of order $\mathcal{O}(d-4)$. We begin by observing that (C.110) can be written as

$$\begin{aligned}\delta\boldsymbol{\mathcal{L}}_2^{(2)} &\propto \int \mathrm{d}\mathcal{M}\,\mathcal{T}^{(2)}(\alpha,\beta,\gamma)\\ &\propto \int_0^1 \mathrm{d}F \int \frac{\mathrm{d}u\mathrm{d}v}{(2\pi\mathrm{i})^2}\alpha^{d-5-u-v}\beta^{d/2-2+u}\gamma^{d/2-2+v}\left(\gamma\tilde{f}(u,v)+\beta\tilde{f}(v,u)\right)\mathcal{T}^{(2)}(\alpha,\beta,\gamma)\ ,\end{aligned} \tag{C.113}$$

where the proportionality constant is regular in the limit $d\to 4$, and we obtained the second line by replacing the measure $\mathrm{d}\mathcal{M}$ with its explicit form (C.107).

We begin with showing that

$$\int_0^1 \mathrm{d}F \int \frac{\mathrm{d}u\mathrm{d}v}{(2\pi\mathrm{i})^2}\alpha^{d-5-u-v}\beta^{d/2-2+u}\gamma^{d/2-1+v}\tilde{f}(u,v)\mathcal{T}^{(2)}(\alpha,\beta,\gamma) \tag{C.114}$$

vanishes for arbitrary d. To see this, we express $\mathcal{T}^{(2)}(\alpha,\beta,\gamma)$ by its integral representation (C.93) and exploit the antisymmetry of the ε-symbol (6.33) to rewrite (C.114) as follows

$$\int \frac{\mathrm{d}F\mathrm{d}u\mathrm{d}v}{(2\pi\mathrm{i})^2}\left(\frac{\gamma^{d/2+v}\tilde{f}(u,v)}{\alpha^{5-d+u+v}\beta^{1-d/2-u}}-\frac{\gamma^{d/2+v}\tilde{f}(u,v)}{\beta^{4-d+u+v}\alpha^{2-d/2-u}}\right)\oint \mathrm{d}^3\tau\varepsilon(\tau)\frac{\sin\tau_{13}\sin^2\frac{\tau_{23}}{2}}{Q^{3d/2-4}}\ . \tag{C.115}$$

Changing variable according to $u'=d/2-3-u-v$ in the second term, we observe that the function $\tilde{f}(u,v)$ (C.108) is left unchanged and the integral vanishes identically. Thus, (C.113) reduces to

$$\begin{aligned}\delta\boldsymbol{\mathcal{L}}_2^{(2)} &\propto \int_0^1 \mathrm{d}F \int \frac{\mathrm{d}u\mathrm{d}v}{(2\pi\mathrm{i})^2}\alpha^{d-5-u-v}\beta^{d/2-1+u}\gamma^{d/2-2+v}\tilde{f}(v,u)\mathcal{T}^{(2)}(\alpha,\beta,\gamma)\\ &\propto 2\int \frac{\mathrm{d}F\mathrm{d}u\mathrm{d}v}{(2\pi\mathrm{i})^2}\left(\frac{\gamma^{d/2-1+v}\tilde{f}(v,u)}{\alpha^{5-d+u+v}\beta^{-d/2-u}}-\frac{\gamma^{d/2-1+v}\tilde{f}(v,u)}{\beta^{4-d+u+v}\alpha^{1-d/2-u}}\right)\oint \mathrm{d}^3\tau\varepsilon(\tau)\frac{\sin\tau_{13}\sin^2\frac{\tau_{23}}{2}}{Q^{3d/2-4}}\\ &\propto 2\left(\boldsymbol{\mathcal{E}}_1^{(2)}(d)-\boldsymbol{\mathcal{E}}_2^{(2)}(d)\right)\ ,\end{aligned} \tag{C.116}$$

where we used (C.93) and introduced the functions

$$\boldsymbol{\mathcal{E}}_1^{(2)}(d)=\int \frac{\mathrm{d}F\mathrm{d}u\mathrm{d}v}{(2\pi\mathrm{i})^2}\frac{\gamma^{d/2-1+v}\tilde{f}(v,u)}{\alpha^{5-d+u+v}\beta^{-d/2-u}}\oint \mathrm{d}^3\tau\varepsilon(\tau)\frac{\sin\tau_{13}\,(1-\cos\tau_{23})}{Q^{3d/2-4}}\ , \tag{C.117}$$

$$\boldsymbol{\mathcal{E}}_2^{(2)}(d)=\int \frac{\mathrm{d}F\mathrm{d}u\mathrm{d}v}{(2\pi\mathrm{i})^2}\frac{\gamma^{d/2-1+v}\tilde{f}(v,u)}{\beta^{4-d+u+v}\alpha^{1-d/2-u}}\oint \mathrm{d}^3\tau\varepsilon(\tau)\frac{\sin\tau_{13}\,(1-\cos\tau_{23})}{Q^{3d/2-4}}\ . \tag{C.118}$$

Let us consider $\boldsymbol{\mathcal{E}}_1^{(2)}(d)$. Replacing $Q^{3d/2-4}$ with its Mellin-Barnes representation (C.94), we can integrate over the contour by (C.139). As a result, (C.117) can be expressed as a four-fold

Mellin-Barnes integral

$$\boldsymbol{\mathcal{E}}_1^{(2)}(d) = \int \frac{\mathrm{d}u\mathrm{d}v\mathrm{d}s\mathrm{d}t}{(2\pi\mathrm{i})^4} \frac{\Gamma(3d/2-4-s-t)\Gamma(-s)\Gamma(-t)\Gamma(-d/2-u-v-s)\Gamma(5-d-t+u)}{2^{3d/2-5}\Gamma(5-d)\Gamma(3d/2-4)} \times \Gamma(d/2+v+t+s)\mathcal{J}(3d/2-4-s-t,s+1,t) \ , \tag{C.119}$$

where $\mathcal{J}(x,y,z)$ is given by (C.139). Expanding the previous expression around $d=4$, we can integrate over s and t by a repeated application of Barnes's first lemma and we find

$$\boldsymbol{\mathcal{E}}_1^{(2)}(d) = 8\pi^2 \int_{\delta-\mathrm{i}\infty}^{\delta+\mathrm{i}\infty} \frac{\mathrm{d}u\mathrm{d}v}{(2\pi\mathrm{i})^2} \frac{\Gamma(1-u)\Gamma(u+2)\Gamma(-v)\Gamma(v)\Gamma(-u-v)\Gamma(u+v+1)}{v\,(1+u+v)} + \mathcal{O}(d-4) \ , \tag{C.120}$$

where $\delta \in (-1,0)$ is the real part of the variables u and v. The integration over u and v is not necessary as $\boldsymbol{\mathcal{E}}_2^{(2)}(d)$ (C.118) reduces to the same integral in the limit $d \to 4$, *i.e.*

$$\boldsymbol{\mathcal{E}}_2^{(2)}(d) \simeq \boldsymbol{\mathcal{E}}_1^{(2)}(d)\Big|_{d=4} + \mathcal{O}(d-4) \ . \tag{C.121}$$

Substituting the previous expression into (C.116), we find that (C.113) vanishes in four-dimensions.

C.3.0.3 Summary of the results

Using the relations obtained in the previous subsections, we can derive the final results for the lifesaver diagrams (C.68). Although the calculations required intricate manipulations, we obtain a remarkably simple form

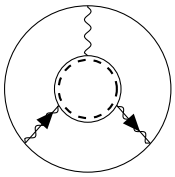

$$\overset{(C.89)}{=} \boldsymbol{\mathcal{L}}^{(1)} + \boldsymbol{\mathcal{L}}^{(2)} \tag{C.122}$$

$$\overset{(C.97,C.112)}{=} \hat{g}_B^6 F_2^{(2)} + \hat{g}_B^6 \frac{5C_F N\beta_0\zeta_3}{2^8\pi^4} + \mathcal{O}(d-4) \ ,$$

where we recall that $F_2^{(2)}$ is the bubble-like contribution (6.52).

C.4 Diagrams with four emissions

Let us now consider the following class of three-loop diagrams

$$\mathcal{W} = \quad , \tag{C.123}$$

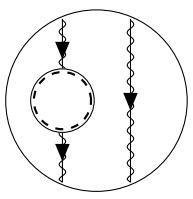

where we recall that the double dashed/continuous internal bubble denotes the one-loop correction to the propagators of the adjoint scalar and gauge field in the difference approach (C.28).

Following the approach outlined in Section C.2, we can apply the decomposition (C.50) and organise the correction (C.123) as follows

$$\boldsymbol{\mathcal{W}} = \boldsymbol{\mathcal{W}}_1 + \boldsymbol{\mathcal{W}}_2 \ , \tag{C.124a}$$

$\boldsymbol{\mathcal{W}}_1 =$ 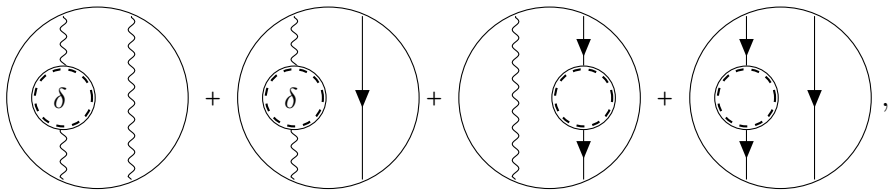 , (C.124b)

$\boldsymbol{\mathcal{W}}_2 =$ 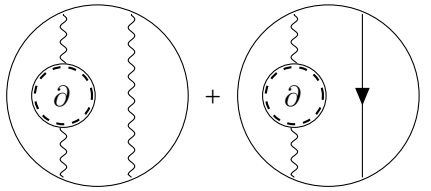 . (C.124c)

Computing $\mathcal{W}_1$

Expanding the Wilson loop operator at order g_B^4 and dressing the Wick contractions with the one-loop correction to the scalar propagator $\Delta^{(1)}(x)$ (C.30) and with the tensor $\delta_{\mu\nu}\Delta^{(1)}(x)$, we find that

$$\begin{aligned}\boldsymbol{\mathcal{W}}_1 = \frac{g_B^4}{N}\int_{\tau_1>\tau_2>\tau_3>\tau_4} \mathrm{d}^4\tau \; & C^{aabb}\left(\widehat{\Delta}(x_{12})\widehat{\Delta}^{(1)}(x_{34}) + \widehat{\Delta}(x_{34})\widehat{\Delta}^{(1)}(x_{12})\right) + \\ & C^{aabb}\left(\widehat{\Delta}(x_{14})\widehat{\Delta}^{(1)}(x_{23}) + \widehat{\Delta}(x_{23})\widehat{\Delta}^{(1)}(x_{14})\right) + \\ & C^{abab}\left(\widehat{\Delta}(x_{13})\widehat{\Delta}^{(1)}(x_{14}) + \widehat{\Delta}(x_{34})\widehat{\Delta}^{(1)}(x_{12})\right) \ ,\end{aligned} \tag{C.125}$$

where we recall that the tensor C^{abcd} is given by (6.20), while $\widehat{\Delta}(x)$ and $\widehat{\Delta}^{(1)}(x)$ are the effective propagators defined in (6.15) and (6.40), respectively.

To further simplify (C.125), we use the non-Abelian exponentiation rules for the Wilson loop and we obtain

$$\boldsymbol{\mathcal{W}}_1 = \mathcal{W}_2\mathcal{W}_4' \ + \frac{g_B^4}{2N}\,\mathrm{tr}\left([T^b,T^a]\right)^2\int_{\mathcal{D}}\mathrm{d}^4\tau\left(\widehat{\Delta}(x_{13})\widehat{\Delta}^{(1)}(x_{24}) + \widehat{\Delta}(x_{24})\widehat{\Delta}^{(1)}(x_{13})\right) \ , \tag{C.126}$$

where $\mathcal{D}$ denotes the ordered region $\tau_1 > \tau_2 > \tau_3 > \tau_4$, the functions $\mathcal{W}_2$ and $\mathcal{W}_4'$ are, respectively, defined in (6.16) and (6.41), while the second term in (C.126) defines the maximally non-Abelian part of the diagram.

Going through the calculation of (C.126), we encounter the integral

$$\int_{\mathcal{D}} \frac{\mathrm{d}^4\tau}{\left(4\sin^2\frac{\tau_{13}}{2}\right)^{d/2-2}\left(4\sin^2\frac{\tau_{24}}{2}\right)^{d-4}} + \frac{\mathrm{d}^4\tau}{\left(4\sin^2\frac{\tau_{24}}{2}\right)^{d/2-2}\left(4\sin^2\frac{\tau_{12}}{2}\right)^{d-4}} \ , \tag{C.127}$$

which arises when the effective propagators $\widehat{\Delta}(x)$ (6.15) and $\widehat{\Delta}^{(1)}(x)$ (6.40) are replaced with their explicit expressions and by employing the coordinate parametrization (5.8). This integral can be calculated following the approach outlined in Section 6.1.2.

In particular, replacing the trigonometric functions in (C.127) by their Fourier expansions (6.23), we find that the nested integration becomes elementary and the correction $\boldsymbol{\mathcal{W}}_1$ (C.126)

assumes a remarkably simple form

$$\boldsymbol{\mathcal{W}}_1 = \hat{g}_B^6 C_F \frac{2N^2-3}{6N} P_2(d) B_1(d) B_2(d) - \frac{\hat{g}_B^6 \beta_0 C_F N 3\zeta_3}{2^8\pi^4} + \mathcal{O}((d-4)^2) \,, \tag{C.128}$$

where the functions $B_n(x)$ and $P_2(x)$ are defined in (6.16) and (6.41), respectively.

Crucially, the ζ_3-term in (C.128) mirrors the contribution generated by the maximally non-Abelian part of the two-loop ladder-like diagram (6.24). In that case, the result was proportional to the evanescent factor $\epsilon = 2 - d/2$ originating from the contour integration. The same factor appears in (C.128), but it cancels against the ultraviolet pole of the one-loop correction $\Delta^{(1)}(x)$ (C.30), leaving a finite contribution.

Computing $\mathcal{W}_2$

Finally, we turn our attention to the correction $\boldsymbol{\mathcal{W}}_2$ (C.124c).

We begin with considering in detail the diagram that only involves the propagation of gauge fields. We expand the Wilson loop operator at order g_B^4, and we dress the relevant Wick contractions by the tensor $\Delta^{(1),\mathrm{g}}_{\mu\nu}(x) \equiv \partial_{1,\mu}\partial_{1,\nu}\Delta^{(1),g}(x)$ (C.31). We have

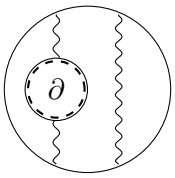

$$\begin{aligned}
&= g_B^4 \oint_{\mathcal{D}} \mathrm{d}^4\tau \; C^{aabb} \left(\dot{x}_1^\mu \dot{x}_2^\nu \Delta^{(1),\mathrm{g}}_{\mu\nu}(x_{12}) \Delta(x_{34}) (\dot{x}_3 \cdot \dot{x}_4) + \begin{pmatrix} 1 \leftrightarrow 3 \\ 2 \leftrightarrow 4 \end{pmatrix} \right) + \\
&\qquad g_B^4 \oint_{\mathcal{D}} \mathrm{d}^4\tau \; C^{abab} \left(\dot{x}_1^\mu \dot{x}_3^\nu \Delta^{(1),\mathrm{g}}_{\mu\nu}(x_{13}) \Delta(x_{24}) (\dot{x}_2 \cdot \dot{x}_4) + \begin{pmatrix} 1 \leftrightarrow 2 \\ 3 \leftrightarrow 4 \end{pmatrix} \right) + \\
&\qquad g_B^4 \oint_{\mathcal{D}} \mathrm{d}^4\tau \; C^{aabb} \left(\dot{x}_1^\mu \dot{x}_4^\nu \Delta^{(1),\mathrm{g}}_{\mu\nu}(x_{14}) \Delta(x_{23}) (\dot{x}_3 \cdot \dot{x}_2) + \begin{pmatrix} 1 \leftrightarrow 2 \\ 4 \leftrightarrow 3 \end{pmatrix} \right) \,.
\end{aligned} \tag{C.129}$$

The previous expression can be further simplified by employing again the non-Abelian exponentiation properties of the Wilson loop. We find that [7]

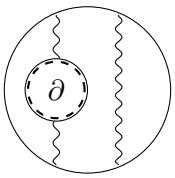

$$\begin{aligned}
&= \frac{g_B^4}{2N} \operatorname{tr}\left([T^a, T^b] \right)^2 \int_{\mathcal{D}} \mathrm{d}^4\tau \left(\dot{x}_1^\mu \dot{x}_3^\nu \Delta^{(1),\mathrm{g}}_{\mu\nu}(x_{13}) \Delta(x_{24}) (\dot{x}_2 \cdot \dot{x}_4) + \begin{pmatrix} 1 \leftrightarrow 2 \\ 3 \leftrightarrow 4 \end{pmatrix} \right) \\
&= g_B^4 \frac{C_F N}{2} \oint \mathrm{d}^2\tau \, (\dot{x}_1 \cdot \dot{x}_2) \, \Delta^{(1),\mathrm{g}}(x_{12}) \Delta(x_{12}) \,,
\end{aligned} \tag{C.130}$$

where we obtained the second equality by integrating by parts twice.

Repeating the same analysis for the second diagram in (C.124c), we find that

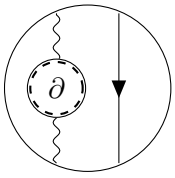

$$= g_B^4 \frac{C_F N}{2} \oint \mathrm{d}^2\tau \left(-R^2 \right) \Delta^{(1),g}(x_{12}) \Delta(x_{12}) \,. \tag{C.131}$$

[7] To obtain (C.130), we neglected terms which yield total derivatives integrated over a closed path.

Combining together (C.130) and (C.131), we find that

$$\mathcal{W}_2 = -g_B^4 \frac{C_F N}{2} \oint \mathrm{d}^2\tau \left(R^2 - \dot{x}_1 \cdot \dot{x}_2\right) \Delta^{(1),\mathrm{g}}(x_{12}) \Delta(x_{12}) = \hat{g}_B^6 F_3^{(2)} \ , \tag{C.132}$$

where $\hat{g}_B = R^{2-d/2} g_B$ and we recall that $F_3^{(2)}$ is the bubble-like contribution (6.52). The last equality can be proved by replacing $\Delta(x)$ and $\Delta^{(1),\mathrm{g}}(x)$ with their explicit forms. These are defined in (6.13) and (C.31), respectively.

Employing (C.132) and (C.128), we finally find that

$$\mathcal{W} = \mathcal{W}_1 + \mathcal{W}_2 = \hat{g}_B^6 F_3^{(2)} + \hat{g}_B^6 C_F \frac{2N^2-3}{6N} P_2(d) B_1(d) B_2(d) - \frac{\hat{g}_B^6 \beta_0 C_F N 3\zeta_3}{2^8 \pi^4} + \mathcal{O}((d-4)^2) \ . \tag{C.133}$$

C.4.1 Trigonometric integrals

As observed in the previous subsections, the perturbative corrections to the expectation value of the supersymmetric Wilson loop involve various trigonometric integrals. The aim of this section is to provide a detailed derivation of those integrals. Our first goal is to review some identities, starting from

$$\begin{aligned} \mathcal{M}(a,b,c) &= \int_0^{2\pi} \mathrm{d}^3\tau \left(\sin^2\frac{\tau_{12}}{2}\right)^a \left(\sin^2\frac{\tau_{13}}{2}\right)^b \left(\sin^2\frac{\tau_{23}}{2}\right)^c \\ &= 8\pi^{3/2} \frac{\Gamma(a+1/2)\Gamma(b+1/2)\Gamma(c+1/2)\Gamma(1+a+b+c)}{\Gamma(1+a+c)\Gamma(1+b+c)\Gamma(1+a+b)} \ , \end{aligned} \tag{C.134}$$

which was originally derived in [147] and can be used to evaluate

$$\begin{aligned} \mathcal{I}[\alpha,\beta,\gamma] = \int_{\tau_1>\tau_2>\tau_3} \mathrm{d}^3\tau \Bigg[& \left(\sin^2\frac{\tau_{12}}{2}\right)^\alpha \left(\sin^2\frac{\tau_{13}}{2}\right)^\beta \left(\sin^2\frac{\tau_{23}}{2}\right)^\gamma \cos\frac{\tau_{23}}{2} \\ & - \left(\sin^2\frac{\tau_{23}}{2}\right)^\alpha \left(\sin^2\frac{\tau_{12}}{2}\right)^\beta \left(\sin^2\frac{\tau_{13}}{2}\right)^\gamma \cos\frac{\tau_{13}}{2} \\ & \left(\sin^2\frac{\tau_{13}}{2}\right)^\alpha \left(\sin^2\frac{\tau_{23}}{2}\right)^\beta \left(\sin^2\frac{\tau_{12}}{2}\right)^\gamma \cos\frac{\tau_{12}}{2} \Bigg] \ , \end{aligned} \tag{C.135}$$

as explained in Appendix G of [170]. Indeed, we find that (C.135) can be reduced to a linear combination of functions (C.134) and the net result takes the following form

$$\mathcal{I}[\alpha,\beta,\gamma] = 4\pi^{3/2} \frac{\Gamma(1+\alpha+\beta+\gamma)\Gamma(1+\alpha)\Gamma(1+\beta)\Gamma\left(1/2+\gamma\right)}{\Gamma\left(3/2+\alpha+\gamma\right)\Gamma\left(3/2+\beta+\gamma\right)\Gamma(1+\alpha+\beta)} \ . \tag{C.136}$$

The three-loop corrections to the Wilson loop expectation value involve the following class of *path-ordered* integrals

$$\mathcal{J}(\alpha,\beta,\gamma) = \oint \mathrm{d}^3\tau \varepsilon(\tau) \sin\tau_{13} \left(\sin^2\frac{\tau_{12}}{2}\right)^\alpha \left(\sin^2\frac{\tau_{13}}{2}\right)^\gamma \left(\sin^2\frac{\tau_{23}}{2}\right)^\beta \ , \tag{C.137}$$

where $\varepsilon(\tau) \equiv \varepsilon(\tau_1,\tau_2,\tau_3)$ is the antisymmetric symbol (6.33). Replacing $\varepsilon(\tau)$ with its explicit form (6.33) and relabelling the integration variables, we find that

$$\mathcal{J}(\alpha,\beta,\gamma) = -2\mathcal{I}(\beta,\alpha,\gamma+1/2) - 2\mathcal{I}(\alpha,\beta,\gamma+1/2) = -4\mathcal{I}(\alpha,\beta,\gamma+1/2) \ , \tag{C.138}$$

where we obtained the last line by observing that $\mathcal{I}(\beta,\alpha,\gamma) = \mathcal{I}(\alpha,\beta,\gamma)$. Using (C.137), we finally find that

$$\mathcal{J}(\alpha,\beta,\gamma) = -16\pi^{3/2}\frac{\Gamma(3/2+\alpha+\beta+\gamma)\Gamma(1+\alpha)\Gamma(1+\beta)\Gamma(1+\gamma)}{\Gamma(2+\alpha+\gamma)\Gamma(2+\beta+\gamma)\Gamma(1+\alpha+\beta)} \ . \tag{C.139}$$

Finally, we will extensively use the identity

$$\frac{1}{(A+B+C)^{\sigma}} = \frac{1}{\Gamma(\sigma)}\int_{-\mathrm{i}\infty}^{+\mathrm{i}\infty}\frac{\mathrm{d}u\,\mathrm{d}v}{(2\pi\mathrm{i})^2}\,\frac{B^u C^v}{A^{\sigma+u+v}}\Gamma(\sigma+u+v)\Gamma(-u)\Gamma(-v) \ , \tag{C.140}$$

where the integration contour runs parallel to imaginary axis in such a way that the increasing and decreasing poles of the gamma functions are separated.

C.4.1.1 Path-ordered integrals

Let us consider the path-ordered integral

$$\begin{aligned}\boldsymbol{\mathcal{Q}}(d) &= \int_0^1 \mathrm{d}\alpha\mathrm{d}\beta\mathrm{d}\gamma\delta(1-\alpha-\beta-\gamma)\,(\alpha\beta\gamma)^{d/2-2}\ \oint \mathrm{d}^3\tau\ \varepsilon(\tau)\frac{\sin\tau_{13}}{Q^{d-3}} \\ &= -8\int_0^1 \mathrm{d}\alpha\mathrm{d}\beta\mathrm{d}\gamma\delta(1-\alpha-\beta-\gamma)\,(\alpha\beta\gamma)^{d/2-2}\ \int_{\tau_1>\tau_2>\tau_3}\mathrm{d}^3\tau\ \frac{\sin\frac{\tau_{13}}{2}\ \sin\frac{\tau_{12}}{2}\ \sin\frac{\tau_{23}}{2}}{Q^{d-3}} \ ,\end{aligned} \tag{C.141}$$

where Q is defined in (6.31) and we obtained the second line by replacing the ε-symbol with its explicit form (6.33).

To proceed with the calculation, we use (C.140) to express Q^{d-3} (6.31) as a two-fold Mellin-Barnes integral

$$\frac{1}{Q^{\sigma}} = \frac{2^{-\sigma}}{\Gamma(\sigma)}\int_{-\mathrm{i}\infty}^{+\mathrm{i}\infty}\frac{\mathrm{d}u\,\mathrm{d}v}{(2\pi\mathrm{i})^2}\ \frac{\Gamma(\sigma+u+v)\Gamma(-u)\Gamma(-v)}{\left(\beta\alpha\sin^2\frac{\tau_{12}}{2}\right)^{\sigma+u+v}\left(\beta\gamma\sin^2\frac{\tau_{23}}{2}\right)^{-u}\left(\gamma\alpha\sin^2\frac{\tau_{31}}{2}\right)^{-v}} \ , \tag{C.142}$$

where the integration path runs parallel to the imaginary axes and separates the increasing and the decreasing poles of the gamma functions.

Substituting (C.142) into (C.141) and performing the integration over α,β and γ, we arrive at the following result

$$\boldsymbol{\mathcal{Q}}(d) = \int\frac{\mathrm{d}u\,\mathrm{d}v}{(2\pi\mathrm{i})^2}\ \frac{\Gamma(d-3+u+v)\Gamma(-u)\Gamma(-v)\Gamma(2-d/2-u)}{\left(\Gamma(2-d/2-v)\Gamma(d/2-1+u+v)\right)^{-1}}\mathcal{Q}(u,v,d) \ , \tag{C.143}$$

where we introduced

$$\begin{aligned}\mathcal{Q}(u,v,d) &= -\frac{2^{6-d}}{\Gamma(3-d/2)\Gamma(d-3)}\ \int_{\tau_1>\tau_2>\tau_3}\mathrm{d}^3\tau\ \frac{\left(\sin^2\frac{\tau_{23}}{2}\right)^{u+1/2}\left(\sin^2\frac{\tau_{31}}{2}\right)^{v+1/2}}{\left(\sin^2\frac{\tau_{12}}{2}\right)^{d-3+u+v-1/2}} \\ &= -\frac{2^{6-d}}{\Gamma(3-d/2)\Gamma(d-3)3!}\oint\ \mathrm{d}^3\tau\ \frac{\left(\sin^2\frac{\tau_{23}}{2}\right)^{u+1/2}\left(\sin^2\frac{\tau_{31}}{2}\right)^{v+1/2}}{\left(\sin^2\frac{\tau_{12}}{2}\right)^{d-3+u+v-1/2}} \\ &= -\frac{2^{9-d}\pi^{3/2}\Gamma(11/2-d)}{\Gamma(3-d/2)\Gamma(d-3)3!}\ \frac{\Gamma(u+1)\Gamma(v+1)\Gamma(4-d-u-v)}{\Gamma(2+u+v)\Gamma(5-d-u)\Gamma(5-d-v)} \ .\end{aligned} \tag{C.144}$$

In the previous expression, we obtained the second line by replacing the nested integration with an integral over the complete circle [8] and we integrated over τ_i by using (C.134).

Substituting (C.144) into (C.143), we find that

$$\mathcal{Q}(d) = -\frac{2^{9-d}\pi^{3/2}\Gamma(11/2-d)}{\Gamma(3-d/2)\Gamma(d-3)3!}\,\mathcal{M}(d)\ , \tag{C.145}$$

where the Mellin amplitude $\mathcal{M}(d)$ is a meromorphic function of the dimension d and is given by

$$\begin{aligned}\mathcal{M}(d) = \int \frac{\mathrm{d}u\,\mathrm{d}v}{(2\pi\mathrm{i})^2}\frac{\Gamma(v+1)\Gamma(-v)\Gamma(2-d/2-v)\Gamma(-u)\Gamma(u+1)\Gamma(2-d/2-u)}{\Gamma(5-d-v)}\times\\ \times\frac{\Gamma(d-3+u+v)\Gamma(4-d-u-v)\Gamma(d/2-1+u+v)}{\Gamma(2+u+v)\Gamma(5-d-u)}\ .\end{aligned} \tag{C.146}$$

Since $\mathcal{Q}(d)$ appears in the calculation of the Wilson loop with an evanescent coefficient (see (6.29)), we only have to determine its behaviour in four dimensions. To do so, we expand the amplitude $\mathcal{M}(d)$ (C.146) around $d=4$ and we obtain

$$\begin{aligned}\mathcal{M}(d)\Big|_{d=4} &= \int_{\delta-\mathrm{i}\infty}^{\delta+\mathrm{i}\infty}\frac{\mathrm{d}v\,\mathrm{d}u}{(2\pi\mathrm{i})^2}\frac{-\pi^3\csc(\pi u)\csc(\pi v)\csc(\pi(u+v))}{(1+u+v)uv}\\ &= 6\zeta_3\ ,\end{aligned} \tag{C.147}$$

where $\delta = \mathfrak{Re}(u) = \mathfrak{Re}(v) \in (-1,0)$. Combining everything together, we finally arrive at

$$\mathcal{Q}(d) = -16\pi^2\zeta_3 + \mathcal{O}(d-4)\ . \tag{C.148}$$

[8] By properly shifting the integration variables u and v, it is straightforward to show that the integrand is fully symmetric under the exchange of the variables τ_i. This means that the integration over the ordered region $\tau_1 > \tau_2 > \tau_3$ is equivalent to one-sixth of the integral over the complete circle.

Bibliography

[1] K. Fujikawa, *Path Integral Measure for Gauge Invariant Fermion Theories*, *Phys. Rev. Lett.* **42** (1979) 1195.

[2] K. Fujikawa, *Path Integral for Gauge Theories with Fermions*, *Phys. Rev. D* **21** (1980) 2848.

[3] G. 't Hooft, *Naturalness, chiral symmetry, and spontaneous chiral symmetry breaking*, *NATO Sci. Ser. B* **59** (1980) 135.

[4] H.A. Kramers and G.H. Wannier, *Statistics of the two-dimensional ferromagnet. Part 1.*, *Phys. Rev.* **60** (1941) 252.

[5] J.M. Maldacena, *The Large N limit of superconformal field theories and supergravity*, *Int.J.Theor.Phys.* **38** (1999) 1113 [hep-th/9711200].

[6] O. Aharony, S.S. Gubser, J.M. Maldacena, H. Ooguri and Y. Oz, *Large N field theories, string theory and gravity*, *Phys.Rept.* **323** (2000) 183 [hep-th/9905111].

[7] E. Witten, *Anti-de Sitter Space and Holography*, *Adv. Theor. Math. Phys.* **2** (1998) 253 [hep-th/9802150].

[8] S. Gubser, I.R. Klebanov and A.M. Polyakov, *Gauge theory correlators from noncritical string theory*, *Phys.Lett.* **B428** (1998) 105 [hep-th/9802109].

[9] V. Pestun et al., *Localization techniques in quantum field theories*, *J. Phys.* **A50** (2017) 440301 [1608.02952].

[10] N.A. Nekrasov, *Seiberg-Witten prepotential from instanton counting*, *Adv. Theor. Math. Phys.* **7** (2003) 831 [hep-th/0206161].

[11] N. Beisert et al., *Review of AdS/CFT Integrability: An Overview*, *Lett. Math. Phys.* **99** (2012) 3 [1012.3982].

[12] A.A. Belavin, A.M. Polyakov and A.B. Zamolodchikov, *Infinite Conformal Symmetry in Two-Dimensional Quantum Field Theory*, *Nucl. Phys. B* **241** (1984) 333.

[13] A.V. Kotikov, L.N. Lipatov, A.I. Onishchenko and V.N. Velizhanin, *Three loop universal anomalous dimension of the Wilson operators in $N = 4$ SUSY Yang-Mills model*, *Phys. Lett. B* **595** (2004) 521 [hep-th/0404092].

[14] A.V. Kotikov, *The Property of maximal transcendentality in the N=4 Supersymmetric Yang-Mills*, pp. 150–174, 5, 2010 [1005.5029].

[15] Z. Bern, L.J. Dixon and V.A. Smirnov, *Iteration of planar amplitudes in maximally supersymmetric Yang-Mills theory at three loops and beyond*, *Phys. Rev. D* **72** (2005) 085001 [hep-th/0505205].

[16] J.M. Henn, *Multiloop integrals in dimensional regularization made simple*, *Phys. Rev. Lett.* **110** (2013) 251601 [1304.1806].

[17] J.M. Henn, G.P. Korchemsky and B. Mistlberger, *The full four-loop cusp anomalous dimension in $\mathcal{N} = 4$ super Yang-Mills and QCD*, *JHEP* **04** (2020) 018 [1911.10174].

[18] S. Moch, J.A.M. Vermaseren and A. Vogt, *The Three loop splitting functions in QCD: The Nonsinglet case*, *Nucl. Phys. B* **688** (2004) 101 [hep-ph/0403192].

[19] N. Seiberg and E. Witten, *Electric - magnetic duality, monopole condensation, and confinement in N=2 supersymmetric Yang-Mills theory*, *Nucl. Phys.* **B426** (1994) 19 [hep-th/9407087].

[20] N. Seiberg and E. Witten, *Monopoles, duality and chiral symmetry breaking in $\mathcal{N} = 2$ supersymmetric QCD*, *Nucl. Phys.* **B431** (1994) 484 [hep-th/9408099].

[21] N. Seiberg, *Electric - magnetic duality in supersymmetric nonAbelian gauge theories*, *Nucl. Phys. B* **435** (1995) 129 [hep-th/9411149].

[22] N. Seiberg, *Exact results on the space of vacua of four-dimensional SUSY gauge theories*, *Phys. Rev. D* **49** (1994) 6857 [hep-th/9402044].

[23] M. Billo', L. Griguolo and A. Testa, *Remarks on BPS Wilson loops in non-conformal $\mathcal{N} = 2$ gauge theories and localization*, *JHEP* **01** (2024) 160 [2311.17692].

[24] M. Billo', L. Griguolo and A. Testa, *1/2 BPS Wilson loops in non-conformal $\mathcal{N} = 2$ gauge theories and localization: a three-loop analysis*, *JHEP* **02** (2025) 076 [2410.14847].

[25] M. Billo', L. Griguolo and A. Testa, *Supersymmetric Localization and Nonconformal N=2 Supersymmetric Yang-Mills Theories in the Perturbative Regime*, *Phys. Rev. Lett.* **134** (2025) 071601 [2407.11222].

[26] M. Billo, L. Griguolo, A. Lerda and A. Testa, *Correlators in non-conformal $\mathcal{N} = 2$ gauge theories from localization*, 2505.03940.

[27] L. Griguolo, L. Guerrini and A. Testa, *Into the wedge of $\mathcal{N} = 2$ superconformal gauge theories*, *JHEP* **07** (2025) 125 [2411.04043].

[28] G.P. Korchemsky and A. Testa, *Correlation functions in four-dimensional superconformal long circular quivers*, *JHEP* **07** (2025) 223 [2501.17223].

[29] M.F. Sohnius, *Introducing Supersymmetry*, *Phys. Rept.* **128** (1985) 39.

[30] J. Wess and J. Bagger, *Supersymmetry and supergravity*, Princeton University Press, Princeton, NJ, USA (1992).

[31] Y. Tachikawa, *N=2 supersymmetric dynamics for pedestrians*, vol. 890 (12, 2013), 10.1007/978-3-319-08822-8, [1312.2684].

[32] S.R. Coleman and J. Mandula, *All Possible Symmetries of the S Matrix*, *Phys. Rev.* **159** (1967) 1251.

[33] M. Bertolini, *Supersymmetry - From the basics to exact results in gauge theories*, World Scientific (1, 2025), 10.1142/14026.

[34] P.H. Ginsparg, *APPLIED CONFORMAL FIELD THEORY*, in *Les Houches Summer School in Theoretical Physics: Fields, Strings, Critical Phenomena*, 9, 1988 [hep-th/9108028].

[35] S. Rychkov, *EPFL Lectures on Conformal Field Theory in D>= 3 Dimensions*, SpringerBriefs in Physics (1, 2016), 10.1007/978-3-319-43626-5, [1601.05000].

[36] J.D. Qualls, *Lectures on Conformal Field Theory*, 1511.04074.

[37] A.B. Zamolodchikov, *Infinite Additional Symmetries in Two-Dimensional Conformal Quantum Field Theory*, *Theor. Math. Phys.* **65** (1985) 1205.

[38] J. Polchinski, *Scale and Conformal Invariance in Quantum Field Theory*, *Nucl. Phys. B* **303** (1988) 226.

[39] R. Jackiw and S.Y. Pi, *Tutorial on Scale and Conformal Symmetries in Diverse Dimensions*, *J. Phys. A* **44** (2011) 223001 [1101.4886].

[40] P. Di Francesco, P. Mathieu and D. Senechal, *Conformal Field Theory*, Graduate Texts in Contemporary Physics, Springer-Verlag, New York (1997), 10.1007/978-1-4612-2256-9.

[41] G. Gibbons, *Quantum field theory in curved spacetime.*, (S. Hawking and W. Israel eds.) Cambridge University Press (1979).

[42] K.G. Wilson, *Nonlagrangian models of current algebra*, *Phys. Rev.* **179** (1969) 1499.

[43] P.S. Howe, K.S. Stelle and P.C. West, *A Class of Finite Four-Dimensional Supersymmetric Field Theories*, *Phys. Lett. B* **124** (1983) 55.

[44] D.R.T. Jones, *Two Loop Diagrams in Yang-Mills Theory*, *Nucl. Phys. B* **75** (1974) 531.

[45] P.S. Howe and P.C. West, *THE TWO LOOP BETA FUNCTION IN MODELS WITH EXTENDED RIGID SUPERSYMMETRY*, *Nucl. Phys. B* **242** (1984) 364.

[46] N. Seiberg, *Supersymmetry and Nonperturbative beta Functions*, *Phys. Lett.* **B206** (1988) 75.

[47] V.A. Novikov, M.A. Shifman, A.I. Vainshtein and V.I. Zakharov, *The beta function in supersymmetric gauge theories. Instantons versus traditional approach*, *Phys. Lett. B* **166** (1986) 329.

[48] V.A. Novikov, M.A. Shifman, A.I. Vainshtein and V.I. Zakharov, *Exact Gell-Mann-Low Function of Supersymmetric Yang-Mills Theories from Instanton Calculus*, *Nucl. Phys. B* **229** (1983) 381.

[49] D.J. Gross and F. Wilczek, *Asymptotically Free Gauge Theories - I*, *Phys. Rev. D* **8** (1973) 3633.

[50] N. Nekrasov and A. Okounkov, *Seiberg-Witten theory and random partitions*, *Prog. Math.* **244** (2006) 525 [hep-th/0306238].

[51] M.F. Sohnius and P.C. West, *Conformal Invariance in N=4 Supersymmetric Yang-Mills Theory*, *Phys. Lett. B* **100** (1981) 245.

[52] S. Mandelstam, *Light Cone Superspace and the Ultraviolet Finiteness of the N=4 Model*, *Nucl. Phys. B* **213** (1983) 149.

[53] L. Brink, O. Lindgren and B.E.W. Nilsson, *The Ultraviolet Finiteness of the N=4 Yang-Mills Theory*, *Phys. Lett. B* **123** (1983) 323.

[54] M.T. Grisaru, M. Rocek and W. Siegel, *Zero Three Loop beta Function in N=4 Superyang-Mills Theory*, *Phys. Rev. Lett.* **45** (1980) 1063.

[55] V. Pestun, *Localization of gauge theory on a four-sphere and supersymmetric Wilson loops*, *Commun. Math. Phys.* **313** (2012) 71 [0712.2824].

[56] S. Cremonesi, *An Introduction to Localisation and Supersymmetry in Curved Space*, *PoS* **Modave2013** (2013) 002.

[57] M. Marino, *Lectures on localization and matrix models in supersymmetric Chern-Simons-matter theories*, *J.Phys.* **A44** (2011) 463001 [1104.0783].

[58] M. Beccaria, M. Billo, F. Galvagno, A. Hasan and A. Lerda, $\mathcal{N} = 2$ *Conformal SYM theories at large* $\mathcal{N}$, *JHEP* **09** (2020) 116 [2007.02840].

[59] G. Festuccia and N. Seiberg, *Rigid Supersymmetric Theories in Curved Superspace*, *JHEP* **06** (2011) 114 [1105.0689].

[60] M. Billò, F. Galvagno and A. Lerda, *BPS wilson loops in generic conformal* $\mathcal{N} = 2$ *SU(N) SYM theories*, *JHEP* **08** (2019) 108 [1906.07085].

[61] R. Andree and D. Young, *Wilson Loops in* $\mathcal{N} = 2$ *Superconformal Yang-Mills Theory*, *JHEP* **09** (2010) 095 [1007.4923].

[62] M. Billo, F. Fucito, A. Lerda, J.F. Morales, Y.S. Stanev and C. Wen, *Two-point correlators in* $N = 2$ *gauge theories*, *Nucl. Phys. B* **926** (2018) 427 [1705.02909].

[63] M. Billo, F. Galvagno, P. Gregori and A. Lerda, *Correlators between Wilson loop and chiral operators in* $\mathcal{N} = 2$ *conformal gauge theories*, *JHEP* **03** (2018) 193 [1802.09813].

[64] L. Bianchi, M. Billo, F. Galvagno and A. Lerda, *Emitted Radiation and Geometry*, *JHEP* **01** (2020) 075 [1910.06332].

[65] M. Billo, M. Frau, F. Galvagno, A. Lerda and A. Pini, *Strong-coupling results for* $\mathcal{N} = 2$ *superconformal quivers and holography*, *JHEP* **10** (2021) 161 [2109.00559].

[66] M. Billo, M. Frau, A. Lerda, A. Pini and P. Vallarino, *Localization vs holography in 4d*$\mathcal{N} = 2$ *quiver theories*, *JHEP* **10** (2022) 020 [2207.08846].

[67] M. Billo, M. Frau, A. Lerda, A. Pini and P. Vallarino, *Three-point functions in a* $\mathcal{N} = 2$ *superconformal gauge theory and their strong-coupling limit*, 2202.06990.

[68] M. Beccaria, G.V. Dunne and A.A. Tseytlin, *Strong coupling expansion of free energy and BPS Wilson loop in* $\mathcal{N} = 2$ *superconformal models with fundamental hypermultiplets*, *JHEP* **08** (2021) 102 [2105.14729].

[69] M. Beccaria, G.P. Korchemsky and A.A. Tseytlin, *Non-planar corrections in orbifold/orientifold $\mathcal{N} = 2$ superconformal theories from localization*, *JHEP* **05** (2023) 165 [2303.16305].

[70] M. Beccaria and G.P. Korchemsky, *Four-dimensional $\mathcal{N} = 2$ superconformal long circular quivers*, *JHEP* **04** (2024) 054 [2312.03836].

[71] J. Russo and K. Zarembo, *Massive $\mathcal{N} = 2$ Gauge Theories at Large N*, *JHEP* **11** (2013) 130 [1309.1004].

[72] S.-J. Rey and T. Suyama, *Exact Results and Holography of Wilson Loops in N=2 Superconformal (Quiver) Gauge Theories*, *JHEP* **01** (2011) 136 [1001.0016].

[73] V. Mitev and E. Pomoni, *Exact effective couplings of four dimensional gauge theories with $\mathcal{N} = 2$ supersymmetry*, *Phys. Rev. D* **92** (2015) 125034 [1406.3629].

[74] B. Fiol, B. Garolera and G. Torrents, *Probing $\mathcal{N} = 2$ superconformal field theories with localization*, *JHEP* **01** (2016) 168 [1511.00616].

[75] V. Mitev and E. Pomoni, *Exact bremsstrahlung and effective couplings*, *JHEP* **06** (2016) 078 [1511.02217].

[76] A. Pini, D. Rodriguez-Gomez and J.G. Russo, *Large N correlation functions $\mathcal{N} = 2$ superconformal quivers*, *JHEP* **08** (2017) 066 [1701.02315].

[77] K. Zarembo, *Quiver CFT at Strong Coupling*, *JHEP* **06** (2020) 055 [2003.00993].

[78] B. Fiol, J. Martfnez-Montoya and A. Rios Fukelman, *The planar limit of $\mathcal{N} = 2$ superconformal quiver theories*, *JHEP* **08** (2020) 161 [2006.06379].

[79] H. Ouyang, *Wilson Loops in Circular Quiver SCFTs at Strong Coupling*, *JHEP* **02** (2021) 178 [2011.03531].

[80] F. Galvagno and M. Preti, *Chiral correlators in $\mathcal{N} = 2$ superconformal quivers*, *JHEP* **05** (2021) 201 [2012.15792].

[81] M. Beccaria and A.A. Tseytlin, *$1/N$ expansion of circular Wilson loop in $\mathcal{N} = 2$ superconformal $SU(N) \times SU(N)$ quiver*, *JHEP* **04** (2021) 265 [2102.07696].

[82] M. Billò, M. Frau, A. Lerda, A. Pini and P. Vallarino, *Structure Constants in N=2 Superconformal Quiver Theories at Strong Coupling and Holography*, *Phys. Rev. Lett.* **129** (2022) 031602 [2206.13582].

[83] N. Arkani-Hamed, A.G. Cohen and H. Georgi, *(De)constructing dimensions*, *Phys. Rev. Lett.* **86** (2001) 4757 [hep-th/0104005].

[84] C.T. Hill, S. Pokorski and J. Wang, *Gauge Invariant Effective Lagrangian for Kaluza-Klein Modes*, *Phys. Rev. D* **64** (2001) 105005 [hep-th/0104035].

[85] M. Billo, M. Frau, A. Lerda, A. Pini and P. Vallarino, *Strong coupling expansions in $\mathcal{N} = 2$ quiver gauge theories*, *JHEP* **01** (2023) 119 [2211.11795].

[86] M. Preti, *Correlators in superconformal quivers made QUICK*, 2212.14823.

[87] C.F. Uhlemann, *Exact results for 5d SCFTs of long quiver type*, *JHEP* **11** (2019) 072 [1909.01369].

[88] C.F. Uhlemann, *AdS_6/CFT_5 with O7-planes*, *JHEP* **04** (2020) 113 [1912.09716].

[89] L. Coccia, *Topologically twisted index of $T[SU(N)]$ at large N*, *JHEP* **05** (2021) 264 [2006.06578].

[90] L. Coccia and C.F. Uhlemann, *On the planar limit of 3d $\mathrm{T}^{\sigma}_{\rho}[\mathrm{SU}(\mathrm{N})]$*, *JHEP* **06** (2021) 038 [2011.10050].

[91] M. Akhond, A. Legramandi, C. Nunez, L. Santilli and L. Schepers, *Matrix models and holography: Mass deformations of long quiver theories in 5d and 3d*, *SciPost Phys.* **15** (2023) 086 [2211.13240].

[92] C. Nunez, L. Santilli and K. Zarembo, *Linear Quivers at Large-N*, 2311.00024.

[93] E. Sobko, *Continuous Quivers*, 2406.14203.

[94] N. Arkani-Hamed, A.G. Cohen, D.B. Kaplan, A. Karch and L. Motl, *Deconstructing (2,0) and little string theories*, *JHEP* **01** (2003) 083 [hep-th/0110146].

[95] N. Lambert, C. Papageorgakis and M. Schmidt-Sommerfeld, *Deconstructing (2,0) Proposals*, *Phys. Rev. D* **88** (2013) 026007 [1212.3337].

[96] J. Hayling, C. Papageorgakis, E. Pomoni and D. Rodríguez-Gómez, *Exact Deconstruction of the 6D (2,0) Theory*, *JHEP* **06** (2017) 072 [1704.02986].

[97] V. Niarchos, C. Papageorgakis and E. Pomoni, *Type-B Anomaly Matching and the 6D (2,0) Theory*, *JHEP* **04** (2020) 048 [1911.05827].

[98] E. Gerchkovitz, J. Gomis, N. Ishtiaque, A. Karasik, Z. Komargodski and S.S. Pufu, *Correlation Functions of Coulomb Branch Operators*, *JHEP* **01** (2017) 103 [1602.05971].

[99] M. Baggio, V. Niarchos and K. Papadodimas, *On exact correlation functions in SU(N) $\mathcal{N} = 2$ superconformal QCD*, *JHEP* **11** (2015) 198 [1508.03077].

[100] D. Rodriguez-Gomez and J.G. Russo, *Operator mixing in large N superconformal field theories on S^4 and correlators with Wilson loops*, *JHEP* **12** (2016) 120 [1607.07878].

[101] C.A. Tracy and H. Widom, *Level spacing distributions and the Bessel kernel*, *Commun. Math. Phys.* **161** (1994) 289 [hep-th/9304063].

[102] M. Beccaria, G.P. Korchemsky and A.A. Tseytlin, *Strong coupling expansion in $\mathcal{N} = 2$ superconformal theories and the Bessel kernel*, *JHEP* **09** (2022) 226 [2207.11475].

[103] P.J. Forrester, *The spectrum edge of random matrix ensembles*, *Nucl. Phys. B* **402** (1993) 709.

[104] C.A. Tracy and H. Widom, *Fredholm Determinants, Differential Equations and Matrix Models*, *Commun. Math. Phys.* **163** (1994) 33 [hep-th/9306042].

[105] A.V. Belitsky and G.P. Korchemsky, *Exact Null Octagon*, *JHEP* **05** (2020) 070 [1907.13131].

[106] A.V. Belitsky and G.P. Korchemsky, *Crossing bridges with strong Szegő limit theorem*, *JHEP* **04** (2021) 257 [2006.01831].

[107] A.V. Belitsky and G.P. Korchemsky, *Octagon at Finite Coupling*, *JHEP* **07** (2020) 219 [2003.01121].

[108] M. Beccaria, M. Billo, M. Frau, A. Lerda and A. Pini, *Exact results in a $\mathcal{N} = 2$ superconformal gauge theory at strong coupling*, *JHEP* **07** (2021) 185 [2105.15113].

[109] Z. Bajnok, B. Boldis and G.P. Korchemsky, *Tracy-Widom Distribution in Four-Dimensional Supersymmetric Yang-Mills Theories*, *Phys. Rev. Lett.* **133** (2024) 031601 [2403.13050].

[110] Z. Bajnok, B. Boldis and G.P. Korchemsky, *Solving four-dimensional superconformal Yang-Mills theories with Tracy-Widom distribution*, 2409.17227.

[111] G.P. Korchemsky, *Lattice path combinatorics in superconformal Yang-Mills theories*, 2508.20901.

[112] G. Ferrando, S. Komatsu, G. Lefundes and D. Serban, *Exact Three-Point Functions in $\mathcal{N} = 2$ Superconformal Field Theories: Integrability vs. Localization*, 2503.07295.

[113] M. Beccaria, G.P. Korchemsky and A.A. Tseytlin, *Exact strong coupling results in $\mathcal{N} = 2$ Sp(2N) superconformal gauge theory from localization*, *JHEP* **01** (2023) 037 [2210.13871].

[114] D. Dorigoni, *An Introduction to Resurgence, Trans-Series and Alien Calculus*, *Annals Phys.* **409** (2019) 167914 [1411.3585].

[115] I. Aniceto, G. Basar and R. Schiappa, *A Primer on Resurgent Transseries and Their Asymptotics*, *Phys. Rept.* **809** (2019) 1 [1802.10441].

[116] "*NIST Digital Library of Mathematical Functions*." `https://dlmf.nist.gov/`, Release 1.2.3 of 2024-12-15.

[117] G. Kallen, *On the definition of the Renormalization Constants in Quantum Electrodynamics*, *Helv. Phys. Acta* **25** (1952) 417.

[118] S. Kachru and E. Silverstein, *4-D Conformal Theories and Strings on Orbifolds*, *Phys. Rev. Lett.* **80** (1998) 4855 [hep-th/9802183].

[119] S. Gukov, *Comments on $\mathcal{N} = 2$ AdS Orbifolds*, *Phys. Lett. B* **439** (1998) 23 [hep-th/9806180].

[120] T. Skrzypek and A.A. Tseytlin, *On AdS/CFT duality in the twisted sector of string theory on $AdS_5 \times S^5/\mathbb{Z}_2$ orbifold background*, *JHEP* **03** (2024) 045 [2312.13850].

[121] J.K. Erickson, G.W. Semenoff and K. Zarembo, *Wilson loops in N=4 supersymmetric Yang-Mills theory*, *Nucl. Phys.* **B582** (2000) 155 [hep-th/0003055].

[122] N. Drukker and D.J. Gross, *An Exact prediction of N=4 SUSYM theory for string theory*, *J. Math. Phys.* **42** (2001) 2896 [hep-th/0010274].

[123] N. Drukker, S. Giombi, R. Ricci and D. Trancanelli, *Supersymmetric Wilson loops on S^3*, *JHEP* **05** (2008) 017 [0711.3226].

[124] V. Pestun, *Localization of the four-dimensional N=4 SYM to a two-sphere and 1/8 BPS Wilson loops*, *JHEP* **12** (2012) 067 [0906.0638].

[125] A. Bassetto and L. Griguolo, *Two-dimensional QCD, instanton contributions and the perturbative Wu-Mandelstam-Leibbrandt prescription*, *Phys. Lett. B* **443** (1998) 325 [hep-th/9806037].

[126] S. Giombi, V. Pestun and R. Ricci, *Notes on Supersymmetric Wilson Loops on a Two-Sphere*, *JHEP* **07** (2010) 088 [0905.0665].

[127] S. Giombi and V. Pestun, *Correlators of local operators and 1/8 BPS Wilson loops on S**2 from 2d YM and matrix models*, *JHEP* **10** (2010) 033 [0906.1572].

[128] B. Fiol and A.R. Fukelman, *The planar limit of $\mathcal{N}$ = 2 chiral correlators*, *JHEP* **08** (2021) 032 [2106.04553].

[129] D. Correa, J. Henn, J. Maldacena and A. Sever, *An exact formula for the radiation of a moving quark in N=4 super Yang Mills*, *JHEP* **06** (2012) 048 [1202.4455].

[130] M. Bonini, L. Griguolo, M. Preti and D. Seminara, *Bremsstrahlung function, leading Lüscher correction at weak coupling and localization*, *JHEP* **02** (2016) 172 [1511.05016].

[131] B. Fiol, E. Gerchkovitz and Z. Komargodski, *Exact Bremsstrahlung Function in N = 2 Superconformal Field Theories*, *Phys. Rev. Lett.* **116** (2016) 081601 [1510.01332].

[132] C. Gomez, A. Mauri and S. Penati, *The Bremsstrahlung function of $\mathcal{N}$ = 2 SCQCD*, *JHEP* **03** (2019) 122 [1811.08437].

[133] A.V. Belitsky and G.P. Korchemsky, *Circular Wilson loop in N=2* super Yang-Mills theory at two loops and localization*, *JHEP* **04** (2021) 089 [2003.10448].

[134] K.G. Wilson, *Confinement of Quarks*, *Phys. Rev. D* **10** (1974) 2445.

[135] J.M. Maldacena, *Wilson loops in large N field theories*, *Phys. Rev. Lett.* **80** (1998) 4859 [hep-th/9803002].

[136] K. Zarembo, *Supersymmetric Wilson loops*, *Nucl. Phys.* **B643** (2002) 157 [hep-th/0205160].

[137] N. Drukker, *1/4 BPS circular loops, unstable world-sheet instantons and the matrix model*, *JHEP* **09** (2006) 004 [hep-th/0605151].

[138] N. Drukker, S. Giombi, R. Ricci and D. Trancanelli, *More Supersymmetric Wilson Loops*, *Phys. Rev. D* **76** (2007) 107703 [0704.2237].

[139] M. Baggio, V. Niarchos, K. Papadodimas and G. Vos, *Large-N correlation functions in $\mathcal{N}$ = 2 superconformal QCD*, *JHEP* **01** (2017) 101 [1610.07612].

[140] D. Rodriguez-Gomez and J.G. Russo, *Large N Correlation Functions in Superconformal Field Theories*, *JHEP* **06** (2016) 109 [1604.07416].

[141] M. Baggio, V. Niarchos and K. Papadodimas, *tt^* equations, localization and exact chiral rings in 4d $\mathcal{N}$ =2 SCFTs*, *JHEP* **02** (2015) 122 [1409.4212].

[142] M. Baggio, V. Niarchos and K. Papadodimas, *Exact correlation functions in $SU(2)\mathcal{N}=2$ superconformal QCD*, *Phys. Rev. Lett.* **113** (2014) 251601 [1409.4217].

[143] S. Giombi and V. Pestun, *Correlators of Wilson Loops and Local Operators from Multi-Matrix Models and Strings in AdS*, *JHEP* **01** (2013) 101 [1207.7083].

[144] M. Billo, F. Fucito, G.P. Korchemsky, A. Lerda and J.F. Morales, *Two-point correlators in non-conformal $\mathcal{N} = 2$ gauge theories*, *JHEP* **05** (2019) 199 [1901.09693].

[145] J. Gatheral, *Exponentiation of eikonal cross sections in nonabelian gauge theories*, *Physics Letters B* **133** (1983) .

[146] J. Frenkel and J. Taylor, *Non-abelian eikonal exponentiation*, *Nuclear Physics B* **246** (1984) .

[147] M. Beccaria, S. Giombi and A. Tseytlin, *Non-supersymmetric Wilson loop in $\mathcal{N} = 4$ SYM and defect 1d CFT*, *JHEP* **03** (2018) 131 [1712.06874].

[148] A.I. Davydychev and J.B. Tausk, *A Magic connection between massive and massless diagrams*, *Phys. Rev. D* **53** (1996) 7381 [hep-ph/9504431].

[149] V.S. Dotsenko and S.N. Vergeles, *Renormalizability of Phase Factors in the Nonabelian Gauge Theory*, *Nucl. Phys.* **B169** (1980) 527.

[150] R.A. Brandt, F. Neri and M.-a. Sato, *Renormalization of Loop Functions for All Loops*, *Phys. Rev. D* **24** (1981) 879.

[151] G.P. Korchemsky and A.V. Radyushkin, *Renormalization of the Wilson Loops Beyond the Leading Order*, *Nucl. Phys. B* **283** (1987) 342.

[152] S. Penati, A. Santambrogio and D. Zanon, *Two point functions of chiral operators in N=4 SYM at order g^4*, *JHEP* **12** (1999) 006 [hep-th/9910197].

[153] S. Penati, A. Santambrogio and D. Zanon, *Correlation functions of chiral primary operators in perturbative N=4 SYM*, hep-th/0003026.

[154] S. Penati, A. Santambrogio and D. Zanon, *More on correlators and contact terms in N=4 SYM at order g^4*, *Nucl. Phys.* **B593** (2001) 651 [hep-th/0005223].

[155] D. Bason and M. Billò, *θ-diagram technique for $\mathcal{N} = 1$, $d = 4$ superfields*, *Eur. Phys. J. C* **83** (2023) 892 [2301.11717].

[156] S.J. Gates, M.T. Grisaru, M. Rocek and W. Siegel, *Superspace Or One Thousand and One Lessons in Supersymmetry*, vol. 58 of *Frontiers in Physics* (1983), [hep-th/0108200].

[157] S. Kovacs, *N=4 supersymmetric Yang-Mills theory and the AdS / SCFT correspondence*, other thesis, 8, 1999, [hep-th/9908171].

[158] S. Kovacs, *A Perturbative reanalysis of N=4 supersymmetric Yang-Mills theory*, *Int. J. Mod. Phys. A* **21** (2006) 4555 [hep-th/9902047].

[159] M. Bianchi, F. Fucito, G.C. Rossi and M. Martellini, *ALE instantons in string effective theory*, *Nucl. Phys.* **B440** (1995) 129 [hep-th/9409037].

[160] M. Bianchi, S. Kovacs, G. Rossi and Y.S. Stanev, *On the logarithmic behavior in N=4 SYM theory*, *JHEP* **08** (1999) 020 [hep-th/9906188].

[161] M. Bianchi and S. Kovacs, *Nonrenormalization of extremal correlators in N=4 SYM theory*, *Phys. Lett. B* **468** (1999) 102 [hep-th/9910016].

[162] M.S. Bianchi, *Protected and uniformly transcendental*, *JHEP* **09** (2023) 121 [2306.06239].

[163] F. Passerini and K. Zarembo, *Wilson Loops in N=2 Super-Yang-Mills from Matrix Model*, *JHEP* **09** (2011) 102 [1106.5763].

[164] J.-E. Bourgine, *A Note on the Integral Equation for the Wilson Loop in* $\mathcal{N} = 2$ $d = 4$ *Superconformal Yang-Mills Theory*, *J. Phys.* **A45** (2012) 125403 [1111.0384].

[165] J.G. Russo and K. Zarembo, *Large N Limit of* $\mathcal{N} = 2$ $SU(N)$ *Gauge Theories from Localization*, *JHEP* **10** (2012) 082 [1207.3806].

[166] K. Zarembo, *Localization and AdS/CFT Correspondence*, *J. Phys.* **A50** (2017) 443011 [1608.02963].

[167] B. Fiol, J. Martínez-Montoya and A. Rios Fukelman, *The planar limit of* $\mathcal{N} = 2$ *superconformal field theories*, *JHEP* **05** (2020) 136 [2003.02879].

[168] A. Grozin, *Lectures on QED and QCD*, in *3rd Dubna International Advanced School of Theoretical Physics*, 8, 2005 [hep-ph/0508242].

[169] A. Bassetto, L. Griguolo, F. Pucci and D. Seminara, *Supersymmetric Wilson loops at two loops*, *JHEP* **06** (2008) 083 [0804.3973].

[170] M.S. Bianchi, L. Griguolo, M. Leoni, A. Mauri, S. Penati and D. Seminara, *The quantum 1/2 BPS Wilson loop in* $\mathcal{N} = 4$ *Chern-Simons-matter theories*, *JHEP* **09** (2016) 009 [1606.07058].